

UNCLASSIFIED

AD NUMBER: AD0269587

LIMITATION CHANGES

TO:

Approved for public release; distribution is unlimited.

FROM:

Distribution authorized to US Government Agencies and their Contractors; Administrative/Operational Use; 1 Oct 1961. Other requests shall be referred to Aeronautical Systems Division, Wright-Patterson AFB, OH, 45433.

AUTHORITY

AFFDL ltr dtd 2 Jul 1974

CLASSIFIED

269 587

*Reproduced
by the*

**TECHNICAL INFORMATION AGENCY
PENTAGON HALL STATION
WASHINGTON 25, VIRGINIA**



CLASSIFIED

NOTICE: When government or other drawings, specifications or other data are used for any purpose other than in connection with a definitely related government procurement operation, the U. S. Government thereby incurs no responsibility, nor any obligation whatsoever; and the fact that the Government may have formulated, furnished, or in any way supplied the said drawings, specifications, or other data is not to be regarded by implication or otherwise as in any manner licensing the holder or any other person or corporation, or conveying any rights or permission to manufacture, use or sell any patented invention that may in any way be related thereto.

CATALOGED BY ASTIA # 269587
AS AD NO.

269587

ASD TECHNICAL REPORT 61-39
PART I

SPACE RADIATOR ANALYSIS AND DESIGN
PART I

D. B. MACKAY
C. P. BACHA

SPACE AND INFORMATION SYSTEMS DIVISION
NORTH AMERICAN AVIATION, INC.

SID 61-66

OCTOBER, 1961

XEROX

62-124

ASTIA
RECEIVED
JAN 15 1962
JIPDB

AERONAUTICAL SYSTEMS DIVISION

NOTICES

When Government drawings, specifications, or other data are used for any purpose other than in connection with a definitely related Government procurement operation, the United States Government thereby incurs no responsibility nor any obligation whatsoever; and the fact that the Government may have formulated, furnished, or in any way supplied the said drawings, specifications, or other data, is not to be regarded by implication or otherwise as in any manner licensing the holder or any other person or corporation, or conveying any rights or permission to manufacture, use, or sell any patented invention that may in any way be related thereto.



Qualified requesters may obtain copies of this report from the Armed Services Technical Information Agency (ASTIA), Arlington Hall Station, Arlington 12, Virginia.



This report has been released to the Office of Technical Services, U. S. Department of Commerce, Washington 25, D. C., for sale to the general public.



Copies of ASD Technical Reports and Technical Notes should not be returned to the Aeronautical Systems Division unless return is required by security considerations, contractual obligations, or notice on a specific document.

**ASD TECHNICAL REPORT 61-30
PART I**

SPACE RADIATOR ANALYSIS AND DESIGN

PART I

**D. B. MACKAY
C. P. BACHA**

**SPACE AND INFORMATION SYSTEMS DIVISION
NORTH AMERICAN AVIATION, INC.**

SID 61-66

OCTOBER, 1961

**FLIGHT ACCESSORIES LABORATORY
CONTRACT AF 33(616)-7635
PROJECT No. 6146
TASK No. 6118**

**AERONAUTICAL SYSTEMS DIVISION
AIR FORCE SYSTEMS COMMAND
UNITED STATES AIR FORCE
WRIGHT-PATTERSON AIR FORCE BASE, OHIO**

FOREWORD

This is one of a series of reports which summarizes the first 6-month phase of a planned 3-year study of thermal and atmospheric control systems of manned and unmanned space vehicles. The study was conducted by the Space and Information Systems Division (S&ID) of North American Aviation, Inc., under AF 33(616)-7635 and was sponsored by the Flight Accessories Laboratory of Aeronautical Systems Division (formerly designated Wright Air Development Division). The Los Angeles Division of North American Aviation and AiResearch Manufacturing Company were subcontractors in the study effort.

The reports comprising the series are as follows:

ASD TR 61-164 (Part I)	Environmental Control Systems Selection for Unmanned Space Vehicles (secret)
ASD TR 61-240 (Part I)	Environmental Control Systems Selection for Manned Space Vehicles, Volume I (unclassified) and Volume II (secret)
ASD TR 61-161 (Part I)	Space Vehicle Environmental Control Requirements Based on Equipment and Physiological Criteria
ASD TR 61-119 (Part I)	Radiation Heat Transfer Analysis for Space Vehicles
ASD TR 61-30 (Part I)	Space Radiator Analysis and Design
ASD TR 61-176 (Part I)	Integration and Optimization Concepts for Space Vehicle Environmental Control Systems
ASD TR 61-162 (Part I)	Analytical Method for Space Vehicle Atmospheric Control Processes

The thermal and atmospheric control program was under the direction of A. L. Ingelfinger and Lieutenant N. P. Jeffries of the Environmental Control Section, Flight Accessories Laboratory. G. Zara of the Environmental Control Section acted as monitor of this report. A. C. Martin served as project engineer at S&ID. The space radiator studies were conducted by D. B. Mackay and C. F. Bacha.

ABSTRACT


The thermal analysis of component elements of space radiators is described herein. Elements include rectangular and circular plates of uniform thickness, triangular and trapezoidal fins, and constant temperature-gradient fins. A complete condenser and a radiator are analyzed and illustrative examples given.

The thermal analyses produced relationships between the physical properties and dimensions, element and environmental temperatures, and rates of heat transfer. These are shown graphically for all types of elements. The optimum proportions of space radiator elements having the greatest ratio of heat radiation rate per pound of weight are also indicated graphically, and procedures for their calculation are shown. The discussions on condensers and radiators include dimensional-thermal relationships and weight-optimizing procedures for complete units.

PUBLICATION REVIEW

This report has been reviewed and is approved.

FOR THE COMMANDER:


WILLIAM C. SAVAGE
Chief, Environmental Branch
Flight Accessories Laboratory

CONTENTS

Section	Page
I INTRODUCTION	1
Study Program	1
Role of Space Radiators	1
Hypothetical Vehicles and Radiator Requirements	2
Nomenclature	3
II DETERMINATION OF SPACE RADIATOR REQUIREMENTS	5
Sources of Heat to be Radiated	5
Heat Quantity and Temperature Determination	5
Conveyance of Heat to Radiators	6
III ANALYSES OF SPACE RADIATOR ELEMENTS	7
Description of Radiator Elements	7
Element Forms	7
Formation of Radiators From Elements	9
Radiation From Elemental Forms	9
Radiant Heat Transfer From Flat Rectangular Plate Uniformly Heated Along One Edge	11
Nomenclature	12
Mathematical Analysis	14
Optimum-Weight Design	18
Design Procedures	22
Radiant Heat Transfer From Flat Circular Plate Uniformly Heated Along Inner Circumference	25
Nomenclature	25
Mathematical Analysis	27
Optimum-Weight Design	30
Radiant Heat Transfer From Constant Temperature- Gradient Fin	37
Nomenclature	38
Mathematical Analysis	40
Design Analysis	49
Optimum-Weight Design	55
Design Procedures	63
Radiant Heat Transfer From Triangular and Trapezoidal Fins	65
Nomenclature	65
Mathematical Analysis	66
Optimum-Weight Design	76
Design Curves	78

Section	Page
Radiant Heat Transfer From Traveling Belt	87
Nomenclature	88
Mathematical Analysis	88
IV DESIGN OF CONDENSERS FOR OPERATION IN SPACE	91
Nomenclature	91
Mathematical Analysis	93
Optimization Procedure	101
Illustrative Problems	104
V DESIGN OF RADIATORS FOR OPERATION IN SPACE	129
Nomenclature	129
Mathematical Analysis	131
Design Factors	143
Illustrative Problems	146
VI REFERENCES	153
VII BIBLIOGRAPHY	155

ILLUSTRATIONS

Figure		Page
1	Various Radiator Elements	8
2	Formation of Radiators From Elemental Forms	10
3	Environment for Flat Plate Analysis	15
4	Dimensional Relationships of Flat Plate Heated Uniformly Along One Edge	17
5	Relationship of Plate Effectiveness to Profile Number of Flat Plate (Rectangular Coordinates)	19
6	Relationship of Plate Effectiveness to Profile Number of Flat Plate (Logarithmic Coordinates)	20
7	Configuration of Circular Plate Fin Acting as Space Radiator	28
8	Dimensional Relationships of Circular Plate Heated Uniformly Along Inner Circumference	28
9	Relationship of Plate Effectiveness to Profile Number of Circular Plate	31
10	Construction of Line of Constant K	33
11	Location of Line of Optimum-Weight Configuration on Plate Effectiveness Versus Profile Number	34
12	Location of Profile Numbers of Maximum Heat Transfer Rate for Circular Plates	35
13	Configuration of Constant Temperature-Gradient Fin	37
14	Dimensional and Temperature Relationships of Constant Temperature-Gradient Fin	41
15	Relationship of Profile Number to Temperature Ratio of Constant Temperature-Gradient Fin	45
16	Relationship of Heat Transfer Number to Fin Profile Number of Constant Temperature-Gradient Fin	51
17	Relationship of Fin Effectiveness to Profile Number of Constant Temperature-Gradient Fin	52
18	Relationship of Weight Number to Profile Number of Constant Temperature-Gradient Fin	53
19	Relationship of Weight/Heat Transfer Ratio to Profile Number of Constant Temperature-Gradient Fin	54
20	Relationship of Fin Differential Ratio Number ζ_d to Profile Number of Constant Temperature-Gradient Fin	56
21	Relationship of Thickness Ratio to Length Ratio of Constant Temperature-Gradient Fin (Operating in Free Space).	57
22	Relationship of Thickness Ratio to Length Ratio of Constant Temperature-Gradient Fin (Operating at Environmental Parameter of 0.2)	58

Figure	Page
23	Relationship of Weight/(Heat Transfer Number) ³ Ratio to Profile Number of Constant Temperature-Gradient Fin 60
24	Relationship of Heat Transfer Number to Weight Number of Constant Temperature-Gradient Fin 62
25	Dimensional Relationships of Trapezoidal Profile Fin 67
26	Relationship of ω to $f(\omega)$ for Triangular and Trapezoidal Fins 74
27	Relationship of Fin Effectiveness to Environmental Parameter and Profile Number of Triangular and Trapezoidal Fins 75
28	Relationship of Fin Effectiveness to Profile Number for Extended-Surface Fins (Two Environmental Parameters) 79
29	Relationship of Fin Effectiveness to Profile Number for Trapezoidal Fin ($\delta_c/\delta_h = 0.75$) 80
30	Relationship of Fin Effectiveness to Profile Number for Trapezoidal Fin ($\delta_c/\delta_h = 0.50$) 81
31	Relationship of Fin Effectiveness to Profile Number for Trapezoidal Fin ($\delta_c/\delta_h = 0.25$) 82
32	Relationship of Fin Effectiveness to Profile Number for Triangular Fin ($\delta_c/\delta_h = 0$) 83
33	Determination of Theoretical Profile for Trapezoidal Fin ($\delta_c/\delta_h = 0.75$) 84
34	Determination of Theoretical Profile for Trapezoidal Fin ($\delta_c/\delta_h = 0.50$) 84
35	Determination of Theoretical Profile for Trapezoidal Fin ($\delta_c/\delta_h = 0.25$) 85
36	Determination of Theoretical Profile for Triangular Fin ($\delta_c/\delta_h = 0$) 85
37	Dimensional Relationships of Traveling Belt Space Radiator 87
38	Dimensional Relationships of Rectangular-Duct Condenser 95
39	Dimensional Relationships of Cylindrical-Tube Condenser With Extended Surfaces of Constant Thickness 96
40	Correction Factors for Interradiation Between Condenser Tubes and Extended Surfaces 98
41	Section of Condenser Showing Incremental Segments 102
42	Relationship of Weight Per Unit of Heat Transfer and Rate of Change of Ratio to Fin Length (Problem 1) 106
43	Relationship of Weight Per Unit of Heat Transfer to Fin Length for Environmental Parameter of Zero (Problem 2) 111
44	Relationship of Weight Per Unit of Heat Transfer to Fin Length for Theoretical Profile (Problem 2) 112
45	Relationship of Weight Per Unit of Heat Transfer to Fin Length for Flat Plate and Triangular Fin (Problem 2) 113
46	Relationship of Weight Per Unit of Heat Transfer and Rate of Change of Ratio to Fin Length (Problem 3) 119
47	Relationship of Area Per Unit of Heat Transfer to Fin Length (Problem 3) 120

Figure		Page
48	Relationship of Temperature Difference Between Vapor and Wall to Vapor Velocity at Tube Entrance (Problem 4)	123
49	Relationship of Tube Length to Vapor Velocity at Tube Entrance (Problem 5)	125
50	Relationship of Tube Inside Diameter to Vapor Velocity (Problem 6)	127
51	Dimensional and Temperature Relationships of Rectangular Cross-Section Duct Radiating Heat From Both Surfaces	132
52	Dimensional and Temperature Relationships of Rectangular Cross-Section Duct Radiating Heat From One Surface	137
53	Dimensional Relationship of Duct and Extended-Surface Heat Exchanger Radiating Heat From Both Surfaces	139
54	Dimensional Relationship of Duct and Extended-Surface Heat Exchanger Radiating Heat From One Surface	142
55	Relationship of Film Resistance Number ψ_1 to Temperature Ratio	144
56	Relationship of Radiation Number ψ_2 to Temperature Ratio	145
57	Configuration of Heat Exchanger (Problem 2)	149

INTRODUCTION

STUDY PROGRAM

The Thermal and Atmospheric Control Study made for the Aeronautical Systems Division is an analytical and experimental program concerned with the problems of the control of the environments of future military space vehicles. Three broadly defined tasks were designated for this study. They are:

1. Development of improved methods of analysis for predicting the requirements for and performance of space environmental control systems
2. Development of improved methods, techniques, systems, and equipment required for this environmental control
3. Development of criteria and techniques for the optimization of environmental control systems and the integration of these systems with other vehicle systems

One endeavor made to accomplish these tasks is a survey of industrial organizations and military establishments to obtain data concerned with current and future state-of-the-art of thermal and atmospheric control. Other endeavors include evaluating existing and newly created methods of analysis, selection, integration, and optimization of control systems and components. The refurbishing and developing of existing and new analog or digital computer programs, applicable to this study, are included. In addition, laboratory verification of analyses and new design concepts form a part of the effort associated with these tasks.

To guide all of the endeavors along lines which would find immediate and practical application, components and systems associated with specific vehicles were studied. The vehicles selected were representative of a number of earth-orbital and cislunar missions. These hypothetical vehicles were carried through preliminary design and used as thermal and atmospheric control models.

Manuscript released by authors April 1961 for publication as an ASD Technical Report.

ROLE OF SPACE RADIATORS

One problem common to all space vehicles is the disposal of waste heat produced by the generation of power, operation of equipment, or physiological functions of the human body. Although transfer of heat within the vehicle may be accomplished by conduction, convection, or radiation, the only practical long-term means of removing heat from a vehicle in space is by radiation. The design of a space radiator to dissipate excess heat, takes on primary importance in the control of the thermal environment of a space vehicle.

The configuration of a space radiator can take any of several forms. For the earlier, smaller vehicles, it has been possible to employ the exterior skin as the radiator. As space vehicles become larger and more complex, necessitating additional power requirements, the skin structure will have to be augmented by auxiliary radiators. Some of the suggested elemental forms of lightweight radiators are the following:

- Flat plates of rectangular form
- Flat plates of circular form
- Fins of trapezoidal cross section
- Fins of triangular cross section
- Fins of tapered cross section and with concave surfaces
- Moving belts

This report documents a study of the thermal behavior of each of these elemental forms. The mathematical relationship between temperature, flow rate, dimensions, and other physical properties is established. The method of finding the dimensions of the optimum-weight configuration is determined for most cases, and the procedure for designing space vehicle condensers and radiators is shown. In performing the analyses, material previously compiled at S&ID was used as well as published literature.

HYPOTHETICAL VEHICLES AND RADIATOR REQUIREMENTS

The type of the space radiator to be used depends to some extent upon the mission to be performed. Thus, vehicles carrying personnel and operating continuously for long periods would require larger radiators than would unmanned vehicles having missions of relatively short duration. To illustrate this with examples, the thermal and atmospheric control program includes the design of several hypothetical space vehicles. Their mission will be assumed to range from relatively short observational surveillance flights to the extended duty of large space stations. Other reports of this program will illustrate the manner of designing these radiators and will compare the designs for the various vehicles.

These vehicles were designed in order to provide a concrete frame of reference for the selection of all types of control systems. Each vehicle presents a series of system problems, the solution of which will serve to demonstrate the principles and procedures presented in the analytic reports of the program. Because of the differences in character and mission of the various vehicles, opportunities occurred for developing a wide range of unique methods of integrating and optimizing components and systems.

In the first phase of the study, one manned and one unmanned vehicle were selected to serve as base point designs; others were developed later in the study. As each of the first two vehicles was developed, its missions, configurations, internal equipment, environments, and other requirements were defined. The objective was not to obtain working drawings from which these vehicles could be constructed; rather, realistic examples of thermal and atmospheric control areas requiring development were derived and the methods and procedures resulting from the thermal and atmospheric control program were tested.

NOMENCLATURE

Because the material for the thermal and atmospheric control study program reports was submitted by several organizations and was written by different authors, an effort was made to establish a nomenclature which is common to all the related reports. Therefore, publication ASA Y10.4-1957 of the American Society of Mechanical Engineers, entitled "Letter Symbols for Heat and Thermodynamics" (Reference 1), was adopted as the standard for the nomenclature and should serve as a useful guide.

It appeared more effective to provide separate nomenclature lists for each analysis of the report. These lists are found near the beginning of each separate discussion.

Section II

DETERMINATION OF SPACE RADIATOR REQUIREMENTS

SOURCES OF HEAT TO BE RADIATED

The first step in the design of space radiators is to determine the amount of heat to be radiated, for this will usually be the principal factor influencing the size of the radiator and other features. To find the required rate of heat dissipation, all possible sources of heat that may exist in a space vehicle or satellite must be considered. The following list has been compiled as a guide to the principal categories of heat sources:

- Propulsion
- Secondary power
- External environment
- Internal environment control
- Ecological systems
- Guidance and attitude control
- Communication
- General and miscellaneous

The categories were made as general as possible so as to cover all types of vehicles. Each has a number of specific sources of excess or unusable heat. For example, communication could include radio, radar, television, and recording equipment.

HEAT QUANTITY AND TEMPERATURE DETERMINATION

Having identified all of the heat sources and sinks that will affect the size and form of a space radiator, the next task of the designer is to determine the quantities and intensities of heat to be conveyed to the radiator. This determination can be made only by an analysis of the thermal characteristics of each source of heat.

It is not the purpose of this report to discuss methods of finding the magnitudes and intensities of heat quantities. Detailed procedures for the computation of heat transfer by conduction and convection can be found in standard texts on the subject. Another report of this study, "Radiation Heat Transfer in Analysis for Space Vehicles," ASD TR 61-119, explains the principles of radiant heat transfer in considerable detail.

CONVEYANCE OF HEAT TO RADIATORS

The radiator is only one part of the system by which excessive or waste heat is rejected to space. Another is the path by which the heat is conveyed from its source to the radiator. After the sources, quantities, and temperatures of heat within a vehicle have been determined, the next step in a thermal study is to establish the routes by which the heat is to travel to the radiator. This is important in radiator design because the final form of the radiator will depend, to a large extent, upon the means of bringing the heat to it. Some of these means are indicated here.

The routes for conveying heat may use one of the three fundamental modes of heat transfer - conduction, convection, and radiation - or any combination. In unmanned vehicles, convection would probably not occur because of the lack of a convective atmosphere. In a manned vehicle operating in zero-gravity, natural convection would be limited but fans or blowers could serve to move portions of the atmosphere in selected directions. Forced convection of fluids in ducts is relatively simple and probably would be used as a method of conveying heat to space radiators and condensers.

Conduction as a means of moving heat would probably be limited to those situations wherein the source of heat is relatively close to the radiator. Because the best conductors are metals, of relatively high density, long conductive paths could add excessive weight to a vehicle. On the other hand, removal of heat by conduction requires no moving parts or fluids, which could result in greater reliability than some other means of conveyance. Other factors to be considered are the radiation from conductors within the vehicle and the need for insulation to reduce this radiation or prevent injury to the crew.

While radiation is the means by which waste heat will ultimately be removed from a space vehicle, this means will ordinarily not be used for conveying heat from the source to the radiator. Heat is transferred by radiation at a relatively low rate, and its flow cannot be directed or channelled. Not that radiation should never be relied upon as a means of cooling components, but rather the heat so dissipated will usually have to be conveyed to the external radiator by some other means.

ANALYSIS OF SPACE RADIATOR ELEMENTS

DESCRIPTION OF RADIATOR ELEMENTS

ELEMENT FORMS

For purposes of the present analysis, space radiators may be divided into two classes: (1) those which are only secondarily radiators and primarily parts of the space vehicle structure, outer skin, or some other functional element, and (2) those which have been designed principally for the emission of radiant energy. The first type may be of a complex configuration resulting from its location on the vehicle. The second class of radiators are usually of simple geometric shape or are composed of combinations of simple elements. The forms most often used in the design of radiators of the second class are described in the following paragraphs and are illustrated in Figure 1.

Rectangular Plates

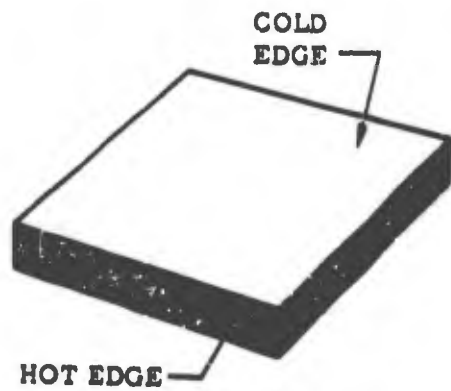
Plates of rectangular shape and uniform thickness forming part of the external surface of a vehicle may function as space radiators. When uniformly heated over one of the large surfaces, their thermal behavior is relatively simple. As space radiators or condensers, however, they will be heated along one edge and heat will be radiated from one or both surfaces. The heat flow rates in this case are much more difficult to determine, and it is this problem that will be analyzed as part of the present report.

Circular Plates

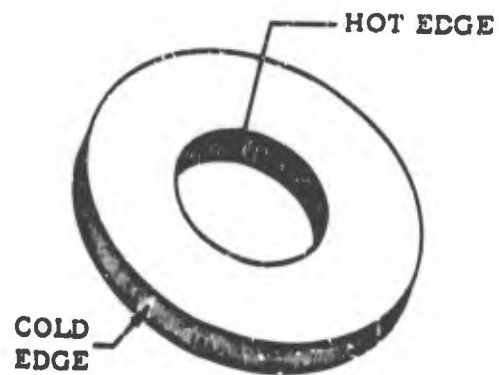
Circular plates may also act as radiators integral with the structure, receiving heat on one surface and emitting radiant energy from the other. They are also used as "fins" or extended surfaces of radiators, receiving heat along the edge of a circular hole concentric with the outer edge of the disc and radiating from one or both plane surfaces.

Trapezoidal and Triangular Fins

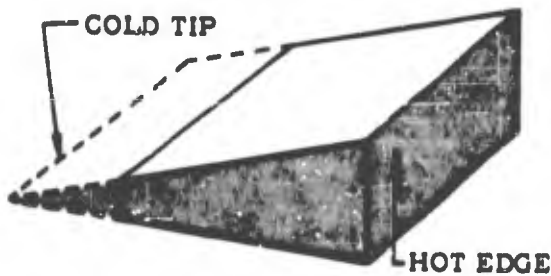
Plates of uniform thickness do not represent the most efficient radiators from a weight standpoint; fins of trapezoidal or triangular cross section have been found to be more effective. The triangular fin is a special trapezoidal fin case. Both types are analyzed here.



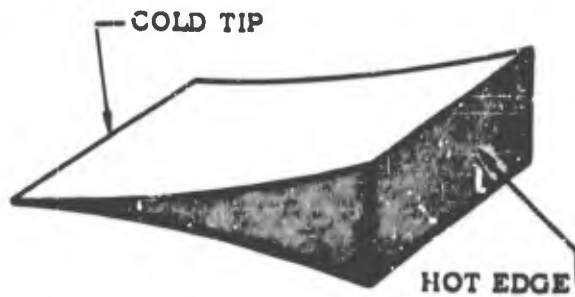
**FLAT PLATE
EXTENDED SURFACE OR FIN**



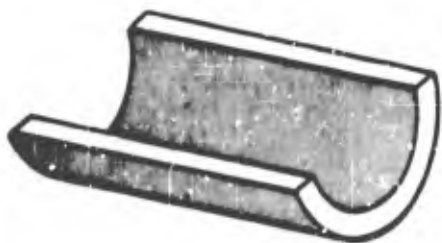
**CIRCULAR PLATE
EXTENDED SURFACE OR FIN**



**TRAPEZOIDAL &
TRIANGULAR FIN**



**CONSTANT TEMPERATURE-GRADIENT
OR "TAPERED" FIN**



SECTION OF CYLINDER



SEGMENT OF SPHERE

Figure 1. Various Radiator Elements

Constant Temperature-Gradient Fins

The fin emitting the most heat for a given weight for which data are available is one that produces a constant temperature gradient from root to tip. Such a fin has curved radiating surfaces, as shown in Figure 1, which taper to a sharp point.

Cylinders

The outer surface of a cylindrical space vehicle may be used as a space radiator. Segments of cylinders can be used as two-sided units, although the effectiveness of the concave side is reduced by elements of the surface "seeing" one another. Cylindrical ducts conveying fluids may also act as radiators. Such tubes may have extended surfaces to assist in heat dissipation.

Spheres

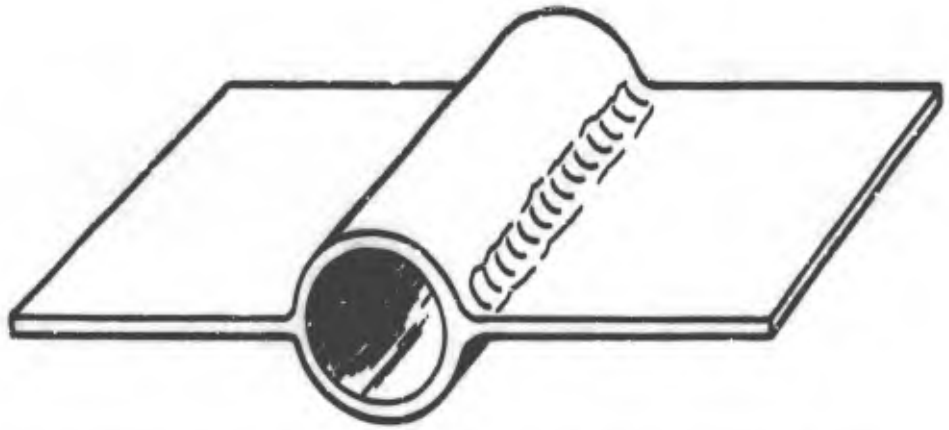
Spheres and spherical segments are similar to cylinders and cylindrical segments in that they are more often a vehicle outer surface than an independent radiator. Although the advantages to be gained in having a separate spherical radiator are nebulous, it would be possible to use radio or radar antennas, shaped as segments of spheres, for thermal radiation.

FORMATION OF RADIATORS FROM ELEMENTS

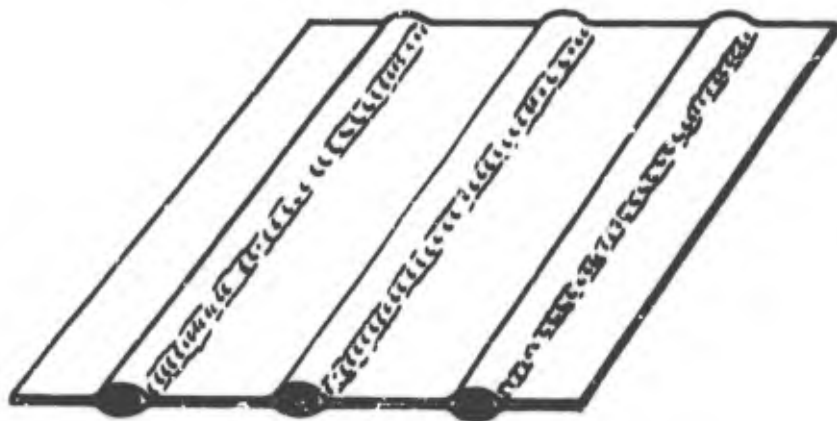
The elemental shapes described here may be combined in a number of ways to produce complete space radiators or condensers. Examples are shown in Figure 2. In Sections IV and V of this report, the thermal behavior of complete condensers and radiators is analyzed and procedures for their design are given.

RADIATION FROM ELEMENTAL FORMS

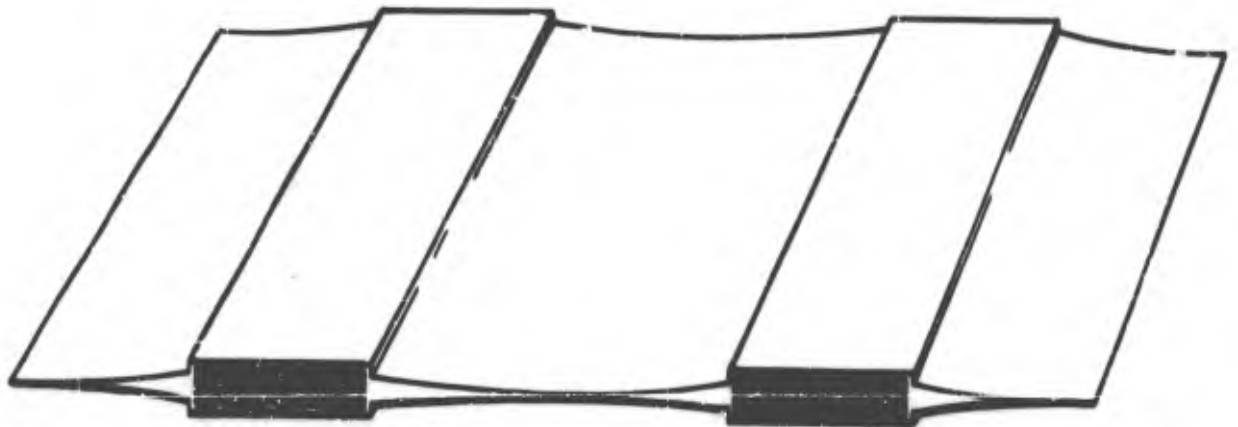
The radiation characteristics of most of the elemental forms just described are analyzed in the following subsections. Some of the material is based on previous studies conducted by S&ID and other companies. Two such early studies are documented in the Appendix of this report in the form of society papers presented by D. B. Mackay of S&ID. In some cases, the previous work has been rewritten for simplicity and clarity. Also, much new material has been added. This additional effort includes the optimization of configurations to produce an extended surface of minimum weight for the heat to be rejected.



Ⓐ CYLINDRICAL DUCT & FLAT PLATE EXTENDED SURFACES



Ⓑ SECTION OF THIN-WALLED TUBE & EXTENDED-SURFACE CONDENSER



Ⓒ SECTION OF SPACE RADIATOR OF RECTANGULAR DUCTS & CONSTANT TEMPERATURE-GRADIENT FINS

Figure 2. Formation of Radiators From Elemental Forms

RADIANT HEAT TRANSFER FROM FLAT RECTANGULAR PLATE UNIFORMLY HEATED ALONG ONE EDGE

In this analysis, relationships are determined between the dimensions, temperatures, and rate of heat dissipation for a flat plate heated at a uniform and constant temperature along one edge. Equations are developed by which the dimensions of an optimum-weight plate may be computed. The final results are presented in terms of several dimensionless numbers. For example, heat transfer is given in terms of plate effectiveness, and effectiveness, in turn, is related to plate profile number. Effectiveness and profile number are both dimensionless groups of variables and constants. Effectiveness is here defined as the ratio of the heat radiated from a plate to that radiated in free space from an identical plate having a uniform temperature equal to that at the hot edge of the first plate.

One advantage of this method of presentation is that complex systems can be analyzed for various aspects of performance, while only the profile number and environmental parameter are used throughout as the basic variables. The environmental parameter is the ratio of the heat received from the environment to that which would be radiated from the plate if it were at a uniform temperature equal to that of its hot edge. These nondimensional numbers are flexible enough to accommodate not only the constants specifically indicated in the analysis, but also such other influencing factors as plate finishes and re-radiation from a number of bodies surrounding the plate under study.

The basic assumptions made for this study include the following:

1. The temperature along the hot edge of the plate is uniform and constant.
2. The flow of heat is in straight lines from the hot to the cold edge of the plate, these lines being normal to the hot edge.
3. Heat leaves the plate by radiation from the two large surfaces only, none being radiated from the edges.
4. The emissivity ϵ of the plate surfaces and the conductivity k of the fin material are independent of variations in temperature.

5. Heat radiates from the surfaces in accordance with the Stefan-Boltzmann law.
6. The total operation is in a steady-state condition.

This analysis is based, in part, upon a report by D. B. Mackay and E. L. Leventhal (Reference 2) of S&ID. New material on the determination of the configuration of plates of optimum weight is also presented.

NOMENCLATURE

- A_p Plate area, $(L_w)(L_h)$, sq ft
- C_1 Radiation constant, $\sigma (\epsilon_a + \epsilon_b)$, Btu/(sq ft) (hr) $(^\circ R)^4$
- C_2 Radiation constant, heat received from environment by unit of fin area, Btu/(sq ft) (hr)
- C_3 Aggregate of thermal and dimensional constants, nondimensional
- F_a Radiation form factor for plate side facing sun, nondimensional
- F_b Radiation form factor for plate side away from sun, nondimensional
- k Thermal conductivity of plate material, Btu/(hr) (ft) $(^\circ R)$
- L Distance from hot edge to a point on plate (variable), ft
- L_h Total plate length, ft
- L_w Width of plate normal to heat flow, ft
- q Heat transfer, Btu/hr
- q_f Net heat radiated from plate, Btu/hr
- q_g External heat into plate, Btu/hr
- q_h Heat transferred by conduction into plate through hot edge, equal to net heat lost by radiation, Btu/hr
- q_i Internal heat transferred across any section of plate, Btu/hr

q_f	Heat lost from plate by radiation, Btu/hr
q_u	Heat transferred from plate in space as if temperature is uniform and equal to root temperature, Btu/hr
S_c	Solar constant, Btu/(hr) (sq ft)
T	Temperature of point on plate (variable), °R
T_c	Temperature of cold end of plate (tip), °R
T_h	Temperature of hot end of plate (root), °R
T_m	Surface temperature of environment, °R
W_f	Extended-surface weight, lb
a_a	Absorptivity of plate surface facing sun, nondimensional
a_b	Absorptivity of plate surface away from sun, nondimensional
δ	Plate thickness, ft
ϵ	Surface emissivity of plate, nondimensional
ϵ_a	Emissivity of plate surface facing sun, nondimensional
ϵ_b	Emissivity of plate surface away from sun, nondimensional
ζ_p	Profile number, nondimensional
θ_m	Angle between sun's rays and a normal to environment surface, deg
θ_p	Angle between sun's rays and a normal to plate surface, deg
ρ	Density of plate material, lb/cu ft
ρ_m	Reflectivity of environmental surface, nondimensional

σ Stefan-Boltzmann radiation constant, 0.1713×10^{-8} Btu/(sq ft)
(hr) (°R)⁴

Ω Plate effectiveness, nondimensional

MATHEMATICAL ANALYSIS

The general case of the problem explored here is illustrated by Figure 3. Heat is transferred into the plate along one edge from some source, such as a condenser tube, at a uniform and constant temperature; the other three edges of the plate are assumed to be thermally insulated. Although this assumption is seldom completely valid, the amount of energy radiated from these edge surfaces is usually small enough to be neglected. Heat entering the plate, from radiant solar and environmental sources only, is given by:

$$q_g = S_c A_p a_a \cos \theta_p + S_c A_p F_a a_m \rho_m \cos \theta_m + S_c A_p F_b a_b \rho_m \cos \theta_m + A_p \epsilon_a \sigma F_a T_m^4 + A_p \epsilon_b \sigma F_b T_m^4 \quad (1)$$

Environmental sources of radiation include the earth and other planets. The heat loss from the plate is:

$$q_f = A_p \epsilon_a \sigma T^4 + A_p \epsilon_b \sigma T^4 \quad (2)$$

The difference between the heat radiated out q_f and that received by radiation q_g is the net heat transferred by radiation q , where

$$q = q_f - q_g$$

or

$$q = A_p \epsilon_a \sigma T^4 + A_p \epsilon_b \sigma T^4 - S_c A_p a_a \cos \theta_p - A_p F_a a_a \rho_m S_c \cos \theta_m - A_p F_b a_b \rho_m S_c \cos \theta_m - A_p F_a \epsilon_a \sigma T_m^4 - A_p F_b \epsilon_b \sigma T_m^4 \quad (3)$$

Letting

$$C_1 = \sigma (\epsilon_a + \epsilon_b) \quad (4)$$

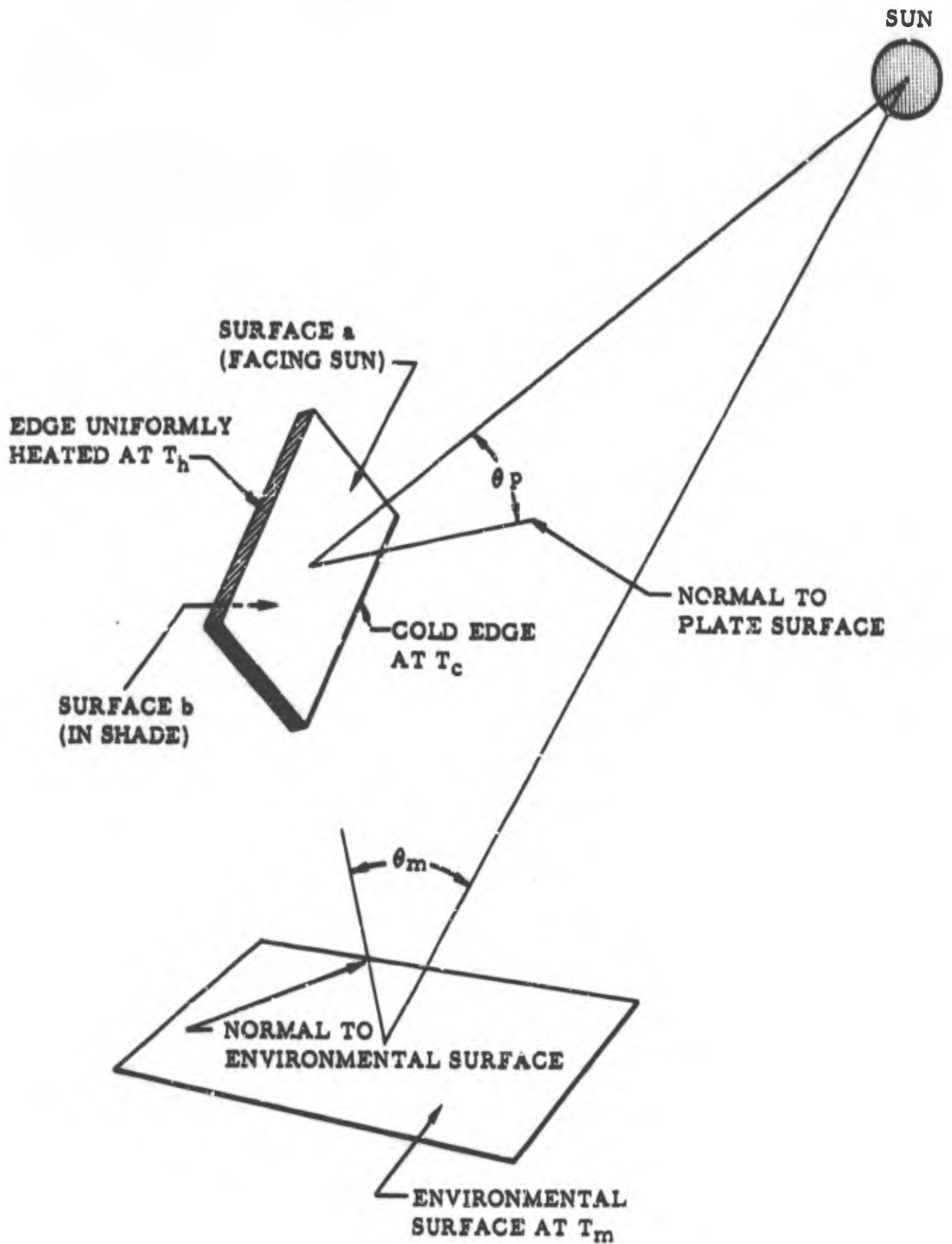


Figure 3. Environment for Flat Plate Analysis

and

$$C_2 = S_c \left(a_a \cos \theta_p + F_a a_a \rho_m \cos \theta_m + F_b a_b \rho_m \cos \theta_m \right) + T_m^4 \sigma (F_a \epsilon_a + F_b \epsilon_b) \quad (5)$$

Equation 3 then becomes

$$q = (C_1 T^4 - C_2) A_p \quad (6)$$

Equation 6 may be considered as a general equation for cases either more or less complicated than that of Figure 3. In all cases, the C_1 group includes the terms multiplied by T^4 and the C_2 group includes all other terms. The differential equation for the heat radiated from a section of the plate is

$$dq = (C_1 T^4 - C_2) L_w dL \quad (7)$$

where L parallels the direction of heat flow through the plate and L_w is normal to it (Figure 4).

The heat transfer by conduction through a section of the plate, at a distance L from the cold end, is expressed as

$$q_1 = -k \delta L_w \frac{dT}{dL} \quad (8)$$

This must be equal to the net heat q radiated from the plate. In any element of the plate, the net heat radiation from the element, dq , is equal to the difference in heat conducted into the element along its hotter edge and that conducted out along the opposite edge, dq_1 . That is

$$dq = dq_1 = -k \delta L_w \frac{d^2 T}{dL^2} dL \quad (9)$$

After equating Equations 7 and 9, integrating in two steps, and determining the value of the constant of integration by the substitution of boundary conditions,

$$\frac{dT}{dL} = - \sqrt{\frac{2C_1 T_c^5}{5k\delta}} \sqrt{\frac{T}{T_c} - 1} \sqrt{\left(\frac{T}{T_c}\right)^4 + \left(\frac{T}{T_c}\right)^3 + \left(\frac{T}{T_c}\right)^2 + \left(\frac{T}{T_c}\right) + 1} - \frac{5C_2}{C_1 T_c^4} \quad (10)$$

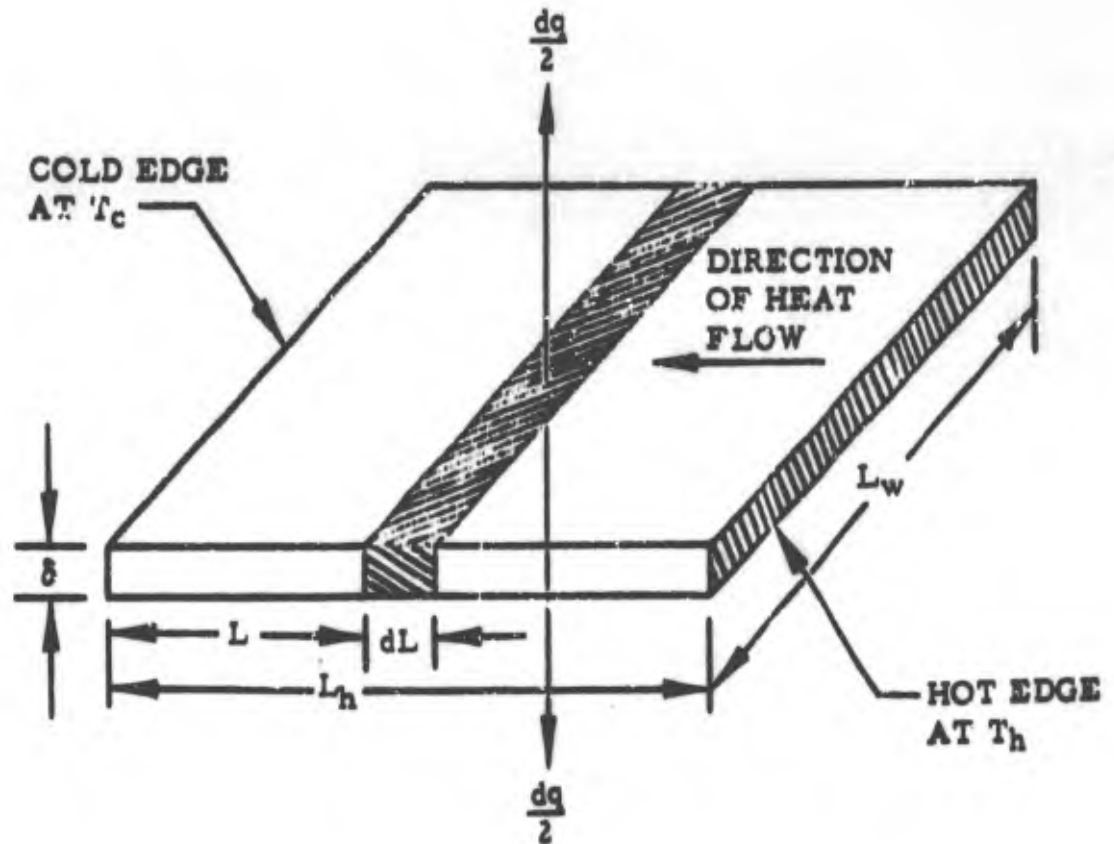


Figure 4. Dimensional Relationships of Flat Plate Heated Uniformly Along One Edge

Equation 10 is difficult to integrate. Graphical solutions (Reference 2) and digital computers (References 3 and 4) have been used for this purpose.

To present the results in a form more useful for radiator design, the rate of heat transfer was converted to plate effectiveness. This term can be defined by first considering the amount of heat that would be transferred if it were to have a uniform temperature equal to the plate hot edge temperature throughout the plate, with no radiant heat being received from any source. This would be

$$q_u = L_h L_w C_1 T_h^4 \quad (11)$$

Plate effectiveness is the ratio of the net heat radiated q_f to this amount of heat q_u , or

$$\Omega = \frac{q_f}{L_h L_w C_1 T_h^4} \quad (12)$$

and

$$q_f = L_h L_w C_1 T_h^4 \Omega \quad (13)$$

The results compiled from the data of References 2 through 4 are shown in rectangular coordinates in Figure 5 and in logarithmic coordinates in Figure 6.

OPTIMUM-WEIGHT DESIGN

In both Figures 5 and 6, a line indicates the optimum-weight configuration (theoretical profile). The determination of this line and its significance is shown in the following analysis.

The weight of a flat plate extended surface is

$$W_f = L_w L_h \delta \rho \quad (14)$$

The abscissas of Figures 5 and 6 are aggregates of dimensional and thermal constants which produce a dimensionless quantity called the profile number ζ_p , where

$$\zeta_p = \frac{C_1 T_h^3 L_h^2}{k \delta} \quad (15)$$

Equating equations 14 and 15 to eliminate δ ,

$$\zeta_p = \frac{C_1 T_h^3 L_h^3 L_w \rho}{k W_f} \quad (16)$$

Solving for L_h ,

$$L_h = \left(\frac{k W_f \zeta_p}{C_1 T_h^3 L_w \rho} \right)^{1/3} \quad (17)$$

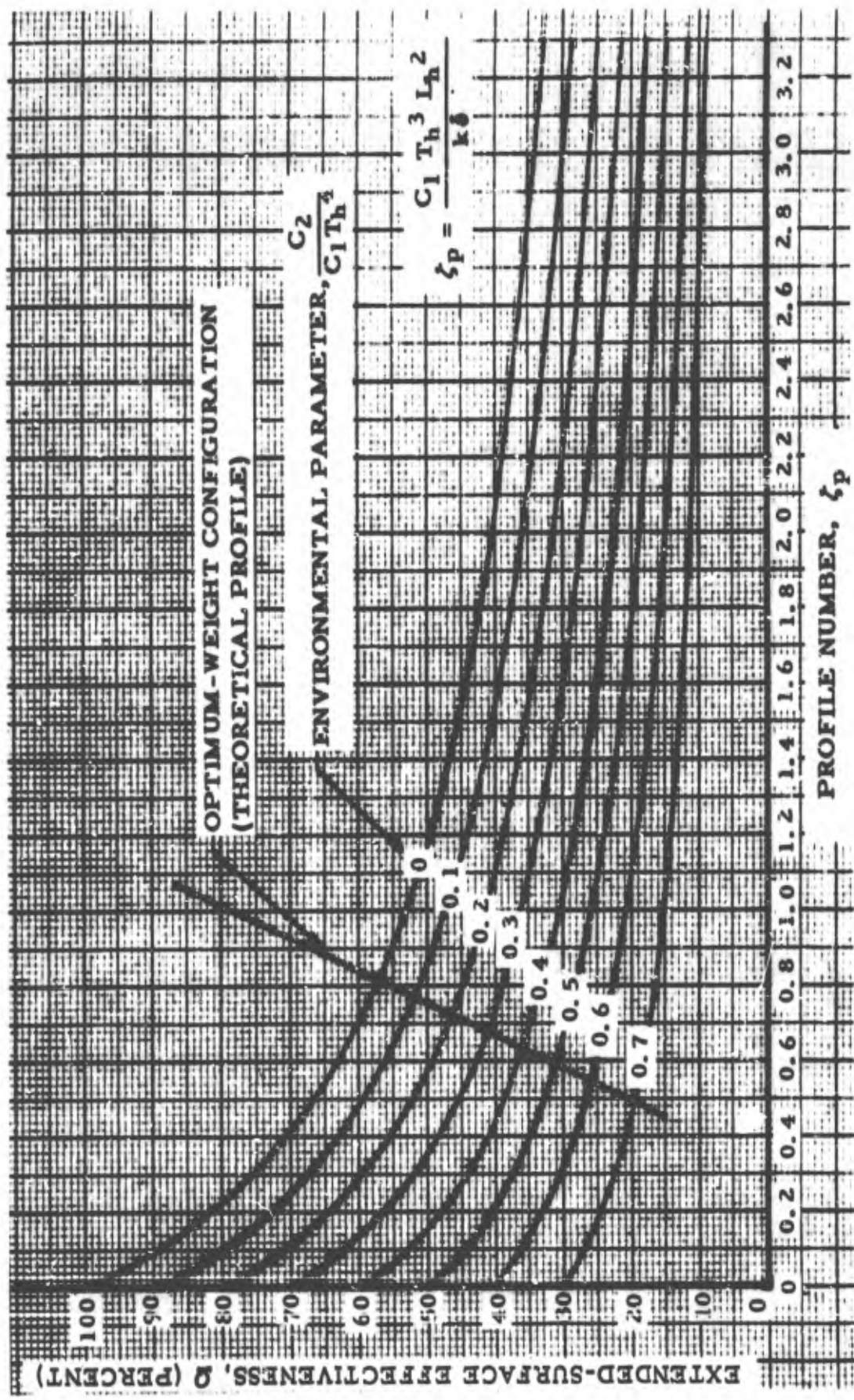


Figure 5. Relationship of Plate Effectiveness to Profile Number of Flat Plate (Rectangular Coordinates)

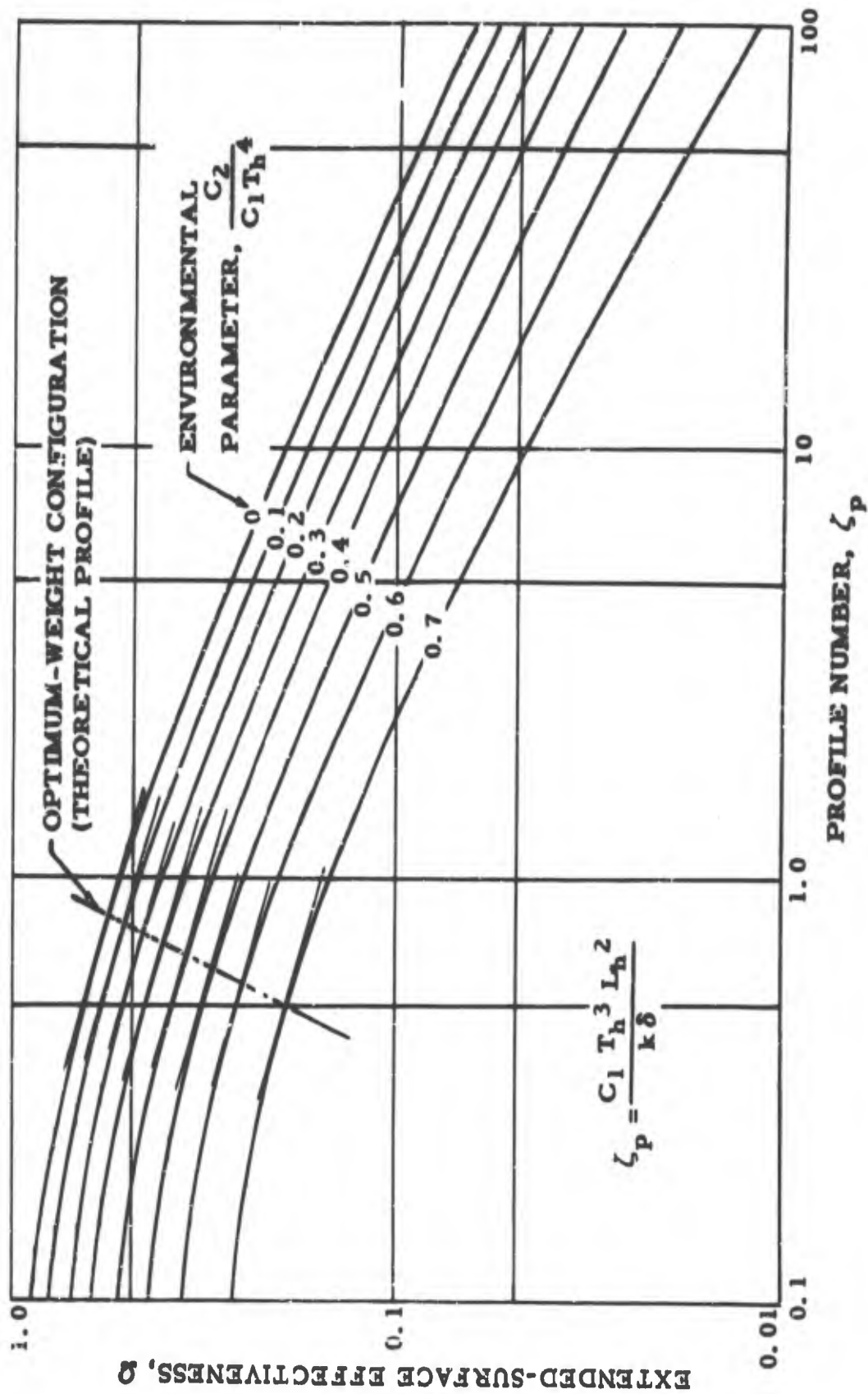


Figure 6. Relationship of Plate Effectiveness to Profile Number of Flat Plate (Logarithmic Coordinates)

Substituting Equation 17 into Equation 13,

$$q_f = \Omega L_w C_1 T_h^4 \left(\frac{k W_f \zeta_p}{C_1 T_h^3 L_w \rho} \right)^{1/3} \quad (18)$$

Solving for W_f ,

$$W_f = \left(\frac{q_f^3 \rho}{k C_1^2 T_h^9 L_w^2} \right) \left(\frac{1}{\Omega^3 \zeta_p} \right) \quad (19)$$

Ordinary methods of calculus can now be used to determine the relationship between these terms which will produce the plate of lowest weight for the dissipation of a fixed heat rate. If the length L_w is fixed or unity, then all terms within the first bracketed group will be constants, or

$$W_f = \frac{C_3}{\Omega^3 \zeta_p} \quad (20)$$

Differentiating Equation 20 with respect to ζ_p ,

$$\frac{dW_f}{d\zeta_p} = - \frac{C_3}{\Omega^6 \zeta_p^2} \left(3\Omega^2 \zeta_p \frac{d\Omega}{d\zeta_p} + \Omega^3 \right) \quad (21)$$

Equating the differentiated equation to zero and rearranging,

$$\frac{\frac{d\Omega}{\Omega}}{\frac{d\zeta_p}{\zeta_p}} = - \frac{1}{3}$$

or

$$\frac{d(\log \Omega)}{d(\log \zeta_p)} = - \frac{1}{3} \quad (22)$$

The optimum-weight configuration for each environmental parameter is then located at the point at which each curve of Figure 6 has a slope of $-1/3$. The loci of these points are indicated in Figures 5 and 6 as the optimum-weight configuration (theoretical profile) line.

Very often, the optimum-weight configuration prescribes a fin so thin that it would be impossible to manufacture. In other cases, the radiator surface area becomes too large for satisfactory usage. In either event, a heavier but more compact design should be used. For these reasons, the minimum-weight profile is designated as the theoretical profile to emphasize that it may not be the "optimum" configuration when requirements other than weight are considered. However, the theoretical profile is the best known starting point for selection of the final configuration.

DESIGN PROCEDURES

The principal worth of the relationships shown in Figures 5 and 6 is that they aid in the rapid and adequate evaluation of a flat extended surface. The key to this is the profile number. If the configuration and thermal characteristics are known, the profile number can be evaluated. For a wide variety of problems, however, the route followed is to determine a profile number from which the dimensions are established. In either event, the profile number is the important criterion.

Where the plate size and shape are known, the normal procedure would be as follows:

1. Evaluate the profile number ζ_p (Equation 15).
2. Evaluate the environmental parameter $C_2/C_1 T_h^4$.
3. Obtain surface effectiveness Ω from Figures 5 or 6 using the profile number and environmental parameter.
4. Compute the heat transfer (Equation 13).

Where the required heat transfer per unit of length L_w is known, a different procedure is followed:

1. Evaluate the environmental parameter $C_2/C_1 T_h^4$.
2. Select the appropriate values of effectiveness and profile number from Figure 5 or 6. If minimum weight is desired, effectiveness and profile number are obtained by the point of intersection of the theoretical profile line with that of the environmental parameter. If higher or lower values of effectiveness are desired, another position on the environmental line is selected.
3. Compute plate length L_h (Equation 13).

4. Compute plate thickness δ using the computed plate length (Equation 15).

Step 2 of this procedure demonstrates another valuable feature of the curves of Figures 5 and 6 — the direct identification of the optimum-weight configuration. In space vehicle design, weight saving is usually of paramount importance. The ability to find, in uncomplicated fashion, the dimensions of the plate having the least weight for a given amount of heat radiation, is a very desirable characteristic of these graphs.

For both procedures given, the assumption was made that the environmental parameter can be evaluated. Reference to Equation 5, however, indicates that to do so requires knowledge of the form factors F^a and F_b , both of which depend upon the size and shape of the plate finally selected. The required procedure must then include assuming the values of these factors, in order to start through the steps, and checking the final results against the assumptions. A series of trials may therefore be required before arrival at a final solution.

RADIANT HEAT TRANSFER FROM FLAT CIRCULAR PLATE UNIFORMLY HEATED ALONG INNER CIRCUMFERENCE

The problem of steady-state radiation from an annular fin is analyzed here. The relationship of fin effectiveness Ω to fin profile number ζ_p is established for a range of ratios of radii ϕ_r . All these three factors are dimensionless numbers.

The first discussion is a mathematical analysis abstracted from a paper by R. L. Chambers and E. O. Somers (Reference 5). In the second discussion, configurations having the least weight for the heat radiated are determined. This analysis is more complex than that for rectangular flat plates because of the presence of an added variable, the radii ratio ϕ_r . The procedures given were developed by D. B. Mackay of S&ID.

NOMENCLATURE

- C_1 Radiation constant, $\sigma(\epsilon_a + \epsilon_b)$, where ϵ_b generally equals zero, Btu/(hr)(sq ft)(°R)⁴
- K Aggregate of constants, nondimensional
- k Thermal conductivity of plate material, Btu/(hr)(ft)(°R)
- m Total number of concentric elements that subdivide the plate, nondimensional
- n Integer, nondimensional
- q_f Rate of heat radiation from plate, Btu/hr
- q_u Rate of heat radiation from plate in free space as if temperature is uniform throughout plate, Btu/hr
- r Distance of any point from plate center, ft
- r_i Inside radius of plate, ft
- r_o Outside radius of plate, ft

T	Temperature of point on plate, °R
T_h	Temperature of point on inner circumference, °R
T_n	Temperature of any concentric element, °R
T_{nm}	Temperature of outer concentric element, °R
Z_h	Ratio of temperatures, T/T_h , nondimensional
Z_n	Ratio of temperatures, T_n/T_h , nondimensional
Z_{nm}	Ratio of temperatures, T_{nm}/T_h , nondimensional
W_{cp}	Weight of circular plate, lb
Δr	Width of concentric element of plate, ft
δ	Plate thickness, ft
ϵ_a	Emissivity of exposed surface, nondimensional
ϵ_b	Emissivity of other surface, nondimensional
ζ_p	Plate profile number, nondimensional
π	Circumference-to-diameter ratio of circle, nondimensional
ρ	Density of plate material, lb/cu ft
σ	Stefan-Boltzmann constant, 0.1713×10^{-8} Btu/(hr)(sq ft)(°R) ⁴
ϕ	Ratio of radii, $(r - r_i)/(r_o - r_i)$, nondimensional
ϕ_n	Ratio of radii, $n\Delta r/(r_o - r_i)$, nondimensional
ϕ_r	Ratio of radii, r_o/r_i , nondimensional
ϕ_Δ	Ratio of radii, $r_i/\Delta r$, nondimensional
Ω	Fin effectiveness, nondimensional

MATHEMATICAL ANALYSIS

The configuration of a circular fin which conforms to this analysis is shown in Figure 7. Heat from some source is conducted through the peg to the circular plate fin. Here the heat is transferred to the inner circumference, and then conducted throughout the plate and radiated into space. For the case illustrated, insulation confines the radiating area to one flat surface of the circular plate and, in effect, dictates zero emissivity of the insulated surface. Any radiation from the exposed end of the peg does not influence the thermal behavior of the circular plate. Figure 8 is a schematic drawing of the plate.

The assumptions for this analysis are essentially the same as those made for the flat plate of rectangular section. The important difference is that the only environmental situation considered is the one in which heat radiates to a space having absolute zero temperature. Further work is required to extend the analysis to other values of the environmental parameter.

The physical laws of heat transfer and the assumptions were combined to produce a second-order nonlinear differential equation describing the heat flow within the fin, as well as two boundary conditions. The differential equation is

$$\frac{d^2 Z_h}{d\phi^2} + \frac{1}{\phi + \frac{1}{\phi_r - 1}} \left(\frac{dZ_h}{d\phi} \right) - \zeta_p Z_h^4 = 0 \quad (23)$$

where

$$\zeta_p = \frac{C_1 T_h^3 (r_o - r_i)^2}{k \delta}$$

The boundary conditions are

$$r = r_i, \phi = 0, Z_h = 1 \quad \text{Inner circumference}$$

$$r = r_o, \phi = 1, \frac{dZ_h}{d\phi} = 0 \quad \text{Outer circumference}$$

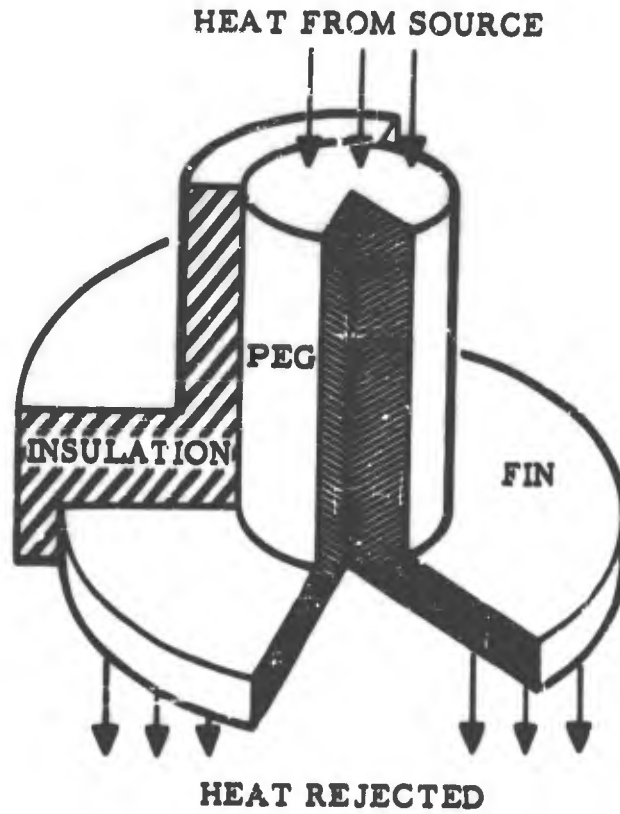


Figure 7. Configuration of Circular Plate Fin Acting as Space Radiator

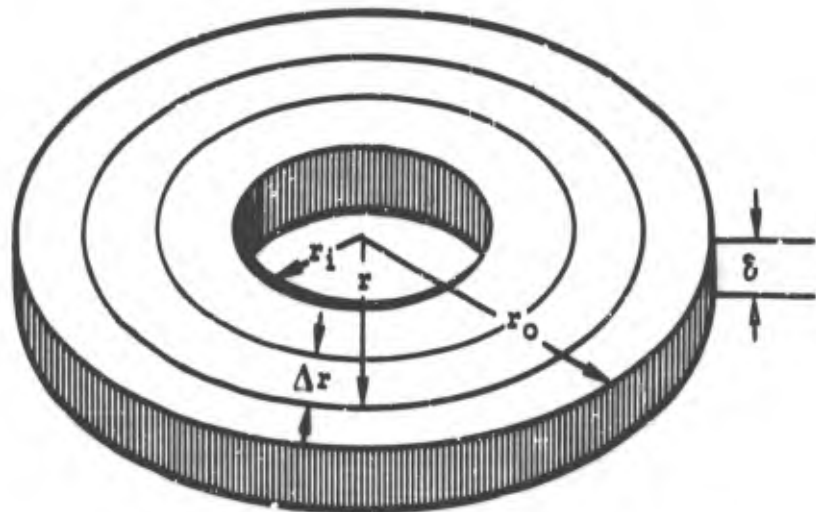


Figure 8. Dimensional Relationships of Circular Plate Heated Uniformly Along Inner Circumference

The solution of Equation 23 was computed numerically for various assumed values of the ratio of radii ϕ_r and profile number ζ_p . The adiabatic boundary condition at $\phi = 1.0$ was checked on an IBM 704 digital computer as zero to within five significant figures. The relationship of Z_h to ϕ is found from the solution of Equation 23.

Several methods of integration may be applied to determine the fin effectiveness. One method was derived by breaking the fin into a series of concentric annuli of radial width Δr , and specifying a fin temperature ratio Z_n at $\phi_n = n \Delta r / (r - r_i)$. By definition, fin effectiveness is

$$\Omega = \frac{q_f}{q_u} \quad (24)$$

where the rate of heat radiation from a fin having the uniform hot end temperature T_h is

$$q_u = C_1 T_h^4 \pi (r_o^2 - r_i^2) \quad (25)$$

The heat flow rate is approximated by

$$q_f = C_1 T_h^4 \Delta r^2 \pi \left\{ \left(\phi_\Delta + \frac{1}{4} \right) + \left(\phi_r \phi_\Delta - \frac{1}{4} \right) Z_{nm}^4 + 2 \sum_{n=1}^{m-1} (n + \phi_\Delta) Z_n^4 \right\} \quad (26)$$

Combining Equations 25 and 26 and reducing the quotient,

$$\Omega = \frac{\left(\phi_\Delta + \frac{1}{4} \right) + \left(\phi_r \phi_\Delta - \frac{1}{4} \right) Z_{nm}^4 + 2 \sum_{n=1}^{m-1} (n + \phi_\Delta) Z_n^4}{\phi_\Delta^2 (\phi_r^2 - 1)} \quad (27)$$

By selecting a sufficiently large number of elements, the approximation of Equation 27 can be made an equality. The effectiveness would then be a function only of the ratio of radii ϕ_r and profile number ζ_p , since Z_h is also a function of ϕ_r and ζ_p .

In Figure 9, effectiveness is plotted against profile number for a range of values of the ratio of radii. Therefore, if the geometry of the fin and the characteristics of its material are known, the effectiveness may be determined from these curves. The quantity of heat radiated from the fin can then be calculated using Equations 24 and 25. The determination and significance of the theoretical profile will be discussed later.

Because of recoding complexities in the IBM program, the work presented in Reference 5 did not consider the case of a straight fin ($\phi_r = 1.000$). However, when values were computed for $\phi_r = 1.001$ and 1.1, the difference in fin effectiveness was found to be negligible. It is therefore reasonable to consider that a straight fin may be approximated by $\phi_r = 1.001$.

OPTIMUM-WEIGHT DESIGN

A relationship exists between the "length" ($r_o - r_i$) of a circular plate and plate thickness δ which will produce a minimum-weight plate for radiating a given quantity of heat. Conversely, if the weight of the plate is specified, then a relationship of dimensions can be found which will radiate a maximum amount of heat. It is assumed in the present analysis that the weight is fixed and that the object is to find the thickness and radii of the extended surface which will enable the greatest quantity of heat to be radiated.

The weight of a circular plate is given by

$$W_{cp} = \rho \delta \pi (r_o^2 - r_i^2) \quad (28)$$

or

$$\delta = \frac{W_{cp}}{\rho \pi (r_o^2 - r_i^2)} = \frac{W_{cp}}{\rho \pi r_i^2 (\phi_r^2 - 1)} \quad (29)$$

The profile number is

$$\zeta_p = \frac{C_1 T_h^3 r_i^2}{k \delta} (\phi_r - 1)^2 \quad (30)$$

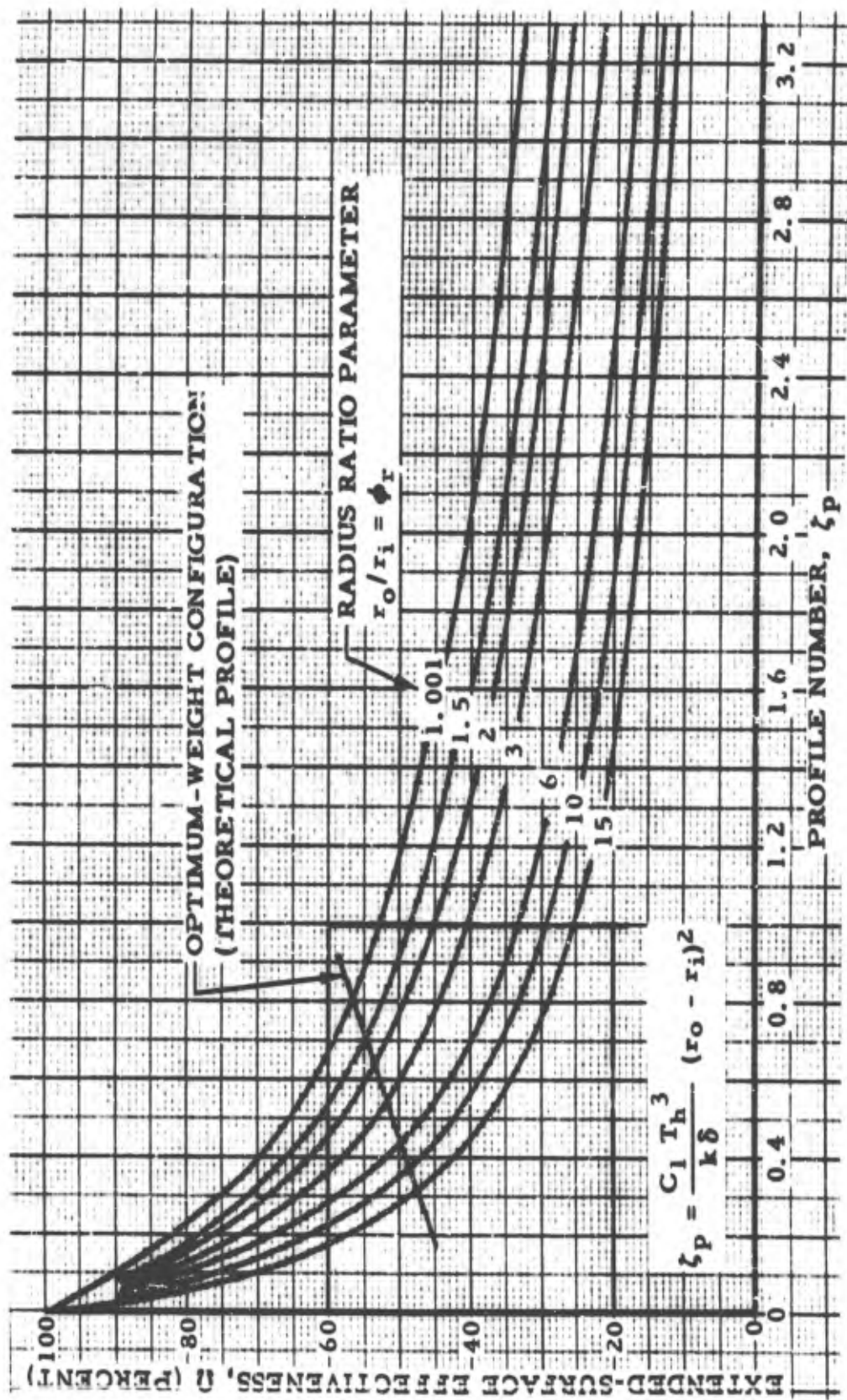


Figure 9. Relationship of Plate Effectiveness to Profile Number of Circular Plate

Substituting Equation 29 into Equation 30.

$$\zeta_p = \frac{C_1 T_h^3 r_i^4 \rho \pi}{k W_{cp}} (\phi_r - 1)^2 (\phi_r^2 - 1) \quad (31)$$

The inner radius r_i is ordinarily fixed by other considerations so that all terms of the first group in Equation 31 are constant. That is,

$$\frac{C_1 T_h^3 r_i^4 \rho \pi}{k W_{cp}} = K \quad (32)$$

where K is a constant. Equation 31 then becomes

$$\zeta_p = K (\phi_r^2 - 1)(\phi_r - 1)^2 \quad (33)$$

Figure 10 is similar to Figure 9 except that curves for only two radii ratios, ϕ_{r1} and ϕ_{r2} , are shown. After selecting any point such as point 1, the value of K can be determined by Equation 33. A second point, having the same value of K but with a radius ratio ϕ_{r2} instead of ϕ_{r1} , is designated as point 2. The profile number of point 2 can be determined by rearranging Equation 33 so that

$$K = \frac{\zeta_p}{(\phi_r^2 - 1)(\phi_r - 1)^2}$$

Since

$$K_1 = K_2$$

then

$$\frac{\zeta_{p1}}{(\phi_{r1}^2 - 1)(\phi_{r1} - 1)^2} = \frac{\zeta_{p2}}{(\phi_{r2}^2 - 1)(\phi_{r2} - 1)^2}$$

or

$$\zeta_{p2} = \zeta_{p1} \frac{(\phi_{r2}^2 - 1)(\phi_{r2} - 1)^2}{(\phi_{r1}^2 - 1)(\phi_{r1} - 1)^2} \quad (34)$$

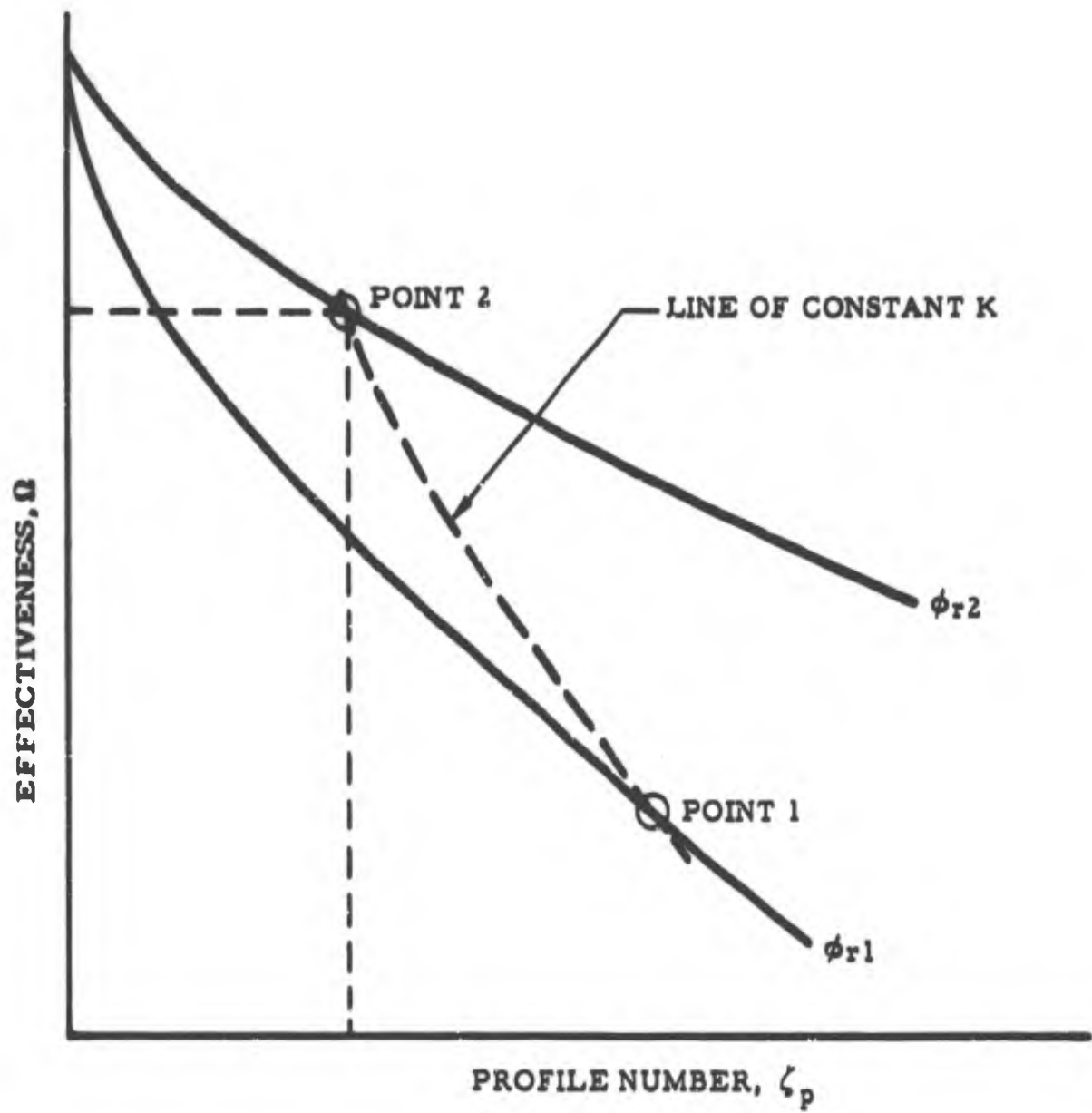


Figure 10. Construction of Line of Constant K

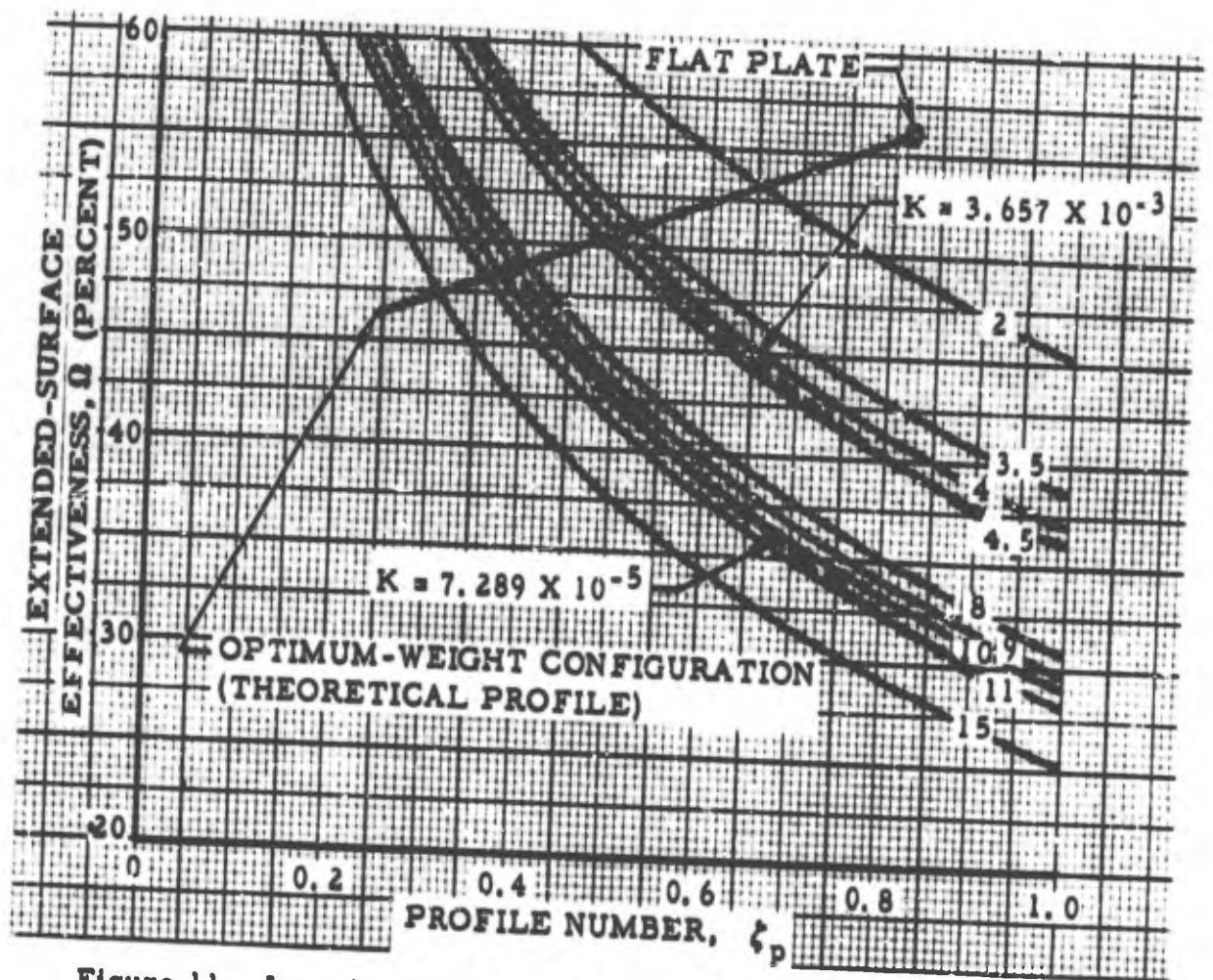


Figure 11. Location of Line of Optimum-Weight Configuration on Plate Effectiveness Versus Profile Number

All quantities of Equation 34 are known except ζ_p , which can now be determined. By choosing successive values of ϕ_r , the loci of the line of constant K can be drawn, as shown in Figure 11.

By combining Equations 24 and 25, the rate of heat radiation is found to be

$$q_f = C_1 T_h^4 \pi r_1^2 (\phi_r^2 - 1) \Omega \quad (35)$$

Since C_1 , T_h , π , and r_1 are all fixed quantities, the heat rate will be maximum when the product $(\phi_r^2 - 1) \Omega$ is maximum. Values of this product are plotted in Figure 12 against profile number for each of the two values of K . The maximum points of these curves establish the values of profile number for which heat transfer is a maximum. In Figure 11, the profile numbers at which these maxima occur are plotted as circles on the lines of constant K . These points locate the values at which the maxima occur. They also mark two points on the line of the optimum-weight configuration. A third point is found on this line by plotting the profile number of the optimum

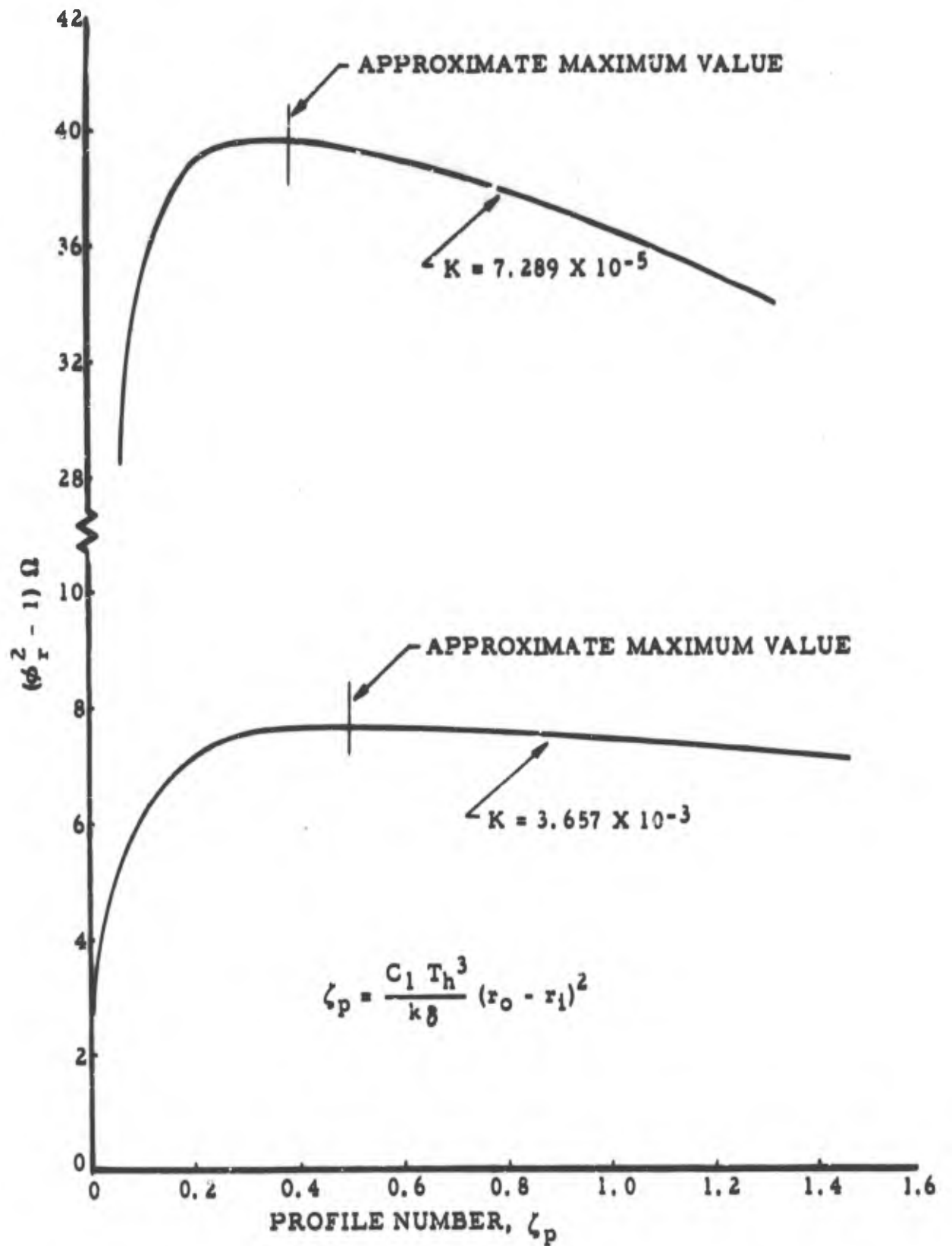


Figure 12. Location of Profile Numbers of Maximum Heat Transfer Rate for Circular Plates

weight flat plate at its corresponding value of effectiveness. The line of the optimum configuration was then transferred to Figure 9. From this line, the combination of radii and thickness that produces the maximum heat radiation for a given weight can be determined.

It should be noted that the curves of Figure 12 are relatively flat in the region of their maximum value. This indicates that the profile number is not critical in this region. Changes in the value of profile number by ± 0.2 from the peak value will reduce the rate of heat transfer by only approximately 2 percent.

Figure 9 can be used by the designer in much the same way as Figure 5 would be used in designing flat plate radiating surfaces. If the dimensions of the circular plate are known, the effectiveness can be read from Figure 9 and the heat that can be radiated calculated. Conversely, with the heat to be dissipated known, a ratio of radii can be selected, the profile number and related effectiveness read from the chart, and the dimensions of the plate calculated. The chosen coordinates are usually in the neighborhood of the line of optimum-weight configuration, but need not be if some requirement prevents this. However, it must be pointed out that Figure 9 is limited to the environmental parameter of free space only and that other similar families of curves are necessary to design for other conditions.

RADIANT HEAT TRANSFER FROM CONSTANT TEMPERATURE-GRADIENT FIN

The term "fin" has been applied to extended surfaces used to dissipate heat by radiation or convection or by a combination of these. This analysis places some restrictions upon this general concept - namely, that no convection exists, and that the temperature of the root of the fin is constant and remains uniform along the entire width of the fin. Another special characteristic of the fin considered here is the linear temperature gradient from the base to the tip of the fin. Attaining this relationship requires a fin that is thickest at its base and tapers to the tip so as to form convex surfaces of the sides. This configuration is shown in Figure 13.

In later analyses, "triangular" and "trapezoidal" fins are considered. The triangular fin differs from the constant temperature-gradient fin in that its surfaces are flat planes; the trapezoidal fin has the profile of a truncated triangle. Constant temperature-gradient fins are of interest because they have a more effective distribution of material and enable more heat to be dissipated per unit of weight.

The thermal analysis has been made for combinations of three variables: (1) the fin root thickness, (2) the fin length from root to tip, and (3) the ratio of the absolute temperatures at the hot (root) and cold (tip) ends

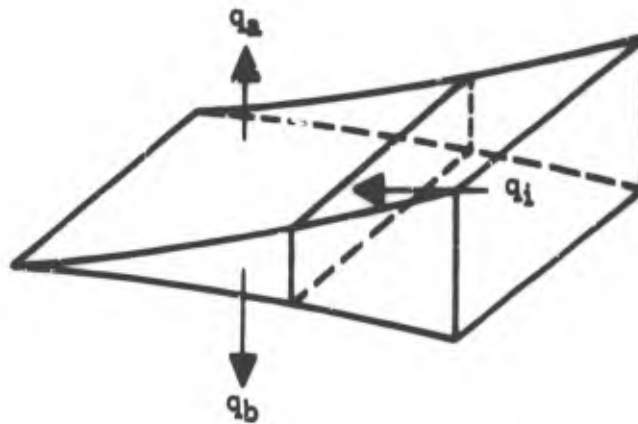


Figure 13. Configuration of Constant Temperature-Gradient Fin

of the fin. The third factor, temperature ratio, in most cases enters equations as complex functions which have been grouped together. Because the evaluation of these equations by hand is very tedious, numerical values have been determined by digital computer for a range of temperature ratios and curves relating the variables have been plotted. Most fin design problems of heat transfer, weight, and contour can be solved by the use of these graphs. The optimum-weight configurations have also been determined and are shown on the appropriate graphs.

The mathematical analysis given here was abstracted from the work of D. B. Mackay listed as Reference 6. (Reference 6 is reproduced in the Appendix of this report.) The discussion on weight optimization was prepared subsequent to Reference 6 and, for this reason, is in greater detail than is the thermal analysis.

NOMENCLATURE

- C_1 Radiation constant, $\sigma(\epsilon_a + \epsilon_b)$, Btu/(sq ft)(hr)(°R)⁴
- C_2 Radiation constant, heat received from environment by unit of fin area, Btu/sq ft
- k Thermal conductivity of fin material, Btu/(hr)(ft)(°R)
- L Fin length measured from tip to root (variable), ft
- L_h Total fin length, ft
- L_w Width of fin normal to heat flow, ft
- q Heat radiated by both sides of fin from tip to section considered, Btu/hr
- q_a Heat radiated by one side of fin from tip to section considered, Btu/hr
- q_b Heat radiated by opposite side of fin from tip to section considered, Btu/hr
- q_f Heat radiated by both sides of entire fin, Btu/hr
- q_i Internal heat transferred past section of fin, Btu/hr
- q_u Heat radiated from fin in free space if as temperature is uniform and equal to root temperature, Btu/hr
- T Temperature of point on fin (variable), °R

T_c	Temperature of cold end of fin (tip), °R
T_h	Temperature of hot end of fin (root), °R
W_s	Weight of fin section, lb
W_f	Total weight of fin, lb
Z	Ratio of temperatures, T_h/T_c , nondimensional
β	Exponent, nondimensional
δ	Fin thickness at any point (variable), ft
δ_h	Fin thickness at hot end (root), ft
ϵ_a	Emissivity of one surface of fin, nondimensional
ϵ_b	Emissivity of opposite surface of fin, nondimensional
ζ_h	Fin heat transfer number, nondimensional
ζ_p	Fin profile number, nondimensional
ζ_r	Fin ratio number, nondimensional
ζ_w	Fin weight number, nondimensional
ζ_d	Fin differential ratio number, nondimensional
ρ	Density of fin material, lb/cu ft
σ	Stefan-Boltzmann constant, 0.1713×10^{-8} Btu/(sq ft)(hr)(°F) ⁴
ϕ_1	Relationship of temperature ratio and environmental parameter, nondimensional
ϕ_2	Second relationship of temperature ratio and environmental parameter, nondimensional
Ω	Fin effectiveness, nondimensional

MATHEMATICAL ANALYSIS

Dimensional and Temperature Relationships

The amount of heat passing a section of a fin that is normal to the direction of heat flow will be, from Figure 13,

$$q_i = -k\delta L_w \frac{dT}{dL} \quad (36)$$

With the physical properties of the fin material known, the heat flow rate may be determined if the temperature gradient dT/dL can be evaluated. One objective of this analysis is to determine the fin profile which will produce the temperature gradient which radiates the most heat per unit weight.

It is demonstrated in References 7 and 8 that, in a gaseous medium with convection, the maximum heat dissipation per unit weight occurs when the temperature gradient is linear along the length L of the fin. For radiation without convection, however, some investigators feel that a modification of this assumption is necessary. From the several temperature gradients proposed, the one most often used is that presented in References 9 and 10. This gradient is mathematically expressed as

$$T = T_h \left(\frac{L}{L_h} \right)^\beta \quad (37)$$

For a minimum fin profile area, and consequently least weight, it has been stated that $\beta = 0.5$.

This gradient, although commonly accepted, appears to have a number of deficiencies. Equation 37 indicates that fin temperature decreases as the tip of the fin is approached, which is a behavior not in itself contrary to actual fin behavior. Equation 37 also expresses the requirement that the temperature at the fin tip be absolute zero; however, this may not always be desirable and may not be attainable in an actual fin. Further, as can be shown, in that part of the dimensional spectrum where most space radiators will be designed, the fin of Equation 37 is not of optimum weight and the constant temperature-gradient fin is lighter.

In the following analysis, it is assumed that a linear temperature-distance relationship exists from the base of the fin outward and that the temperature at the fin tip is not at absolute zero. Although these assumptions do not represent the best contour, they produce only a slight weight increase over a hypothetical optimum configuration and may be further justified by the simplification they produce in the analysis.

The general shape of a minimum-weight fin and its temperature gradient relationship are shown in Figure 14. The temperature T at any section is

$$T = T_c + \frac{L}{L_h} (T_h - T_c) \quad (38)$$

or

$$\frac{T}{T_c} = 1 + \frac{L}{L_h} \left(\frac{T_h}{T_c} - 1 \right) \quad (39)$$

Differentiating Equation 38 with respect to L ,

$$dT = \left(\frac{T_h - T_c}{L_h} \right) dL \quad (40)$$

Substituting in Equation 36,

$$q_1 = - \frac{k \delta L_w}{L_h} (T_h - T_c) \quad (41)$$

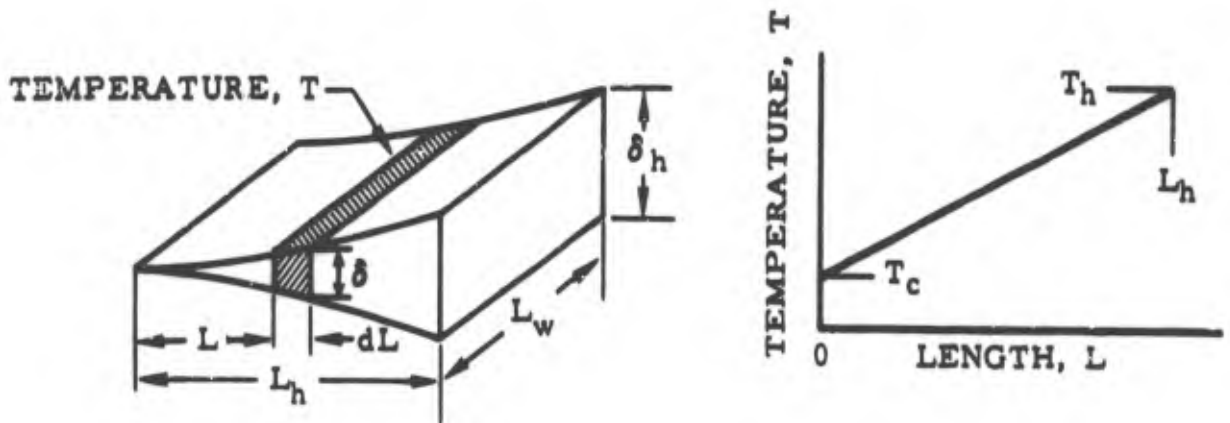


Figure 14. Dimensional and Temperature Relationships of Constant Temperature-Gradient Fin

This is the quantity of heat radiated from both sides of the fin between the tip and the section, or, from Figure 13,

$$-q_1 = q_a + q_b \quad (42)$$

With end effects neglected and a small taper, the heat can be assumed to radiate from both sides of the projected area. The heat lost from the elemental area of the configuration shown in Figure 14 is

$$dq = (C_1 T^4 - C_2) L_w dL \quad (43)$$

where

$$C_1 = \sigma (e_a + e_b)$$

and C_2 accounts for heat transfer from the environment, as described in Equations 4 and 5 for flat plates.

If C_1 and C_2 remain fixed in value, Equation 43 can be integrated over the fin surface. Combining Equations 40 and 43 and setting limits of integration,

$$q = \int_0^q dq = \int_{T_c}^T \frac{L_w L_h}{T_h - T_c} (C_1 T^4 - C_2) dT \quad (44)$$

This is the rate at which heat is radiated by the fin surface from the tip of the section being considered.

Integrating Equation 44 and combining with Equations 41 and 42,

$$\frac{k \delta L_w}{L_h} (T_h - T_c) = \frac{C_1 L_w L_h T_c^4}{5} \left[\frac{\left(\frac{T}{T_c}\right)^5 - 1}{Z - 1} \right] - \frac{C_2 L_w L_h}{Z - 1} \left(\frac{T}{T_c} - 1\right) \quad (45)$$

where

$$Z = \frac{T_h}{T_c} \quad (46)$$

Substituting Equation 39 into Equation 45 and solving for fin thickness,

$$\delta = \left\{ \frac{C_1 T_h^3 L_h^2}{5kZ^3(Z-1)^2} \right\} \left\{ \left[1 + \frac{L}{L_h}(Z-1) \right]^5 - 1 - \frac{5C_2}{C_1 T_h^4} (Z^4)(Z-1) \left(\frac{L}{L_h} \right) \right\} \quad (47)$$

Equation 47 relates fin thickness δ to length L in terms of fin material constants and temperature variables and makes possible the determination of an exact fin profile for any set of conditions. However, it must be noted that values of Z cannot be chosen indiscriminately. It is obvious from the nature and function of space radiators that the minimum value of Z must be 1.0 ($T_c = T_h$). The maximum value of Z is shown in Reference 6 to be

$$Z_{\max} = \sqrt[4]{\frac{C_1 T_h^4}{C_2}} \quad (48)$$

Combining Equations 46 and 48,

$$(T_c)_{\min} = \sqrt[4]{\frac{C_2}{C_1}} \quad (49)$$

This restriction produces configurations having the fin tip in equilibrium with the environment with zero heat flow to and zero radiation from the tip element of the fin. In free space, both the minimum tip temperature and C_2 are absolute zero; under other environmental conditions, the minimum tip temperature will not be zero.

Evaluations of Equation 48 appear on Figures 15 through 19 as the locus of theoretical limit line. Temperature ratio Z must be numerically below that limit.

Fin Profile and Profile Number

At the hot (root) end of the fin, L and L_h are equal. The maximum thickness, as obtained from Equation 47, is now

$$\delta_h = \frac{C_1 T_h^3 L_h^2}{5kZ^3(Z-1)^2} \left[Z^5 - 1 - \frac{5C_2}{C_1 T_h^4} (Z^4)(Z-1) \right] \quad (50)$$

An expression for the fin thickness δ at any distance L from the tip may be obtained as a percentage of the maximum thickness by combining Equations 47 and 50.

$$\frac{\delta}{\delta_h} = \frac{\left[1 + \frac{L}{L_h}(Z - 1)\right]^5 - 1 - \frac{5C_2}{C_1 T_h^4} (Z^4)(Z - 1)\left(\frac{L}{L_h}\right)}{Z^5 - 1 - \frac{5C_2}{C_1 T_h^4} (Z^4)(Z - 1)} \quad (31)$$

Equation 50 may be rearranged as

$$\frac{C_1 T_h^3 L_h^2}{k \delta_h} = \frac{5Z^3(Z - 1)^2}{Z^5 - 1 - \frac{5C_2}{C_1 T_h^4} (Z^4)(Z - 1)} \quad (52)$$

The left-hand side of Equation 52 is almost identical with the aggregate of constants of Equation 15, identified as the plate profile number ζ_p . A profile number for the constant temperature-gradient fin is, from Equation 52,

$$\zeta_p = \frac{C_1 T_h^3 L_h^2}{k \delta_h} \quad (53)$$

The value of the profile number, for various values of temperature ratio, has been computed from Equation 52 and is plotted in Figure 15. The profile number increases rapidly as the temperature ratio increases. This is especially true for those cases having high environmental parameters or where the environment greatly affects the heat transfer.

Heat Transfer Relationships

Relationships between the principal variables of heat transfer properties, temperatures, and dimensions have been established. The heat transfer rate q_f from the entire fin can be obtained by integrating Equation 44 and substituting T_h for T in the limits of integration. This, then, becomes

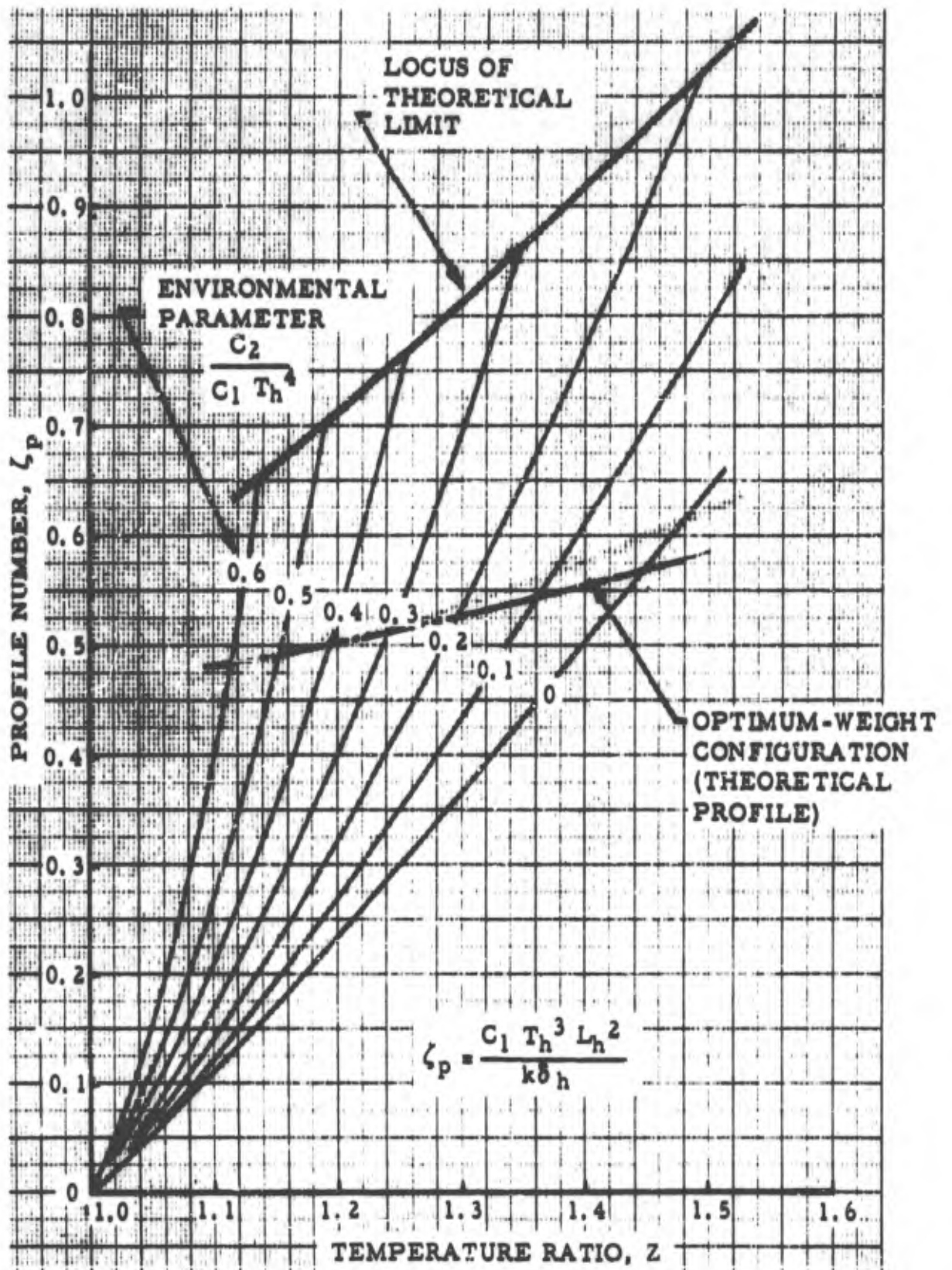


Figure 15. Relationship of Profile Number to Temperature Ratio of Constant Temperature-Gradient Fin

$$q_f = \frac{C_1 L_w L_h T_c^4 (Z^5 - 1)}{5(Z - 1)} - C_2 L_w L_h \quad (54)$$

An alternate equation for expressing the heat transfer from a fin is obtained by combining Equations 50 and 54 and simplifying.

$$q_f = L_w \sqrt{C_1 T_h^5 k \delta_h} \zeta_h \quad (55)$$

where ζ_h is identified as the heat transfer number and is defined as

$$\zeta_h = \sqrt{\frac{Z^5 - 1 - \frac{5C_2}{C_1 T_h^4} (Z^4)(Z - 1)}{5Z^5}} \quad (56)$$

Fin Effectiveness

As for other extended surfaces, a measure of the performance of a given fin is a comparison between the heat that it radiates and the heat which would be radiated from the same fin in free space at a constant and uniform temperature equal to that at the fin root T_h . The ratio of the two heat quantities is called fin effectiveness Ω . As a measure of merit, this term has the deficiency of being unable to indicate the benefit of any fin over no fin. It is a convenient method, however, of comparing different configurations. The equation for fin effectiveness is

$$\begin{aligned} \Omega = \frac{q_f}{q_u} &= \frac{q_f}{C_1 L_w L_h T_h^4} \\ &= \frac{\frac{C_1 L_w L_h T_c^4 (Z^5 - 1)}{5(Z - 1)} - C_2 L_w L_h}{C_1 L_w L_h T_h^4} \end{aligned} \quad (57)$$

or

$$\Omega = \frac{Z^5 - 1}{5Z^4(Z - 1)} - \frac{C_2}{C_1 T_h^4} \quad (58)$$

Fin Weight

The weight of a differential element of Figure 14 is

$$dW_f = \rho \delta L_w dL$$

Substituting the relationship of Equation 47 for fin thickness δ and then integrating, over the entire fin length

$$W_f = \frac{\rho C_1 L_w L_h^3 T_h^3}{5kZ^3 (Z-1)^3} \left[\frac{Z^6}{6} - Z + \frac{5}{6} - \frac{5}{2} \left(\frac{C_2}{C_1 T_h^4} \right) (Z^4)(Z-1)^2 \right] \quad (59)$$

Another useful equation is obtained when L_h^3 in Equation 59 is eliminated and Equation 52 is combined with Equation 59.

$$W_f = \rho L_w \left(\frac{k \delta_h^3}{C_1 T_h^3} \right)^{1/2} \zeta_w \quad (60)$$

where ζ_w is identified as the weight number and is defined as

$$\zeta_w = \frac{\sqrt{5Z^3} \left[\frac{Z^6}{6} - Z + \frac{5}{6} - \frac{5}{2} \left(\frac{C_2}{C_1 T_h^4} \right) (Z^4)(Z-1)^2 \right]}{\left[Z^5 - 1 - \frac{5C_2}{C_1 T_h^4} (Z^4)(Z-1) \right]^{3/2}} \quad (61)$$

Weight/Heat Transfer Ratio

The fin weight per unit of heat dissipated to space is often of interest in preliminary design. This ratio can be obtained by dividing the value of W_f given in Equation 59 by the heat rejected to the environment from the fin as expressed by Equation 55. Dividing Equation 59 by Equation 55, substituting value of L_h given by Equation 52, and simplifying,

$$\frac{W_f}{q_f} = \left(\frac{\rho \delta_h}{C_1 T_h^4} \right) \zeta_r \quad (62)$$

where ζ_r is identified as the ratio number and is defined as

$$\zeta_r = \frac{5Z^4 \left[\frac{Z^6}{6} - Z + \frac{5}{6} - \frac{5}{2} \left(\frac{C_2}{C_1 T_h^4} \right) (Z^4) (Z-1)^2 \right]}{\left[(Z^5 - 1) - 5 \left(\frac{C_2}{C_1 T_h^4} \right) (Z^4) (Z-1) \right]^2} \quad (63)$$

As an aid in the weight optimization of a condenser or heat exchanger, it is desirable to know the ratio of increase in weight to increase in heat transfer which results from an increase in fin length. This ratio, dW_f/dq_f , was evaluated in Reference 6, which presents the following pertinent equations.

$$\frac{dW_f}{dq_f} = \left(\frac{\rho \delta_h}{C_1 T_h^4} \right) \zeta_d \quad (64)$$

where ζ_d is identified as the differential ratio number and is defined as

$$\zeta_d = \frac{Z^4}{(\phi_2)^2} \left\{ \frac{2Z \left(\frac{d\phi_1}{dZ} \right) + 3\phi_1 \left[1 - \frac{Z}{\phi_2} \left(\frac{d\phi_2}{dZ} \right) \right]}{\frac{Z}{5\phi_2} \left(\frac{d\phi_2}{dZ} \right) - 1} \right\} \quad (65)$$

and where

$$\phi_1 = \frac{z^6}{6} - z + \frac{5}{6} - \frac{5}{2} \left(\frac{C_2}{C_1 T_h^4} \right) (z^4)(z-1)^2 \quad (66)$$

$$\frac{d\phi_1}{dz} = z^5 - 1 - 5 \left(\frac{C_2}{C_1 T_h^4} \right) (z^3)(3z-2)(z-1) \quad (67)$$

and

$$\phi_2 = z^5 - 1 - 5 \left(\frac{C_2}{C_1 T_h^4} \right) (z^4)(z-1) \quad (68)$$

$$\frac{d\phi_2}{dz} = 5z^4 \left[z \left(1 - \frac{5C_2}{C_1 T_h^4} \right) + \frac{4C_2}{C_1 T_h^4} \right] \quad (69)$$

DESIGN ANALYSIS

The equations of the mathematical analysis discussion have the disadvantage of containing complex temperature ratio functions which make the determination of desired information a long and often repetitious process. To assist in the design of these fins, the graphs of Figures 16 through 21 have been prepared. The variable groups and parameters were evaluated by use of a digital computer.

Basic fin properties have been grouped together to form the profile number ζ_p defined in Equation 53. This profile number is very similar to that of a flat plate of uniform thickness, and is identical to the one to be discussed for a fin of triangular or trapezoidal profile. The difference between this and the flat plate number is the use of the fin root thickness δ_h instead of the thickness δ of the uniform plate. A comparison of thermal behavior of tapered fins and flat plates can therefore be made upon the basis of the same root thickness.

Heat Transfer

The heat radiated from a fin may be found from Equations 55 and 56, or from Figure 16 where heat transfer number ζ_h is plotted against profile number. It is seen that the curve of heat transfer number, and consequently the radiation, rises quite rapidly with the first increase of profile number above zero. It then becomes relatively flat, showing that radiating power cannot be improved greatly by increasing the value of fin profile number alone.

Fin Effectiveness

The relationship of fin effectiveness to fin profile number is shown in Figure 17. Effectiveness is seen to decrease with increasing values of the profile number, comparatively rapidly at first and then more slowly as the locus of theoretical limit is approached.

Fin effectiveness Ω can be used to obtain the rate of heat radiation q_f by means of Equation 57. This method may have some advantages, in certain design procedures, over the use of Figure 16.

Fin Weight

Figure 18 shows the relationship of weight to fin profile number. A striking feature is the small difference in fin weight, for low values of the fin profile number, caused by the variation of environmental parameter. However, the difference does become significant in the region of the optimum-weight profile number.

Weight/Heat Transfer Ratio

The ratio of weight to heat transfer rate of a fin may be obtained from Figure 19. Since both abscissa and ordinate contain the root thickness term, δ_h , it is difficult to observe the effect upon the weight/heat transfer ratio of root thickness alterations. However, with a fixed value of δ_h , it is possible to observe the result of changing fin length L_h . As this dimension increases, the weight/heat transfer ratio at first increases quite rapidly but then its rate of increase falls off. The difference in the ratio for two different lengths is enhanced by the appearance of fin length as a squared term in the abscissa.

An evaluation of the differential ratio number ζ_d was made using Equations 64 through 69. Because the algebraic manipulations are complex, a digital computer was used to determine the coordinates of these curves. The value of ζ_d increases markedly with increase in profile number, especially for high values of the environmental parameter. Further, since the profile number itself is a function of the fin length to the second power,

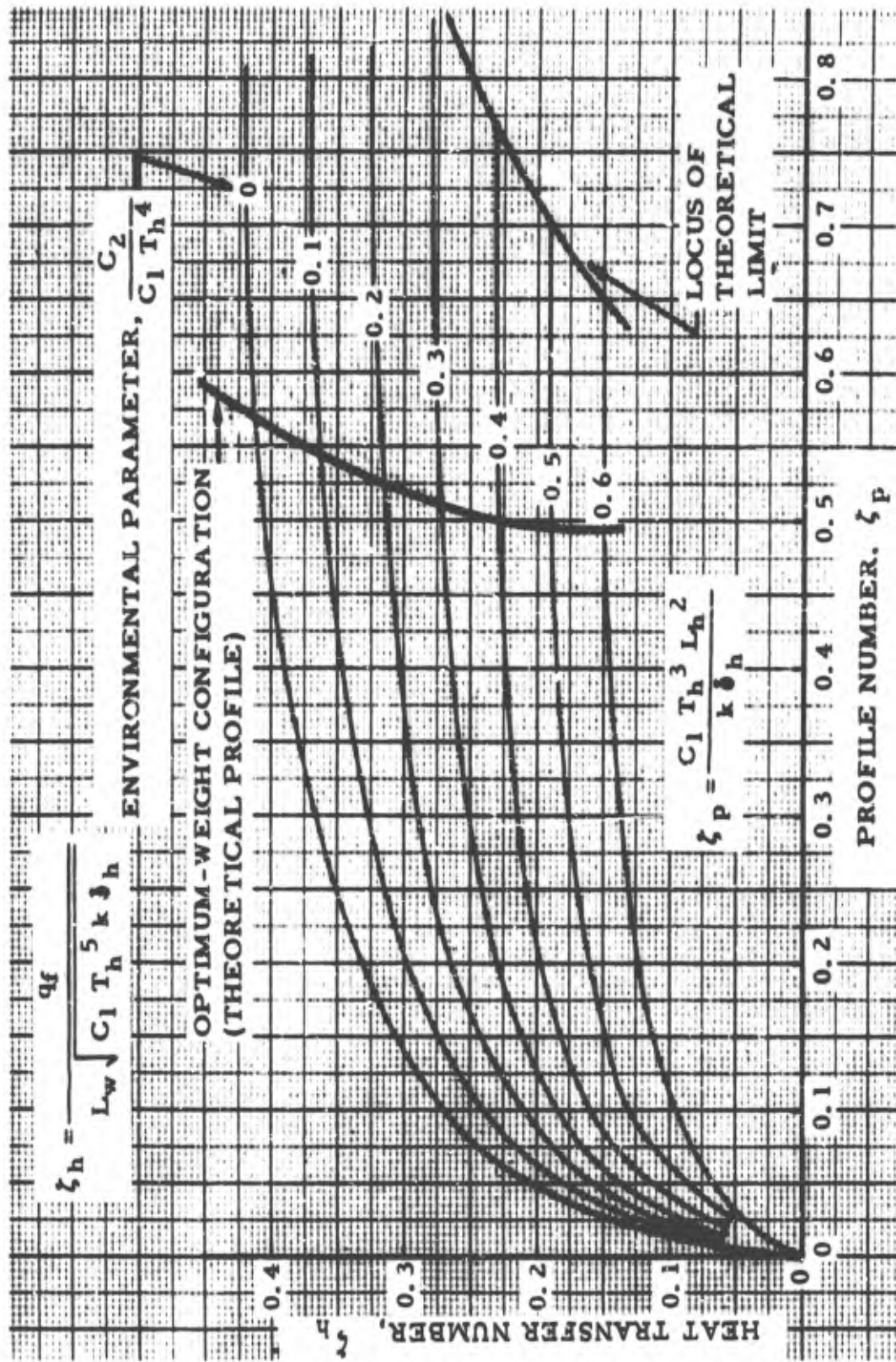


Figure 16. Relationship of Heat Transfer Number to Fin Profile Number of Constant Temperature-Gradient Fin

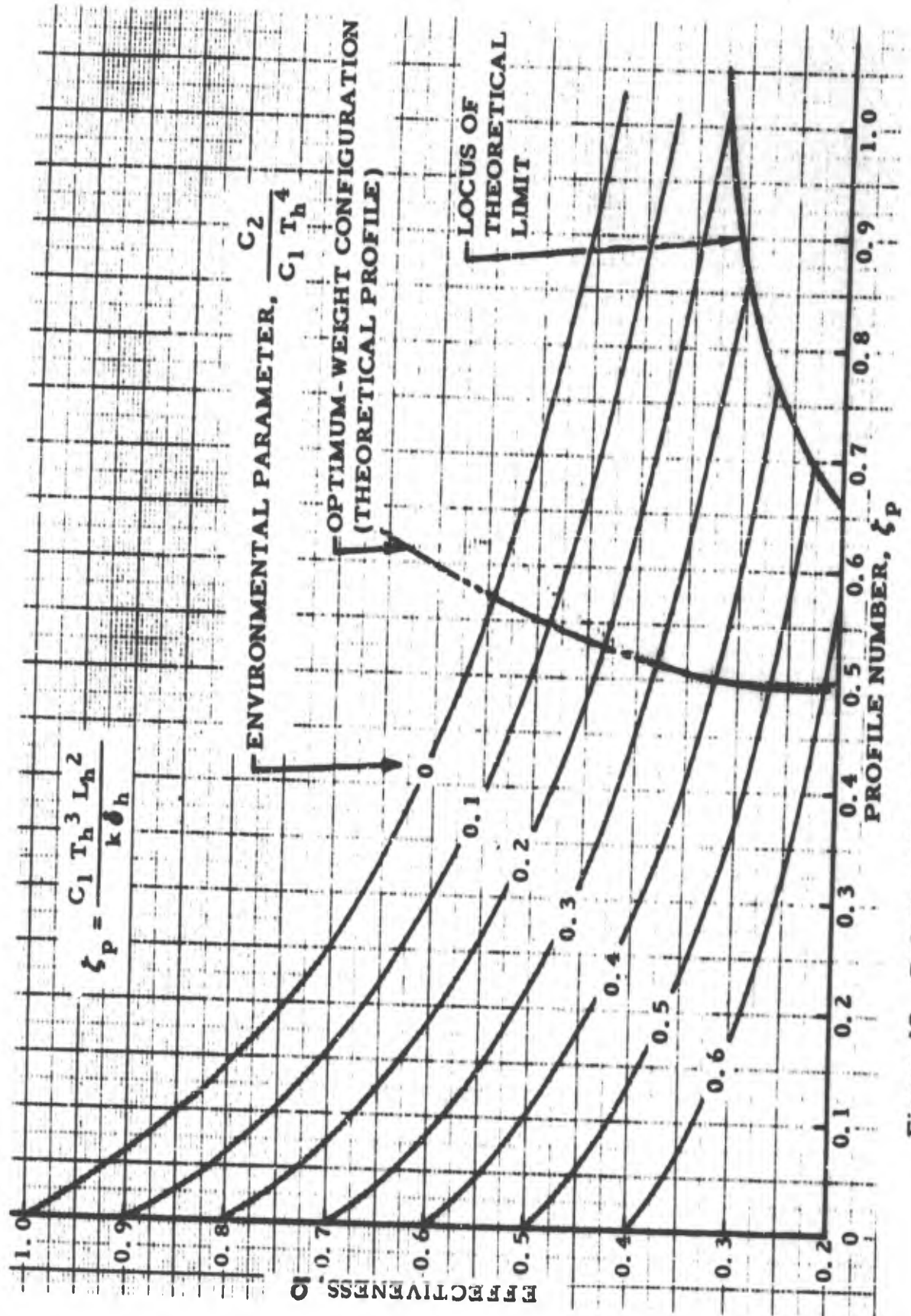


Figure 17. Relationship of Fin Effectiveness to Profile Number of Constant Temperature-Gradient Fin

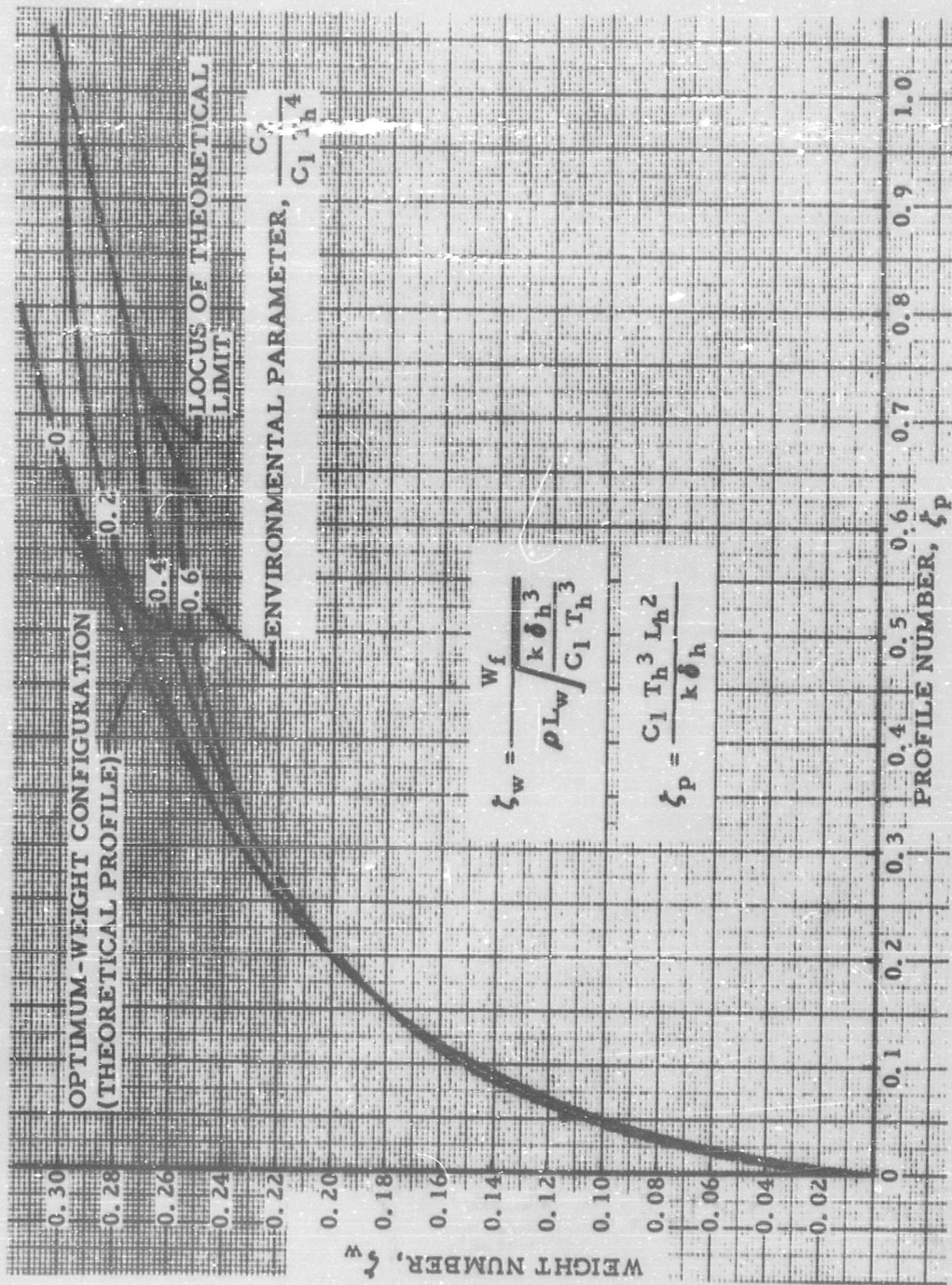


Figure 18. Relationship of Weight Number to Profile Number of Constant Temperature-Gradient Fin

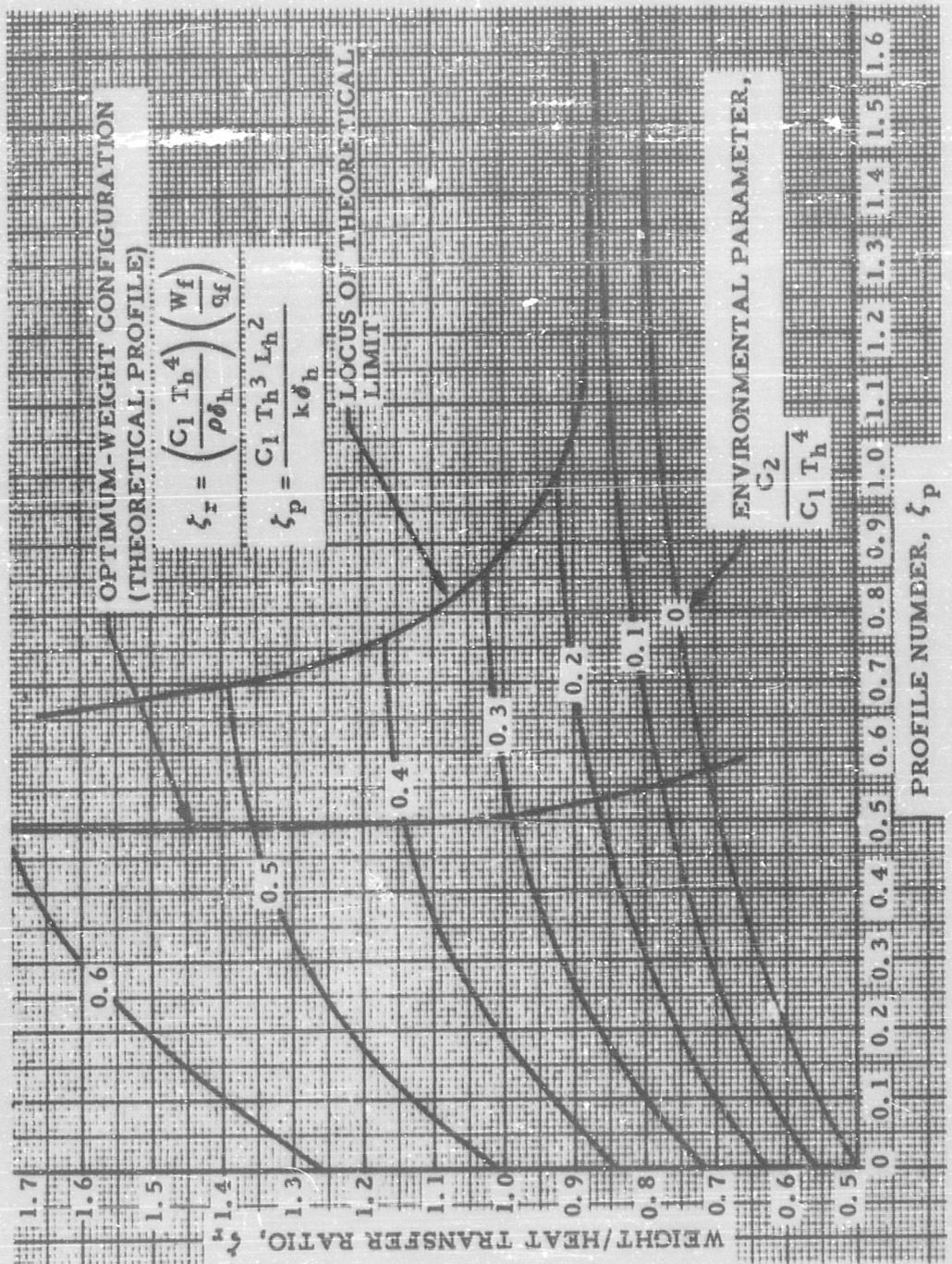


Figure 19. Relationship of Weight/Heat Transfer Ratio to Profile Number of Constant Temperature-Gradient Fin

the values of ζ_h and of the ratio dW_f/dq_f increase very rapidly with an increase in fin length.

Therefore, when designing a optimum-weight condenser, a modest fin length should be expected. Numerical quantities obtained from Figure 20 will necessarily be less exact than those obtained by direct substitution in the related equation. However, they should be adequate for most design purposes.

Fin Shape

In Figures 21 and 22, the thickness ratio δ/δ_h is plotted against the length ratio L/L_h for various values of temperature ratio Z and for the environmental parameters of 0 and 0.2. The resulting curves are relative portraits of the fin cross section, the profile becoming more and more concave as the temperature ratio increases.

The effect of increasing the environmental parameter is to increase the concavity of the fin, for values of Z greater than 1.0. For an environmental parameter of 0.2, the maximum temperature ratio Z at the theoretical limit is 1.49735. When Z is 1.5, theory predicts a "negative thickness" at the tip, which is not apparent on the graph because of the scale. This curve does serve to emphasize the sharpness of the fin at its end section when conditions near the theoretical limit of Z are approached. Difficulties in fabrication and handling would make fins of extreme concavity undesirable.

OPTIMUM-WEIGHT DESIGN

The determination of the optimum-weight fin profile, the one for which the ratio of heat radiated to weight is greatest, is important in space radiator design. Although this configuration may not be desirable for all intended applications because of fabrication or some other difficulties, it can serve as a base point for arriving at an acceptable design.

Two useful dimensionless numbers have been developed. The fin heat transfer number (Equation 55) is

$$\zeta_h = \frac{q_f}{L_w \sqrt{C_1 T_h^5 k \delta_h}}$$

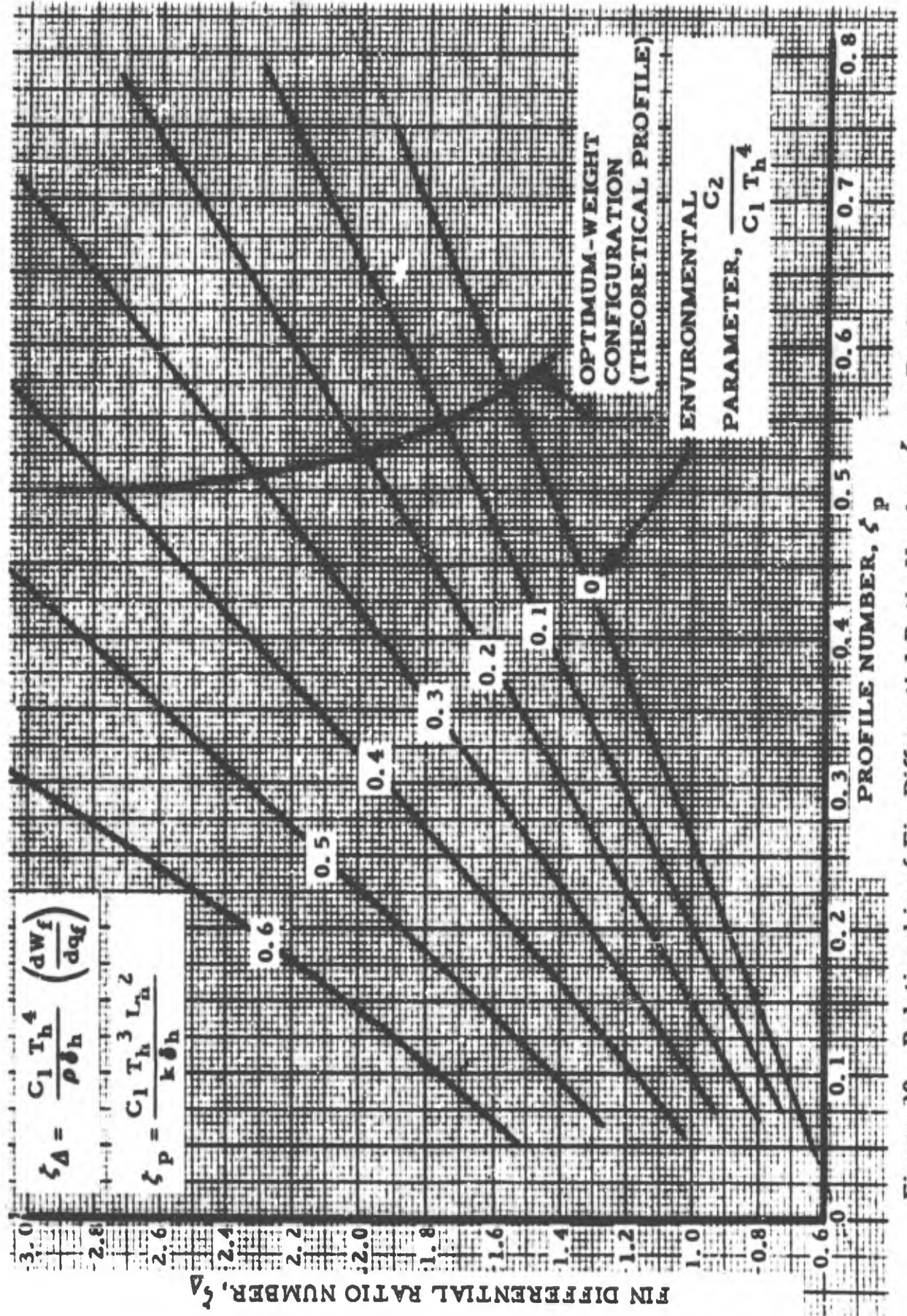


Figure 20. Relationship of Fin Differential Ratio Number ζ_A to Profile Number of Constant Temperature-Gradient Fin

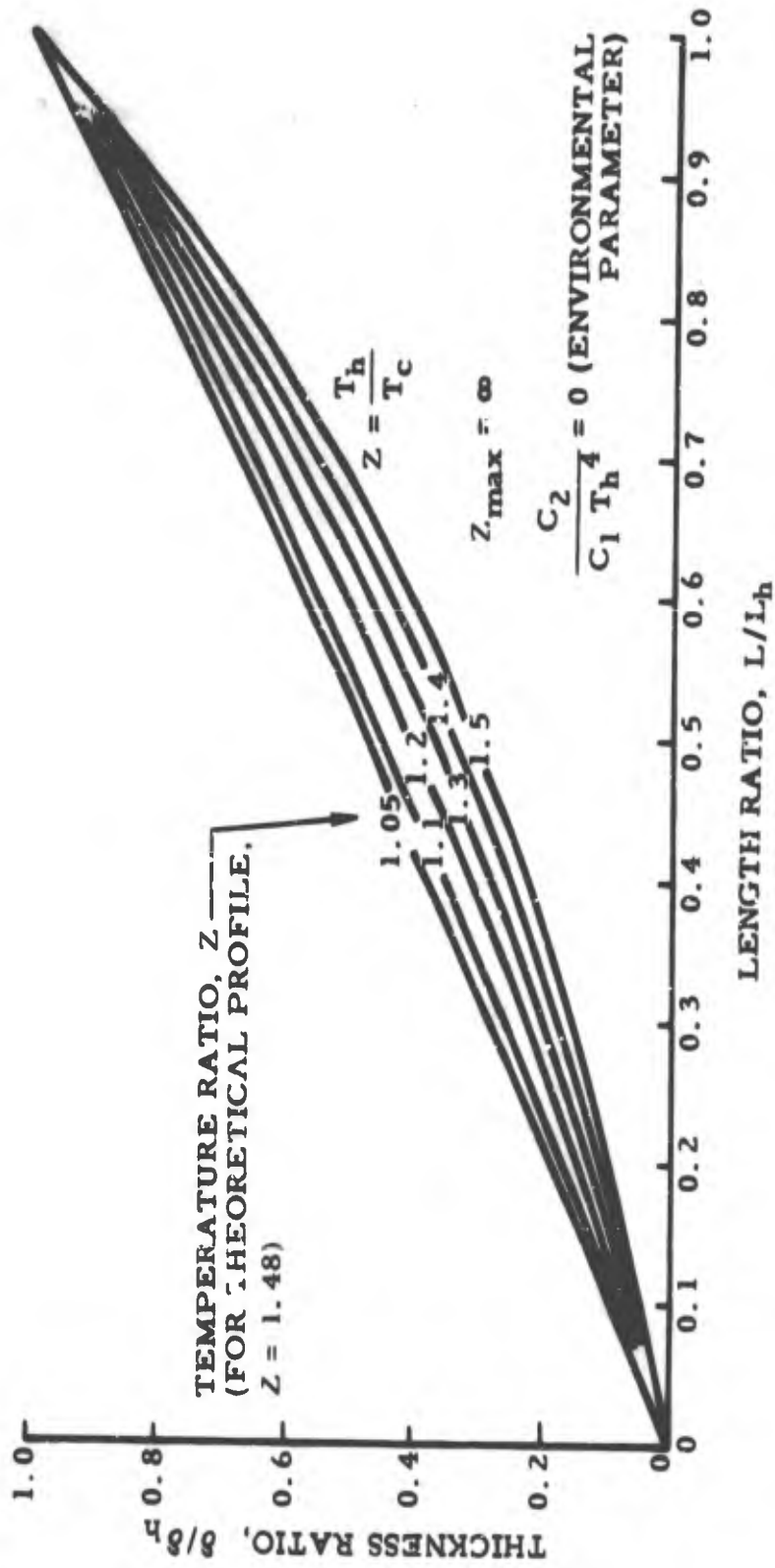


Figure 21. Relationship of Thickness Ratio to Length Ratio of Constant Temperature-Gradient Fin (Operating in Free Space)

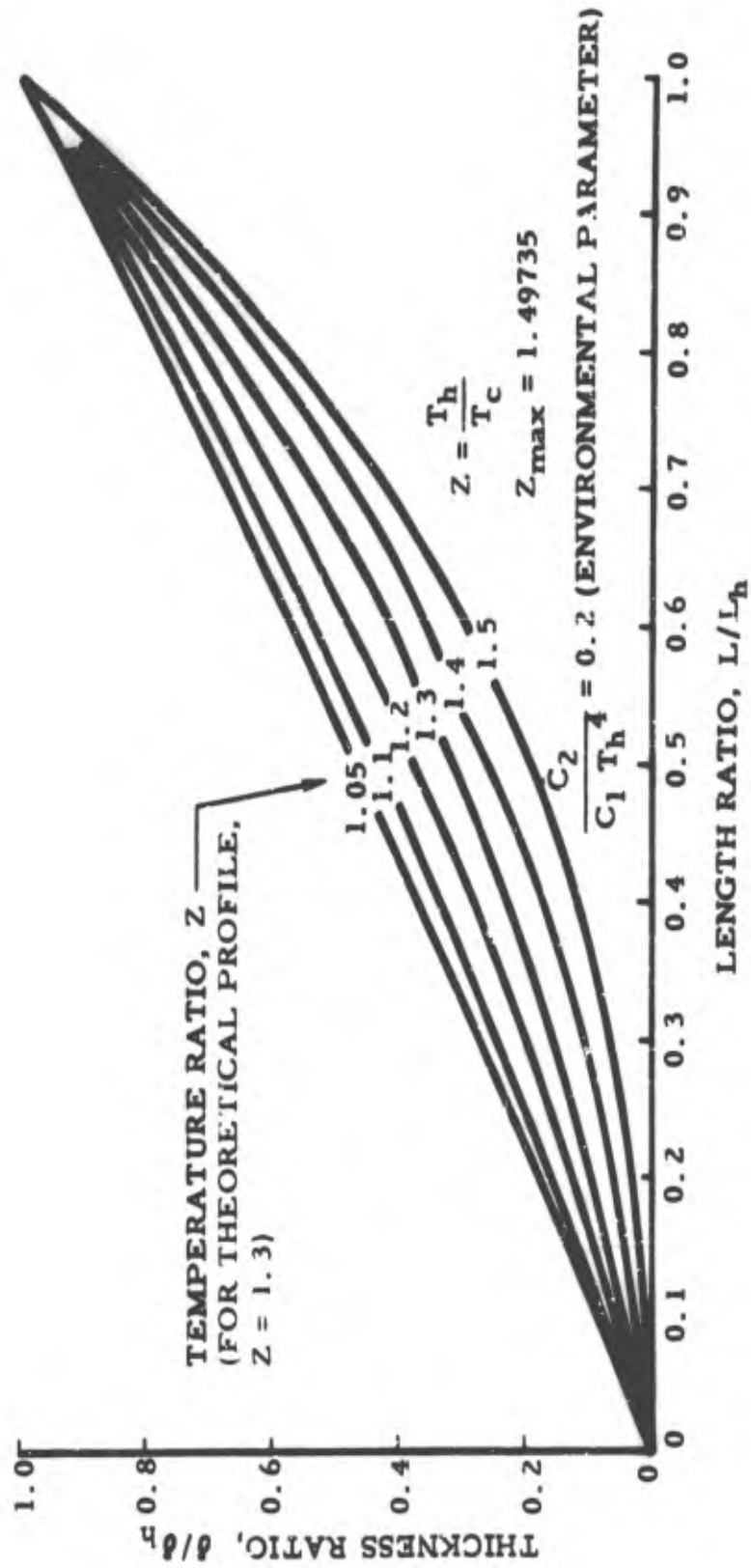


Figure 22. Relationship of Thickness Ratio to Length Ratio of
Constant Temperature-Gradient Fin
(Operating at Environmental Parameter of 0.2)

and the fin weight number (Equation 60) is

$$\zeta_w = \frac{W_f}{\rho L_w \sqrt{\frac{k \delta_h^3}{C_1 T_h^3}}}$$

Rearranging Equation 55,

$$\sqrt{\delta_h} = \frac{q_f}{\zeta_h L_w \sqrt{C_1 T_h^5 k}} \quad (70)$$

Substituting Equation 70 into Equation 60, simplifying, and rearranging,

$$W_f = \frac{\rho q_f^3}{L_w^2 C_1^2 T_h^9 k} \left(\frac{\zeta_w}{\zeta_h^3} \right) \quad (71)$$

For any given situation, the radiated heat q_f is a constant, as is the quantity $\rho/L_w^2 C_1^2 T_h^9 k$. Fin weight W_f therefore depends only on the value of the ratio ζ_w/ζ_h^3 , and the weight is least when this ratio has the lowest value. Since both numbers are functions of profile number, the ratio can be plotted against ζ_p , as shown in Figure 23.

The flatness of the curves of Figure 23 shows that the ratio of weight and heat transfer numbers is not very sensitive to variation in profile number in the region of the optimum-weight fin. A fairly wide range of profile numbers can therefore be used without an appreciable change in fin weight. In fact, because it is difficult to locate the minimum-ratio profile number for most of the environmental parameters, a second method was developed to improve accuracy.

In this alternate approach, Equation 71 was differentiated with respect to profile number ζ_p so that, with a constant value of $\rho q_f^3/L_w^2 C_1^2 T_h^9 k$,

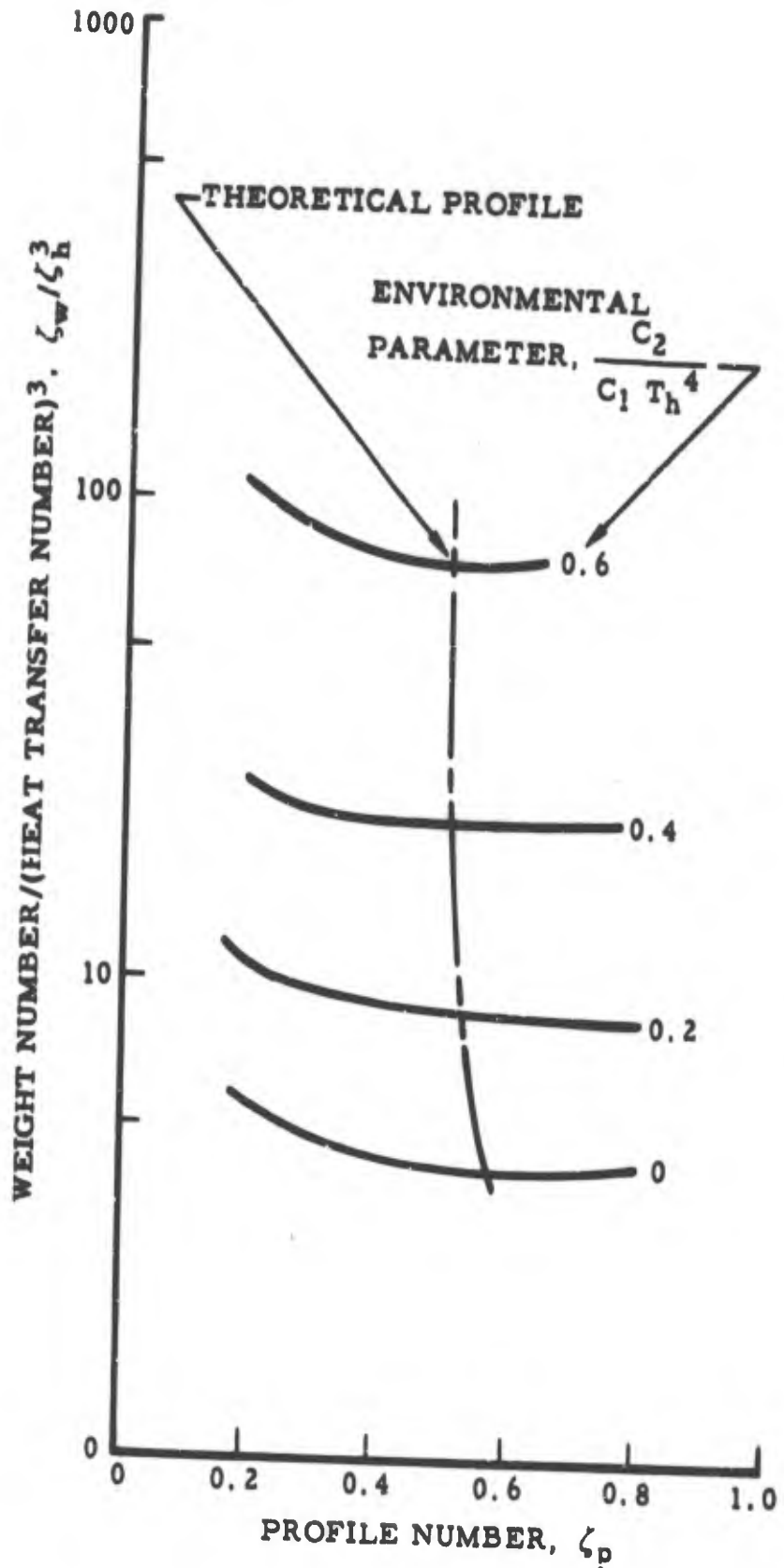


Figure 23. Relationship of Weight / (Heat Transfer Number)³ Ratio to Profile Number of Constant Temperature-Gradient Fin

$$\frac{dW_f}{d\zeta_p} = \frac{\rho q_f^3}{L_w^2 C_1^2 T_h^9 k \zeta_h^6} \left[\zeta_h^3 \left(\frac{d\zeta_w}{d\zeta_p} \right) - 3\zeta_w \zeta_h^2 \left(\frac{d\zeta_h}{d\zeta_p} \right) \right] \quad (72)$$

For the condition of minimum weight, $dW_f/d\zeta_p$ is zero, from which

$$\zeta_h^3 \left(\frac{d\zeta_w}{d\zeta_p} \right) = 3\zeta_w \zeta_h^2 \left(\frac{d\zeta_h}{d\zeta_p} \right) \quad (73)$$

or

$$\frac{d\zeta_w}{\zeta_w d\zeta_p} = \frac{3}{\zeta_h} \left(\frac{d\zeta_h}{d\zeta_p} \right) \quad (74)$$

This may be expressed as

$$\frac{1}{3} \left[\frac{d(\log \zeta_w)}{d\zeta_p} \right] = \frac{d(\log \zeta_h)}{d\zeta_p} \quad (75)$$

or

$$\frac{1}{3} d \log \zeta_w = d \log \zeta_h \quad (76)$$

Solutions can be found for Equation 76 by plotting ζ_w against ζ_h on logarithmic coordinates, or $\log \zeta_w$ against $\log \zeta_h$ on rectangular coordinates, and locating the point at which the slope of the curve is 1/3. The first of these procedures is shown in Figure 24. The points of tangency, which can be easily detected, are joined by a smooth curve. The values of abscissa and ordinate from this curve were used to produce

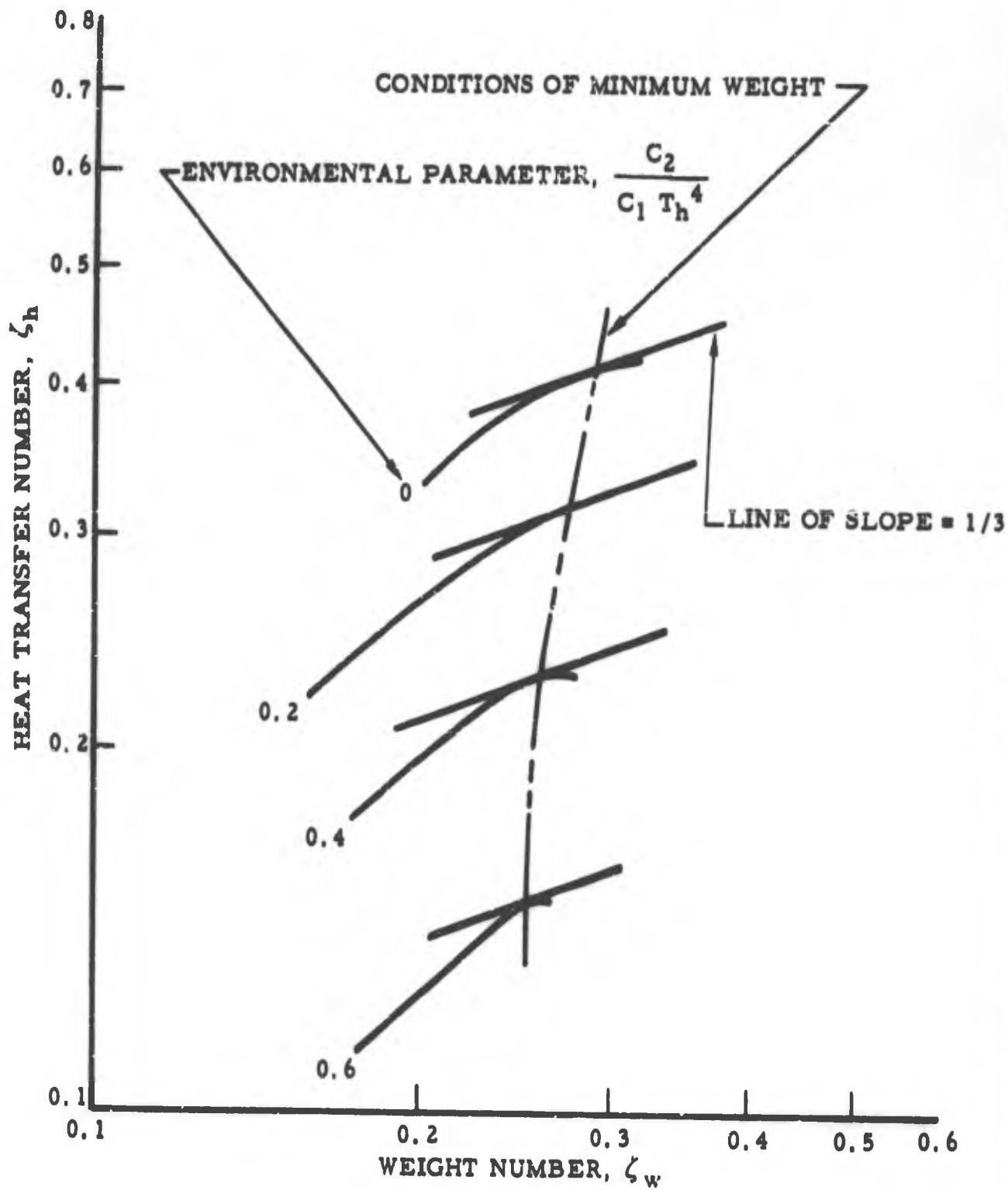


Figure 24. Relationship of Heat Transfer Number to Weight Number of Constant Temperature-Gradient Fin

the optimum-weight configuration (theoretical profile) lines of Figures 15 through 19.

DESIGN PROCEDURES

In designing constant temperature-gradient fins, the procedures outlined in the discussion on flat plates may be followed. The practical necessity for obtaining high radiator effectiveness generally dictates the use of profile numbers lower than those indicated for the optimum-weight configuration. The use of lower profile numbers could produce stubbier fins of greater root thickness and lesser area than those having theoretical profiles.

RADIANT HEAT TRANSFER FROM TRIANGULAR AND TRAPEZOIDAL FINS

The advantage of triangular and trapezoidal fins over flat plates is that they radiate almost as much heat from a given area but weigh considerably less. The advantage they possess over the constant temperature-gradient fin is the comparative simplicity of their profile and, therefore, of their fabrication. It will soon be evident, however, that the thermal analysis of triangular and trapezoidal is much more complex because of the nonlinear gradient of temperature from tip to root. Pioneering investigations of this profile have been conducted by Wilkins (Reference 11) and Nilson and Curry (Reference 12).

NOMENCLATURE

- C_1 Radiation constant, $\sigma(\epsilon_a + \epsilon_b)$, Btu/(sq ft)(hr)(°R)⁴
- C_2 Radiation constant, heat received from environment by unit of fin area, Btu/sq ft
- K_1 Thermal and configuration ratio, 1/ft
- K_2 Configuration ratio, ft
- K_3 Thermal and configuration ratio, (Btu/hr)³
- k Thermal conductivity of fin material, Btu/(hr)(ft)(°R)
- L Fin length measured from tip toward root (variable), ft
- L_h Total fin length, ft
- L_w Width of fin normal to heat flow, ft
- q Heat transfer rate from both sides of fin from tip to section considered, Btu/hr
- q_f Heat transfer rate from both sides of entire fin, Btu/hr
- q_i Internal heat transferred past section of fin, Btu/hr
- S_f Configuration ratio (slope), nondimensional

T	Temperature of point on fin (variable), °R
T_c	Temperature of cold end of fin (tip), °R
T_h	Temperature of hot end of fin (root), °R
W_f	Fin weight, lb
Z_c	Ratio of temperatures, nondimensional
δ	Fin thickness at any point, ft
δ_c	Fin thickness at cold end (tip), ft
δ_h	Fin thickness at hot end (root), ft
ζ_p	Fin profile number, nondimensional
ρ	Density of fin material, lb/cu ft
Ω	Fin effectiveness, nondimensional
ω	Variable relating dimensional and thermal characteristics, nondimensional
ω_h	Evaluation of ω at root end, nondimensional
ω_c	The evaluation of ω at tip end, nondimensional

MATHEMATICAL ANALYSIS

The form of trapezoidal fin to be analyzed is shown in Figure 25. Although the profile of the actual radiating surface would probably be an isosceles trapezoid, the form shown assists the analysis without changing the results. Triangular fins may be considered as special forms of trapezoidal fins.

The internal heat transfer across the indicated section is

$$q_1 = -k L_w \delta \frac{dT}{dL} \quad (77)$$

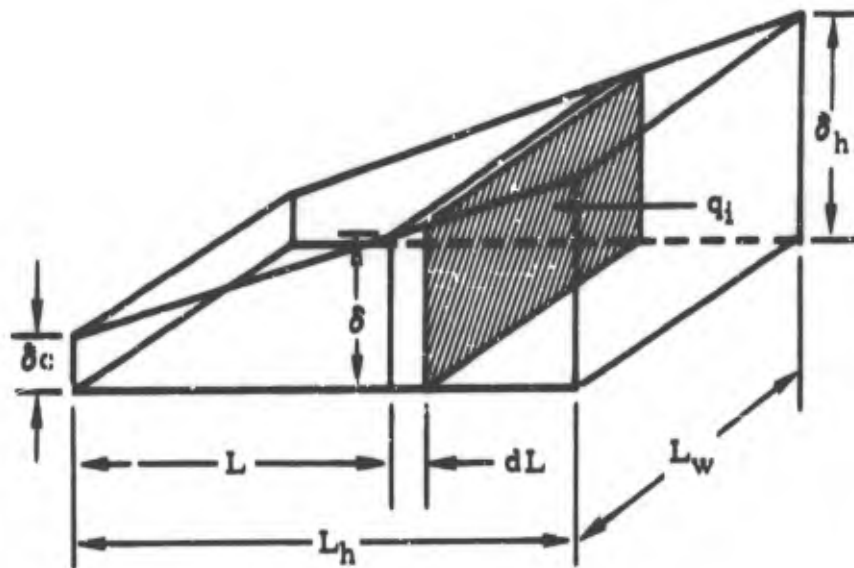


Figure 25. Dimensional Relationships of Trapezoidal Profile Fin

Differentiated with respect to L this becomes

$$dq_i = -k L_w \frac{d}{dL} \left(\delta \frac{dT}{dL} \right) dL \quad (78)$$

The heat lost by radiation from an element of the fin is

$$dq = (C_1 T^4 - C_2) L_w dL \quad (79)$$

Since the heat lost by radiation represents the difference in heat passing across the two internal faces of the element, then

$$dq = -dq_i \quad (80)$$

and

$$C_1 T^4 - C_2 = k \frac{d}{dL} \left(\delta \frac{dT}{dL} \right) \quad (81)$$

From the geometry of Figures 25,

$$\delta = \delta_c + (\delta_h - \delta_c) \frac{L}{L_h} = S_f \left(\frac{\delta_c}{S_f} + L \right) \quad (82)$$

where

$$S_f = \frac{\delta_h - \delta_c}{L_h} \quad (83)$$

Equation 81 is operated upon by dividing both sides by $C_1 T_c^4$ and substituting Equation 82 for δ . After rearranging, this becomes

$$\left(\frac{T}{T_c} \right)^4 - \frac{C_2}{C_1 T_c^4} = \frac{d}{dL} \left[\frac{k S_f}{C_1 T_c^4} \left(\frac{\delta_c}{S_f} + L \right) \frac{dT}{dL} \right] \quad (84)$$

Letting

$$\frac{C_1 T_c^3}{k S_f} = K_1 \quad (85)$$

$$\frac{\delta_c}{S_f} = K_2 \quad (86)$$

$$\frac{T}{T_c} = Z_c \quad (87)$$

Then

$$T_c \left(\frac{dZ_c}{dL} \right) = \frac{dT}{dL} \quad (88)$$

After substituting, Equation 84 becomes

$$Z_c^4 - \frac{C_2}{C_1 T_c^4} = \frac{d}{dL} \left[\frac{1}{K_1} (K_2 + L) \frac{dZ_c}{dL} \right] \quad (89)$$

Introducing a new variable into Equation 89, wherein

$$\omega = K_1 (K_2 + 1) \quad (90)$$

and

$$\frac{d\omega}{dL} = K_1 \quad (91)$$

Then

$$\frac{dZ_c}{dL} = \frac{dZ_c}{d\omega} \left(\frac{d\omega}{dL} \right) = K_1 \left(\frac{dZ_c}{d\omega} \right) \quad (92)$$

Substituting values and rearranging terms,

$$\frac{d}{dL} \left[\frac{dL}{d\omega} \left(\frac{\omega}{K_1} \right) K_1 \frac{dZ_c}{d\omega} \right] - Z_c^4 + \frac{C_2}{C_1 T_c^4} = 0 \quad (93)$$

which becomes

$$\frac{d}{d\omega} \left(\omega \frac{dZ_c}{d\omega} \right) - Z_c^4 + \frac{C_2}{C_1 T_c^4} = 0 \quad (94)$$

The ratio of the temperature at a section to that at the cold end, or tip temperature, is dependent upon the value of ω . This can be written as

$$Z_c = f(\omega) \quad (95)$$

Equation 94 then becomes

$$\omega f''(\omega) + f'(\omega) - \left[f(\omega) \right]^4 + \frac{C_2}{C_1 T_c^4} = 0 \quad (96)$$

Equation 96 is an important expression of the relationship between the variables. Since it is a nonlinear differential equation, its solution is numerical, but even the solution must be modified somewhat before it can be used for actual problems.

Where the profile length L_h and root temperature T_h are known, the heat transfer is established in terms of these quantities. The environmental term $C_2/C_1 T_c^4$ of Equation 96 can be converted into the normal environmental parameter by the operation

$$\left(\frac{C_2}{C_1 T_c^4}\right)\left(\frac{T_c}{T_h}\right)^4 = \frac{C_2}{C_1 T_h^4} \quad (97)$$

From Equations 87 and 95,

$$f(\omega) = \frac{T}{T_c} \quad (98)$$

Letting subscript h denote the condition where $L = L_h$,

$$f(\omega_h) = \frac{T_h}{T_c} \quad (99)$$

From Equation 97,

$$\frac{C_2}{C_1 T_c^4} = \frac{C_2}{C_1 T_h^4} \left[f(\omega_h) \right]^4 \quad (100)$$

Placing Equation 91 in a form to be integrated,

$$K_1 \int_{\omega_c}^{L_h} dL = \int_{\omega_c}^{\omega_h} d\omega \quad (101)$$

The lower integration limit, ω_c , is obtained from Equation 90 at $L = 0$, as

$$\omega_c = K_1 K_2 \quad (102)$$

After substitution and integration, Equation 101 becomes

$$K_1 L_h = \int_{K_1 K_2}^{\omega_h} d\omega \quad (103)$$

The term K_1 can be expressed in terms of L_h by combining Equations 83 and 85 and substituting, so that

$$K_1 = \frac{C_1 T_c^3 L_h}{k (\delta_h - \delta_c)} = \frac{C_1 T_h^3 L_h}{k \delta_h \left(1 - \frac{\delta_c}{\delta_h}\right)} \left(\frac{T_c}{T_h}\right)^3 \quad (104)$$

By combining Equations 99 and 104,

$$K_1 L_h = \left(\frac{C_1 T_h^3 L_h^2}{k \delta_h}\right) \left\{ \frac{1}{\left[f(\omega_h)\right]^3 \left(1 - \frac{\delta_c}{\delta_h}\right)} \right\} \quad (105)$$

The first parenthetical expression is recognized as the profile number ζ_p , or

$$\zeta_p = \frac{C_1 T_h^3 L_h^2}{k \delta_h} \quad (106)$$

Combining Equations 103, 105, and 106,

$$\zeta_p = \left[f(\omega_h) \right]^3 \left(1 - \frac{\delta_c}{\delta_h} \right) \int_{K_1 K_2}^{\omega_h} d\omega \quad (107)$$

Since the profile number can be obtained directly from the physical properties and shape of the extended surface, and can also be determined at any value of ω_h during the numerical integration process, it is an extremely valuable group of terms. In fact, all performance characteristics of these extended surfaces will be presented as a function of the profile number. Further, since ζ_p is a fundamental property, the results of specific examples can be converted into generalized data by the use of this number.

During the numerical integration process, it is desirable to evaluate ζ_p at any value of ω_h along the extended surface. The corresponding value of δ_h at the end of a given section is evaluated from Equations 82, 86, and 103 as

$$\delta_h = S_f \left[K_2 + \frac{1}{K_1} \int_{K_1 K_2}^{\omega_h} d\omega \right] \quad (108)$$

Dividing both sides of Equation 108 by δ_c and combining with Equation 86,

$$\frac{\delta_h}{\delta_c} = 1 + \frac{1}{K_1 K_2} \int_{K_1 K_2}^{\omega_h} d\omega \quad (109)$$

Substituting the value of δ_h/δ_c given by Equation 109 into Equation 107, and simplifying,

$$\zeta_p = \frac{\left[f(\omega_h) \right]^3 \left(\int_{K_1 K_2}^{\omega_h} d\omega \right)^2}{K_1 K_2 + \int_{K_1 K_2}^{\omega_h} d\omega} \quad (110)$$

The heat transfer from an extended surface such as that shown in Figure 25 can be obtained by combining Equations 77 and 80.

$$q_f = k L_w \delta_h \left(\frac{dT}{dL} \right)_{L=L_h} \quad (111)$$

Substituting values from Equations 87, 88, 92, and 95,

$$q_f = k L_w \delta_h T_c K_1 \left[f'(\omega_h) \right] \quad (112)$$

The heat transfer from an extended surface can also be expressed as a surface effectiveness, similar to that defined for flat plates or for surfaces contoured to give a constant temperature-gradient. Thus

$$q_f = C_1 T_h^4 L_h L_w \Omega \quad (113)$$

Equating Equations 112 and 113 and simplifying,

$$\Omega = \frac{k \delta_h T_c K_1}{C_1 T_h^4 L_h} \left[f'(\omega_h) \right] \quad (114)$$

Combining Equations 103, 108, and 114,

$$\Omega = \frac{k S_f}{C_1 T_h^4} \left[K_2 + \frac{1}{K_1} \int_{K_1 K_2}^{\omega_h} d\omega \right] \left[\frac{T_c K_1 f'(\omega_h)}{\frac{1}{K_1} \int_{K_1 K_2}^{\omega_h} d\omega} \right] \quad (115)$$

However, by combining Equations 85, 87, 95, and 115,

$$\Omega = \frac{f'(\omega_h) \left[K_1 K_2 + \int_{K_1 K_2}^{\omega_h} d\omega \right]}{\left[f(\omega_h) \right]^4 \int_{K_1 K_2}^{\omega_h} d\omega} \quad (116)$$

The desired results can be obtained using these equations and a digital computer. Details of the procedure can be best explained by referring to Figure 26.

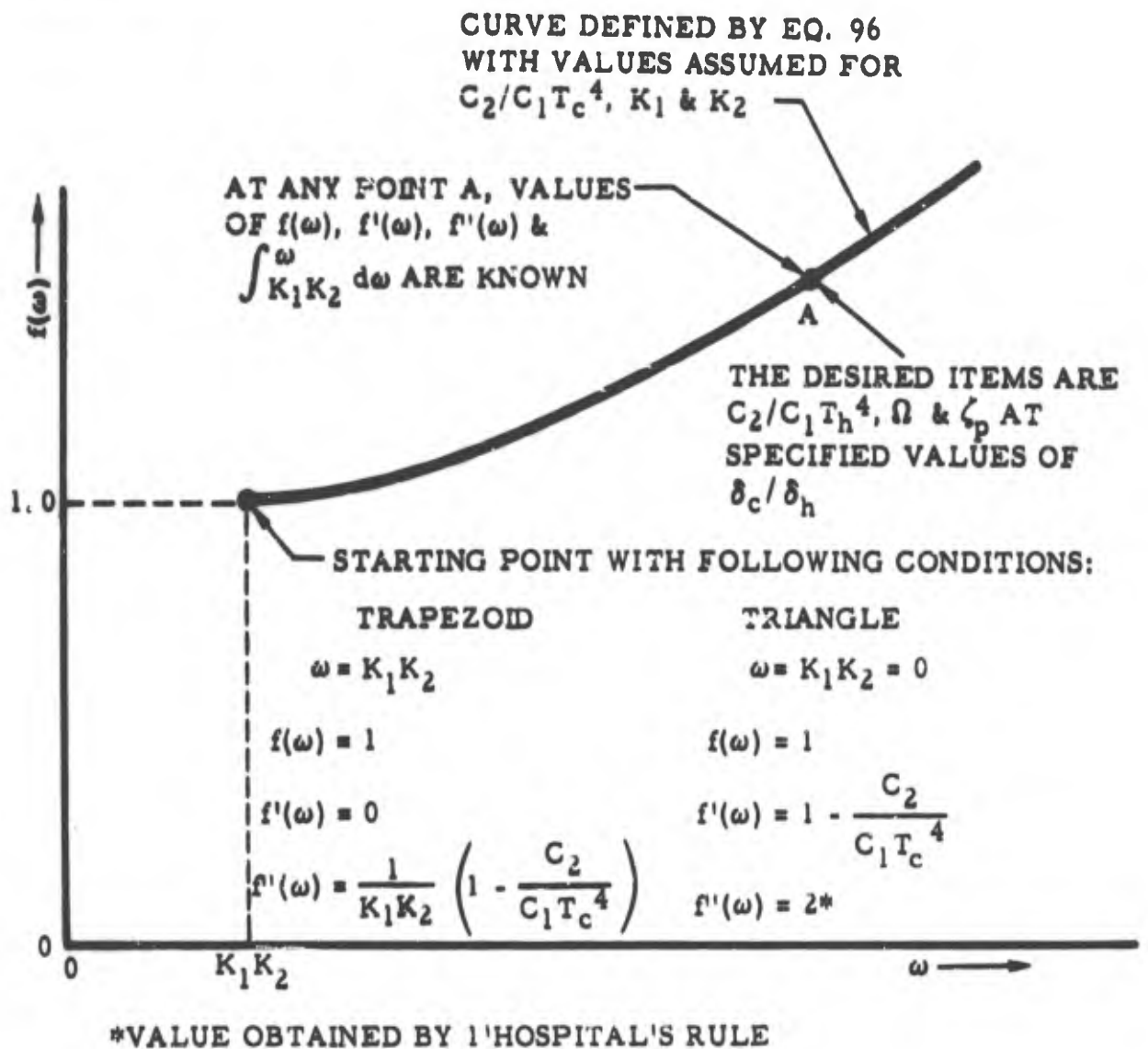


Figure 26. Relationship of ω to $f(\omega)$ for Triangular and Trapezoidal Fins

For an assumed set of values for $C_2/C_1 T_c^4$, K_1 , and K_2 , a curve such as that illustrated in Figure 26 can be obtained by the numerical integration of Equation 96. During the iteration process, the known differential quantities can be used to compute the desired items by using Equations 100, 110, and 116. However, for the purposes of obtaining useful points along the curve, only those giving prescribed values of δ_c/δ_h need be considered. The environmental parameter, effectiveness, and profile number (as well as the desired thickness ratio δ_c/δ_h) were printed out by the computing machine at these prescribed points. The process was repeated several times for successive changes in one of the initial variables.

The actual programming for most of the work presented here was for a fixed value for both $C_1 T_c^4$ and δ_c . For a given set of data, a value of C_2 was chosen, and the slope S_f was varied so as to obtain the desired spread of data. The work was then repeated for another value of C_2 with a variety of slopes. The corresponding data for successive runs were plotted on a double graph, as shown in Figure 27. The values of effectiveness and

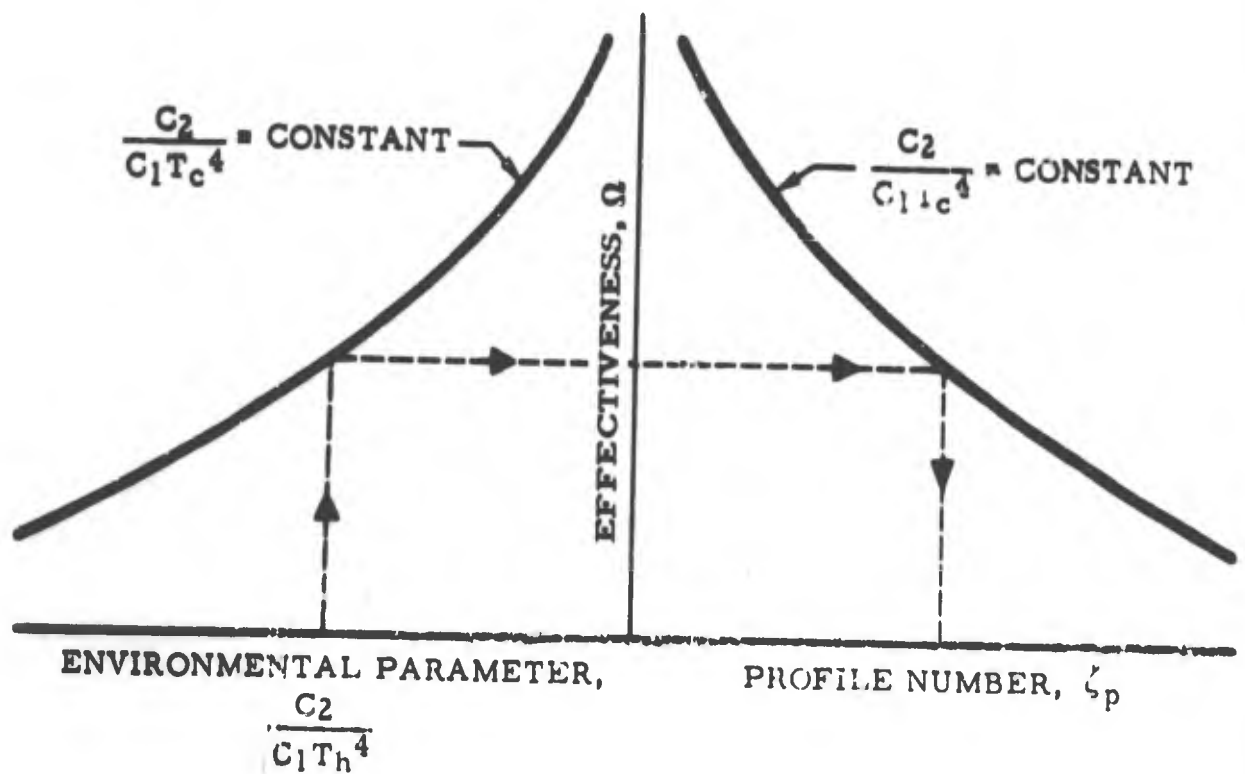


Figure 27. Relationship of Fin Effectiveness to Environmental Parameter and Profile Number of Triangular and Trapezoidal Fins

profile number, for the desired environmental parameters, were then obtained by following the dashed line from the desired environmental parameter to the profile number as illustrated.

Obtaining data for the triangular fin is somewhat easier than for the trapezoidal fin. In this case, $\delta_c = K_2 = 0$, and the data can be printed out from the machine at any desired value of the environmental parameter. The data can then be used directly and no cross-plotting is necessary.

OPTIMUM-WEIGHT DESIGN

Equation 113 can be modified to take the form

$$q_f = \frac{C_1 T_h^3 L_h^2}{\delta_h} (\delta_h L_h) (k T_h L_w) \left(\frac{\Omega}{L_h^2} \right) \quad (117)$$

An expression for the weight of a trapezoidal fin is

$$W_f = \frac{\rho L_w L_h \delta_h}{2} \left(1 + \frac{\delta_c}{\delta_h} \right) \quad (118)$$

Combining Equations 117 and 118,

$$q_f = \zeta_p \left[\frac{2W_f k T_h}{\rho \left(1 + \frac{\delta_c}{\delta_h} \right)} \right] \left(\frac{\Omega}{L_h^2} \right) \quad (119)$$

Substituting an expression for L_h obtained from Equation 113,

$$q_f^3 = \zeta_p \left[\frac{2W_f k T_h^9 C_1^2 L_w^2 \Omega^3}{\rho \left(1 + \frac{\delta_c}{\delta_h} \right)} \right] \quad (120)$$

Then, in order to simplify Equation 120, let

$$K_3 = \frac{2W_f k T_h^4 C_1^{2.2} w}{\rho \left(1 + \frac{\delta_c}{\delta_h}\right)}$$

so that

$$q_f^3 = K_3 \zeta_p \Omega^3 \quad (121)$$

In differential form, Equation 121 becomes

$$3q_f^2 dq_f = K_3 (\Omega^3 d\zeta_p + 3\zeta_p \Omega^2 d\Omega) \quad (122)$$

To determine the relationship producing minimum weight, Equation 122 is equated to zero, or

$$\Omega^3 d\zeta_p + 3\zeta_p \Omega^2 d\Omega = 0$$

and

$$\Omega d\zeta_p + 3\zeta_p d\Omega = 0$$

Then

$$\frac{d\Omega}{\Omega} = -\frac{1}{3} \left(\frac{d\zeta_p}{\zeta_p} \right)$$

$$d \log \Omega = -\frac{1}{3} d \log \zeta_p$$

so that

$$\frac{d \log \Omega}{d \log \zeta_p} = -\frac{1}{3} \quad (123)$$

The optimum-weight configuration is then located at a point where the curves plotted on log paper, of the relationship of effectiveness Ω to profile number ζ_p have a slope of $-1/3$.

DESIGN CURVES

From the data computed for trapezoidal and triangular fins, a comparison of several types of profiles was plotted in Figure 28 for two environment parameters. The flat plate has the highest effectiveness, for a given profile number, while the constant temperature-gradient has the lowest. However, it must be remembered that the flat plate is also the heaviest. The flat plate weighs twice as much as a triangular fin of the same root thickness and transmits only about 12 percent more heat (in the vicinity of the theoretical profile). Therefore, an appreciable weight saving is realized by using the triangular profile. A similar but not nearly so striking comparison can be made between triangular and constant temperature-gradient fins, with the latter having the advantage. The curve separation is slightly greater for free space operation ($C_2 = 0$) than for operation in the other environment. Actually, the little difference in effectiveness between the different profiles may be somewhat surprising.

Data for trapezoidal fins with thickness ratios δ_c/δ_h of 0.75, 0.50, and 0.25 (triangular) are shown in Figures 29 through 32 for a wide variety of environmental parameters and for profile numbers up to approximately 2.0. Theoretical profile points or conditions of minimum weight were obtained by plotting the data shown in Figures 33 through 36 and transferring the tangent points back to Figures 29 through 32. All curves are uniform, and the data can be used in a similar manner as for flat or constant temperature-gradient profiles.

It can be seen in Figures 33 through 36 that the curvature of the lines is so slight that the exact points of tangency are difficult to locate. This makes the theoretical profile difficult to define exactly. However, fairly wide deviations from the theoretical profile can be tolerated without large weight penalties.

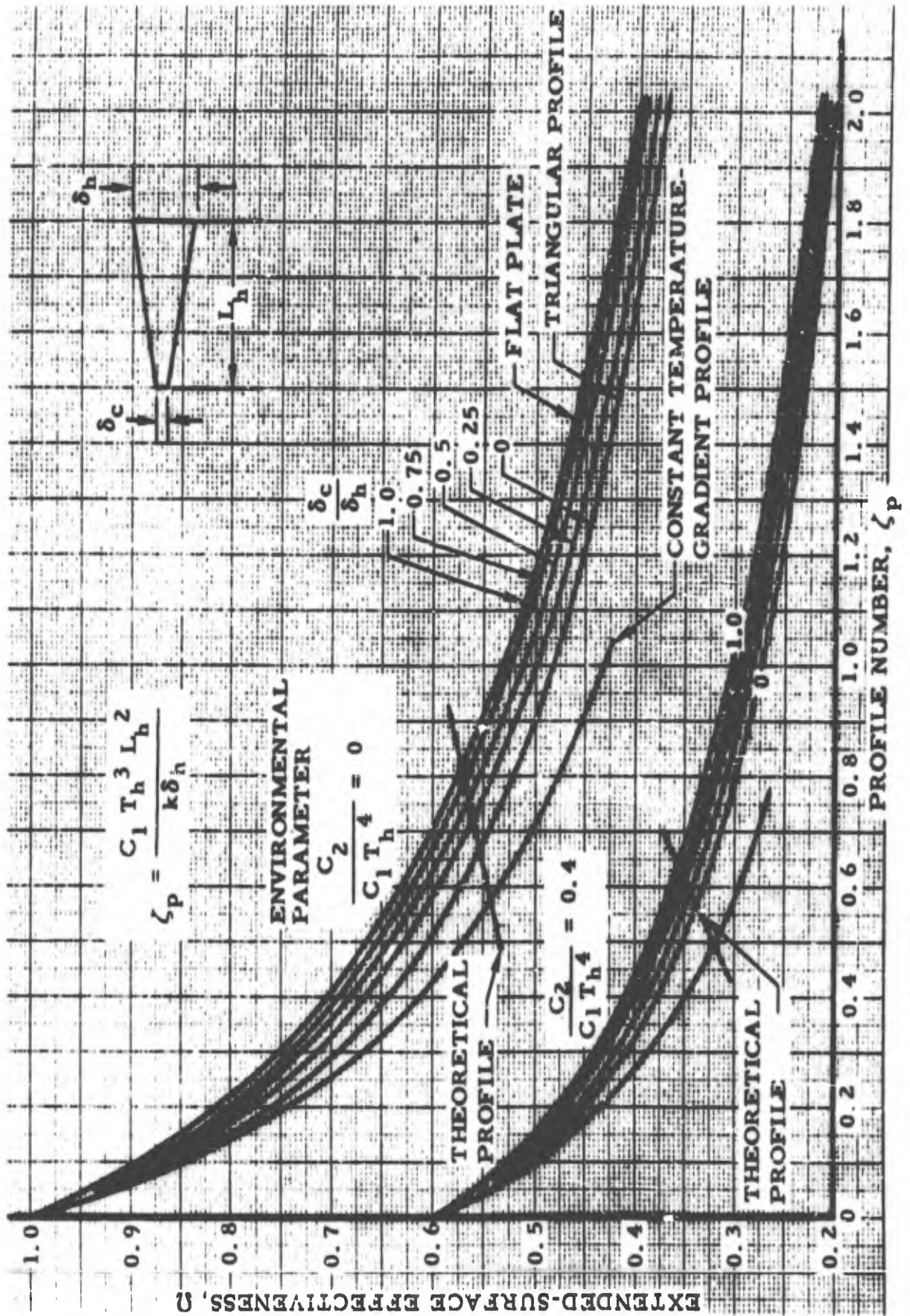


Figure 28. Relationship of Fin Effectiveness to Profile Number for Extended-Surface Fins (Two Environmental Parameters)

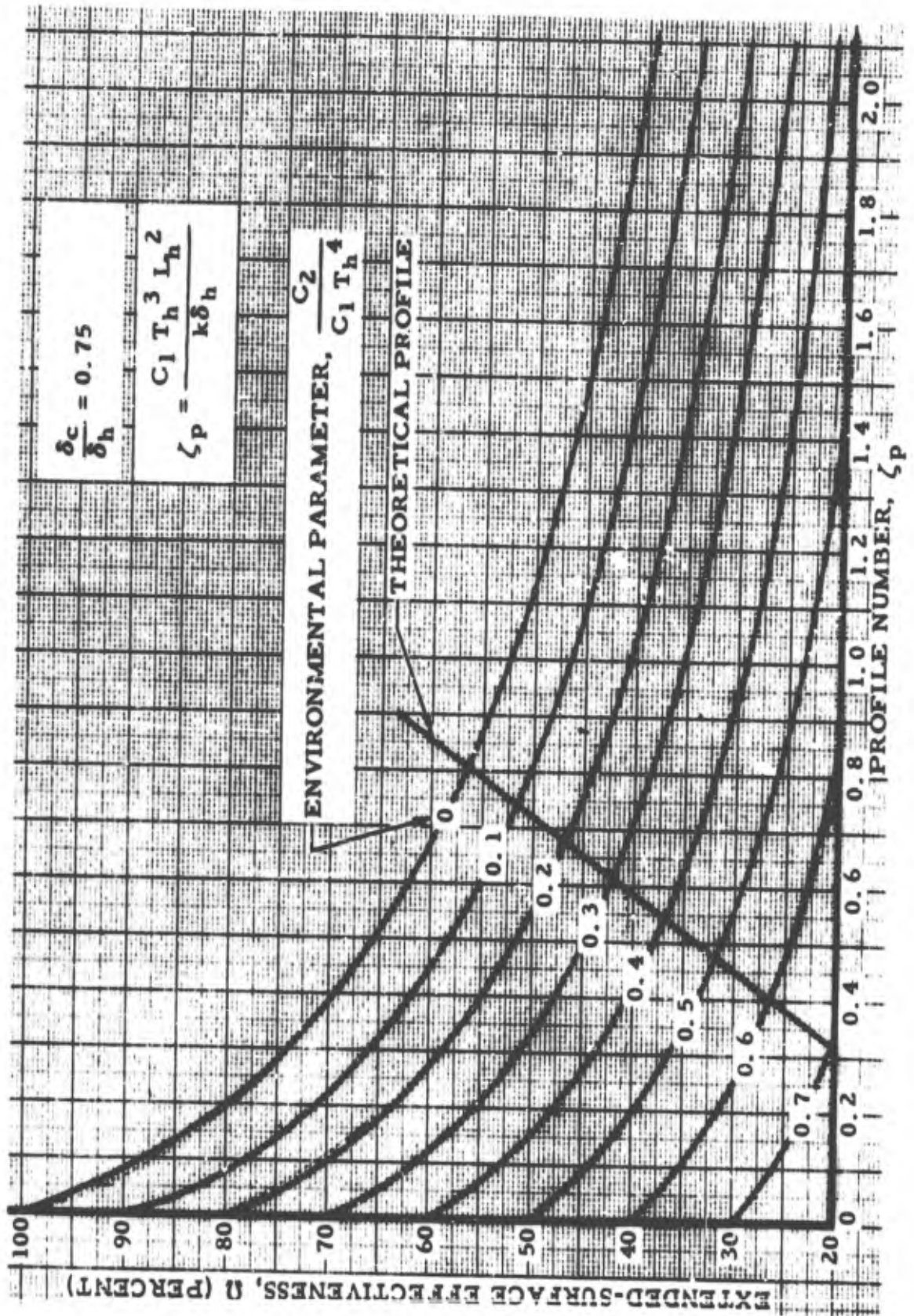


Figure 29. Relationship of Fin Effectiveness to Profile Number for Trapezoidal Fin ($\delta_c / \delta_h = 0.75$)

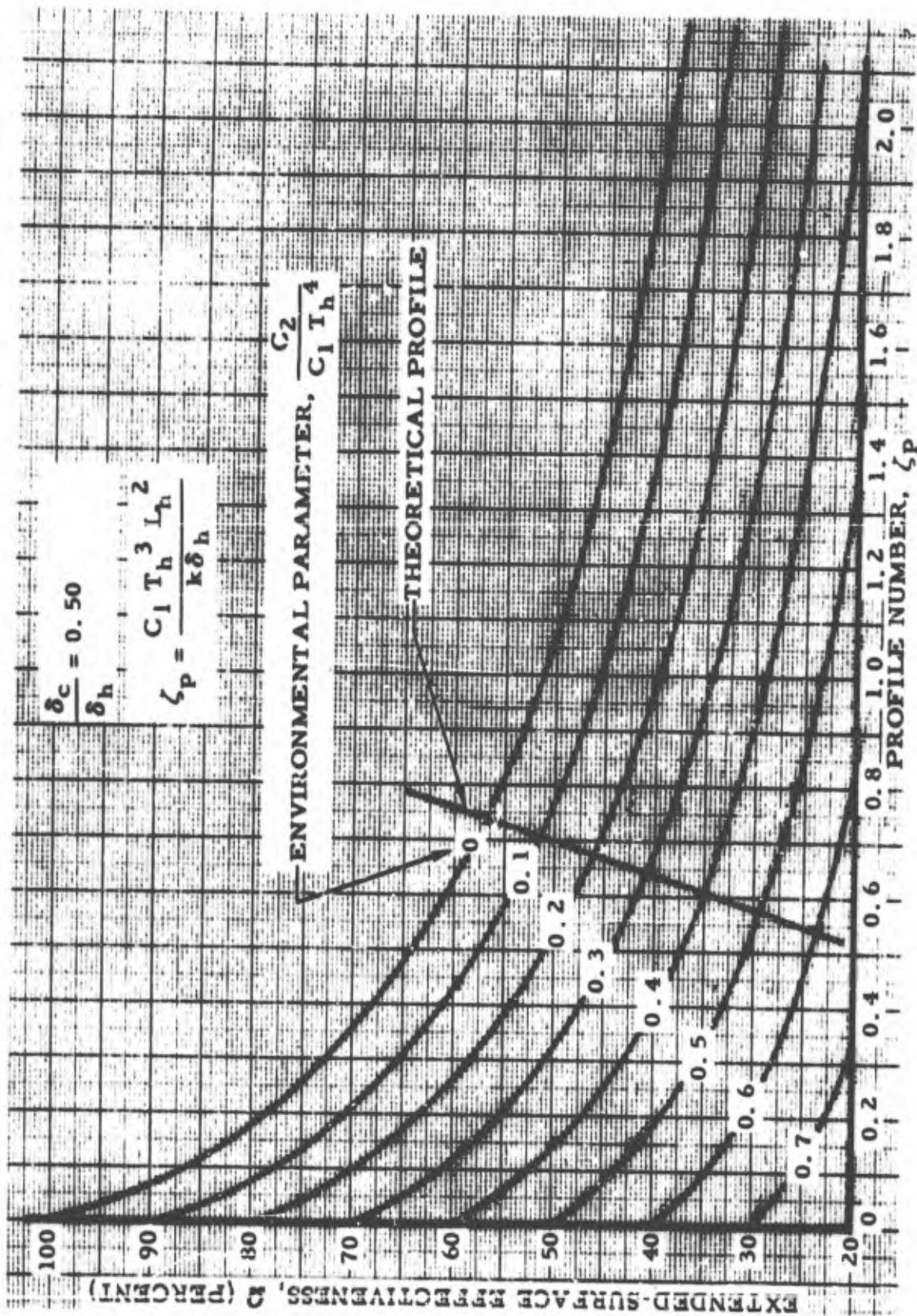


Figure 30. Relationship of Fin Effectiveness to Profile Number for Trapezoidal Fin ($\delta_c/\delta_h = 0.50$)

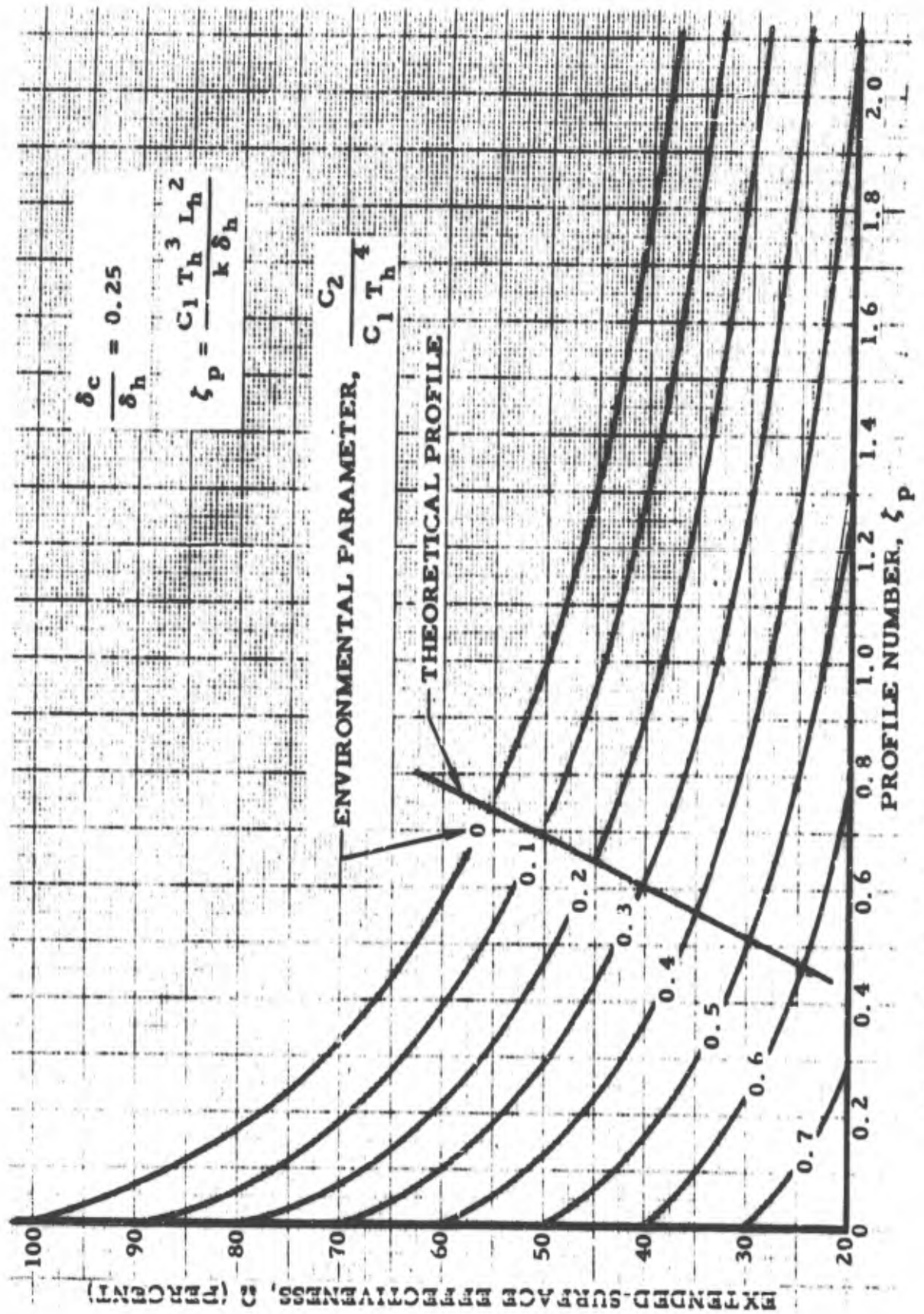


Figure 31. Relationship of Fin Effectiveness to Profile Number for Trapezoidal Fin ($\delta_c/\delta_h = 0.25$)

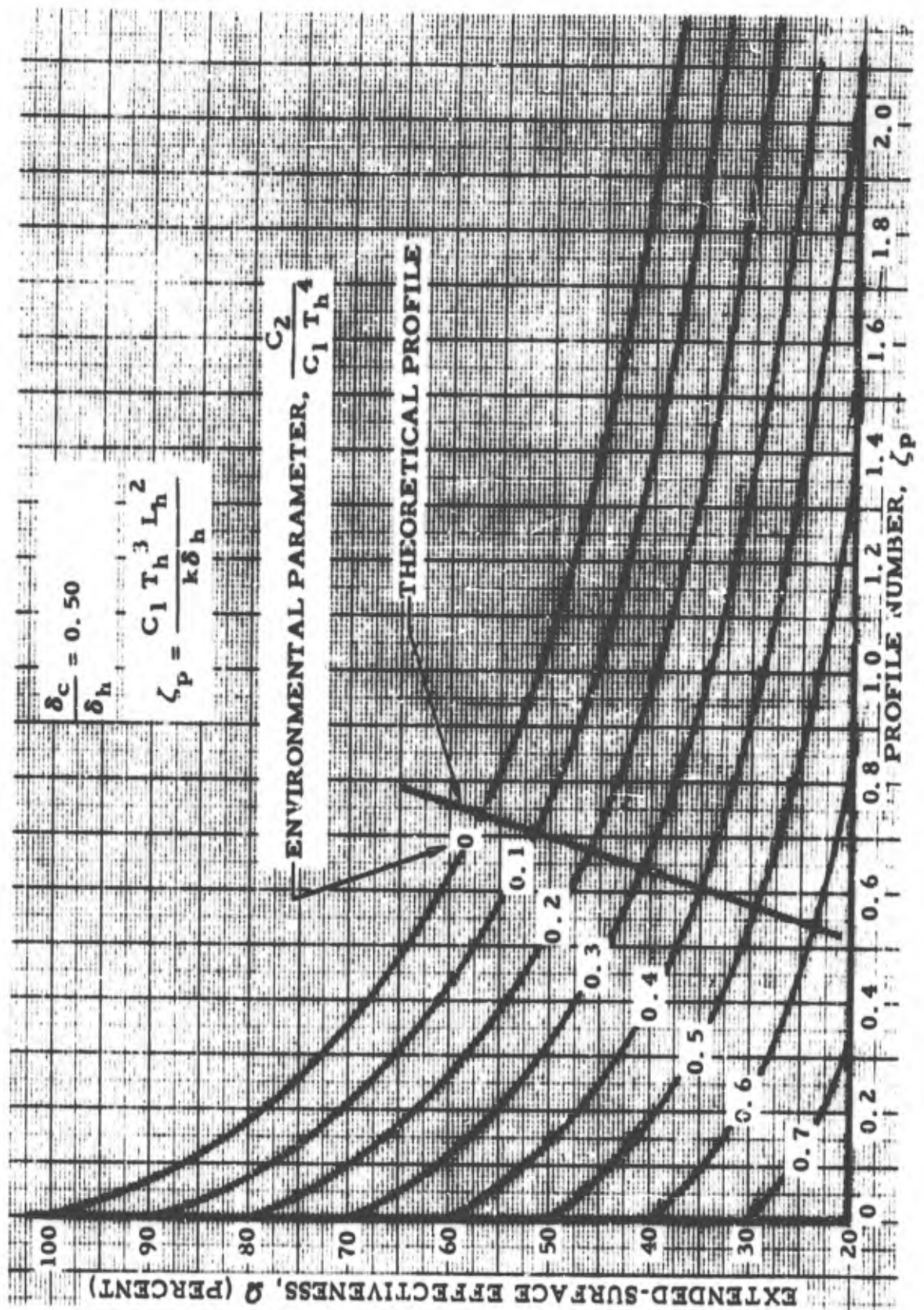


Figure 30. Relationship of Fin Effectiveness to Profile Number for Trapezoidal Fin ($\delta_c/\delta_h = 0.50$)

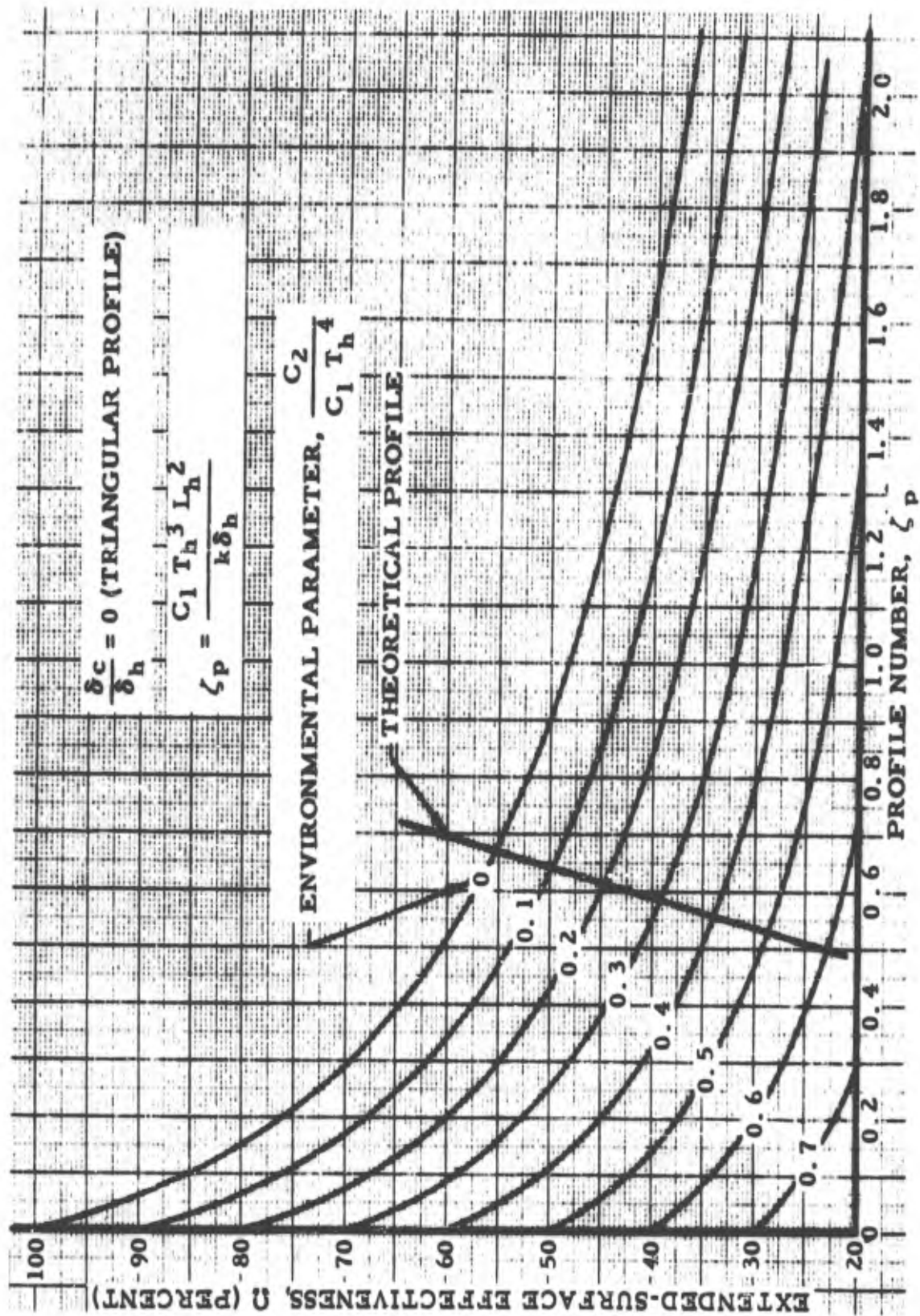


Figure 32. Relationship of Fin Effectiveness to Profile Number for Triangular Fin ($\delta_c/\delta_h = 0$)

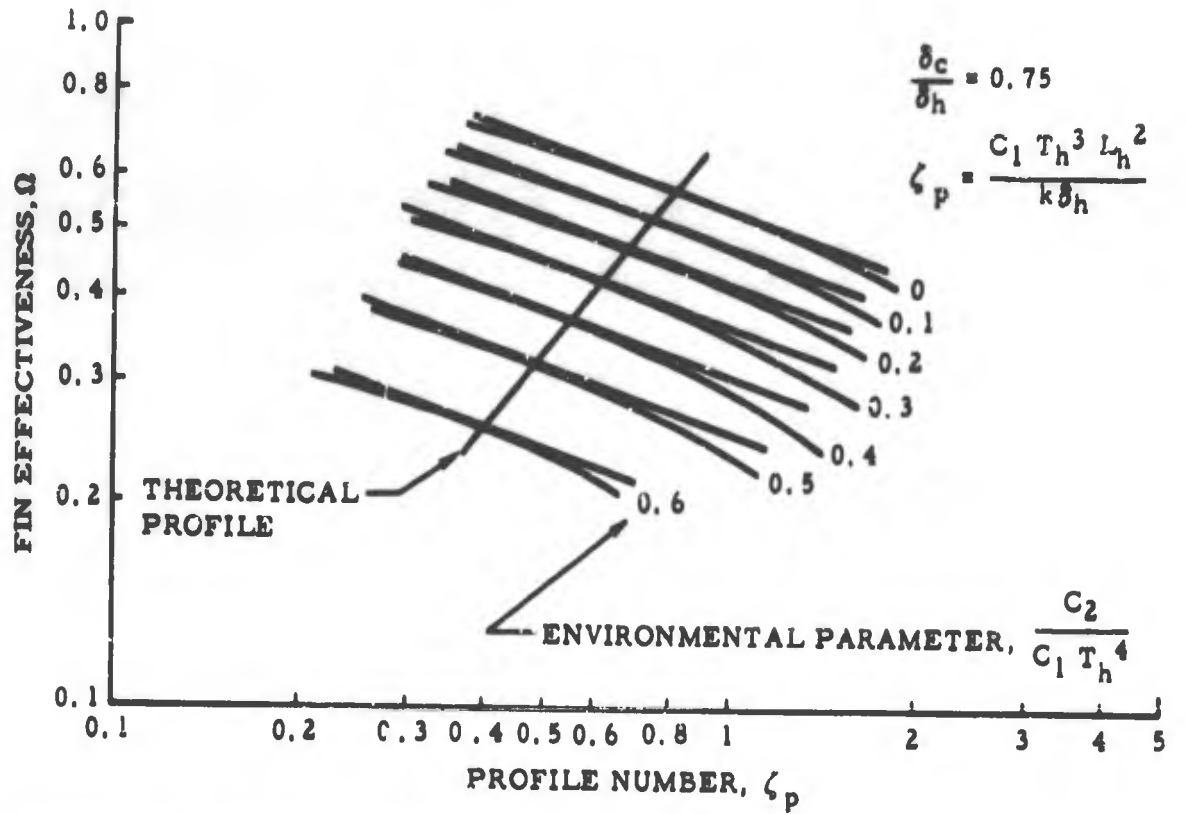


Figure 33. Determination of Theoretical Profile for Trapezoidal Fin ($\delta_c/\delta_h = 0.75$)

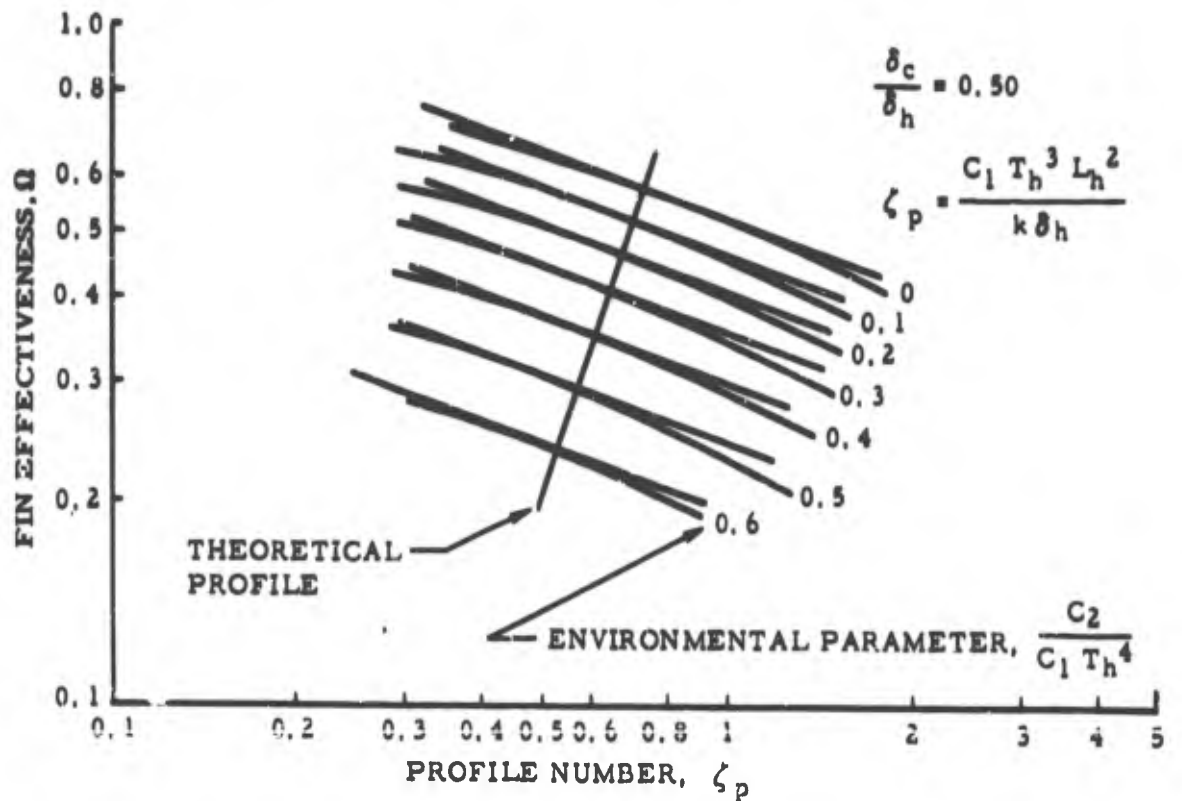


Figure 34. Determination of Theoretical Profile for Trapezoidal Fin ($\delta_c/\delta_h = 0.50$)

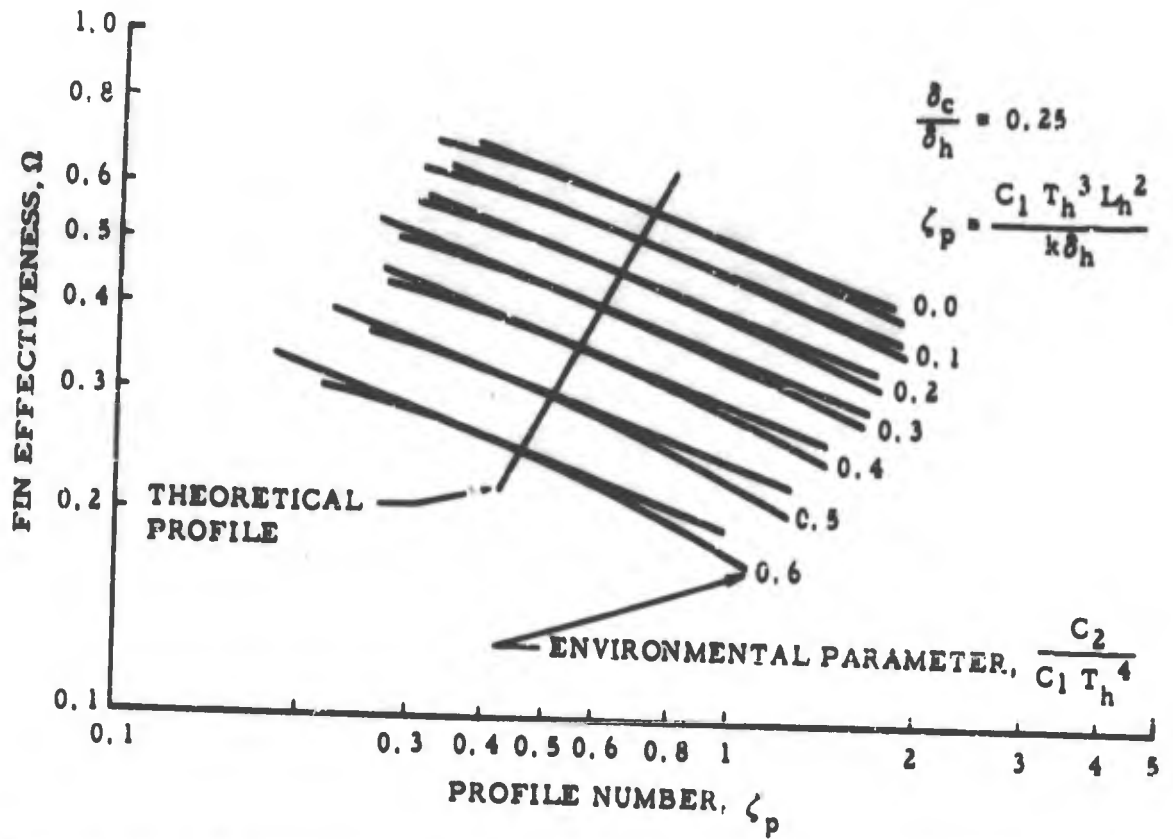


Figure 35. Determination of Theoretical Profile for Trapezoidal Fin ($\delta_c/\delta_h = 0.25$)

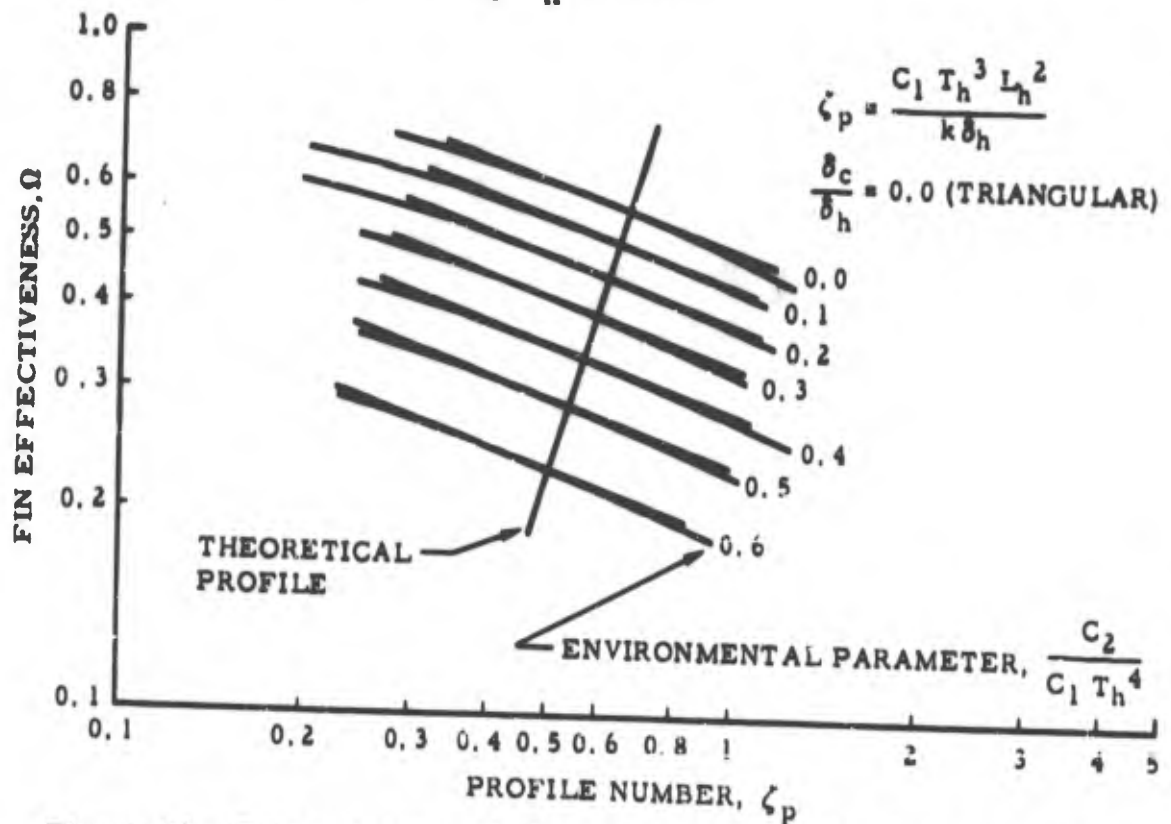


Figure 36. Determination of Theoretical Profile for Triangular Fin ($\delta_c/\delta_h = 0$)

RADIANT HEAT TRANSFER FROM TRAVELING BELT

The use of a traveling belt as a space radiator has been recently advocated for satellites. The advantages claimed are its ability to operate in spite of damage by meteoroids, to be rolled into a small package at take-off, and to meet changing load requirements by changes in speed.

In operation, a section of the belt is in contact with part of the surface of a rotating drum. The drum acts as a sink for the heat to be rejected from the vehicle. The heated segment of the belt moves out so that heat can be radiated into space. Figure 37 is a schematic representation of the system.

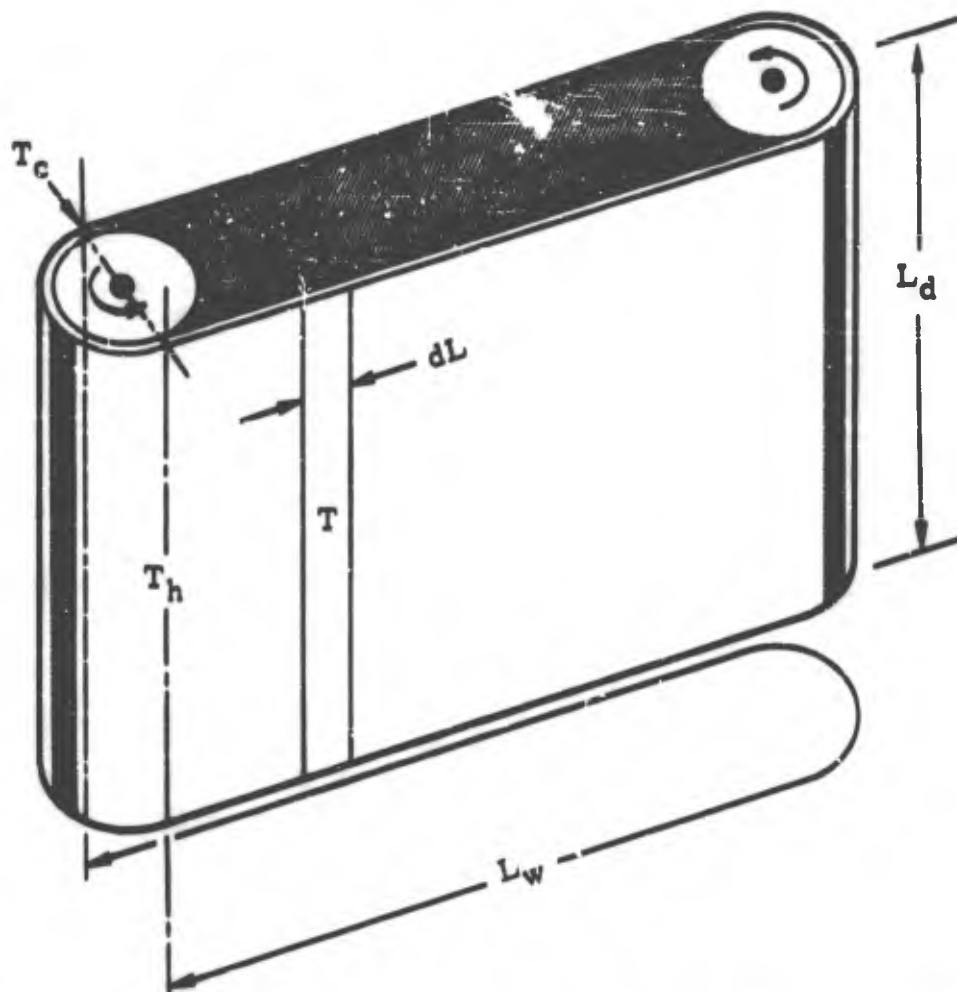


Figure 37. Dimensional Relationships of Traveling Belt Space Radiator

NOMENCLATURE

C_1	Radiation constant, $\sigma (\epsilon_a + \epsilon_b)$, Btu/(sq ft)(hr)(°R) ⁴
C_2	Radiation constant, heat received from environment by belt, Btu/(sq ft)(hr)
c	Specific heat of belt material, Btu/(lb)(°R)
L_d	Belt width, ft
L_w	Effective length of belt, ft
dL	Length of element of belt, ft
q	Heat transfer rate, Btu/hr
T	Temperature at point on belt, °R
T_c	Temperature at cold end of belt, °R
T_h	Temperature at hot end of belt, °R
V	Belt velocity, ft/hr
W_b	Weight rate of belt travel, lb/hr
δ	Belt thickness, ft
ρ	Belt density, lb/cu ft
ψ_2	Radiation number, nondimensional

MATHEMATICAL ANALYSIS

The heat radiated from an element of the belt is

$$dq = (C_1 T^4 - C_2) L_d dL \quad (124)$$

Difficulty will be encountered in evaluating C_2 exactly because it is dependent upon the view factor between the element and the opposite side of the belt and the drum or rollers. The temperature of the opposite side of the belt and the idling roller may also be elusive. All heat may be assumed, for some configurations, to be transferred from the outside of the belt, or an average

temperature of the opposite face may be assumed. Equation 124 can then be solved without difficulty.

Another expression for the heat given up by the element of the belt is

$$dq = -W_b c dT \quad (125)$$

Equating Equations 124 and 125

$$-W_b c dT = (C_1 T^4 - C_2) L_d dL \quad (126)$$

Arranging in a form for integration,

$$\int_0^{L_w} dL = -\frac{W_b c}{L_d} \int_{T_h}^{T_c} \frac{dT}{C_1 T^4 - C_2} \quad (127)$$

The integration of Equation 127 leads to complex relationships, and a step-by-step procedure can be found in Section V of this report. The integrated form of Equation 127 may be written as

$$L_w = \left(\frac{W_b c}{6C_1 T_h^3 L_d} \right) \psi_2 \quad (128)$$

The term ψ_2 is defined as a radiation number and its mathematical expression is given in Equation 163. Values of this term for various temperature ratios and environmental parameters are plotted in Figure 56.

An expression for the weight rate at which the belt travels is

$$W_b = \rho V \delta L_d \quad (129)$$

Substituting Equation 129 into Equation 128,

$$L_w = \left(\frac{\rho V c \delta}{6C_1 T_h^3} \right) \psi_2 \quad (130)$$

The distance L_w required to cool the belt from temperature T_h to T_c can be determined from Equation 130. If L_w is known, ψ_2 can be evaluated and temperature T_c computed.

DESIGN OF CONDENSERS FOR OPERATION IN SPACE

Analyses have been made of such heat radiating surfaces as plates, fins, and moving belts. The purpose of this section is to present the procedures and data needed to design an optimum-weight condenser intended for operation in space or on the lunar surface.

The heat to be rejected from space vehicles or extraterrestrial installations will be primarily from power-generating or refrigeration equipment, the chief difference in these being their temperature. The heat to be radiated may be assumed here to have originated at either source. This analysis of condenser design is based upon a paper by D. B. Mackay (Reference 13). The presentation of the interradiation correction factor and the first two sample problems to illustrate the optimization procedures are new and do not appear in Reference 13.

NOMENCLATURE

- A_d Inside cross-sectional area of duct, sq ft
- C_1 Radiation constant, $\sigma(\epsilon_a + \epsilon_b)$, Btu/(sq ft)(hr)(° R⁴)
- C_2 Radiation constant, heat received from environment by unit of fin area, Btu/(sq ft)(hr)
- D_i Inside diameter of circular section duct, ft
- D_o Outside diameter of circular section duct, ft
- F_a Radiation form factor for one side of fin, nondimensional
- F_b Radiation form factor for other side of fin, nondimensional
- F_r Interradiation correction factor, nondimensional
- h Heat transfer coefficient, Btu/(sq ft)(hr)(° R)
- h_{fg} Latent heat of vaporization or condensation, Btu/lb
- K_1 Aggregate of constant terms, ft

K_2	Aggregate of constant terms, ft
k	Thermal conductivity of fin material, Btu/(hr)(ft)(°R)
L_d	Duct width, ft
L_e	Equivalent length, ft
L_h	Length of extended surface, ft
L_w	Length of condenser section (parallel to tube), ft
P	Effective wetted perimeter of vapor passageway, ft
P_t	Total wetted perimeter of vapor passageway, ft
q	Heat transfer rate (during condensation), Btu/hr per section
q_d	Heat transfer rate from entire duct surface, Btu/hr per section
q_f	Heat transfer rate from fin, Btu/hr per section
q_t	Heat transfer rate from one-quarter of tube surface, Btu/hr per section
S_c	Solar constant, Btu/(hr)(sq ft)
T_f	Temperature of fluid in duct, °R
T_h	Temperature of hot end of plate (root), °R
T_m	Temperature of surface of environment, °R
T_w	Temperature of tube wall, °R
V	Velocity of fluid at entrance of duct, ft/hr
v	Specific volume of vapor, cu ft/lb
v_f	Specific volume of saturated liquid, cu ft/lb
v_{fg}	Change of specific volume of fluid during condensation, cu ft/lb
v_g	Specific volume of saturated vapor, cu ft/lb
W	Weight of section of condenser, lb/ft of length
W_d	Weight of vapor duct, lb per section

- W_f Weight of fin, lb per section
 W_t Weight of circular section tube, lb/ft of length
 w Weight rate of fluid being condensed, lb/hr
 x Quality of fluid entering condenser, nondimensional
 α_a, α_b Absorptivity of surfaces, nondimensional
 δ_c Extended surface thickness at cold end, ft
 δ_d Thickness of wall of vapor passageway, ft
 δ_h Extended surface root thickness, ft
 ϵ_a, ϵ_b Emissivity of surfaces, nondimensional
 θ_m Angle between sun's rays and a normal to environmental surface, deg
 θ_p Angle between sun's rays and a normal to plate surface, deg
 ζ_p Extended-surface profile number, nondimensional
 ζ_w Extended-surface weight number, nondimensional
 ζ_d Extended-surface differential ratio number, nondimensional
 ρ Density of condenser material, lb/cu ft
 ρ_m Reflectivity of environmental surface, nondimensional
 σ Stefan-Boltzmann constant, 0.1713×10^{-8} Btu/(hr)(sq ft)(°R)⁴
 Ω Extended surface effectiveness, nondimensional
 Ω_a Actual integrated effectiveness of plate surface, nondimensional

MATHEMATICAL ANALYSIS

Rectangular Vapor Duct

Condensers for space applications differ from those of land-based installations principally in the method of heat dissipation. In space, heat must be rejected by radiation, whereas convection plays the most important role in gaseous environments. Space condensers, as a result, will usually consist of ducts with extended surfaces, the overall configuration being essentially a flat plane. To design an optimum condenser, it is therefore

necessary to consider the heat to be taken from the fluid, the surface over which this transfer will occur, the area from which heat will be rejected to space, and the weight of the related ducts and extended surfaces.

The configuration of Figure 38 may be assumed to represent a section of a typical space condenser. The heat transferred from the small external vertical surface of the vapor passageway may be neglected. Therefore, from a given linear section, the heat rejected is that from the top and bottom surfaces of the duct or vapor passageway and from the top and bottom of the extended surfaces. If the emissivity of all surfaces is the same, then

$$q = (C_1 T_w^4 - C_2) L_d L_w + 2C_1 T_w^4 \Omega L_h L_w \quad (131)$$

A correction factor F_r may be applied to Equation 131 to account for the interradiation between the duct and the extended surfaces. Equation 131 then becomes

$$q = \left[(C_1 T_w^4 - C_2) L_d L_w + 2C_1 T_w^4 \Omega L_h L_w \right] F_r \quad (132)$$

Rearranging Equation 132,

$$q = (C_1 T_w^4 - C_2) L_w \left\{ \left(L_d + \frac{2\Omega L_h}{1 - \frac{C_2}{C_1 T_w^4}} \right) F_r \right\} \quad (133)$$

The bracketed term may be considered to be the width of an area which is equivalent in radiation effect to a section of the condenser such that

$$q = (C_1 T_w^4 - C_2) L_w L_e \quad (134)$$

where L_e is the equivalent length, or

$$L_e = \left(L_d + \frac{2\Omega L_h}{1 - \frac{C_2}{C_1 T_w^4}} \right) F_r \quad (135)$$

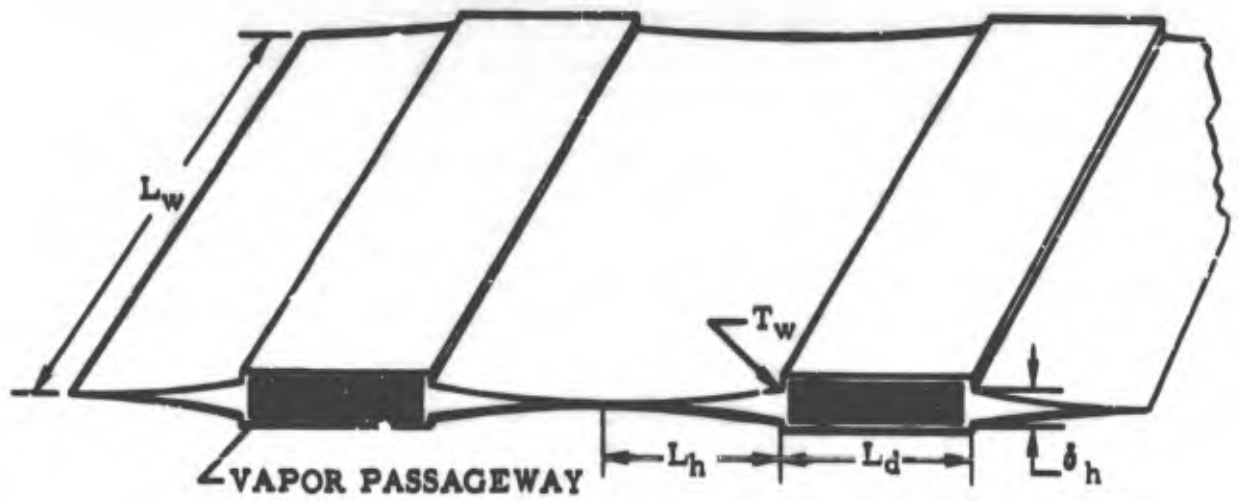


Figure 38. Dimensional Relationships of Rectangular-Duct Condenser

Interradiation Correction Factor

Although the correction factor is negligible for the flat ducts of Figure 38, there may be a considerable interchange for an arrangement of large tubing and extended surface such as that in Figure 39. The direct effect of this interchange is an increase in the temperature of the extended surface, which results in an increase in radiation rate from these surfaces. For tubes of relatively small diameter, interchange effects are small, and the projected diameter D_o can be used as a constant-temperature duct width to replace the term L_d in Equation 135. When large-diameter tubes are encountered, it is advisable to determine a correction factor that is at least approximately correct.

Values of the correction factor F_r are not yet available for all types of extended surfaces. The special case of the flat plate in free space with a surface emissivity of 1.0 is considered in Reference 14. These data have been analyzed and put into a form compatible with the present discussion. An expression for the correction factor is found in the following manner.

Equation 24b of Reference 14 was rephrased to conform with the nomenclature of this report and adapted to the configuration of Figure 39. It becomes

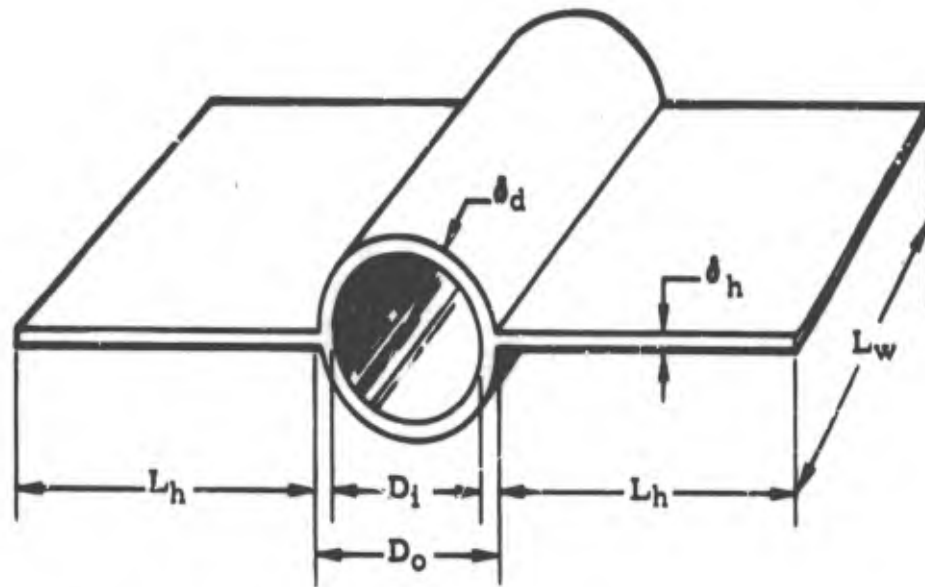


Figure 39. Dimensional Relationships of Cylindrical-Tube Condenser With Extended Surfaces of Constant Thickness

$$q = C_1 T_w^4 L_w \left\{ \frac{\pi}{2} D_o \left[\frac{4q_t}{C_1 T_w^4 \left(\frac{\pi}{2}\right) D_o L_w} \right] + 2L_h \Omega \left(\frac{\Omega_a}{\Omega} \right) \right\} \quad (136)$$

where Ω_a is an integrated effectiveness accounting for losses in heat transfer caused by the interception of radiant energy by tube surfaces and by the non-uniform distribution of temperature in the extended surfaces. Rewriting Equation 132 for free-space conditions,

$$q = C_1 T_w^4 L_w (D_o + 2\Omega L_h) F_r \quad (137)$$

Equating Equations 136 and 137 and rearranging,

$$F_r = \frac{\frac{\pi}{2} \left(\frac{D_o}{L_h} \right) \left(\frac{8q_t}{C_1 T_w^4 \pi D_o L_w} \right) + 2\Omega \left(\frac{\Omega_a}{\Omega} \right)}{\frac{D_o}{L_h} + 2\Omega} \quad (138)$$

Values of Ω_a/Ω and of $8q_t/C_1 T_w^4 \pi D_o L_w$ are found in Reference 14 (Figures 2 and 4), plotted against profile number ζ_p . The conventional plate effectiveness Ω may be obtained from the Reference 14 or from Figure 5 of this document. These data were used to prepare the relationships of Figure 40. The dashed lines of Figure 40 signify that these curves were prepared from extrapolated data. The significance of the theoretical profile will be discussed later.

The highest practical limit of the profile number ζ_p and of the dimensional parameter D_o/L_h is about 1.0. This results in a probable maximum correction factor of 1.07, a surprisingly small number.

It would appear, therefore, that use of projected areas of the tube in the calculations is highly accurate. A further conclusion is that the correction factors for all extended surfaces (triangular, trapezoidal, and constant temperature-gradient fins) also require small correction factors, if any. Figure 40, then, can well serve for all extended surfaces and for all environments.

Duct Length and Diameter Relationships

The heat radiated from fin or plate surfaces is equal to that given up during the condensation of the vapor in the ducts. Assuming no subcooling of the condensate, this may be expressed as

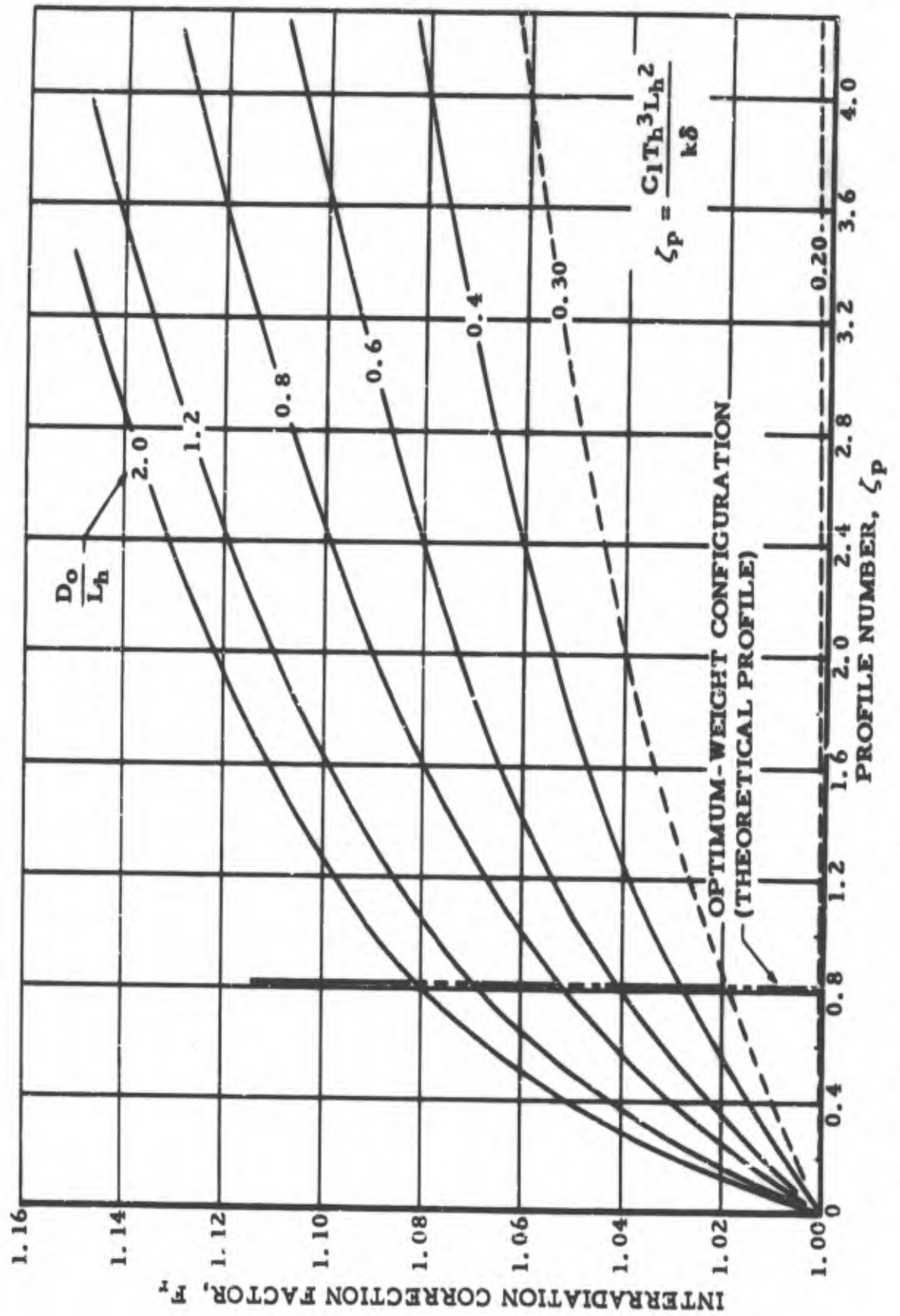


Figure 40. Correction Factors for Irradiation Between Condenser Tubes and Extended Surfaces

$$q = x h_{fg} w = x h_{fg} \left(\frac{A_d V}{v} \right) = x h_{fg} \left(\frac{A_d V}{v_f + x v_{fg}} \right) \quad (139)$$

where x is the quality of the entering vapor.

If the quality of the entering vapor mixture is high, Equation 139 may be reduced to

$$q = \frac{h_{fg} A_d V}{v_g} \quad (140)$$

Combining Equations 134 and 140,

$$L_w = \frac{h_{fg} A_d V}{v_g (C_1 T_w^4 - C_2) L_e} \quad (141)$$

It is evident from Equation 141 that the duct length L_w becomes fixed only when a duct external configuration and an inlet velocity are specified for a particular vapor. Further fixing of the area A_d causes the length to vary directly and only with the velocity. Fixing of the velocity does not create a direct relationship between length and area because of the implicit presence of the tube diameter D_o in the equivalent length term L_e . The tube length L_w is just long enough to produce complete condensation with no subcooling.

When low-vapor-pressure fluids such as sodium or potassium are to be condensed, the specific volume of the entering vapor is large and the duct length short. To minimize the effect of these conditions on weight, passages which taper to a smaller exit diameter have been proposed.

For a straight circular duct, as in Figure 39, the tube diameter for a given tube length L_w is found by combining Equations 133 and 140.

$$\frac{h_{fg} A_d V}{v_g} = (C_1 T_w^4 - C_2) L_w \left(D_o + \frac{2 \Omega L_h}{1 - \frac{C_2}{C_1 T_w^4}} \right) F_r \quad (142)$$

Since

$$A_d = \frac{\pi D_1^2}{4}$$

$$D_o = D_1 + 2\delta_d \quad (143)$$

Equation 142 becomes

$$D_1^2 - K_1 D_1 - K_1 K_2 = 0 \quad (144)$$

where

$$K_1 = \frac{4v_g L_w F_r (C_1 T_w^4 - C_2)}{\pi h_{fg} V} \quad (145)$$

and

$$K_2 = 2 \left(\delta_d + \frac{\Omega L_h}{1 - \frac{C_2}{C_1 T_w^4}} \right) \quad (146)$$

The only usable root of Equation 144 is found to be

$$D_1 = \frac{K_1}{2} \left(1 + \sqrt{1 + \frac{4K_2}{K_1}} \right) \quad (147)$$

Equation 147, together with Equation 141, is very useful for determining the size of heat exchanger elements. It must be noted that Equations 141 and 147 are mutually dependent. In other words, one of the two dimensions, D_1 or L_h , must be assumed, if only temporarily, before the other can be determined.

The weight of ducts, of any shape, per unit of heat radiated is higher than that of extended surfaces. It is therefore desirable that ducts be relatively small. Diameters, as shown in Equation 147, are strongly influenced by K_1 , which in turn depends directly on the value of the vapor specific volume. It follows that condensers for low-density vapors will tend to be heavier than those for vapors of high density. However, in determining the total weight of an actual condenser, it is necessary to include the weight of fluid it contains. This may be a major part of the total weight.

OPTIMIZATION PROCEDURE

A procedure is given here which can be used in determining the optimum configuration, from a weight standpoint, of a finned radiator-condenser. It will be seen that the procedure is directed primarily toward establishing the configuration of the extended surfaces.

It is not sufficient for optimization to know only the weight and heat transfer characteristics of the profile of an extended surface. For example, equations in Reference 6 predict that the fin weight per Btu will be numerically less for shorter as opposed to longer fin lengths or for thinner as opposed to thicker root sections. A literal extension of this reasoning leads to the incorrect conclusion that the "optimum" fin is of zero length and thickness, leaving the tubes and headers as the total heat transfer systems. A realistic procedure must include the consideration of all the factors which make the heat dissipation system.

The form of a section of the condenser to be considered is shown in Figure 41. The fins form an integral part of the fluid duct, although they are not necessarily of the same material. The optimum values of root thickness δ_h and fin length L_h are to be found.

Three dimensions that can be incremented are indicated as dL_w and the two identical segments marked dL_h . The first results in an increment of the basic condenser length, and the others in increments to the basic fin length. By analyzing the heat transfer and weight of first the basic section and then the differential areas, the optimum configuration can be established. The heat outputs and weights of duct and of fins are computed separately, the total heat transferred q being the sum of the two quantities. Heat transfer from the top and bottom of the duct, assuming no temperature gradient across, is found by the Stefan-Boltzmann equation; heat transfer from the fin sections is found by the equations derived in Section III.

The optimum-weight configuration is the one giving the best ratio of weight to heat transfer, although this may not be the most practicable configuration. For the original condenser section, the ratio is W/q . If the size of the radiator is increased by extending the condenser (e. g., by the addition of dL_w), the ratio of the added weight to the added heat transfer

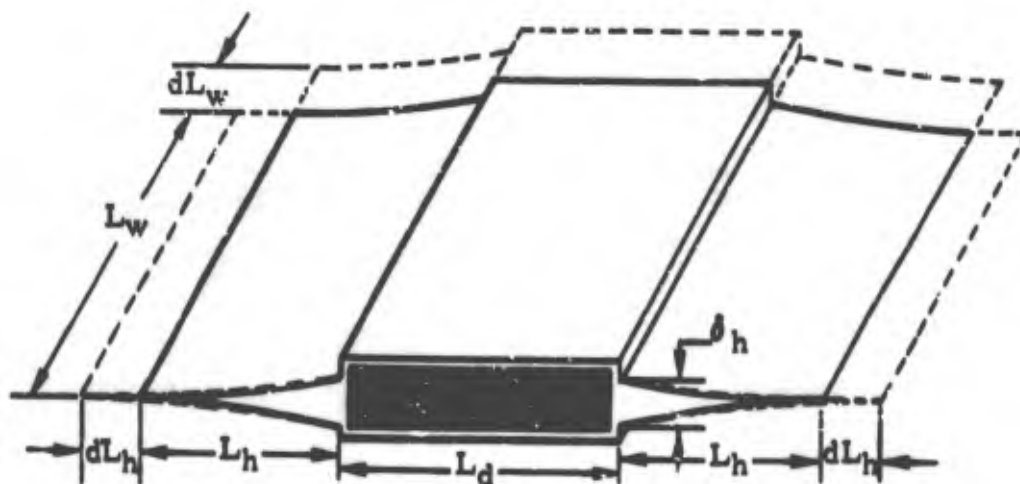


Figure 41. Section of Condenser Showing Incremental Segments

should have the same numerical value as the original ratio, W/q . Changes in flow of the condensing fluid caused by extending tube length are considered negligible.

The ratio of the changes resulting from increasing the fin length is dW_f/dq_f . Ordinarily, this is different from W/q . It should be noted that dW_f does not represent the weight of the added segment dL_h only, because the addition of this segment requires the thickening of the entire fin profile from the root outward. The total change of fin weight is dW_f and the total change of heat transfer is dq_f .

The method of determining the optimum dimensions is now arrived at by the following reasoning. If the ratio dW_f/dq_f is less than the ratio W/q for the original section, it is profitable to reduce the section length L_w and extend the fin length L_h . With this change, the same amount of heat can then be dissipated from a radiator of lower overall weight. Changes in this direction are continued until a point is reached at which dW_f/dq_f is equal to W/q . Since the extension of L_h always causes an increase in the ratio of weight to heat rejected, continuing the extension of fin length beyond the point where the ratios were equal is unprofitable.

Having thus established the optimum lengths L_w and L_h for a given root thickness δ_h , the next step is to investigate the effects of changing the root thickness. This is done by determining the weight/heat transfer ratio for successive decrements in root thickness while maintaining the optimum lengths. The root thickness which yields the lowest ratio is optimum from a weight standpoint. Again, it must be pointed out that the fin thickness for this condition may be too thin for use on an actual vehicle.

The rate-of-change ratio is obtained from Figure 20 where the fin differential ratio number ζ_d is plotted against fin profile number. Recalling that, from Equation 64,

$$\zeta_d = \frac{C_1 T_h^4}{\rho \delta_h} \left(\frac{dW_f}{dq_f} \right)$$

the desired ratio can be obtained for a given root thickness. Since C_1 , T_h , and ρ are known when plotted against fin length, the intersection of this curve with that for W/q fixes the weight-optimum fin length for that fin thickness δ_h . Repeating this process for a series of fin thicknesses, the intersection of the W/q and dW_f/dq_f curves produces a curve, the minimum point of which is the weight-optimum profile. This procedure is presented in detail in illustrative problem 1.

The procedure just outlined is completely satisfactory for many design problems. It should be recognized, however, that a number of omissions make the process not entirely complete. Some of these omissions are the following:

1. The effect of length on pressure drop is not considered.
2. The effects of changes in duct shape (e. g. , tapered tubes) are not considered.
3. Changes in heat transfer rates with fluid state changes are not considered.

A complete analysis should include the weight of the fluid condensing in the duct, its condensation behavior in zero-gravity, latent heat of vaporization, and fluid-to-wall heat transfer characteristics. The foregoing list is not intended to minimize the value of the suggested procedure but rather to point the direction for further investigation. The influence of some of the listed factors is certainly minor at best; however, not enough is presently known to permit any one of them to be discarded.

ILLUSTRATIVE PROBLEMS

As an aid in designing and optimizing a condenser for space use, a number of sample problems are included here. These have been selected to cover as many principles and important points as possible.

Problem 1: Design of Constant Temperature-Gradient Fin for Space Condenser

Given

The condenser of a refrigeration plant is to operate in free space, oriented so that no face is directed toward the sun. The vapor passageway is aluminum tubing and the extended surfaces are of the same material.

Required

To determine the dimensions of a constant temperature-gradient fin of optimum weight to be attached to the vapor passageway.

Data

$$T_h = 215F = 675R$$

$$D_o = 3/8 \text{ in.}$$

$$\delta_d = 0.028 \text{ in.}$$

$$k = 133 \text{ Btu/(hr)(ft)(}^\circ\text{R)}$$

$$\rho = 172.8 \text{ lb/cu ft}$$

$$\epsilon_a = \epsilon_b = 0.95$$

$$\alpha_a = \alpha_b = 0.18$$

$$W_t = 0.037 \text{ lb/ft}$$

$$F_r = 1.00 \text{ (assumed)}$$

Procedure

The heat radiated from a 1-foot section of tubing is found from Equation 137.

$$q_d = C_1 T_h^4 D_o = \sigma(\epsilon_a + \epsilon_b) T_h^4 D_o$$

$$= (0.1713 \times 10^{-8})(0.95 + 0.95)(675)^4 \left(\frac{0.375}{12}\right) = 21.1 \text{ Btu/(hr)(ft)}$$

The steps of the procedure used are as follows:

1. The optimum weight profile number of 0.571 and the fin effectiveness of 0.543 were obtained from Figure 17, at an environmental parameter of 0.
2. A number of fin lengths L_h were assumed.
3. Using these values of L_h and Equation 137, the total heat radiated from a condenser section 1 foot long was determined.
4. The fin root thickness associated with the assumed fin lengths were calculated from Equation 53.
5. Using the profile number of 0.571, a value of 0.288 was obtained from Figure 18 for the weight number ζ_w .
6. Weights for each fin of the set were obtained by using ζ_w in Equation 60.
7. The total weight of two fins and the tube were determined for each set.
8. The weight per unit of heat transfer was obtained by dividing the total weight from step 6 by the total heat transfer from step 3.
9. The results were plotted in Figure 42 as weight per unit of heat transfer versus fin length.

Data fixing other variables was also obtained, using a slightly different procedure. For this part of the analysis:

10. A fin root thickness was specified arbitrarily.
11. A variety of fin lengths L_h were assumed, compatible with this root thickness.
12. The profile number for each fin length was calculated using Equation 53.

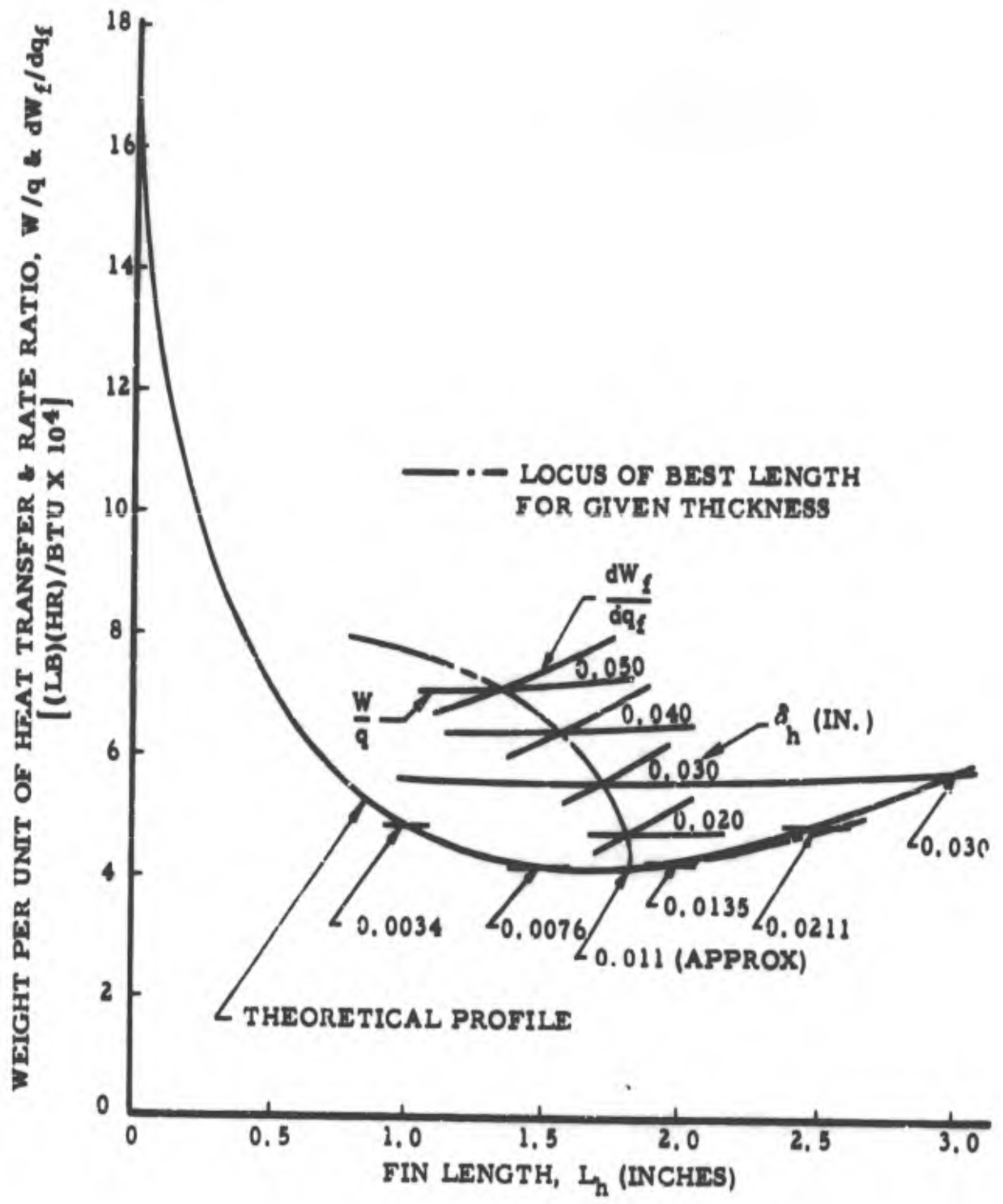


Figure 42. Relationship of Weight Per Unit of Heat Transfer and Rate of Change of Ratio to Fin Length (Problem 1)

13. Using the profile number, the fin effectiveness was found from Figure 17.
14. Using Equation 57 and the assumed fin lengths, the heat transfer from each of a set of 1-foot fins was determined.
15. The total heat transfer was obtained by adding together the heat transferred from the tube and two fins.
16. Using the profile number for each fin of the set, values of the weight number ζ_w were read from Figure 18.
17. Fin weight was then obtained using the thickness assumed in step 10, and the weight number ζ_w from step 16.
18. The total weight of two fins and a tube were then computed.
19. The weight per unit of heat transfer was calculated by dividing the total weight from step 18 by the total heat transfer from step 15.
20. The value of ζ_Δ was read from Figure 20, using the profile number of step 12.
21. Using ζ_Δ (step 20), the root thickness (step 10), and Equation 64, the value of dW_f/dq_f was computed.
22. Steps 10 through 21 were repeated for various root thicknesses.
23. The values for W/q and dW_f/dq_f versus L_h were plotted, as shown in Figure 42.

The pertinent information needed to make a fin selection can be obtained from the curves of Figure 42. The weight per unit of heat transfer along the theoretical profile is shown to be lowest for a root thickness of approximately 0.009 inch and a fin length of 1.82 inch. As expected from the theory, a reasonable tolerance in thickness and length give almost the same results. However, the fabrication of fins so thin in section would be difficult if not impossible. Therefore, it will probably be necessary to use other configurations than that of the theoretically minimum weight.

Comment

The values of W/q for a fixed root thickness are seen in Figure 42 to be very flat over a wide range of fin length. This relationship for a root thickness of 0.030 inch has been extended for emphasis. Using data read from curves such as these, it is impossible to precisely locate the minimum point. A close approach is made by the use of the dW_f/dq_f ratio which

theoretically crosses the W/q curves at the minimum point. Obviously, a deviation from the lowest value will result in only a slight weight penalty.

The locus line through the intersection points demonstrates the potentialities of the system. The lowest point is where the locus line intersects the theoretical profile. For this case, a ratio of weight to heat transfer of 4.25×10^{-4} pound-hours per Btu is obtained. Thicker root sections along the locus line show a rapid rise in the ratio of weight to heat transfer. For root thicknesses greater than 0.050 inch, fin length diminishes rapidly and the computation of intersecting points becomes impossible because of the errors encountered in reading curve values.

It may be desirable from a standpoint of meteoritic protection to use fin lengths greater than those shown by the locus line. The longer fins transmit more heat (at reduced effectiveness) and require less tube length, thereby reducing vulnerability. Shorter lengths may also be considered when radiator area is critical. A shorter fin is more effective and permits a reduction in total radiator area while at the same time dictating an increase in the actual tube area and, therefore, an increase in vulnerability to meteorites. The best fin is that having the optimum combination of practical thickness, low weight per unit of heat transfer, and the required reliability. A more detailed study of manufacturing processes, tolerances, and other factors is needed to fully establish the best fin length and thickness.

Problem 2: Comparison of Flat Plate and Triangular Fin Extended Surfaces

Given

A powerplant condenser is to be installed on the external wall of a space vehicle. The condenser tubes are circular cylinders of stainless steel and the extended surfaces are of the same material.

Required

To determine the dimensions of the weight-optimum flat plate and the weight-optimum triangular fin capable of rejecting the stipulated amount of heat.

Data

$$L_w = 1 \text{ ft}$$

$$T_w = T_h = 700 \text{ F (1160R)}$$

$$D_o = 5/16 \text{ in.}$$

$$\delta_d = 0.010 \text{ in.}$$

$$k = 16.2 \text{ Btu/(hr)(ft)(}^\circ\text{R)}$$

$$\rho = 0.286 \text{ lb/cu in. (tube, plate, and fin)}$$

$$\epsilon = 0.90$$

$$W_t = 0.0313 \text{ lb/ft}$$

$$F_r = 1.00 \text{ (assumed)}$$

$$C_1 T_h^3 = 0.9 (0.1713 \times 10^{-8}) (1160)^3 = 2.43 \text{ Btu/(hr)(sq ft)(}^\circ\text{R)}$$

$$C_1 T_h^4 = 2.43 (1160) = 2820 \text{ Btu/(hr)(sq ft)}$$

From the data, the following evaluations may be made:

$$(a) \quad q_t = C_1 T_h^4 D_o = \frac{2920 (5/16)}{12} = 73.5 \text{ Btu/(hr)(ft)}$$

$$(b) \quad W_t = \frac{\pi [D_o^2 - (D_o - 2\delta_d)^2]}{4} (0.286) = 0.0313 \text{ lb/ft}$$

$$(c) \quad 2q_f = 2C_1 T_h^4 \left(\frac{L_h}{12}\right) \Omega = 470 L_h \Omega \text{ Btu/(hr)(ft)}$$

$$(d) \quad \zeta_p = \frac{C_1 T_h^3 L_h^2}{k \delta_h} = \frac{2.43 L_h^2}{16.2 (144) \left(\frac{\delta_h}{12}\right)} = 0.0126 \left(\frac{L_h^2}{\delta_h}\right)$$

$$(e) \quad 2W_f = 2(12)\rho L_h \delta_h = 24(0.286) L_h \delta_h = 6.86 L_h \delta_h \text{ per foot for two flat plates}$$

$$(f) \quad 2W_f = 2(12)\rho L_h \left(\frac{\delta_h}{2}\right) = 12(0.286) L_h \delta_h = 3.43 L_h \delta_h \text{ per foot for two triangular plates}$$

Procedure

The steps taken in the case of flat plates are as follows:

1. The value of the fin profile number for several lengths and thicknesses was computed by Equation d.

2. A value for each corresponding plate effectiveness was found from Figure 5.
3. Values of heat ejected by plates of various length and thickness were found from Equation c and that ejected by the tube from Equation a.
4. Heat ejected from the tube and fins was found by addition.
5. The weight of plates for various lengths and thicknesses was computed by Equation e.
6. The weight of the tube was computed by Equation b.
7. The total weight of tube and fins was found by addition.
8. The weight/heat transfer ratios were found by dividing the results of step 7 by the results of step 4.
9. The results obtained were plotted in Figures 43 through 45 as functions of fin length L_h .

The same basic steps were taken in the case of triangular fins, except that the weight was computed by Equation f and the surface effectiveness was found from Figure 32.

Comment

Some results of these calculations are shown in Figure 43. The weight/heat transfer ratio is plotted against fin length L_h for various values of flat plate profile number ζ_p . The pattern for all profile numbers is one of sharp decrease in weight/heat transfer ratio as the fin length increases, the reaching of a minimum point, and then a rapid increase of ratio with increased fin length. Since the profile number equation for this problem reduces to

$$\zeta_p = 0.0126 \left(\frac{L_h^2}{\delta_h} \right)$$

it is apparent that holding this parameter constant fixes only the relationship between length and thickness, not the size of the fin.

The significance of the 0.815 profile number can be noted by referring to Figure 5. It is seen that the profile number for the optimum-weight plate is 0.815, for a value of the environment parameter of 0. The other profile numbers of Figure 43 were arbitrarily selected.

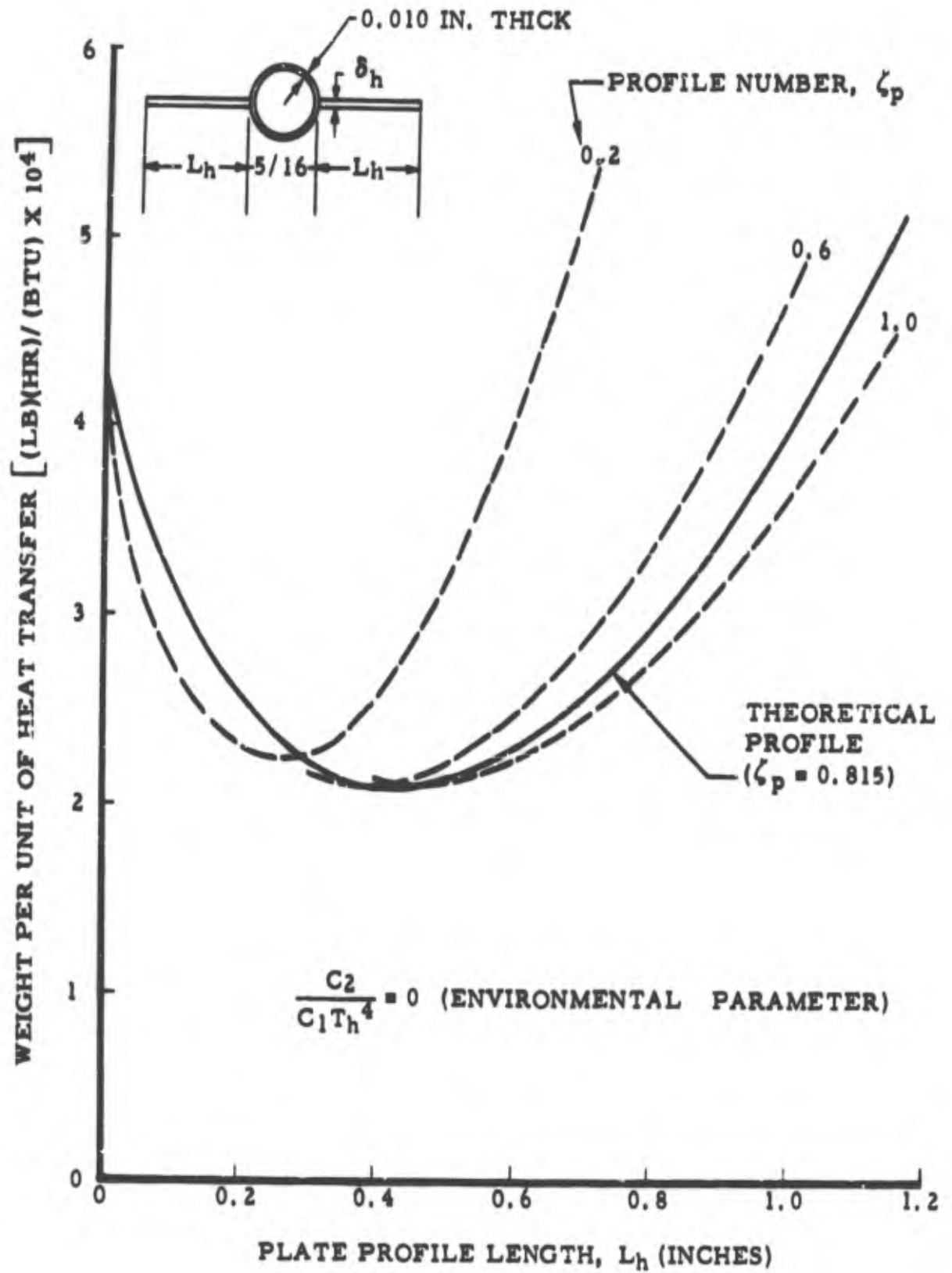


Figure 43. Relationship of Weight Per Unit of Heat Transfer to Fin Length for Environmental Parameter of Zero (Problem 2)

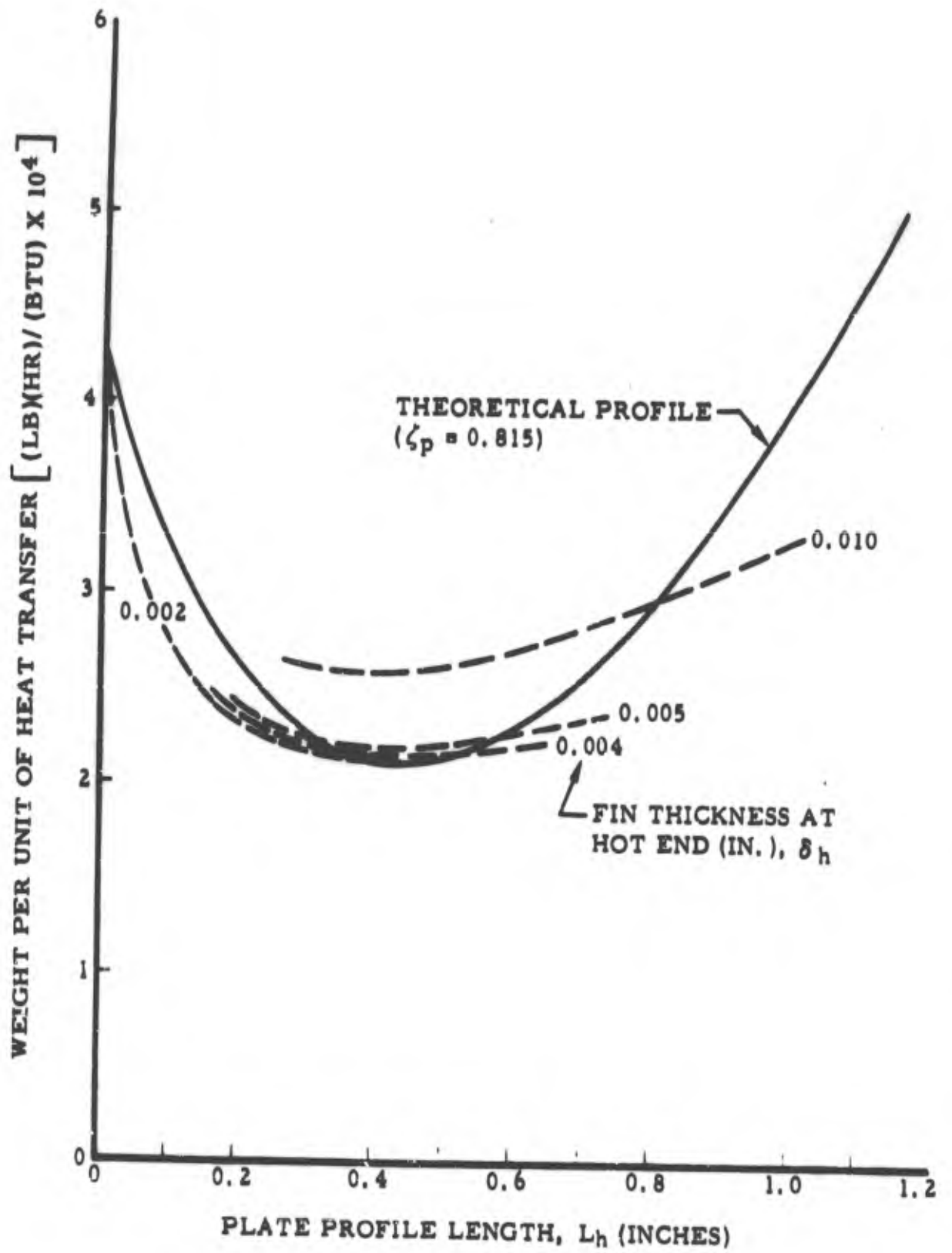


Figure 44. Relationship of Weight Per Unit of Heat Transfer to Fin Length for Theoretical Profile (Problem 2)

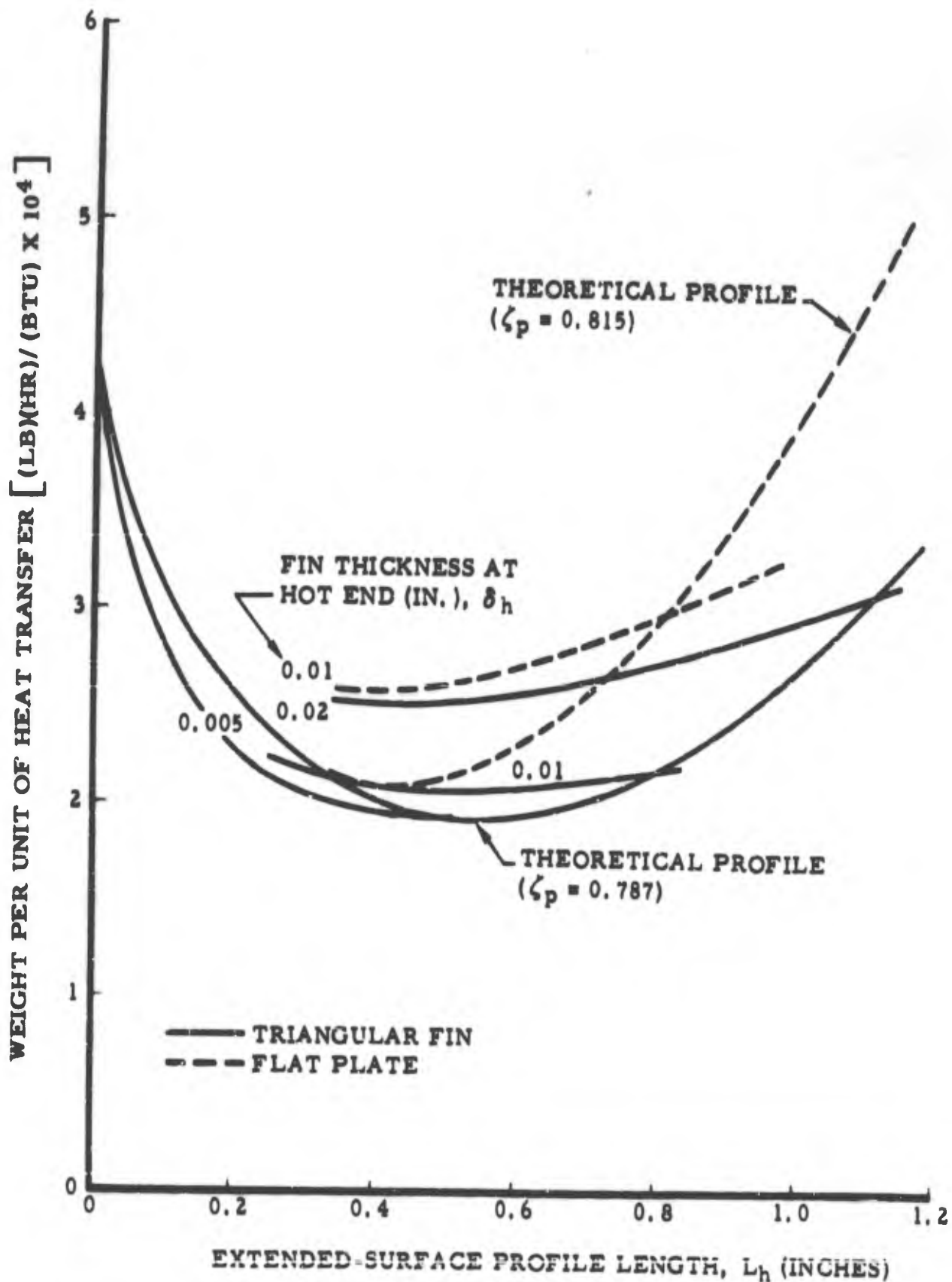


Figure 45. Relationship of Weight Per Unit of Heat Transfer to Fin Length for Flat Plate and Triangular Fin (Problem 2)

While the 0.815 curve reaches the lowest ratio, the minimum points of the 0.6 and 1.0 curves are not very much different, and the minimum value of the 0.2 curve is only 7 percent higher. It must be remembered, however, that while the ratio for the 0.6, 0.815, and 1.0 profile numbers are very nearly the same for a fin length of 0.4 to 0.45 inch, the amount of heat radiated is different in each case.

Another point is the effect created by adding any extended surfaces to a radiator tube. It can be seen that for the "best" plate length, the weight/heat transfer ratio is about one-half that for zero plate length. This is a significant reduction, but not nearly as great as might be expected. Further reductions could be made by using a material for the fins of a density lower than that for the tube.

In Figure 44, the parameter of plate thickness is introduced into the weight/heat transfer ratio and extended-surface length relationship. The positions of lowest ratio are seen to be occupied by the thinner plates, some so thin as to be more in the nature of metal foils. The fabrication and handling of extended surfaces 0.002 inch thick would present insolvable problems. It is necessary, therefore, to consider the effects of the deliberate use of off-design thicknesses.

Assume, for example, that computations have indicated the use of a plate 0.002 inch thick and 0.4 inch long, or one having very nearly the minimum weight/heat transfer ratio possible. Assume, further, that the thinnest plate that can be used is 0.010 inch thick. If the plate length remains fixed, the profile is no longer of optimum weight. On the other hand, reference to Figure 5 shows that with the plate five times as thick, so that the profile number is now one-fifth its original value, the effectiveness increases from 57.2 percent to about 84 percent. This increase in effectiveness of almost 30 percent implies an ability to reduce the radiating area, since

$$\Omega_1 A_1 = \Omega_2 A_2$$

Then

$$\begin{aligned} A_2 &= \left(\frac{\Omega_1}{\Omega_2} \right) A_1 \\ &= \left(\frac{57.2}{84} \right) A_1 = 0.69 A_1 \end{aligned}$$

A saving in area can therefore be made by the reduction of length L_w in the direction of fluid flow or normal to the direction of heat flow. This may be sufficient justification for taking on the extra weight of the thicker plate. It

should be noted that this analysis is not entirely accurate; the effect of the tube or duct surfaces has been ignored. However, with small tubes, this procedure may be considered sufficiently accurate.

It would be possible, as seen in Figure 44, to maintain an optimum weight profile for the 0.010-inch fin by increasing its length to 0.8 inch. This would permit much more heat to be radiated, but this is not required in this problem. There would also be twice as much area and hence weight. The additional area could be used to increase reliability in a meteoritic environment.

It would also appear that extending the 0.010-inch curve to the left would cause it to intersect a second time with the optimum-weight profile line, resulting in two fins of the same thickness and different lengths. This point of intersection is without significance; the substitution of this length does not satisfy the equation for profile number.

In Figure 45, comparisons are made between flat plates and triangular fins as extended surfaces for the radiator under consideration. The weight-minimum configuration has a profile number of 0.787 for the triangular fin (Reference 9). The minimum ratio is 1.92×10^{-4} pounds per Btu-hour compared with 2.08×10^{-4} for the flat plate. (Computations more recently performed by D. B. Mackay show that the triangular fin profile number for optimum weight is 0.67.)

For a root thickness δ_h of 0.010 inch, the triangular fin length is about 0.50 inch, at a minimum weight-heat ratio of about 2.07×10^{-4} pounds per Btu-hour. This represents an increase in weight of approximately 21 percent for the entire section, including the tube, over the optimum triangular fin having a root thickness of 0.005 inch. Reference to Figure 28, however, shows that the effectiveness is increased by about 30 percent, thereby permitting a correspondingly large reduction in radiating area. These results serve to point up the fallacy of specifying the lightest configuration without further analysis. Light weight is almost always associated with lower effectiveness, and therefore with large radiating areas.

An interesting comparison can be made between the flat plate 0.010 inch thick and the triangular fin having a root thickness of 0.020 inch. Both weigh the same for any profile length L_h and have nearly the same weight/heat transfer ratios. However, the triangular section is more effective and will dissipate more heat from a given area because of a more favorable distribution of material for conductive heat transfer.

Conclusions

This example shows that an optimum-weight approach to extended surface design results in thin profiles, some so thin that an arbitrary

thickening of several hundred percent is required to reach the realm of practicality. It is then found that a compensation exists for this added weight in the form of a reduction in required area.

Also found was that little difference in performance is expected between flat plates and triangular fins in the region of the minimum weight/heat transfer ratio. This raises the question of whether there is a need for complex profiles, such as those of constant temperature-gradient fins with their concave surfaces. The answer to these and other related questions can only be found when all requirements and restrictions are known.

Problem 3: Effect of Fin Materials

Given

A turbine discharges wet vapor into a stainless steel cylindrical condenser tube. Extended surfaces on the tube are in the form of fins of constant temperature gradient. The condenser is mounted vertically on a level area of the moon terrain at a subsolar point. The fins and tubing are coated with a material having an emissivity of 0.90.

Required

To determine the optimum configuration of fins made of aluminum, beryllium, and copper.

Data

$$T_w = 1450 \text{ R}$$

$$\delta_d = 0.035 \text{ in.}$$

$$D_o = 1.0 \text{ in.}$$

$$S_c = 430 \text{ Btu/(hr)(sq ft)}$$

$$\theta_p = 0 \text{ deg}$$

$$\theta_m = 90 \text{ deg}$$

$$F_a = F_b = 0.5$$

$$r_m = 0.13$$

$$T_m = 674 \text{ R}$$

$$a_a = a_b = 0.18$$

$$\epsilon_a = \epsilon_b = 0.90$$

$$F_r = 1.0 \text{ (assumed)}$$

The thermal conductivity and density of the three materials are as follows:

Material	Thermal Conductivity, k [Btu/(hr)(ft)(°R)]	Density, ρ (lb/cu ft)
Aluminum	155 (at 1392° R)	172.8
Beryllium	124 (at 852° R)	114.05
Copper	205 (at 1392° R)	559

The equations used and numerical values of terms are as follows:

$$C_1 = (\epsilon_a + \epsilon_b)\sigma$$

$$= (0.9 + 0.9)(0.1713 \times 10^{-8}) = 0.30834 \times 10^{-8}$$

$$C_2 = S_c (a_a \cos \theta_p + F_a a_a \rho_m \cos \theta_m + F_b a_b \rho_m \cos \theta_m) + \sigma T_m^4 (F_a \epsilon_a + F_b \epsilon_b)$$

$$= 341 \text{ Btu/(hr)(sq ft)}$$

$$C_1 T_w^3 = 9.4$$

$$C_1 T_w^4 = 13,630$$

$$\frac{C_2}{C_1 T_w^4} = 0.025$$

Procedure

Various fin lengths and thicknesses were assumed for each material, and the heat rejected from a 1-foot section of each configuration computed by Equation 133. Fin effectiveness Ω was determined in each case by

reference to Figure 17 or by the use of the appropriate equations. The weight of each fin configuration was found by using Figure 18. For each case, the ratio W/q was computed and the ratio dW/dq was computed or taken from Figure 20. The data were then plotted as shown in Figure 46.

Comment

The intersections of the W/q and dW_f/dq_f lines mark the optimum fin length L_h for each root thickness δ_h considered. A line connecting these optimum points, for one material, has as its minimum point the optimum fin length and root thickness.

For copper, the line of fin thickness of 0.020 inch lies very near the minimum point. For aluminum and beryllium, the values are approximately 0.40 and 0.085 inch, respectively. The lowest weights were found for the design using beryllium fins. The optimum aluminum fin configuration is only 4 percent heavier, but the copper fin configuration is approximately 30 percent heavier. It is questionable if a saving of only 4 percent of beryllium over aluminum can justify the selection of beryllium, since it is such difficult material to handle and so much more expensive.

For practical reasons, a root thickness larger than that shown at the minimum point on Figure 46 should be used. The exact thickness and length depend somewhat upon the area the condenser requires to dissipate a unit of heat to the environment. The data plotted in Figure 47 present a comparison of the configurations. As longer and thinner fins are used, the condenser area increases sharply.

For example, with copper fins, the condenser area increases by approximately 16 percent, and the weight decreases by 3 percent when fin thickness is reduced from 0.30 to 0.020 inch. An even more striking comparison is obtained with aluminum where reducing the root thickness from 0.075 to 0.050 inch results in an area increase of 19 percent and a weight saving of only 3 percent. A similar comparison can be made for beryllium. For these configurations, it appears that a root thickness approximately 50 percent larger than the minimum point gives a reasonable compromise between area and weight.

In Figure 46, the loci of the points of intersection of the ratio and change-of-ratio curves form a curve which is markedly different from that formed in Figure 42. The reason for this difference has not yet been investigated. It has been suggested that the difference may result from the fact that, in one case, the tube and fins are of the same material whereas, in the other case, the tube and the fins are of different materials. An attempt will be made to find the exact cause of this apparent anomaly, and the results will be reported.

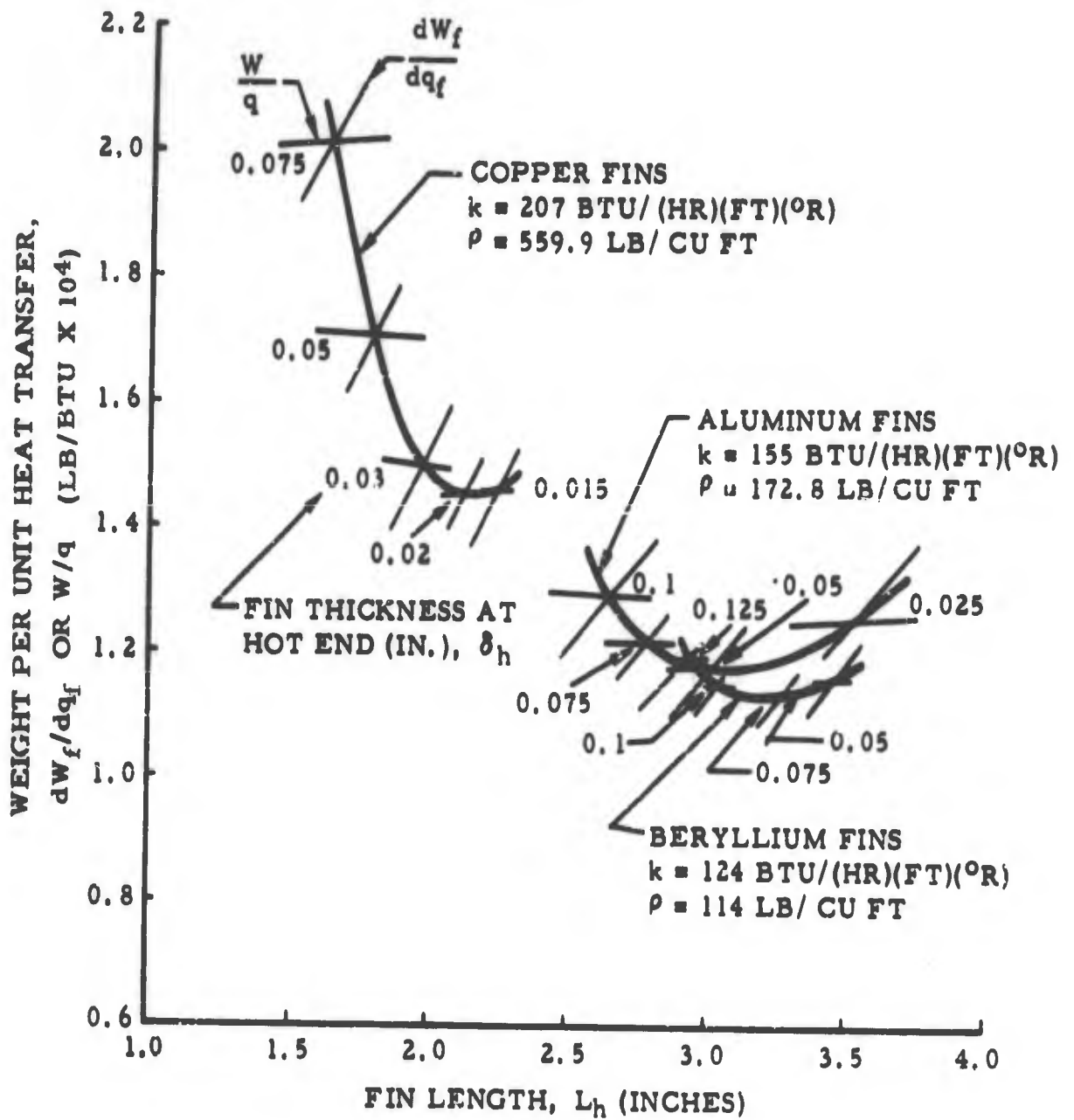


Figure 46. Relationship of Weight Per Unit of Heat Transfer and Rate of Change of Ratio to Fin Length (Problem 3)

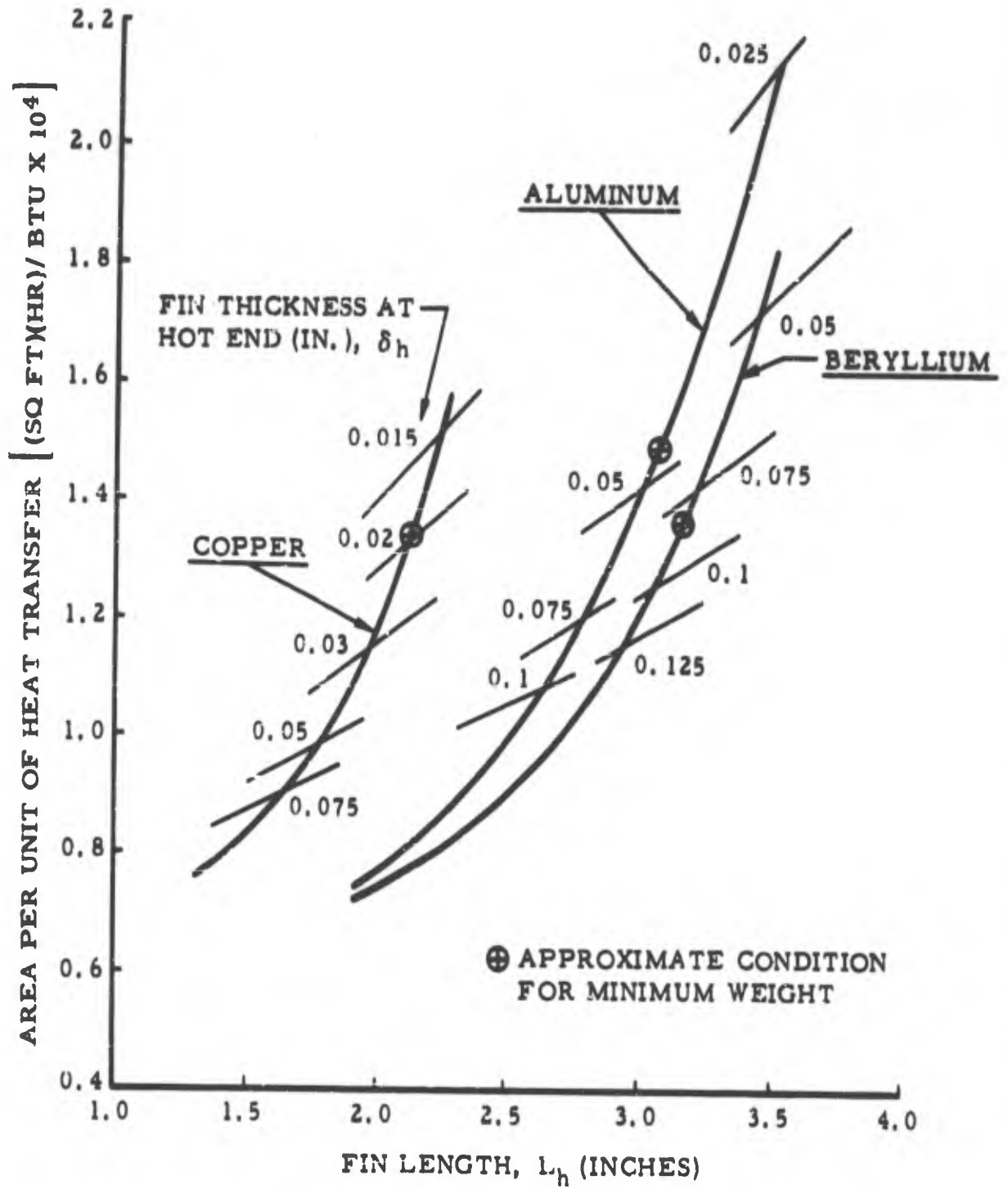


Figure 47. Relationship of Area Per Unit of Heat Transfer to Fin Length (Problem 3)

Problem 4: Determination of Fluid-Wall Temperature Difference

Given

The condenser designed in problem 3 is assumed.

Required

To determine the difference between the condensing vapor temperature T_f and the tube wall temperature T_w when the fluids are mercury, rubidium, potassium, and sodium.

Data

The fins are aluminum with root thickness δ_h of 0.070 inch and length L_h of 2.8 inch. The vapor tube inside diameter D_i is 0.93 inch. The vapor tube is mounted vertical to the lunar surface. The quality of vapor entering the condenser is 85 percent. The gravity of the moon produces an acceleration of 71×10^6 (foot/hour)/hour.

Procedure

Evaluating the fin profile number,

$$\zeta_p = \frac{C_1 T_h^3 L_h^2}{k \delta_h} = \frac{9.4 (2.8)^2}{155 \left(\frac{0.07}{12}\right) (12)^2} = 0.565$$

From Figure 17, fin effectiveness Ω is 0.528

From Equation 135,

$$L_e = \left(L_d + \frac{2\Omega L_h}{1 - \frac{C_2}{C_1 T_w^4}} \right) F_r = \left[\frac{1}{12} + \frac{2(0.528)(2.8)}{(1 - 0.025) 12} \right] 1.0 = 0.3364 \text{ ft}$$

From Equation 143,

$$A_d = \frac{\pi D_1^2}{4}$$

$$= \frac{\pi(0.93^2)}{4(144)} = 4.72 \times 10^{-3} \text{ sq ft}$$

Using the method of Reference 15 (p 335) and the fluid properties found in Reference 16, the following values of heat transfer coefficient were obtained:

Inlet Velocity (ft/sec)	Heat Transfer Coefficient, h [Btu/(hr)(sq ft)(°R)]			
	Mercury	Rubidium	Potassium	Sodium
100	96,000	33,500	68,500	277,000
300	145,800	36,300	45,900	175,000
500	177,000	41,000	39,100	136,800
700	277,000	44,700	35,200	133,700

An expression for the temperature difference is

$$T_f - T_w = \frac{(C_1 T_w^4 - C_2) L_s}{ph} \quad (148)$$

Since all the necessary terms are known, this difference can be determined and is found to be quite small, as indicated in Figure 48. Hence, it can be neglected in most cases. The reason for the small difference is the high value of the heat transfer coefficient, h. These would not be so large in land-based powerplants because of the presence of noncondensable gases in the condenser. Such gases should be more readily eliminated or reduced in a space powerplant, so that values approaching those listed above would be realized.

Problem 5: Determination of Tube Length

Given

The condenser of problems 3 and 4 is assumed.

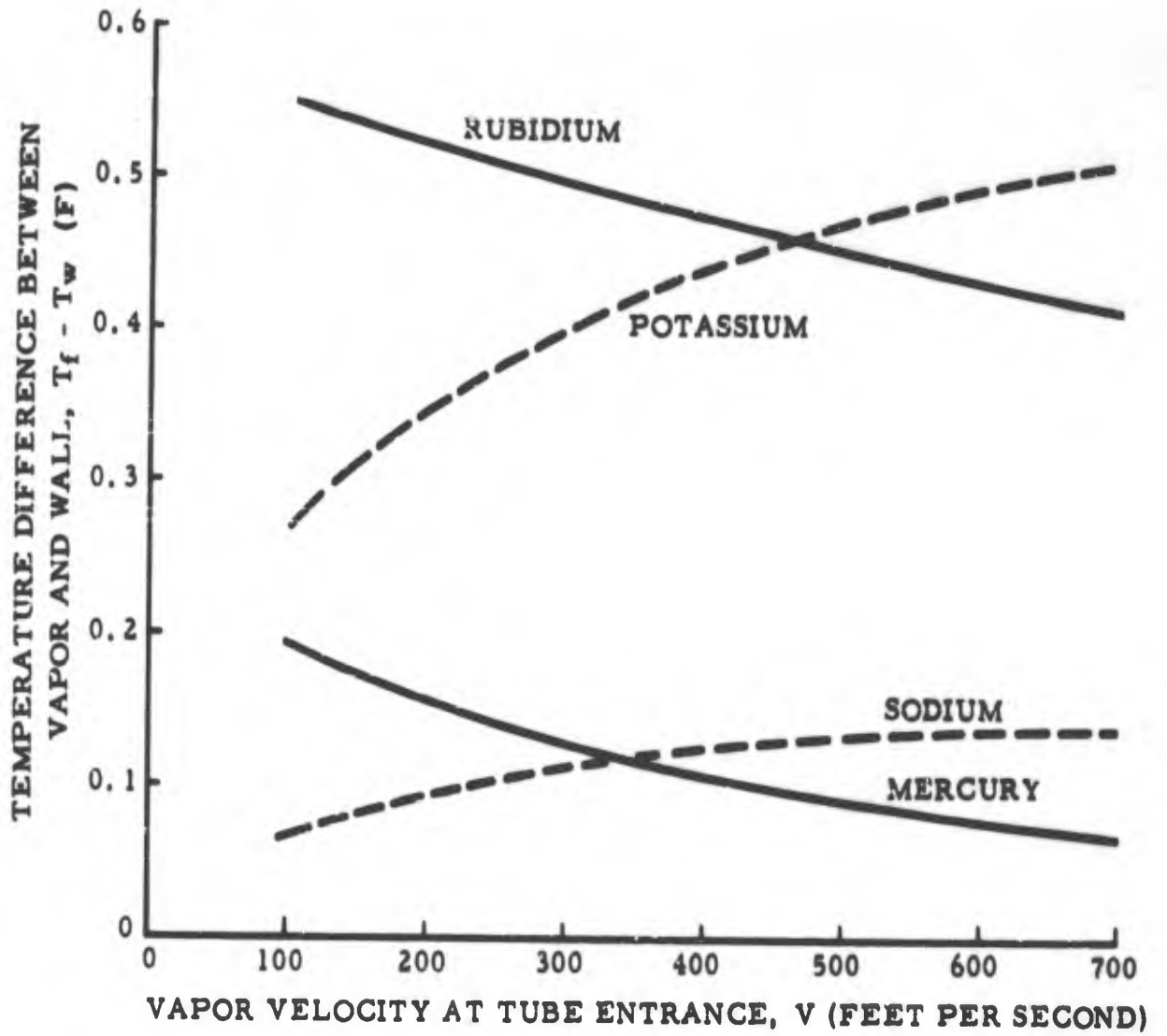


Figure 48. Relationship of Temperature Difference Between Vapor and Wall to Vapor Velocity at Tube Entrance (Problem 4)

Required

To determine the lengths L_w of condenser tubes required for condensing mercury, rubidium, potassium, and sodium.

Procedure

Using Equation 141 and the data of the previous problems, the results presented in Figure 49 are obtained.

Comment

The curves of Figure 49 offer striking comparisons of the effects of working fluid on tube length. While the required lengths for three materials are quite similar, that for mercury is much different.

The use of rubidium, potassium, and sodium will probably require the use of tapered vapor passageways to obtain a reasonable compromise between tube lengths and weight. With mercury, in spite of the extended tube lengths indicated, considerable weight saving can be realized because of the smaller tube diameters required.

Problem 6: Determination of Tube Diameter

Given

The condenser of the previous problems, with aluminum fins, is assumed.

Required

To compare the required tube diameters for the working fluids mercury, rubidium, potassium, and sodium.

Data

$$L_h = 2.5 \text{ in.}$$

$$L_w = 5 \text{ ft}$$

$$\delta_h = 0.075 \text{ in.}$$

$$k = 155 \text{ Btu/(hr)(ft)(}^\circ\text{R)}$$

$$T_w = 1450 \text{ R}$$

$$\delta_d = 0.035 \text{ in.}$$

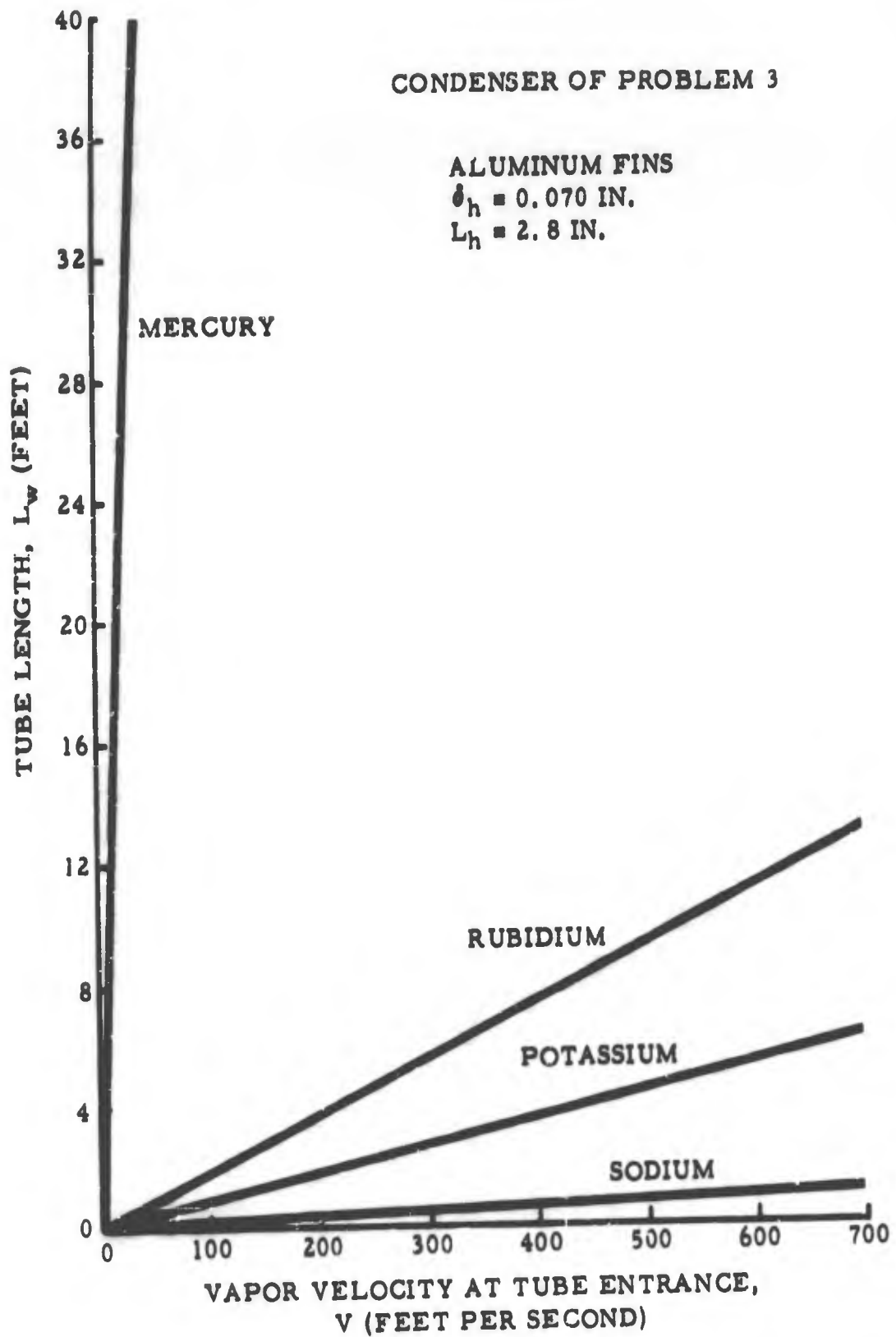


Figure 49. Relationship of Tube Length to Vapor Velocity at Tube Entrance (Problem 5)

$$C_1 = 0.30834 \times 10^{-8}$$

$$C_2 = 341 \text{ Btu/(hr)(sq ft)}$$

$$C_1 T_w^3 = 9.4$$

$$C_1 T_w^4 = 1.363 \times 10^4 \text{ Btu/(hr)(sq ft)}$$

$$\frac{C_2}{C_1 T_w^4} = 0.025$$

Procedure

The inside diameter D_1 is to be computed with the aid of Equation 147.

$$D_1 = \frac{K_1}{2} \left(1 + \sqrt{1 + \frac{4K_2}{K_1}} \right)$$

Since Equation 146 states

$$K_2 = 2 \left(\delta_d + \frac{\Omega L_h}{1 - \frac{C_2}{C_1 T_w^4}} \right)$$

it is necessary to obtain the fin effectiveness Ω from Figure 17. The value of K_1 was obtained from Equation 145 for a number of fluid velocities, using data obtained from Reference 16. The results of these computations are shown in Figure 50.

Comment

It is evident from the solution of this problem that the tube forming the vapor passageway of the condenser is extremely large for sodium and extremely small for mercury. In condenser design, this gives mercury a distinct advantage over the other fluids, since the vapor passageway is considerably heavier than the extended surfaces per unit of heat transfer. This is especially true when a light material such as aluminum is used for the fins and steel is used for the vapor passageway. Within the passageway, however, the vapor pressure is higher for mercury and progressively less for rubidium, potassium, and sodium. Their lower pressures may help reduce, to some extent, the weight of the vapor conduits. In any event, the large passageways required by sodium, potassium, and rubidium increase the condenser weight over that required for mercury.

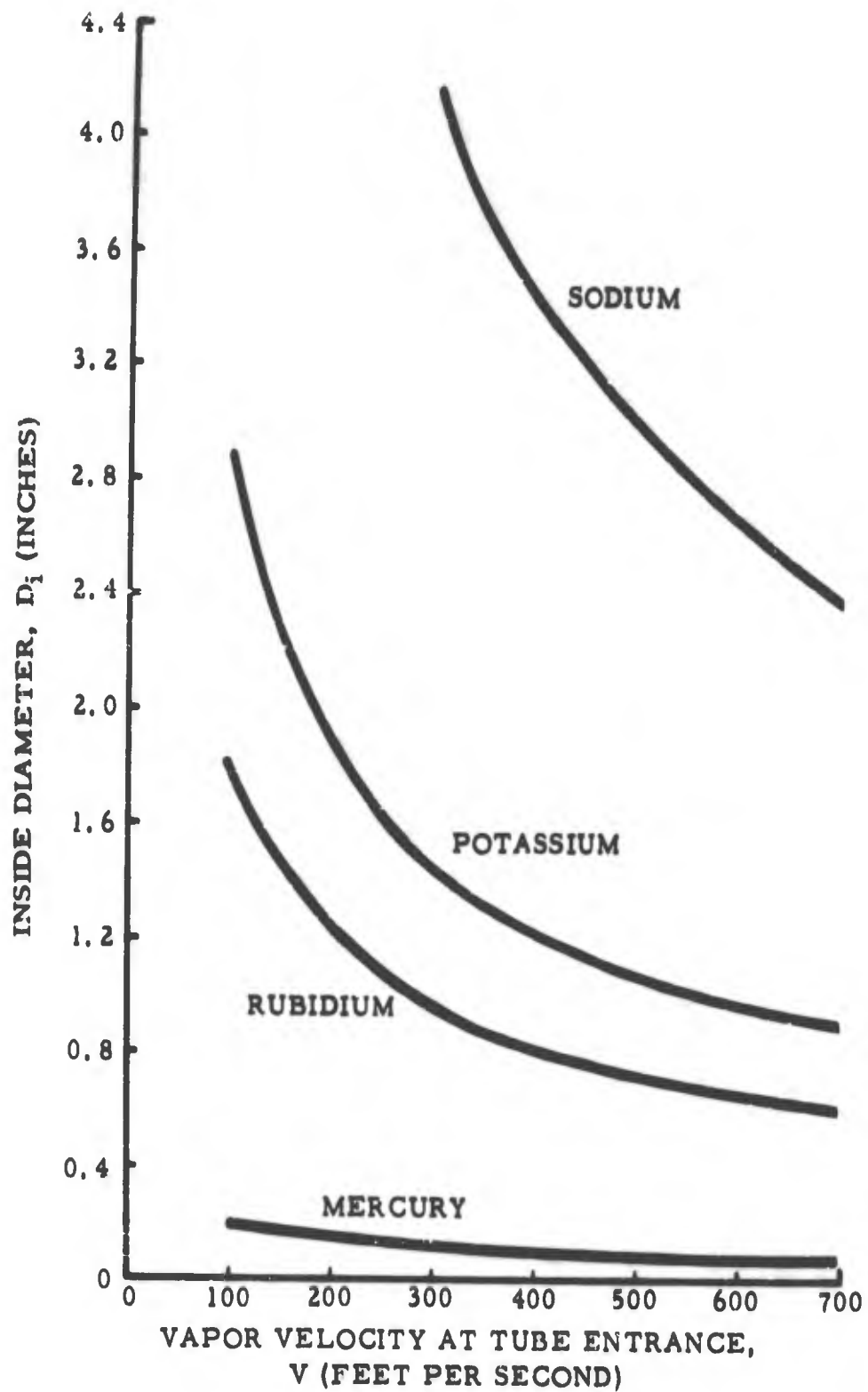


Figure 50. Relationship of Tube Inside Diameter to Vapor Velocity (Problem 6)

The results obtained for this problem illustrate one of the dilemmas facing the radiator designer. A vapor passageway of small cross-sectional area designed for a minimum-weight system dictates the use of small, lightweight extended surfaces. By further reducing the area of the extended surfaces, tubes of a still smaller cross-sectional area can be used. In like fashion, large ducts theoretically require large extended surfaces. If still larger areas are used, radiation increases and subcooling of the liquid occurs so that still larger ducts with greater flow rates are needed. This type of reasoning chain must be broken in order to achieve the design of a practicable combination of tube and extended surface. Good judgment will be required as well as the ability to manipulate the appropriate equations and charts if appropriate solutions are to be found.

DESIGN OF RADIATORS FOR OPERATION IN SPACE

Because the temperature of the fluid changes from entrance to exit, the analysis of the heat transfer characteristics of a radiator may be more complex than that of a condenser in which temperature of the fluid is assumed to be uniform and constant from end to end. Both devices reject heat by radiation, and therefore both may be termed radiators. The distinction made here, however, although somewhat arbitrary, is useful.

The heat transfer behavior of a series of radiators is analyzed in this section. Four configurations were considered: a rectangular section duct and a circular section duct with extended surfaces, each first with two and then with one emitting surface. Illustrative examples are included to demonstrate use of the derived equations. This section was abstracted from a report by D. B. Mackay (Reference 17).

NOMENCLATURE

- A_d Cross-sectional area of duct, sq ft
- C_1 Radiation constant, $\sigma(\epsilon_a + \epsilon_b)$, Btu/(sq ft)(hr)(°R)⁴
- C_2 Radiation constant, heat received from environment by radiating surfaces, Btu/(sq ft)(hr)
- C_3 Ratio of constants, environmental parameter, nondimensional
- c_p Specific heat at constant pressure, Btu/(lb)(°R)
- D_h Hydraulic diameter, ft
- D_i Tube inside diameter, ft
- F_r Interradiation correction factor, nondimensional
- G Mass velocity, lb/(hr)(sq ft)

h	Heat transfer coefficient, Btu/(sq ft)(hr)(° R)
k	Thermal conductivity, Btu/(ft)(hr)(° R)
L	Duct length (variable), ft
L_d	Duct width, ft
L_e	Section effective width, ft
L_h	Extended surface width, ft
L_w	Duct length, ft
P	Effective wetted perimeter, ft
P_t	Total wetted perimeter, ft
q	Heat transfer rate, Btu/hr
S_c	Solar constant, Btu/(sq ft)(hr)
T_f	Temperature of fluid at any point, ° R
T_{f1}	Temperature of fluid at duct entrance, ° R
T_{f2}	Temperature of fluid at duct exit, ° R
T_r	Equivalent temperature, ° R
T_w	Temperature of duct wall at any point, ° R
T_{w1}	Temperature of duct wall at duct entrance, ° R
T_{w2}	Temperature of duct wall at exit, ° R
V	Fluid velocity, ft/hr
w	Weight rate of flow, lb/hr

a_a, a_b	Surface absorptivity, nondimensional
δ_d	Tube wall thickness, ft
δ_h	Extended surface root thickness, ft
ϵ_a, ϵ_b	Surfaces emissivity, nondimensional
ρ	Density of fluid, lb/cu ft
σ	Stefan-Boltzmann constant, 0.1713×10^{-8} Btu/(hr)(sq ft)(°R) ⁴
ψ_1	Film resistance number, nondimensional
ψ_2	Radiation number, nondimensional
Ω	Extended surface effectiveness, nondimensional
Ω_1	Extended surface effectiveness at duct entrance, nondimensional
Ω_2	Extended surface effectiveness at duct exit, nondimensional

MATHEMATICAL ANALYSIS

Radiation From Two Sides of Rectangular Duct (No Extended Surfaces)

Figure 51 shows a duct of rectangular cross section which radiates heat extracted from the conveyed fluid. As the fluid moves from one end to the other, a distance L_w , its temperature falls from T_{f1} to T_{f2} . The corresponding temperatures of the duct wall are T_{w1} and T_{w2} . The relationship of these temperatures to duct length is also shown in Figure 51.

Assuming that the outside wall temperature is equal to the inside wall temperature T_w , and is the same for both faces of the duct, the heat radiated from an element of the duct will be

$$dq = (\bar{C}_1 T_w^4 - \bar{C}_2) L_d dL \quad (149)$$

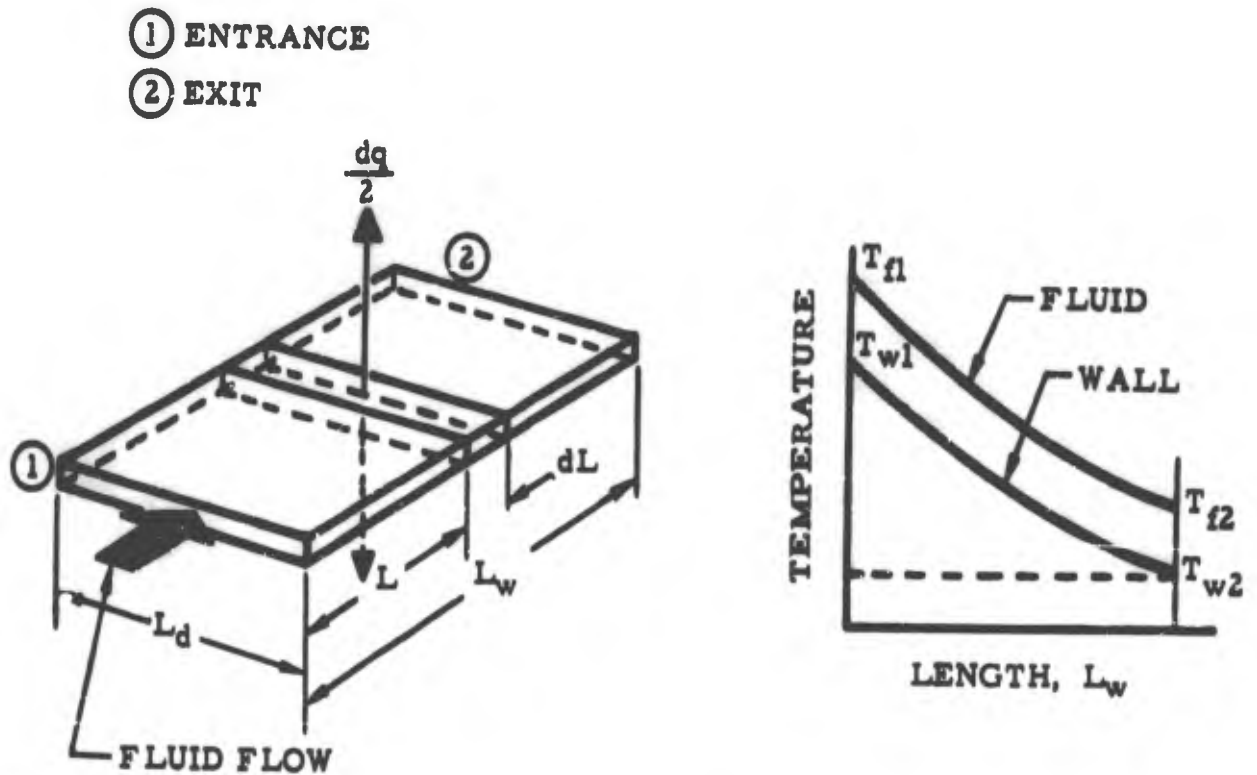


Figure 51. Dimensional and Temperature Relationships of Rectangular Cross-Section Duct Radiating Heat From Both Surfaces

The heat given up by the fluid to the walls, then, is

$$dq = -w c_p dT_f \quad (150)$$

The same quantity of heat must be transferred across the fluid boundary layer, or

$$dq = ph(T_f - T_w)dL \quad (151)$$

Equations 149, 150, and 151 can be combined to obtain expressions for determining the required dimensions of an exchanger.

As a first step toward obtaining the required length L_w of the exchanger, Equations 149 and 151 are combined.

$$ph(T_f - T_w) = (C_1 T_w^4 - C_2)L_d \quad (152)$$

After differentiating and rearranging,

$$dT_f = \left(\frac{4C_1 T_w^3 L_d}{ph} + 1 \right) dT_w \quad (153)$$

Combining Equations 149 and 150,

$$(C_1 T_w^4 - C_2) L_d dL = -w c_p dT_f \quad (154)$$

Substituting Equation 153 in Equation 154,

$$(C_1 T_w^4 - C_2) L_d dL = -w c_p \left(\frac{4C_1 T_w^3 L_d}{ph} + 1 \right) dT_w \quad (155)$$

If C_1 and C_2 are constant along the heat exchanger, Equation 155 can be integrated along dimension L .

An intermediate step to the solution produces the following set of relationships.

$$\left(\frac{ph}{w c_p} \right) L_w = \psi_1 + \left(\frac{ph}{6C_1 T_{w1}^3 L_d} \right) \psi_2 \quad (156)$$

where

$$\psi_1 = - \int_{T_{w1}}^{T_{w2}} \frac{4C_1 T_w^3 dT_w}{C_1 T_w^4 - C_2} \quad (157)$$

and

$$\psi_2 = -6C_1 T_{w1}^3 \int_{T_{w1}}^{T_{w2}} \frac{dT_w}{C_1 T_w^4 - C_2} \quad (158)$$

The terms ψ_1 and ψ_2 defined in Equations 157 and 158 are important in obtaining the heat exchanger length; charts of their values appear later in this report. Solving Equation 156 for the length gives

$$L_w = \left(\frac{wc}{ph} \right) \psi_1 + \left(\frac{wc}{6C_1 T_{w1}^3 L_d} \right) \psi_2 \quad (159)$$

If the heat transfer coefficient h is high, little temperature drop ($T_f - T_w$) occurs between the fluid and the duct wall. The coefficient of ψ_1 is small, and the product of the coefficient and ψ_1 is likewise small. For this case, the heat exchange length is controlled almost completely by the value of ψ_2 and its coefficient. The term ψ_1 can be considered as arising from the resistance to heat transfer in the fluid film and has, therefore, been given the identifying name of film resistance number. Likewise, the term ψ_2 is more closely associated with external radiation resistance and is identified as a radiation number.

Integration of Equation 157 produces

$$\psi_1 = \log_e \frac{1 - C_3}{\left(\frac{T_{w2}}{T_{w1}} \right)^4 - C_3} \quad (160)$$

where

$$C_3 = \frac{C_2}{C_1 T_{w1}^4} \quad (161)$$

The film resistance number ψ_1 can be evaluated by means of Equation 160 for all values of C_3 , including zero. The evaluation of the radiation number ψ_2 is somewhat more involved. In free space, where radiation from the sun or other sources may be blocked or may be negligible in value, C_2 and C_3 are zero and

$$\psi_2 = 2 \left[\frac{1}{\left(\frac{T_{w2}}{T_{w1}} \right)^3} - 1 \right] \quad (162)$$

If C_2 is not zero,

$$\psi_2 = \frac{3}{2C_3^{3/4}} \log_e \frac{\frac{\sqrt[4]{C_3} + \frac{T_{w2}}{T_{w1}}}{\sqrt[4]{C_3} - \frac{T_{w2}}{T_{w1}}}}{\frac{\sqrt[4]{C_3} + 1}{\sqrt[4]{C_3} - 1}} + \quad (163)$$

$$\frac{3}{C_3^{3/4}} \left(\tan^{-1} \frac{\frac{T_{w2}}{T_{w1}}}{\sqrt[4]{C_3}} - \tan^{-1} \frac{1}{\sqrt[4]{C_3}} \right)$$

Substituting Equations 160 and 163 into Equation 156 ($C_3 \neq 0$),

$$\frac{ph L_w}{w c_p} = \log_e \frac{1 - C_3}{\left(\frac{T_{w2}}{T_{w1}}\right)^4 - C_3} + \frac{ph}{4L_d \sqrt[4]{C_1 C_2^3}} \log_e \frac{\left(\sqrt[4]{C_3} + \frac{T_{w2}}{T_{w1}}\right)\left(\sqrt[4]{C_3} - 1\right)}{\left(\sqrt[4]{C_3} - \frac{T_{w2}}{T_{w1}}\right)\left(\sqrt[4]{C_3} + 1\right)} + \quad (164)$$

$$\frac{ph}{2L_d \sqrt[4]{C_1 C_2^3}} \left(\tan^{-1} \frac{\frac{T_{w2}}{T_{w1}}}{\sqrt[4]{C_3}} - \tan^{-1} \frac{1}{\sqrt[4]{C_3}} \right)$$

Substituting Equations 160 and 162 into Equation 156 produces a much simpler relationship ($C_3 = 0$).

$$\frac{ph L_w}{w c_p} = \log_e \left(\frac{T_{w1}}{T_{w2}}\right)^4 + \frac{ph}{3C_1 L_d} \left(\frac{1}{T_{w2}^3} - \frac{1}{T_{w1}^3}\right) \quad (165)$$

In all equations, in order to avoid imaginary answers, it is necessary that

$$\frac{T_{w2}}{T_{w1}} > \sqrt[4]{C_3}$$

or

$$\frac{T_{w2}}{T_{w1}} > \sqrt[4]{\frac{C_2}{C_1 T_{w1}^4}} \quad (166)$$

or

$$T_{w2} > \sqrt[4]{\frac{C_2}{C_1}}$$

The equations developed thus far are all functions of wall temperature T_{w1} and T_{w2} . The corresponding fluid temperatures at the entrance and the exit of the duct are usually known; the relationship between the two sets of temperatures is given by Equation 152. However, the solution of this equation is awkward, requiring trial-and-error efforts. On the other hand, the total quantity of heat transferred by the exchanger can be easily computed by using the integrated form of Equation 150, which is simply

$$q = w c_p (T_{f1} - T_{f2}) \quad (167)$$

In some cases it may be desirable to determine an equivalent or effective radiator temperature (e. g., a uniform temperature T_r at which the same amount of heat could be rejected from the exchanger when located in free space). The equation for the heat transferred would then be expressed by

$$q = C_1 T_r^4 L_d L_w \quad (168)$$

Combining Equations 167 and 168,

$$T_r = \sqrt[4]{\frac{w c_p}{L_d L_w C_1} (T_{f1} - T_{f2})} \quad (169)$$

The dimensions of a heat exchanger of rectangular section, radiating from both sides of the duct, can now be determined. In some applications, such as where the radiating surface is a part of the external surface of the vehicle, it may not be possible to reject heat from both surfaces of the duct. This case is considered next.

Radiation From One Side of Rectangular Duct

A rectangular duct radiating heat from one surface only is illustrated in Figure 52 along with the corresponding temperature history. The equations developed for two-sided radiation, with only small changes in some of the constants or dimensions, can be used for this case.

The heat radiated to space is expressed by Equation 149.

$$dq = (C_1 T_w^4 - C_2) L_d dL$$

In this case, no heat is leaving one side of the duct, which is the same as equating the emissivity of that surface to zero. Thus C_1 is the product of

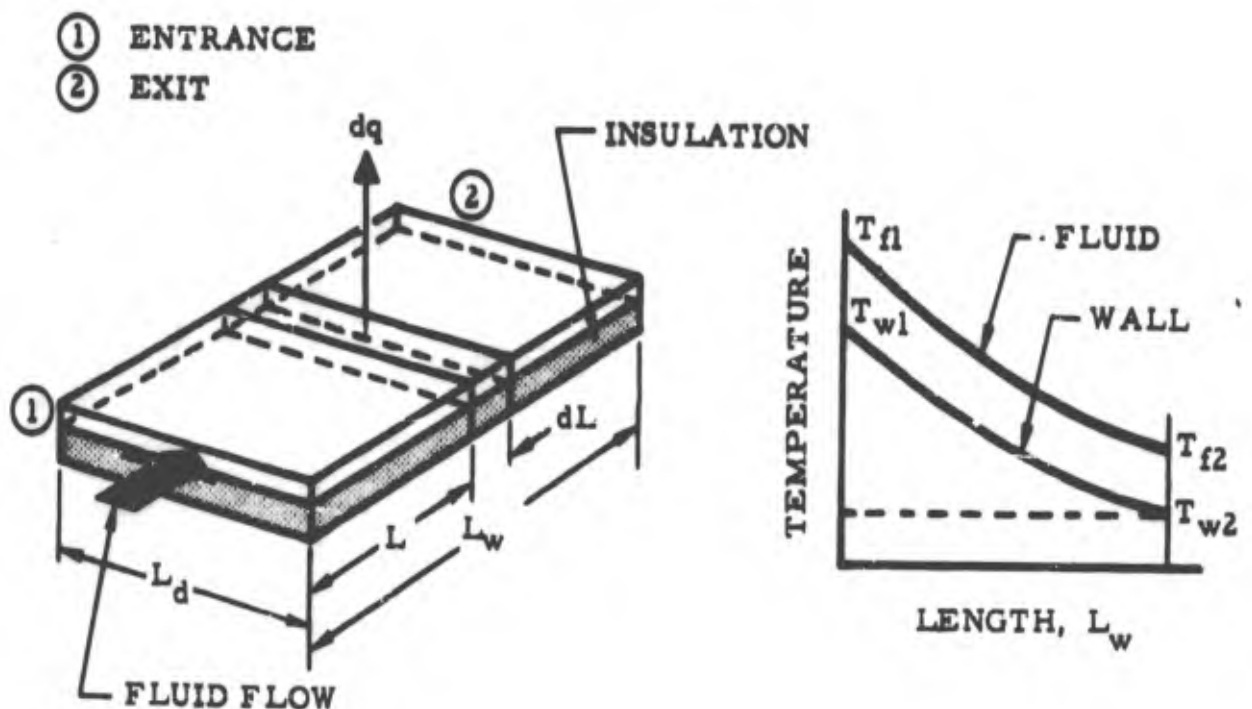


Figure 52. Dimensional and Temperature Relationships of Rectangular Cross-Section Duct Radiating Heat From One Surface

emissivity of the single radiating surface and the Stefan-Boltzmann constant, or

$$C_1 = \sigma \epsilon_a$$

instead of

$$C_1 = \sigma (\epsilon_a + \epsilon_b)$$

and C_2 is the heat reaching a unit area of the radiating surface from the environment instead of heat reaching unit areas of both surfaces.

The heat transferred from the fluid to the radiating wall is, as expressed by Equation 151,

$$dq = ph (T_f - T_w) dL$$

where

$$p = L_d$$

instead of

$$p = 2L_d$$

Radiation From Duct and Extended Surfaces (Heat Loss From Two Sides)

Because of its weight advantage, the extended-surface radiator is expected to be used more commonly in space applications than single rectangular ducts. Unfortunately, there are many variables in such structures, and exact mathematical analysis is difficult. The following procedure, however, is sufficiently accurate for most preliminary design purposes, and the analysis is equally valid for all extended-surface radiators (i. e., flat plates, trapezoidal profile, and constant temperature-gradient fins).

A section of radiator using tapered fins with a constant temperature-gradient is represented in Figure 53. As in simple rectangular radiators, the fluid enters the duct at temperature T_{f1} and leaves at some lower temperature, T_{f2} . The corresponding wall temperatures are T_{w1} and T_{w2} .

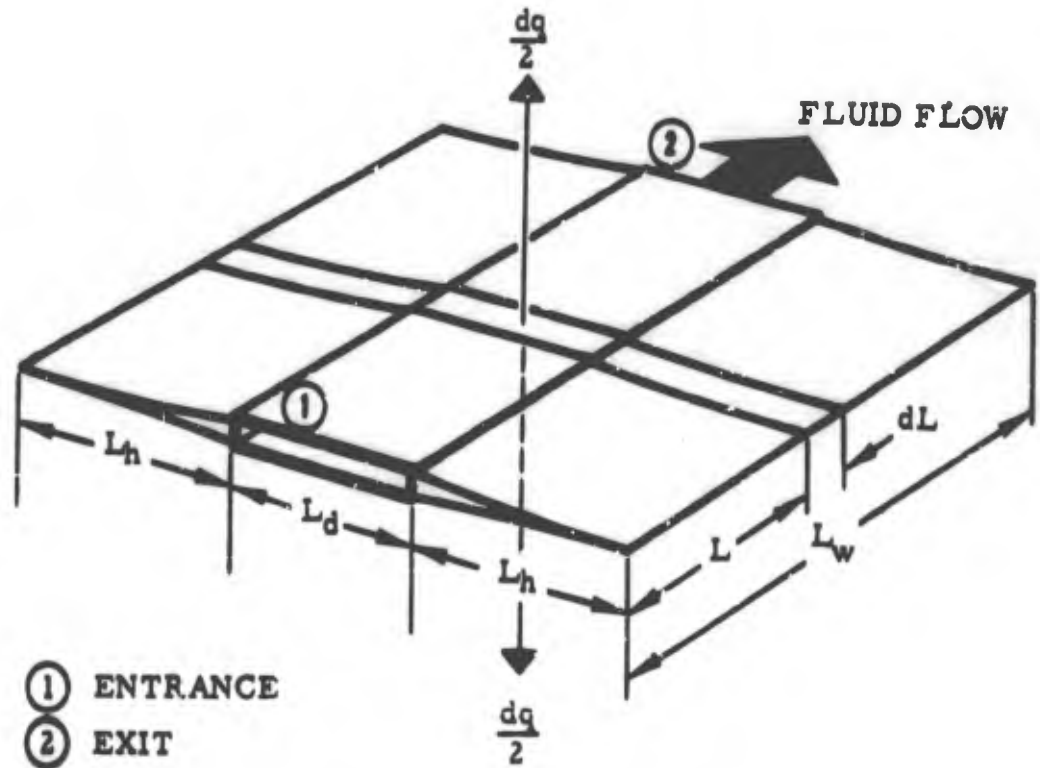


Figure 53. Dimensional Relationship of Duct and Extended-Surface Heat Exchanger Radiating Heat From Both Surfaces

Assuming a constant temperature in the duct wall over the length dL of a differential element, the heat transfer to space can be written as

$$dq = \left[(C_1 T_w^4 - C_2) L_d dL + 2C_1 T_w^4 \Omega L_h dL \right] F_r \quad (170)$$

Rearranging terms,

$$dq = (C_1 T_w^4 - C_2) \left[\left(L_d + \frac{2\Omega L_h}{1 - \frac{C_2}{C_1 T_w^4}} \right) F_r \right] dL \quad (171)$$

The bracketed term in Equation 171 can be defined as the effective width L_e of the heat exchanger (i. e., a width of duct and extended surfaces over which a uniform temperature T_w would radiate the same amount of heat as the actual width, $L_d + 2L_h$, with its nonuniform temperature). Thus,

$$L_e = \left(L_d + \frac{2\Omega L_h}{1 - \frac{C_2}{C_1 T_w^4}} \right) F_r \quad (172)$$

Substituting Equation 172 into Equation 171,

$$dq = (C_1 T_w^4 - C_2) L_e dL \quad (173)$$

The heat transferred from the fluid to the duct can be written as

$$dq = ph (T_f - T_w) dL \quad (174)$$

Equating Equations 173 and 174,

$$(C_1 T_w^4 - C_2) L_e = ph (T_f - T_w) \quad (175)$$

Writing Equation 175 in differential form,

$$4C_1 L_e T_w^3 dT_w = ph (dT_f - dT_w) \quad (176)$$

or

$$dT_f = \left(\frac{4C_1 L_e T_w^3}{ph} + 1 \right) dT_w \quad (177)$$

Combining Equations 150, 173, and 177,

$$(C_1 T_w^4 - C_2) L_e dL = -w c_p \left(\frac{4C_1 L_e T_w^3}{ph} + 1 \right) dT_w \quad (178)$$

Equation 178 can be solved if C_1 , C_2 , and L_e are assumed constant throughout the length of the heat exchanger. An evaluation of Equation 172 averaged over the whole length L_w of the exchanger can be used for L_e , since, in most instances, the equivalent length does not change greatly from one end of the heat exchanger to the other. If large changes are encountered, however, the heat exchanger should be sectionalized and each section treated independently.

Equation 178 can be rearranged and integrated to produce Equation 179, which is identical to Equation 156 except that L_e replaces L_d in the third term.

$$\frac{phL_w}{w c_p} = 1 + \left(\frac{ph}{6C T_{w1}^3 L_e} \right)_{avg} \psi_2 \quad (179)$$

where ψ_1 and ψ_2 are defined by Equations 157 and 158 or by Equations 160, 161, and 163. With these numbers evaluated, Equation 179 can be solved.

The total quantity of heat removed from the fluid in the duct can be computed using Equation 167. The presence of extended surfaces does not affect this relationship in any way.

An effective temperature T_r can be evaluated for the extended-surface radiator in the same manner as for the rectangular duct alone. The heat transfer from the fluid (Equation 167) is

$$q = w c_p (T_{f1} - T_{f2})$$

When heat is radiated to free space from the surfaces of the exchanger, the heat transfer rate may be expressed as

$$q = C_1 T_r^4 L_w L_e (avg) \quad (180)$$

Then

$$C_1 T_r^4 L_w L_e (avg) = w c_p (T_{f1} - T_{f2})$$

and

$$T_r = \sqrt[4]{\frac{w c_p (T_{f1} - T_{f2})}{C_1 L_w L_e (avg)}} \quad (181)$$

Radiation From Duct and Extended Surfaces (Heat Loss From One Side)

The configuration of this exchanger (Figure 54) is similar to that shown in Figure 53 except for the addition of insulation to the underside.

The equation for the heat radiated from an element of length dL (Equation 170) can be written as

$$dq = (C_1 T_w^4 - C_2) L_d dL + 2C_1 T_w^4 \Omega L_h dL$$

as in the case of two-sided radiation. The constants C_1 and C_2 have the significance as before in that a value of zero is used for the underside surface emissivity ϵ_b . The value of effectiveness Ω must be determined for the same condition.

The equation for heat radiated, on an equivalent length basis, is expressed by Equation 173.

$$dq = (C_1 T_w^4 - C_2) L_e dL$$

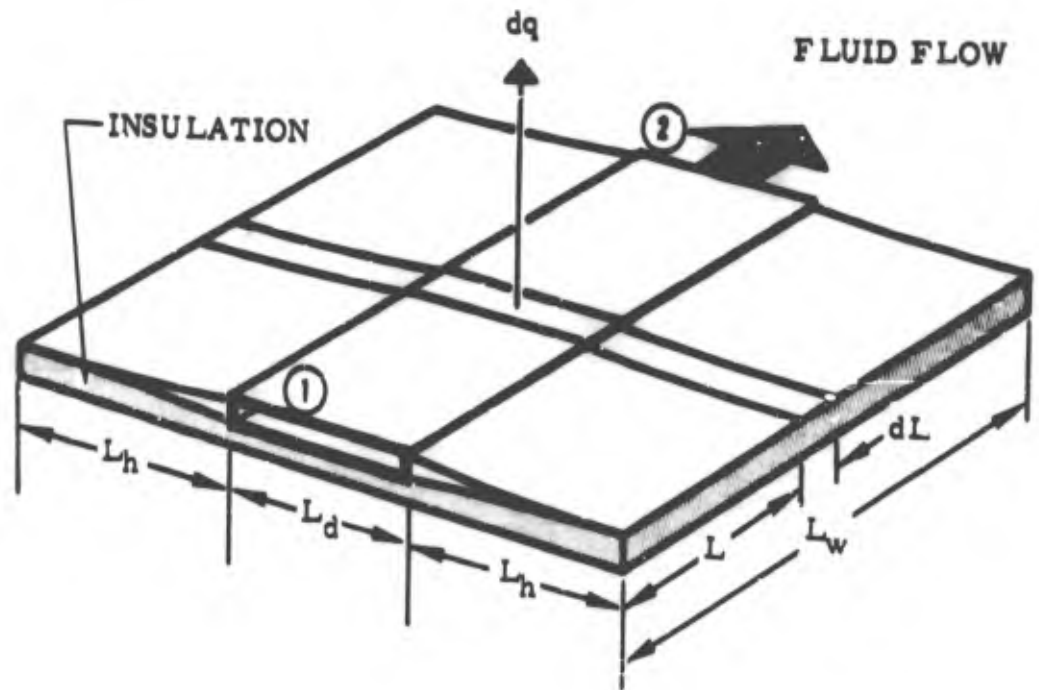


Figure 54. Dimensional Relationship of Duct and Extended-Surface Heat Exchanger Radiating Heat From One Surface

The transfer of heat from fluid to duct wall remains as expressed by Equation 174.

$$dq = ph (T_f - T_w) dL$$

The determination of effective wetted perimeter p , however, may be much more complex in this case due to the fact that part of the insulated portion of the duct may reach and remain at the fluid temperature, thereby reducing the rate of heat flow. Once the extent of this effect has been established, the effective perimeter can be evaluated and Equation 174 solved. With attention to these provisions, the equations derived for two-sided radiators can also be used for single-surface heat exchangers.

DESIGN FACTORS

Although the equations derived in the mathematical analysis are sufficient to design a radiator, the use of graphs is sometimes more convenient for obtaining values for the numbers ψ_1 and ψ_2 . The graphs of Figures 55 and 56 were plotted from Equations 160, 162, and 163. These graphs can be used to compute the dimensions of an exchanger and are especially helpful in obtaining preliminary estimates.

The radiator dimensions computed from Equations 156 and 179 depend directly on the values of ψ_1 and ψ_2 . Large values for these numbers dictate the use of a long radiator. It can be seen in Figures 55 and 56 that the values of ψ_1 and ψ_2 are large for low temperature ratios and high values of C_3 . For example, Equations 160, 162, and 163 give values approaching infinity for ψ_1 and ψ_2 at a temperature ratio of 0.88 when C_3 is 0.6. This effect is to be expected, since only a small temperature drop in the fluid can be obtained when the heat exchanger receives so much heat from the environment.

It should be noted in Equations 156 and 179 that the multipliers applied to the radiation number ψ_2 are usually much larger than those associated with the film resistance number ψ_1 . Also, when Figures 55 and 56 are compared, it is evident that the numerical value of ψ_2 is somewhat larger than that of ψ_1 . Therefore, ψ_2 usually plays the predominant role in heat exchanger design.

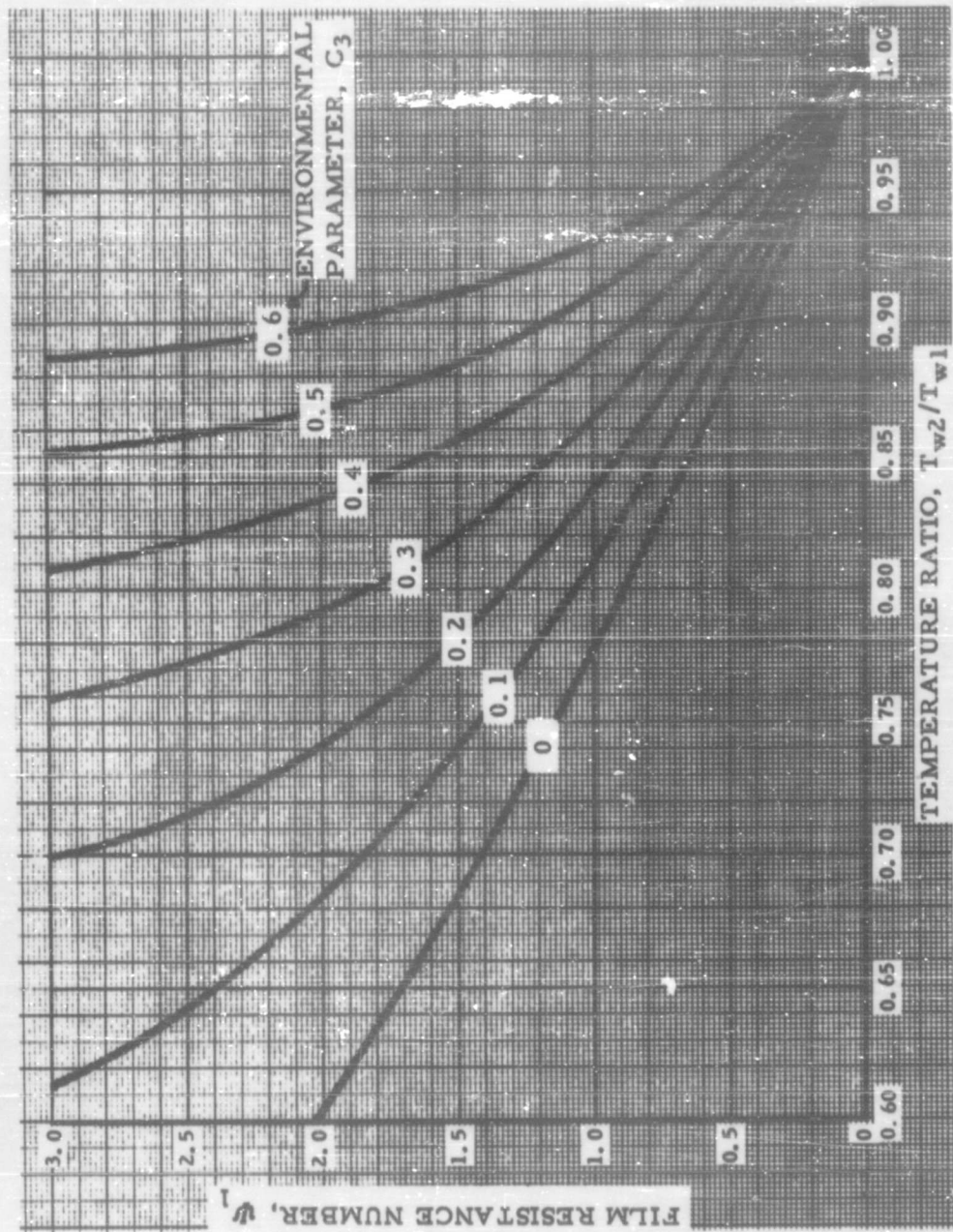


Figure 55. Relationship of Film Resistance Number ψ_1 to Temperature Ratio

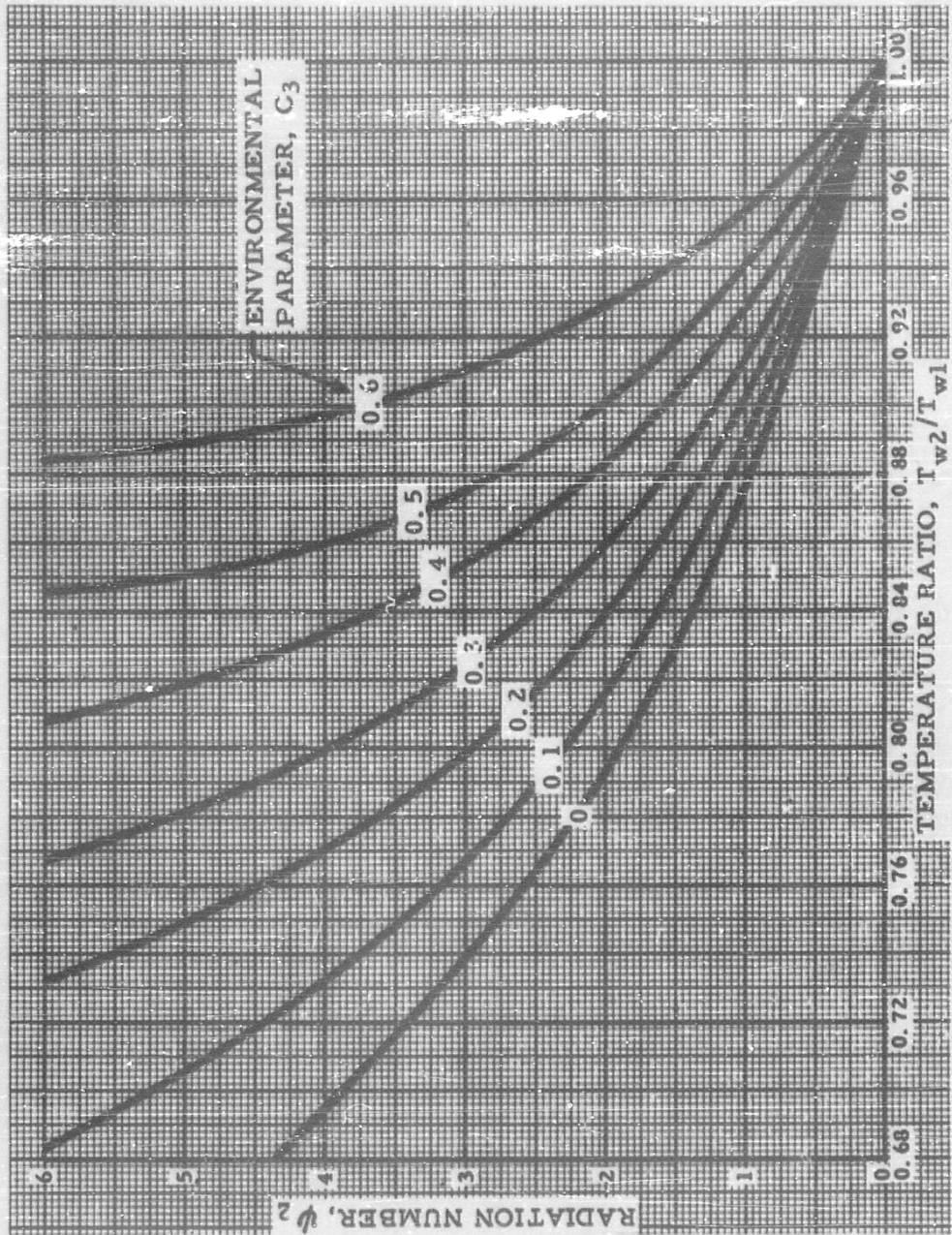


Figure 56. Relationship of Radiation Number ψ_2 to Temperature Ratio

ILLUSTRATIVE PROBLEMS

Problem 1: Determination of Exchanger Length

Given

A horizontal rectangular duct heat exchanger with no extended surfaces is to be mounted on the flat roof of a manned lunar base. Its purpose is to cool the air of the building.

Required

To find the required length L_w of a heat exchanger of a given cross-sectional configuration.

Data

Air density at inlet	0.0663 lb/cu ft
Air temperature at inlet	120 F (580 R)
Air temperature at exit	45 F (505 R)
Air velocity at heat exchanger entrance	40 ft/sec
Air passage height	1/8 in. (0.01042 ft)
Heat exchanger surface coating	Magnesium oxide
Heat exchanger surface absorptivity	0.08
Heat exchanger surface emissivity	0.90

The weight rate of flow w and the duct width are unspecified. The underside of the duct is insulated so that no heat can be transmitted from that surface. The position of the sun is directly overhead.

Procedure

The heat transfer coefficient h is found from Reference 15 (page 226) to be

$$h = \frac{0.0144 c P G^{0.8}}{D_h^{0.2}}$$

where

$$G = V\rho = (40 \times 3600)(0.0663) = 9500 \text{ lb}/(\text{sq ft})(\text{hr})$$

and

$$D_h = \frac{4 A_d}{P_t} = \frac{4 (0.01042 L_d)}{2 L_d} = 0.02084 \text{ ft}$$

Note that although the total perimeter is called for here, the end dimensions are negligible in comparison with the duct width. Also,

$$c_p = 0.24 \text{ Btu/(lb)(}^\circ\text{R)}$$

Then,

$$\begin{aligned} h &= \frac{0.0144(0.24)(9550^{0.8})}{0.02084^{0.2}} \\ &= 11.4 \text{ Btu/(hr)(sq ft)(}^\circ\text{R)} \end{aligned}$$

The constant C_1 is

$$\begin{aligned} C_1 &= \sigma' a \\ &= 0.90 (0.1713 \times 10^{-8}) = 0.1542 \times 10^{-8} \end{aligned}$$

and the solar heat absorbed by the exchanger surface is the product of the solar constant and surface absorptivity, or

$$\begin{aligned} C_2 &= S_c a \\ &= 430 (0.08) = 34.4 \text{ Btu/(sq ft)(hr)} \end{aligned}$$

The wall temperatures T_{w1} and T_{w2} were obtained by trial-and-error solutions of Equation 152 as 569 and 499.6 R, respectively, and

$$\frac{T_{w2}}{T_{w1}} = \frac{499.6}{569} = 0.877$$

Also

$$\begin{aligned} C_3 &= \frac{C_2}{C_1 T_{w1}^4} \\ &= \frac{34.4}{0.1542 \times 10^{-8} (569^4)} = 0.214 \end{aligned}$$

From Equation 160,

$$\psi_1 = 0.742$$

and from Equation 163,

$$\psi_2 = 1.37$$

The weight rate of flow is determined by the equation of continuity as

$$\begin{aligned} w &= \rho V A_d \\ &= 0.0663 (40 \times 3600) (0.01042 L_d) = 99.5 L_d \end{aligned}$$

Rewriting Equation 156,

$$\frac{ph L_w}{w c_p} = \psi_1 + \left(\frac{ph}{6C_1 T_{w1}^3 L_d} \right) \psi_2$$

$$\frac{L_d (11.4) L_w}{99.5 (L_d) 0.24} = 0.742 + \left(\frac{L_d (11.4)}{6 (0.1542 \times 10^{-8}) (568^3) L_d} \right) 1.37$$

$$L_w = 20.8 \text{ ft}$$

Note that the perimeter p used here is the width L_d of the radiating surface only.

This length for a heat exchanger appears to be prohibitive, and some compromise or change of design would probably be made. One possible change is the addition of extended surfaces.

Problem 2: Determination of Extended-Surface Exchanger Length

Given

The same conditions as problem 1 and the exchanger configuration of Figure 57 are assumed.

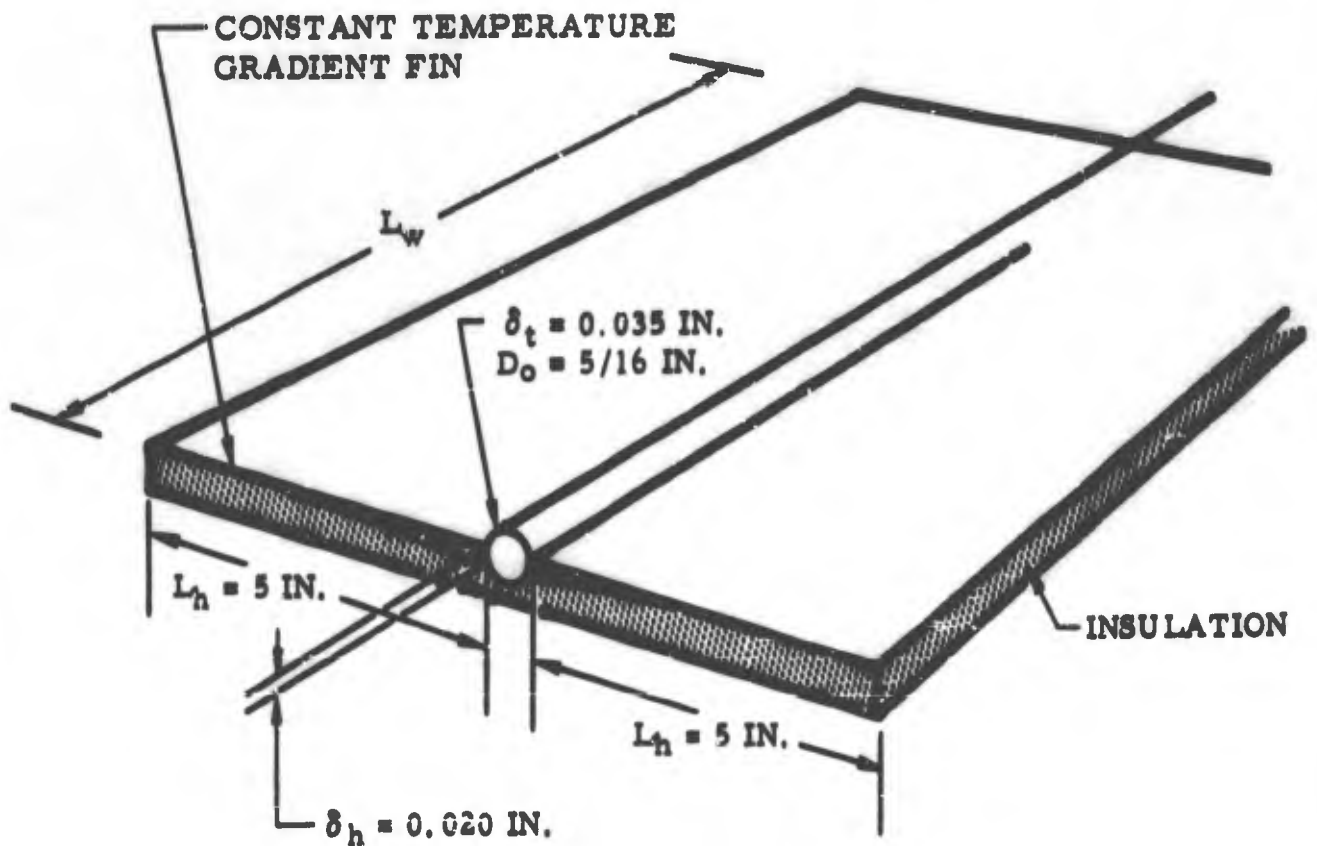


Figure 57. Configuration of Heat Exchanger (Problem 2)

Required

To find the required length L_w of a heat exchanger of the given configuration.

Data

The same conditions obtain as in problem 1, except that duct diameter is known. The exchanger tube and extended areas are made of aluminum, and

$$k = 118 \text{ Btu}/(\text{hr})(\text{ft})(^\circ\text{R})$$

Procedure

The heat transfer coefficient is found, from the equation of Reference 15, to be

$$h = 11.25 \text{ Btu}/(\text{sq ft})(\text{hr})(^\circ\text{R})$$

From problem 1,

$$C_1 = 0.1542 \times 10^{-8}$$

$$C_2 = 34.4$$

The value of duct width L_d was assumed, conservatively, to be equal to the tube diameter, or

$$L_d = 0.3125 \text{ in.} = 0.026 \text{ ft}$$

The effective perimeter for this case is approximately equal to the inside perimeter of the tube, or

$$\begin{aligned} p &= \pi D_1 \\ &= \frac{\pi(0.2425)}{12} = 0.0635 \text{ ft} \end{aligned}$$

The wall temperatures T_{w1} and T_{w2} were obtained by a multiple-step trial-and-error process, as follows:

1. The wall temperature was assumed equal to the adjacent fluid temperature.
2. The values of effectiveness Ω were obtained from Figure 17 for the fin at the tube entrance and exit.
3. The interradiation correction factor F_r was checked and found to be nearly equal to 1.0.
4. The equivalent length L_e at entrance and exit were computed by using Equation 172.
5. The "new" wall temperatures T_{w1} and T_{w2} were then obtained, by trial-and-error, using Equation 175.
6. With these wall temperatures, steps 2, 4, and 5 were repeated until consistent values of effectiveness and wall temperature were obtained.

The following results were obtained after calculation:

$$T_{w1} = 516.25 \text{ R}$$

$$T_{w2} = 468.0 \text{ R}$$

$$\frac{T_{w1}}{T_{w2}} = 0.9065$$

$$C_3 = \frac{C_2}{C_1 T_{w1}^4} = 0.327$$

$$\frac{C_2}{C_1 T_{w2}^4} = 0.477$$

and

$$\Omega_1 = 0.478$$

$$\Omega_2 = 0.412$$

Also

$$L_{e1} = 0.6185$$

$$L_{e2} = 0.6835$$

$$L_e = 0.651 \text{ (average)}$$

and

$$w = \rho V A_d$$

$$= 0.0663 (40 \times 3600) (3.205 \times 10^{-4}) = 3.06 \text{ lb/hr}$$

From Figures 55 and 56,

$$\psi_1 = 0.67$$

$$\psi_2 = 1.18$$

Rewriting Equation 179,

$$\frac{ph L_w}{w c_p} = \psi_1 + \left(\frac{ph}{6C_1 L_e T_{w1}^3} \right) \psi_2$$

$$\frac{0.0635 (11.25) L_w}{3.06 (0.24)} = 0.67 + \frac{0.0635 (11.25)(1.18)}{6 (0.1542 \times 10^{-8}) (0.651) (516.25^3)}$$

$$L_w = 1.735 \text{ ft} = 20.8 \text{ in.}$$

Heat exchangers of these dimensions would seem to be convenient for their intended use and to offer no difficulty in fabrication. Other applications may present problems requiring several trials before arriving at a satisfactory solution.

REFERENCES

The following references are listed in the order in which they are encountered in the text of this report.

1. American Standards Association, "Letter Symbols for Heat and Thermodynamics," ASAY10.4-1957, Published by American Society of Mechanical Engineers.
- *2. Mackay, D. B., and Leventhal, E. L., "Radiant Heat Transfer From a Flat Plate Uniformly Heated Along One Edge," Paper 23, American Institute of Chemical Engineers, August 1960.
3. Lieblein, S., "Analysis of Temperature Distribution and Radiant Heat Transfer Along a Rectangular Fin of Constant Thickness," Technical Note D-196, National Aeronautics and Space Administration, November 1959.
4. Bartis, J. G., and Sellers, W. H., "Radiation Fin Effectiveness," Journal Heat Transfer, Transactions of the American Society of Mechanical Engineers, Vol 82, 1960, p 73-75.
5. Chambers, R. L., and Somers, E. V., "Radiation Fin Efficiency for One-Dimensional Heat Flow in a Circular Fin," Journal Heat Transfer, Transactions of the American Society of Mechanical Engineers, Paper 59-HT-8.
- *6. Mackay, D. B., "Radiant Heat Transfer From Tapered Fin With Constant Temperature-Gradient, Uniformly Heated at Root Section," Paper 24, American Institute of Chemical Engineers, August 1960.
7. Schmidt, E., "Die Wärmeübertragung durch Rippen," Zeitschrift des Vereines Deutscher Ingenieure, Vol 70, 1926, p 885-889.
8. Duffin, R. J., "A Variational Problem Relating to Cooling Fins," Journal of Mathematics and Mechanics, Vol 8, 1959, p 47-56.

*Included in Appendix

9. Wilkins, J. E., Jr., "Minimizing the Mass of Thin Radiating Fins," Journal of Aero/Space Sciences, Vol 27, February 1960, p 145-147.
10. Wilkins, J. E., Jr., "Minimum Mass Thin Fins Which Transfer Heat Only by Radiation to Surroundings at Absolute Zero," Journal of the Society for Industrial and Applied Mathematics, December 1960.
11. Wilkins, J. E., Jr., "Minimum Mass Thin Fins for Space Radiators," Proceedings of 1960 Heat Transfer and Fluid Mechanics Institute, Stanford University, 15-17 June 1960, p 228-243.
12. Nilson, E. N., and Curry, R., "The Minimum Weight Straight Fin of Triangular Profile Radiating to Space," Journal of Aero/Space Sciences, Vol 27, 1960, p 146.
13. Mackay, D. B., "Condenser Design for Space Systems," Space and Information Systems Division, North American Aviation, Inc., Report MD 60-206, 15 July 1960.
14. Sparrow, E. M., and Eckert, E. R. G., "Radiant Interaction Between Fin and Base Surface," Paper 61-AV-30, American Society of Mechanical Engineers, March 1961.
15. McAdams, W. H., Heat Transmission, Third Edition, McGraw-Hill, Inc., New York, 1954.
16. Weatherford, W. D., Jr., Tyler, J. C., Ku, P. M., "Properties of Inorganic Working Fluids and Coolants for Space Applications" (Southwest Research Institute), Wright Air Development Division, WADD TR 59-598, December 1959.
17. Mackay, D. B., "Techniques for Space Heat Exchanger Design," Space and Information Systems Division, North American Aviation, Inc., MD 60-111, 1960.

Section VII

BIBLIOGRAPHY

This bibliography is divided into three parts, with the sources in each part listed in alphabetic order. The three divisions cover (1) the general field of radiation in space, radiators and condensers, (2) heat transfer and fluid flow in heat exchanger tubes, and (3) the protection of radiating surfaces from meteoritic damage.

SPACE RADIATION AND RADIATOR DESIGN

1. Bartas, J. G., and Sellers, W. H., "Radiation Fin Effectiveness" Transactions of the American Society of Mechanical Engineers, Vol 82, 1960, p 73-75.
2. Chambers, R. L., and Somers, E. V., "Radiation Fin Efficiency for One-Dimensional Heat Flow in a Circular Fin," Transactions of the American Society of Mechanical Engineers, Vol 81, 1959, p 327-329.
3. Charnes, A., and Raynor, S., "Solar Heating of a Rotating Cylindrical Shape in Space," ARS Journal, Vol 30, No. 5, May 1960, p 479-484.
4. Coombs, M. G., and Stone, R. A., "SNAP 2 Radiative-Condenser Design," Space Power Systems Conference, American Rocket Society, Paper 1328-60, September 1960.
5. Cornog, Robert, "Design Optimization of Thermal Radiators for Space Vehicles," Western National Meeting, American Astronautical Society, 4-5 August 1959.
6. Duffin, R. J., "A Variational Problem Relating to Cooling Fins," Journal of Mathematics and Mechanics, Vol 8, 1959, p 47-56.

7. Eckert, E. R. G. , Irvine, T. F. , Jr. , and Sparrow, E. M. , "Analytical Formulation for Radiating Fins With Mutual Irradiation, " ARS Journal, Vol 30, 1960, p 644-646.
8. Holden, P. C. , and Stump, F. C. , "Optimized Condenser-Radiator for Space Applications, " American Society of Mechanical Engineers, Publication 60-AV-16, 1960.
9. Lieblein, S. , "Analysis of Temperature Distribution and Radiant Heat Transfer Along a Rectangular Fin of Constant Thickness, " Technical Note D-196, National Aeronautics and Space Administration, November 1959.
10. Mackay, D. B. , "Techniques for Space Heat Exchanger Design, " Space and Information Systems Division, North American Aviation, Inc. , Report MD 60-111, 1960.
11. Mackay, D. B. , "Condenser Design for Space Systems, " Space and Information Systems Division, North American Aviation, Inc. , Report MD 60-206, 1960.
12. Mackay, D. B. , "Radiant Heat Transfer From Tapered Fins, " Space and Information Systems Division, North American Aviation, Inc. , Report MD 60-211, 1960.
13. Mackay, D. E. , and Leventhal, E. L. , "Radiant Heat Transfer From a Flat Plate Uniformly Heated Along One Edge, " American Institute of Chemical Engineers, Paper 23, August 1960.
14. Mackay, D. B. , "Temperature Control for Lunar Vehicles, " Space and Information Systems Division, North American Aviation, Inc. , Report MD 59-15, 1959.
15. Nilson, E. N. , and Curry, R. , "The Minimum Weight Straight Fin of Triangular Profile Radiating to Space, " Journal of Aero/Space Sciences, Vol 27, 1960, p 146.
16. Ross, D. P. , Ray, E. , and Haller, H. C. , "Heat Rejection From Space Vehicles, " American Astronautical Society, Preprint 60-39, January 1960.
17. Schmidt, E. , "Die Warmeubtragung durch Rippen, " Zeitschrift des Vereines Deutscher Ingenieure, Vol 70, 1926, p 885-889.

18. Sparrow, E. M., and Eckert, E. R. G., "Radiant Interaction Between Fin and Base Surface," Paper 60-AV-30, American Society of Mechanical Engineers, March 1961.
19. Tatom, J. W., "Steady State Behavior of Extended Surfaces in Space," ARS Journal, Vol 30, 1960, p 118.
20. Weatherford, W. D., Jr., Tyler, J. C., Ku, P. M., "Properties of Inorganic Working Fluids and Coolants for Space Applications" (Southwest Research Institute), Wright Air Development Division, WADD TR 59-598, December 1959.
21. Weatherston, R. C., and Smith, W. E., "A Method for Heat Rejection From Space Powerplants" ARS Journal, Vol 30, No. 3, March 1960, p 268-269.
22. Wilkins, J. E., Jr., "Minimizing the Mass of Thin Radiating Fins," Journal of Aero/Space Sciences, Vol 27, February 1960, p 145-147.
23. Wilkins, J. E., Jr., "Minimum Mass Thin Fins for Space Radiators" Proceedings of 1960 Heat Transfer and Fluid Mechanics Institute, Stanford University, 15-17 June 1960, p 228.
24. Wilkins, J. E., Jr., "Minimum Mass Thin Fins Which Transfer Heat Only by Radiation to Surroundings at Absolute Zero," Journal of Society for Industrial and Applied Mathematics, December 1960.

HEAT TRANSFER AND FLUID FLOW

1. Abramson, A. E., "Investigation of Annular Liquid Flow with Co-current Air Flow in Horizontal Tubes," Journal of Applied Mechanics, Vol 19, 1952, p 267.
2. Adler, C. R., Mark, A. M., Marshall, W. R., Jr., and Parent, R. J., "A Scanning Device for Determining the Size Distribution of Spray Droplets," Chemical Engineering Progress, Vol 50, 1954, p 14.
3. Akers, W. W., and Rosson, H. F., "Condensation Inside a Horizontal Tube," Heat Transfer Conference, American Society of Mechanical Engineers/American Institute of Chemical Engineers, Preprint 114, 9-12 August 1959.
4. Alexander, L. G., and Coldren, C. W., "Droplet Transfer From Suspending Air to Duct Walls," Industrial and Engineering Chemistry, Vol 43, 1951, p 1325.

5. Allen, W. F., "Flow of Flashing Mixture of Water and Steam Through Pipes and Valves," Transactions of the American Society of Mechanical Engineers, Vol 73, 1951, p 257.
6. Altman, M., Norris, R. H., and Staub, F. W., "Local Heat Transfer and Pressure Drop for Refrigerant-22 Condensing in Horizontal Tubes," Heat Transfer Conference, American Society of Mechanical Engineers/American Institute of Chemical Engineers, Preprint 115, 9-12 August 1959.
7. Alves, G. E., "Co-Current Liquid Gas Flow in a Pipe-Line Contractor," Chemical Engineering Progress, Vol 50, 1954, p 449.
8. Badger, W. L., "How a Long-Tube Evaporator Works," Chemical and Metallurgical Engineering, Vol 46, 1939, p 640.
9. Bailey, J. F., "Metastable Flow of Saturated Water," Transactions of the American Society of Mechanical Engineers, Vol 73, 1951, p 1109.
10. Baker, Q., "Design of Pipelines for the Simultaneous Flow of Oil and Gas," The Oil and Gas Journal, 26 July 1954.
11. Barbet, E., "Evaporation in the Sugar Industry," Bulletin de l'association chimistes de sucrerie, de distillerie et des industries agricoles de France et des colonies, Vol 32, No. III, 1914.
12. Baron, T., Sterling, C. S., and Schueler, A. P., "Viscosity of Suspensions: Review and Application to Two-Phase Flow," Third Midwestern Conference on Fluid Mechanics, University of Minnesota, 23-25 March 1953, p 103-128.
13. Beatty, K. O., and Nandapurkar, S. S., "Condensation on a Horizontal Rotating Disc," Heat Transfer Conference, American Society of Mechanical Engineers/American Institute of Chemical Engineers, Preprint 112, 9-12 August 1959.
14. Begell, W., and Hoopes, J. W., Jr., "Acceleration Pressure Drops in Two-Phase Flow," Technical Information Service, Atomic Energy Commission, Report Cu-18-54-At-dP-Ch, 1954.
15. Benjamin, M. W., and Miller, J. G., "The Flow of Saturated Water Through Throttling Orifices," Transactions of the American Society of Mechanical Engineers, Vol 63, 1941, p 419.

16. Benjamin, M. W., and Miller, J. G., "The Flow of a Flashing Mixture of Water and Steam Through Pipes," Transactions of the American Society of Mechanical Engineers, Vol 64, 1942, p 657.
17. Bergelin, O. P., "Flow of Gas-Liquid Mixtures" Chemical Engineering, Vol 56, 1949, p 104.
18. Bergelin, O. P., and Dukler, A. E., "The Characteristics of Flow in the Falling Liquid Films," Paper Obtained From A. E. Dukler, 1952.
19. Bergelin, O. P., and Gazley, C., Jr., "Co-Current Gas-Liquid Flow: I. Flow in Horizontal Tubes," Heat Transfer and Fluid Mechanics Institute, American Society of Mechanical Engineers, 1949.
20. Bergelin, O. P., Kegel, P. K., Carpenter, F. G., and Gazley, C., Jr., "Co-Current Gas-Liquid Flow: II. Flow in Vertical Tubes," Heat Transfer and Fluid Mechanics Institute, American Society of Mechanical Engineers, 1949, p 19-28.
21. Boelter, L. M. K., and Kepner, R. C., "Pressure Drop Accompanying Two-Component Flow Through Pipes," Industrial and Engineering Chemistry, Vol 31, 1939, p 426.
22. Bolstad, M. M., and Jordan, R. C., "Theory and Use of the Capillary Tube Expansion Device," Refrigeration Engineering, Vol 56, 1948, p 519.
23. Bolstad, M. M., and Jordan, R. C., "Theory and Use of the Capillary Tube Expansion Device. Part II. Nonadiabatic Flow," Refrigeration Engineering, Vol 57, 1949, p 577.
24. Bonilla, C. F., et al, "Boiling and Condensing of Liquid Metals," Atomic Energy Commission, Report NYO-314, February 1952.
25. Bottomley, W. T., "The Flow of Saturated Water Through Throttling Orifices," Transactions of the North-East Coast Institution of Engineers and Shipbuilders, Vol 53, 1937, p 65.
26. Bridge, T. E., "How To Design the Piping for Conveying Flashing Hot Water," Heating, Piping and Air Conditioning, March 1949 (p 63-73), April 1949 (p 92-96), and May 1949 (p 98-100).
27. Brooks, C. H., and Badger, W. L., "Heat Transfer Coefficients in the Boiling Section of a Long-Tube, Natural-Circulation Evaporator," Transactions of the American Institute of Chemical Engineers, Vol 33, 1937, p 392.

28. Burnell, J. C. , "Flow of Boiling Water Through Nozzles, Orifices and Pipes," Engineering, Vol 164, 1947, p 572.
29. Calvert, S. , "Vertical, Upward, Annular, Two-Phase in Smooth Tubes," Doctorate Thesis, University of Michigan, 1952.
30. Chenoweth, J. M. , and Martin, M. W. , Petroleum Refiner, Vol 34, 1955, p 151.
31. Chiarulli, P. , and Pressler, R. F. , "Condensation Interfaces in Two-Phase Flows," Journal of Applied Physics, Vol 28, 1957, p 990.
32. Chisholm, D. , Laird, A. D. K. , "Two-Phase Flow in Rough Tubes" Transactions of the American Society of Mechanical Engineers, Vol 80, 1958, p 276.
33. Cromer, S. , and Huntington, R. L. , "Visual Studies of the Flow of Air-Water Mixtures in a Vertical Pipe," Transactions of the American Institute of Mining, Metallurgical, and Petroleum Engineers, Vol 136, 1940, p 79.
34. Davidson, W. F. , Hardie, P. H. , Hymphreys, C. G. R. , Markson, A. A. , Mumford, A. R. , and Ravese, T. , "Studies of Heat Transmission Through Boiler Tubing at Pressures From 500-3300 Psi," Transactions of the American Society of Mechanical Engineers, Vol 65, 1943, p 544.
35. Dengler, C. E. , "Heat Transfer and Pressure Drop for Evaporation of Water in a Vertical Tube," Doctorate Thesis, Massachusetts Institute of Technology, 1952.
36. Dittus, F. W. , and Hildebrand, A. , "A Method of Determining the Pressure Drop for Oil-Vapor Mixtures Flowing Through Furnace Coils," Transactions of the American Society of Mechanical Engineers, Vol 64, 1942, p 185.
37. Dukler, E. , "Fluid Mechanics and Heat Transfer in Vertical Falling Film Systems," Heat Transfer Conference, American Society of Mechanical Engineers/American Institute of Chemical Engineers, Preprint 101, 9-12 August 1959.
38. Dusinberre, G. M. (Discussion of M. W. Benjamin and J. G. Miller), "The Flow of a Flashing Mixture of Water and Steam Through Pipes," Transactions of the American Society of Mechanical Engineers, Vol 64, 1942, p 666.

39. Eckert, E. R. G., and Drake, R. M., Jr., Heat and Mass Transfer, Second Edition, McGraw-Hill Book Company, New York, 1959.
40. Eddy, K. C., "Pressure Drops in Two-Phase Flow," Masters Thesis, University of Minnesota, 1954.
41. Feldman, S., "On the Hydrodynamic Stability of Two Viscous Incompressible Fluids in Parallel Uniform Shearing Motion," Journal of Fluid Physics, Vol 2, Part 4, June 1957, p 343.
42. Folz, H. L., and Murray, R. G., "Two-Phase Flow Rates and Pressure Drops in Parallel Tubes," Heat Transfer Conference, American Society of Mechanical Engineers/American Institute of Chemical Engineers, Preprint 109, 9-12 August 1959.
43. Fried, L., "Pressure Drop and Heat Transfer for Two-Phase, Two-Component Flow," Chemical Engineering Progress Symposium Series, Vol 50, No. 9 (Published by American Institute of Chemical Engineers), 1954, p 47.
44. Galegar, W. C., "Simultaneous Fluid Flow of Water and Air In Vertical Pipes," Masters Thesis, University of Oklahoma, 1953.
45. Gazley, C., Jr., "Co-Current Gas-Liquid Flow: III. Interfacial Shear and Stability," Heat Transfer and Fluid Mechanics Institute, American Society of Mechanical Engineers, 1949, p 29.
46. Harvey, B. F., and Foust, A. S., "Two-Phase One Dimensional Flow Equations and Their Application to Flow in Evaporator Tubes," Chemical Engineering Progress Symposium Series, Vol 49, No. 5 (Published by American Institute of Chemical Engineers), 1953, p 91.
47. Haywood, R. W., "Research Into the Fundamentals of Boiler Circulation Theory," Discussion on Heat Transfer (London), Institute of Mechanical Engineers, 11-13 September 1951, p 20-22.
48. Heinrich, G., "The Equations of Flow of a Gas/Liquid Mixture," Zeitschrift für angewandte Mathematik and Mechanik, Vol 22, No. 2, 1942, p 117.
49. Hodkinson, B., "The Flow of Hot Water Through a Nozzle," Engineering, Vol 143, 1937, p 629.
50. Homes, Flooding Velocities in Empty Vertical Tubes: Chemical Engineers' Handbook (J.H. Perry, Editor), Third Edition, McGraw-Hill Book Company, New York, 1950, p 686 (Fig. 17 and 18).

51. Hughes, R. R. , Evans, H. D. , and Sternling, C. V. , "Flash Vaporization," Chemical Engineering Progress, Vol 49, 1953, p 78.
52. Ingersoll, L. R. , Zobel, O. J. , and Ingersoll, A. C. , Heat Conduction, University of Wisconsin Press, 1954, p 190-199.
53. Isbin, H. S. (Discussion of J. L. Schweppe and A. S. Foust), "Effect of Forced Circulation Rate on Boiling-Heat Transfer and Pressure Drop in a Short Vertical Tube," Chemical Engineering Progress Symposium Series, Vol 49, No. 5, (Published by American Institute of Chemical Engineers), 1953, p 77.
54. Isbin, H. S. , Moy, J. E. , DaCruz, A. J. R. , "Two-Phase Stream Water Critical Flow," American Institute of Chemical Engineering Journal, Vol 3, No. 3, September 1957, p 361-365.
55. Jackson, C. B. (Editor in Chief), Liquid Metals Handbook, Sodium NaK Supplement, Atomic Energy Commission and Department of the Navy, Washington, D. C. , July 1955, p 85-88.
56. Jenkins, R. , "Two-Phase Two-Component Flow of Air and Water," Masters Thesis, University of Delaware, 1947.
57. Jens, W. H. (Discussion of J. A. Clark and W. M. Rohsenow), "Local Boiling Heat Transfer to Water at Low Reynolds Numbers at High Pressures," Transactions of the American Society of Mechanical Engineers, Vol 76, 1954, p 561.
58. Johnson, H. A. , and Abou-Sabe, A. H. , "Heat Transfer and Pressure Drop for Turbulent Flow of Air-Water Mixtures in a Horizontal Pipe," Transactions of the American Society of Mechanical Engineers, Vol 74, 1952, p 977.
59. Kirschbaum, E. , Kranz, B. , and Starck, D. , "Heat Transfer With a Vertical Vaporizing Tube," Zeitschrift des Vereines Deutscher Ingenieure, Forschungsheft, 1935, p 375.
60. Kosterin, S. I. , "An Investigation of the Influence of the Diameter and the Attitude of a Pipe on the Hydraulic Resistances and on the Structure of Flow of a Gas-Liquid Mixture," Izvestia Akademii Nauk, SSSR Otdelenie Tekhnicheskii Nauk, July-December 1949, p 1864.
61. Kosterin, S. I. , and Rubanovich, M. N. , "The Effect of Surface Tension of a Liquid on the Hydraulic Resistance and the Structure of Flow of a Gas-Liquid Mixture in Pipes," Izvestia Akademii Nauk, SSSR Otdelenie Tekhnicheskii Nauk, July-December 1949, p 1085.

62. Krasiakova, L., "Some Characteristic Flows of a Two-Phase Mixture in a Horizontal Pipe," Zhurnal Technicheskoi Fiziki, Vol 22, No. 4, 1952, p 656.
63. Kreith, F., Heat Transfer and Fluid Mechanics Institute, University of California, 1958.
64. Laird, A.D.K., "Stability of Gas Flow in a Tube as Related to Vertical Annular Gas-Liquid Flow," Transactions of the American Society of Mechanical Engineers, Vol 76, 1959, p 1005.
65. Ledinegg, M., "Flow Distribution in Forced Circulation Boilers," The Engineers' Digest, Vol 10, 1949, p 85.
66. Leib, E.F. (Discussion of J. van Brunt), "A Study of Circulation in High-Pressure Boilers and Water-Cooled Furnaces," Transactions of the American Society of Mechanical Engineers, Vol 63, 1941, p 344.
67. Leppert, G., "Pressure Drop During Forced-Circulation Boiling," Doctorate Thesis, Illinois Institute of Technology, 1954.
68. Levy, S., "Theory of Pressure Drop and Heat Transfer for Two-Phase Two-Component Annular Flow in Pipes," Ohio State University Engineering Experiment Station, Bulletin 149 (Proceedings of the Second Midwestern Conference on Fluid Mechanics, 1952, p 337).
69. Lewis, W.Y., and Robertson, S.A., "The Circulation of Water and Steam in Water-Tube Boilers, and the Rational Simplification of Boiler Design," Proceedings of the Institute of Mechanical Engineers (London), Vol 143, 1940, p 147.
70. Lieberon, N.G., "Two-Phase Flow in Vertical Pipes," Masters Thesis, Massachusetts Institute of Technology, 1952.
71. Linning, D.L., "The Adiabatic Flow of Evaporating Fluids in Pipes of Uniform Bore," Proceedings of the Institute of Mechanical Engineers (London), Vol 1B, No. 2, 1952.
72. Lockhart, R.W., and Martinelli, R.C., "Proposed Correlation of Data for Isothermal Two-Phase, Two-Component Flow in Pipes," Chemical Engineering Progress, Vol 45, 1949, p 39.
73. Luborsky, Bernard, and Kaufman, S.J., "Review of Experimental Investigations of Liquid Metal Heat Transfer," National Advisory Committee for Aeronautics, NACA TN 3336, March 1955.

74. Marcy, G. P., "Pressure Drop With Change of Phase in a Capillary Tube," Refrigerating Engineering, Vol 57, 1949, p 53.
75. Markson, A.A., Ravese, T., and Humphreys, C.G.R., "A Method of Estimating the Circulation in Steam-Boiler-Furnace Circuits," Transactions of the American Society of Mechanical Engineers, Vol 64, 1942, p 275.
76. Martinelli, R.C., Boelter, L.M.K., Taylor, T.H.M., Thomsen, E.G., and Morrin, E.H., "Isothermal Pressure Drop for Two-Phase Two-Component Flow in a Horizontal Pipe," Transactions of the American Society of Mechanical Engineers, Vol 66, 1944, p 139.
77. Martinelli, R.C., "Heat Transfer to Molten Metals," Transactions of the American Society of Mechanical Engineers, November 1947, p 947-959.
78. Martinelli, R.C., and Nelson, D.B., "Prediction of Pressure Drop During Forced-Circulation in Boiling of Water," Transactions of the American Society of Mechanical Engineers, Vol 70, 1948, p 695.
79. Martinelli, R.C., Pulnam, J.A., and Lockhart, R.W., "Two-Phase, Two-Component Flow in the Viscous Region," Transactions of the American Institute of Chemical Engineers. Vol 42, 1946, p 681.
80. McAdams, W.H., Heat Transmission, Third Edition, McGraw-Hill Book Company, New York 1954.
81. McAdams, W.H., Woods, W.K., and Heroman, L.C., Jr., "Vaporization Inside Horizontal Tubes: II. Benzene-Oil Mixtures," Transactions of the American Society of Mechanical Engineers, Vol 64, 1942, p 193.
82. Misra, B., and Bonilla, C.F., "Heat Transfer in the Condensation of Metal Vapors," Chemical Engineering Progress Symposium Series, Vol 52, No. 18, 1956, p 7-21.
83. Moore, T.V., and Wilde, H.D., Jr., "Experimental Measurement of Slippage in Flow Through Vertical Pipes," Transactions of the American Institute of Mining, Metallurgical, and Petroleum Engineers, Vol 92, 1931, p 296.
84. Nusselt, W., Zeitschrift des Vereines Deutscher Ingenieure, Vol 60, p 541-569, 1916.

85. Pasqua, P.F., "Metastable Flow of Freon-12," Refrigerating Engineering, Vol 61, 1953, p 1084A.
86. Radford, B.A., "Gas-Liquid Flow in Vertical Pipes: A Preliminary Investigation," Masters Thesis, University of Alberta, 1949.
87. Rateau, A., "Experimental Researches on the Flow of Steam Through Nozzles and Orifices, to Which Is Added a Note on the Flow of Hot Water," A. Constable and Company, Ltd., London, 1905.
88. Reveal, W.S., "Heat Transmission Studies in a Natural Circulation Evaporator," Doctorate Thesis, University of Minnesota, 1946.
89. Rogers, J.D., "Two-Phase Flow of Hydrogen in Horizontal Tubes," Depository Library, Atomic Energy Commission, Report AECU-2203.
90. Rohsenow, W.M., "Heat Transfer and Temperature Distribution in Laminar-Film Condensation," Transactions of the American Society of Mechanical Engineers, Vol 78, 1956, p 1645-1948.
91. Schneider, P.J., Conduction Heat Transfer, Addison-Wesley, Massachusetts, 1955, p 3-7, 26-29.
92. Schlichting, H., Boundary Layer Theory, McGraw-Hill Book Company, New York, 1955.
93. Schneider, F.N., White, P.D., and Huntington, R.L., "Some Aspects of Simultaneous Horizontal Two-Phase Fluid Flow Through Pipelines," Petroleum Branch Meeting, American Institute of Mining, Metallurgical, and Petroleum Engineers, 19-21 October, 1953.
94. Schueler, A.P., "Momentum Transfer in Two-Phase Flow," Masters Thesis, University of Illinois, 1951.
95. Schurig, W., "Water Circulation in Steam Boilers and the Motion of Liquid-Gas Mixtures in Tubes," Zeitschrift des Vereines Deutscher Ingenieure, Forschungsheft 365, 1934.
96. Seban, R.A., "Remarks on Film Condensation with Turbulent Flow," Transactions of the American Society of Mechanical Engineers, Vol 76, 1954, p 299-303.
97. Shaw, S.F., "Flow Characteristics of Gas Lift in Oil Production," Texas A & M Engineering Experiment Station, Bulletin 113, 1 July 1947.

98. Shugaev, V., and Sorokin, S., "The Hydraulic Resistance of a Two-Phase Mixture," Zhurnal Tekhnicheskoi Fiziki, Vol IX, No. 20, 1939, p 1854.
99. Silver, R.S., "A Thermodynamic Theory of Circulation in Water-Tube Boilers," Proceedings of the Institute of Mechanical Engineers, Vol 153, 1945, p 261.
100. Silver, R.S., "Temperature and Pressure Phenomena in the Flow of Saturated Liquid," Proceedings of the Royal Society (London), Series A, Vol 194, 1948, p 464.
101. Silver, R.S., and Mithcell, J.A., "The Discharge of Saturated Water Through Nozzles," Mechanical World, Vol 119, 1946, p 92.
102. Sobocuski, E.P., and Huntington, R.L., "Concurrent Flow of Air, Gas-Oil and Water in a Horizontal Pipe," Transactions of the American Society of Mechanical Engineers, Vol 80, 1958, p 252.
103. Sparrow, E.M., and Gregg, J.L., "A Boundary Layer Treatment of Laminar Film Condensation," Transactions of the American Society of Mechanical Engineers, Vol 81, Series C, 1959, p 13-18.
104. Sparrow, E.M., and Gregg, J.L., "Laminar Condensation Heat Transfer on a Horizontal Cylinder," Transactions of the American Society of Mechanical Engineers, Vol 81, Series C, 1959, p 291-296.
105. Stein, R.P., Hoopes, J.W., Jr., Markels, M., Jr., Selke, W.A., Bandler, A.J., and Bonilla, C.F., "Pressure Drop and Heat Transfer to Nonboiling and Boiling Water in Turbulent Flow in an Internally Heated Annulus," Chemical Engineering Progress Symposium Series, Vol 50, No. 11, 1954, p 115.
106. Stovall, W.B., "Two-Phase Vertical Flow of Kerosene and Air," Masters Thesis, University of Oklahoma, 1953.
107. Strocbe, G.W., Baker, E.M., and Badger, W.L., "Boiling-Film Heat Transfer Coefficients in a Long-Tube Vertical Evaporator," Industrial and Engineering Chemistry, Vol 31, 1939, p 200.
108. Stuart, M.C., and Yarnall, D.R., "Fluid Flow Through Two Orifices in Series," Mechanical Engineering, Vol 58, 1939, p 479.
109. Styrikovich, M.A., and Miropolski, Z.L., "Flow Lamination of a High-Pressure Steam-Water Mixture in a Heated Horizontal Pipe," Doklady Akademii Nauk, SSSR, Vol 71, No. 2, 1950.

110. Tangren, R.F., Dodge, C.H., and Seifert, H.S., "Compressibility Effects in Two-Phase Flow," Journal of Applied Physics, Vol 20, 1949, p 637.
111. Tchen, C., "Approximate Theory on the Stability of Interfacial Waves Between Two Streams," Journal of Applied Physics, Vol 27, 1956, p 1533.
112. Untermeyer, S., "Boiling Reactors: Direct Steam Generation for Power," Nucleonics, Vol 12, No. 7, 1954, p 43.
113. Uren, L.C., Gregory, P.P., Hancock, R.A., and Feskov, G.V., "Flow Resistance of Gas-Oil Mixtures Through Vertical Pipes," Transactions of the American Institute of Mining, Metallurgical, and Petroleum Engineers, Vol 86, 1930, p 209.
114. Van Wingen, N., "Pressure Drop for Oil-Gas Mixtures in Horizontal Flow Lines," World Oil, Vol 129, No. 7, 1949, p 156.
115. Versluys, J., "Mathematical Development of the Theory of Flowing Oil Wells," Transactions of the Institute of Mining, Metallurgical, and Petroleum Engineers, Vol 86, 1930, p 192.
116. Vorkauf, H., "Flow in Evaporating Tubes Arranged in Parallel-Influence of Tube Nozzles on Water Circulation," Archiv für Waermewirtschaft, Vol 18, 1937, p 75.
117. Ward, C.N., and Kessler, L.H., "Experimental Study of Air Lift Pumps and Application of Results to Design," University of Wisconsin, Bulletin 1265, Engineering Series, Vol 9, No. 4, 1924.
118. Weatherford, W.D., Jr., Tyler, J.C., and Ku, P.M., "Properties of Inorganic Working Fluids and Coolants for Space Applications," (Southwest Research Institute). Wright Air Development Center, WADC TR 59-598 (AD 230065), December 1959.
119. Weining, F.S., "Some Properties of Foam and the Possible Use of Foam for Model Test Especially in Hypersonic Range," Midwestern Conference on Fluid Mechanics, University of Minnesota, 23-25 March 1953, p 515-528.
120. Weiss, D.H., "Pressure Drop in Two-Phase Flow," Masters Thesis, Illinois Institute of Technology, 1952.
121. Yellot, J.I., and Holland, C.K., "The Condensation of Flowing Steam: Part I. Condensation in Diverging Nozzles," Transactions of the American Society of Mechanical Engineers, Vol 59, 1937, 171.

122. "Radiator-Condenser for Space Environment," Wright Air Development Division, WADD TR 61-20, 31 October 1960.

METEORITIC PROTECTION

1. Aller, L., The Atmosphere of the Sun and Stars, The Ronald Press, New York, 1953, p 8.
2. Baldwin, R.B., The Face of the Moon, University of Chicago Press, 1949.
3. Bjork, R.L., "Effects of a Meteoroid Impact on Steel and Aluminum in Space," RAND Corporation, Report P-1662, December 1958.
4. Bjork, R.L., "Meteoroids Versus Space Vehicles," Semiannual Meeting, American Rocket Society, 9-12 May 1960.
5. Buwalda, P., and Hibbs, A.R., "Scientific Measurements by Explorers I and III," Jet Propulsion Laboratory, Publication 538, 1 August 1958.
6. Clay, W., and Partridge, W., "Wax Modeling Studies of High Speed Impact," Department of Electrical Engineering, University of Utah, Report OSR-5, 1956.
7. Cole, R.H., Underwater Explosions, Princeton University Press, 1948.
8. Coombs, M.G., and Stone, R.A., "SNAP-2 Radiative-Condenser Design," Space Power Systems Conference, American Rocket Society, Paper 1328-60, 27-30 September 1960.
9. Diamond, P.M., "The Central Problem of Large Scale Power Generation in Space-Waste Heat," Institute of Aeronautical Sciences, Paper 59-96, 1959.
10. Dubin, Maurice, "The Meteoritic Environment from Direct Measurements," National Aeronautics and Space Administration.
11. Gazley, C., Jr., Kellogg, W.W., and Vestine, E.H., "Space Vehicle Environment," The RAND Corporation, Report P-1335, 7 July 1958, p 24-41.
12. Goetzman, R.C., "Measurement of Satellite Erosion Rates by the Backscattering of β -Rays," Jet Propulsion, November 1958.

13. Grimminger, G., "Possibility That a Meteorite Will Hit or Penetrate a Body Situated in the Vicinity of the Earth," Applied Physics, Vol 19, October, 1948.
14. Hawkins, G., "Meteor Ionization and Its Dependence on Velocity," Astrophysical Journal, Vol 124, July 1956, p 1.
15. Helle, F., "Portions of 'Traite de Ballistique Experimentale' Which Deal With Terminal Ballistics" (Chapters III, IV, V, and XIV, Paris, 1884), Translated by J.S. Rinehart, Naval Ordnance Test Station, Technical Memo RRB-75, 1 May 1950.
16. Hertzberg, A., "The Application of the Shock Tube to the Study of the Problems of Hypersonic Flight," Jet Propulsion, July 1956, p 549.
17. Hoenig, S.A., "Meteoritic Dust Erosion Problem and Its Effect on the Earth Satellite," Aeronautical Engineering Review, July 1957, p 37-40.
18. Huth, J.H., Thompson, J.S., and Van Valkenburg, M.E., "Some New Data on High Speed Impact Phenomena," Journal of Applied Mechanics, Vol 24, No. 1, March 1957, p 65-68.
19. Kaiser, T. (Editor) "Meteors," Journal of Atmospheric and Terrestrial Physics, Special Supplement, Vol II, 1955.
20. Kornhauser, M., "Prediction of Cratering by Meteoroid Impacts," Fourth Annual Meeting, American Astronautical Society, 29-31 January 1958.
21. McKinley, D., "Meteor Velocities From Radar Observations," Astrophysical Journal, Vol 124, July 1956, p 1.
22. Mitra, S., The Upper Atmosphere, Royal Asiatic Society of Bengal (Calcutta, India), 1947.
23. Opik, E., Harvard University, Reprint No. 100, 1937.
24. Ovenden, M., "Meteor Hazards to Space Station," Journal of the British Interplanetary Society, Vol 10, p 275.
25. Pawsey, V., and Bracewell, R., Radio Astronomy, Oxford University Press, 1955.
26. Rinehart, J.S., "Some Observations on High-Speed Impact" Naval Ordnance Test Station, Technical Memo RRB-50, 1 November 1950.

27. Rinehart, J.S., Pearson, J., "Behavior of Metals Under Impulsive Loads," American Society for Metals, 1954.
28. Rinehart, J.S., White, W.C., "Shapes of Craters Formed in Plaster of Paris by Ultra-Speed Pellets," American Journal of Physics, Vol 20, No. 1, January 1952.
29. Robey, D.H., "Meteoritic Dust and Ground Simulation of Impact on Space Vehicles," Journal of the British Interplanetary Society, Vol 17, 1959-60.
30. Silvern, D.H., Fischer, J.H., "Study of Heat Rejection in Space," Electro-Optical Systems, Inc., Report 250-IR-1.
31. Singer, S., "The Effect of Meteoric Particles on a Satellite," American Rocket Society, June 1956.
32. Summers, J.L., and Charters, A.C., "High Speed Impact of Metal Projectiles in Targets of Various Materials" (Edited by F. Genevese), Third Symposium on Hypervelocity Impact, Armour Research Foundation, Illinois Institute of Technology, 1959.
33. Taylor, D.W., Whitman, R.V., "The Behavior of Soils Under Dynamic Loadings: 2. Interim Report on Wave Propagation and Strain-Rate Effect," Massachusetts Institute of Technology, Report AFSWQ-117, July 1953.
34. Van Valkenburg, M.E., Clay, W.G., and Huth, J.H., "Impact Phenomena at High Speeds," Journal of Applied Physics, Vol 27, No. 10, October 1956.
35. Watson, F.S., Between the Planets, The Blakiston Company, Philadelphia, Pennsylvania, 1941.
36. Whipple, F.L., "Exploration of the Upper Atmosphere by Meteoritic Techniques," Harvard College Observatory, Naval Research Contract N50R1-07647, Air Force Contract AF 19(122)-482.
37. Whipple, F.L., "The Meteoritic Risk to Space Vehicles," Proceedings of the Eighth International Astronautical Congress (Barcelona, Spain), 1957.
38. Wyatt, S., and Whipple, F., "The Poynting-Robertson Effect on Meteor Orbits" Astrophysical Journal, Vol III, No. 1, 1950, p 134.

39. "Study and Development Program for a 15 KW Solar-Mechanical Power System," AiResearch Manufacturing Company and Electro-Optical Systems, Inc., Report SY-5166-R, Vol III, 30 December 1959.
40. "Liquid Propellant Losses During Space Flight, First Quarterly Progress Report," Arthur D. Little, Inc., NASA Contract NAS5-664, January 1961.
41. "Radiator-Condenser for Space Environment," Wright Air Development Division, WADD TR 61-20, 31 October 1960.

APPENDIX A

RADIANT HEAT TRANSFER FROM FLAT PLATE UNIFORMLY HEATED ON ONE EDGE

**Donald B. Mackay
E. Lee Leventhal**

**Space and Information Systems Division
North American Aviation, Inc.**

This paper is included because it contains intermediate steps of derivation and development not included in the corresponding sections of the report. This should enable the user to follow the complete analyses which produce the physical and thermal relationships of the flat plate.

This analysis is reproduced here in the form in which it was submitted for publication and presentation at the meeting of the American Institute of Chemical Engineers in August 1960 at Buffalo, New York. It is identified as Paper No. 23.

**RADIANT HEAT TRANSFER FROM FLAT PLATE
UNIFORMLY HEATED ON ONE EDGE**

by

**Donald B. Mackay
E. Lee Leventhal**

**Missile Division
North American Aviation, Inc.
Downey, California**

ABSTRACT

Basic relationships are derived for the parameters affecting heat transfer by radiation from a plate which is uniformly heated on one end. Graphs are plotted to help the designer choose the optimum plate dimensions, and instructions are given on how to take into account more complicated conditions than those shown. An illustrative problem indicates how to optimize a plate for minimum weight.

INTRODUCTION

An ever present problem in space vehicles is the disposal of waste heat produced by generation of power, by operation of equipment, or by human beings. Due to the absence of any matter around the vehicle the only feasible mechanism for disposing of this heat is by radiation.

A study was made of the factors that affect this means of heat transfer. The factors were combined into parameters by the use of constants which include groupings of physical properties representing either the material or the environment. With the help of the data presented here, complicated systems can be analyzed without altering the basic parameter relationships. The parameters presented are flexible so that they can include not only the constants specifically mentioned but also any other influencing factors, such as different plate finishes or reradiation from a number of bodies surrounding the radiating plate.

This discussion is divided into two parts. The first part presents the solution to the heat transfer problem of a plate heated on one edge and thermally insulated on the other three edges. The plate loses heat into free space solely by radiation from the two remaining flat surfaces. In an actual problem, the three

narrow edges of the plate are not usually insulated but the area involved is often small enough that the heat transfer effects can be neglected. The second part gives the solution of heat transfer from a plate wherein the transfer of heat is affected by the environment.

RADIATION HEAT TRANSFER TO FREE SPACE

In the configuration shown in Figure 1, heat enters the hot surface of the plate, flows toward the cold end, and leaves the plate from the flat surfaces by radiation. A heat balance can be written for the differential element whose width is L_w and length is dL . The heat being transferred through the plate into this differential element is

$$Q_1 = -kt L_w \left(\frac{dT_p}{dL} \right)_1 \quad (1)$$

The heat leaving the element is

$$Q_2 = -kt L_w \left(\frac{dT_p}{dL} \right)_2 \quad (2)$$

and the loss of heat by radiation from the element is

$$dQ_R = 2\epsilon\sigma T_p^4 L_w dL \quad (3)$$

It follows from the steady-state heat transfer condition that the radiant heat leaving the surface must equal the difference in the amount of heat entering and the amount of heat leaving the element. Therefore

$$dQ_R = Q_1 - Q_2$$

or

$$dQ_R = -ktL_w \left[\left(\frac{dT_p}{dL} \right)_1 - \left(\frac{dT_p}{dL} \right)_2 \right] \quad (4)$$

The temperature gradient at 2 (in Figure 1) can be written as

$$\left(\frac{dT_p}{dL} \right)_2 = \left(\frac{dT_p}{dL} \right)_1 + \frac{d^2 T_p}{dL^2} dL$$

Substituting this condition into Equation 4,

$$dQ_R = ktL_w \left(\frac{d^2 T_p}{dL^2} \right) dL \quad (5)$$

Combining Equations 3 and 5 gives

$$\frac{d^2 T_p}{dL^2} = \frac{2\epsilon\sigma T_p^4}{kt} \quad (6)$$

This differential equation can be integrated in two steps, the first being

$$\frac{dT_p}{dL} = -2\sqrt{\frac{\epsilon\sigma T_p^3}{5kt}} + D$$

where D is an integration constant which can be determined from boundary conditions. When L_t is equal to the total length of the plate, $dT_p/dL = 0$ because it is assumed that no heat is transferred from the end of the plate. For these conditions,

$$D = - \frac{\epsilon \sigma T_c^5}{5kt}$$

and

$$\frac{dT_p}{dL} = -2\sqrt{\frac{\epsilon \sigma}{5kt}} \sqrt{T_p^5 - T_c^5} \quad (7)$$

Rearranging Equation 7 in a form for integration,

$$\int_{T_h}^{T_c} \frac{dT_p}{T_p^{5/2} \sqrt{1 - \left(\frac{T_c}{T_p}\right)^5}} = -2\sqrt{\frac{\epsilon \sigma}{5kt}} \int_0^{L_1} dL \quad (8)$$

However, equation 8 cannot be readily integrated. To obtain a more satisfactory form, a transformation was used. Setting

$$\left(\frac{T_c}{T_p}\right)^5 = W \quad (9)$$

then

$$dT_p = - \frac{T_c dW}{5W^{6/5}} \quad (10)$$

and

$$T_p^{5/2} = \sqrt{\frac{T_c^5}{W}} \quad (11)$$

Substituting the values shown in Equations 9, 10, and 11 into

Equation 8,

$$\int_{W_1 = \frac{1}{2^5}}^{W_2 = 1} \frac{W^{-7} (1-W)^{-5} dW}{5T_c^{3/2}} = 2\sqrt{\frac{\epsilon \sigma}{5kt}} \int_0^{L_1} dL \quad (12)$$

where $Z = T_h/T_c$

Equation 12 can be further modified to

$$\int_{W_1 = \frac{1}{Z}}^{W_2 = 1} W^{-.7} (1-W)^{-.5} dW = \sqrt{\frac{20.46 T_c^3}{kt}} \int_0^{L_1} dL \quad (13)$$

Equation 13 can be numerically integrated by use of the tables of the incomplete beta function*. The incomplete beta function can be written in terms of the variable W as

$$\beta W(p,q) = \int_0^W W^{(p-1)} (1-W)^{(q-1)} dW \quad (14)$$

For the case considered here, $p = 0.3$ and $q = 0.5$.

The tables for Equation 14 use limits of integration extending from 0 to W , but in Equation 13 the limits extend from W_1 to 1. Therefore, before the required values for Equation 13 could be obtained, the difference in table values from $W = W_1$ to $W = 1$ had to be computed. Also, the tables are normalized so that the differences between the limits $W = W_1$ and $W = 1$ must be multiplied by the complete beta function evaluated from 0 to 1. Equation 13 can be written to use the normalized data as

$$\int_{W_1}^1 W^{(p-1)} (1-W)^{(q-1)} dW = \beta(p,q) [1 - I_{W_1}(p,q)] \quad (15)$$

* Pearson, Karl (Editor), "Tables of the Incomplete Beta-Function," Cambridge University Press (Proprietors of Biometrika), 1934

where $\beta(p, q)$ is the complete beta function evaluated from the integration limit of 0 to 1 and $I_{W_1}(p, q)$ is the normalized value obtained from the tables.

Unfortunately, the required values of $p = 0.3$ were outside the range given in the tables. To approximate the required values, Equation 15 was evaluated for the condition where $p = 0$ and $q = 0.5$ and can be written as

$$\int_{W_1}^1 \frac{dW}{W\sqrt{1-W}} = \beta(p, q) [1 - I_{W_1}(p, q)] \quad (16)$$

Equation 16 can then be integrated to give

$$\beta(p, q) [1 - I_{W_1}(p, q)] = 2[\tan^{-1} \sqrt{1-W}]_{W_1}^1$$

where $p = 0$ and $q = 0.5$

This equation was solved for a number of W_1 values, as shown in Figure 2, and plotted along the abscissa, $p = 0$. Also plotted in Figure 2 were other ordinate values for $q = 0.5$ and $p = 0.5, 1.0, \text{ and } 1.5$ which were obtained from the tables. Smooth curves were drawn through the points, and readings were taken at the intersections of the curves with the line $p = 0.3$. These results were plotted on Figure 3 as a function of the integration limits.

In plotting the curve of Figure 3, the values of W_1 shown in Figure 2 were replaced by the corresponding values of Z . This curve shows the relationship existing between the temperature ratio Z at the hot and cold ends of the plate and the corresponding plate parameter $L_t \sqrt{20 \epsilon \sigma T_c^3 / kt}$.

The quantity of heat entering the plate was then computed using Equation 7. When $L = 0$, the temperature T_p is equal to T_h and Equation 7 can be written as

$$\left. \frac{dT_p}{dL} \right|_{L=0} = -2 \sqrt{\frac{\epsilon \sigma}{5kt}} \times \sqrt{T_h^3 - T_c^3} \quad (17)$$

The heat entering the plate can be computed by substituting Equation 17 into Equation 1 and simplifying

$$Q_p = 2L_w \sqrt{\frac{\epsilon \sigma kt}{5}} \times \sqrt{T_h^3 - T_c^3}$$

This equation can also be written as

$$Q_p = 2T_h^{3/2} L_w \sqrt{\frac{\epsilon \sigma kt}{5}} \times \sqrt{1 - \frac{1}{Z^3}} \quad (18)$$

Equation 18 gives the total heat transferred into the plate or, its equal, the heat transferred away from the plate by radiation.

The efficiency of the plate for transferring heat can be expressed as a ratio between the heat actually transferred (expressed in Equation 18) and the heat which would be transferred

from the same plate at a uniform temperature T_h . This condition can be expressed mathematically as

$$\Omega = \frac{Q}{Q_{T_h}} \quad (19)$$

The denominator of Equation 19 can be written as

$$Q_{T_h} = 2L_1L_w\epsilon\sigma T_h^4 \quad (20)$$

Using Equation 20 for the ideal quantity of heat and Equation 18 for the actual heat, the efficiency becomes

$$\Omega = \frac{2T_h^{3/2}L_w\sqrt{\frac{\epsilon\sigma ki}{5}} \times \sqrt{1 - \frac{1}{Z^2}}}{2L_1L_w\epsilon\sigma T_h^4}$$

which can be rearranged into the form

$$\Omega = \frac{2\sqrt{\frac{1}{Z^2} - \frac{1}{Z^3}}}{L_1\sqrt{\frac{20\epsilon\sigma}{ki} T_h^3}} \quad (21)$$

Equation 21 was used to compute the plate efficiency, and the results are plotted in Figure 4. Values of Z were assumed, and the corresponding values of the denominator read from Figure 3. Figure 4 shows a useful relationship between the plate efficiency and the temperature ratio. Equation 21 can also be put into the form

$$L_1\sqrt{\frac{5\epsilon\sigma}{ki}} = \frac{\sqrt{1 - \frac{1}{Z^2}}}{\Omega T_h^{3/2}} \quad (22)$$

Values of Z were selected and the corresponding values of Ω read from Figure 4. These values of Z and Ω were substituted into Equation 22 and a series of values computed for $L_t \sqrt{5 \epsilon \sigma / kt}$ at various assumed temperatures T_h . The results are shown in Figure 5.

The heat transferred from a plate can be computed readily using Figure 5. The heat transferred from a plate at a uniform temperature T_h can be computed using Equation 20. The plate parameter $L_t \sqrt{5 \epsilon \sigma / kt}$ (ordinate of Figure 5) can be evaluated and the efficiency Ω obtained for a value of T_h . Using the values thus obtained for Q_{T_h} and Ω in Equation 19, the actual heat Q_p can be calculated.

RADIATION HEAT TRANSFER TO ENVIRONMENT

Presented herein are data for determining the heat radiated from a plate heated on one end and situated in an environment which influences the heat transfer. Although only a general case, such as shown in Figure 6, has been analyzed, a more complicated environment can also be solved by these data. For the case shown in Figure 6, the external heat coming into the plate is

$$Q_g = SA_p \alpha_a \cos \theta_p + SA_p F_a \alpha_a r_m \cos \theta_m + SA_p F_b \alpha_b r_m \cos \theta_m + A_p \epsilon_a \sigma F_a T_m^4 + A_p \epsilon_b \sigma F_b T_m^4 \quad (23)$$

The heat loss from the plate can be written as

$$Q_L = A_p \epsilon_a \sigma T_p^4 + A_p \epsilon_b \sigma T_p^4 \quad (24)$$

The difference in heat lost and heat received is equal to the net internal heat supplied to an element of the plate, or

$$Q_p = Q_L - Q_g \quad (25)$$

and

$$Q_p = A_p \epsilon_a \sigma T_p^4 + A_p \epsilon_b \sigma T_p^4 - SA_p \alpha_a \cos \theta_p - A_p F_a \alpha_a r_m S \cos \theta_m - A_p F_b \alpha_b r_m S \cos \theta_m - A_p F_a \epsilon_a \sigma T_m^4 - A_p F_b \epsilon_b \sigma T_m^4 \quad (26)$$

Letting

$$C_1 = \sigma (\epsilon_a + \epsilon_b) \quad (27)$$

and

$$C_2 = S(\alpha_a \cos \theta_p + F_a \alpha_a r_m \cos \theta_m + F_b \alpha_b r_m \cos \theta_m) + T_m^4 \sigma [F_a \epsilon_a + F_b \epsilon_b] \quad (28)$$

then

$$Q_p = (C_1 T_p^4 - C_2) A_p \quad (29)$$

It should be noted that Equation 29 also applies to a heat transfer environment which is more complicated than that considered in the example. In this case, the constant C_1 includes the terms which are multiplied by T_p^4 , and C_2 includes all others.

Equation 29 can be rewritten in differential form as

$$dQ_p = (C_1 T_p^4 - C_2) L_w dL \quad (30)$$

The last two terms in Equation 30 represent the differentiated area A_p of an element having width L_w in the direction normal to the heat flow and width dL in the other direction. The internal heat transferred past a section of the plate is equal to

$$Q_p = -kL_w \frac{dT_p}{dL} \quad (31)$$

Also, as derived in Equation 5, the heat radiated out of any element of the plate is equal to the change in the internal heat transfer from one side of the element to the other side. This relationship can be represented by

$$dQ_p = -kL_w \frac{d^2 T_p}{dL^2} dL \quad (32)$$

Equating Equations 30 and 32, and simplifying,

$$\frac{d^2 T_p}{dL^2} = -\frac{C_1}{kt} T_p^4 + \frac{C_2}{kt} \quad (33)$$

Equation 33 was integrated by steps, the first of which is

$$\frac{dT_p}{dL} = -\sqrt{\frac{2C_1}{5kt} T_p^5 - \frac{2C_2}{kt} T_p + C_3} \quad (34)$$

where C_3 is the integration constant which can be evaluated using boundary conditions. At the cool end of the plate,

$$\frac{dT_p}{dL} = 0, \quad L = L_f, \quad T_p = T_c$$

Then

$$C_3 = -\frac{2C_1}{5kt} T_c^5 + \frac{2C_2}{kt} T_c \quad (35)$$

Substituting the value of C_3 into Equation 34,

$$\frac{dT_p}{dL} = -\sqrt{\frac{2C_1}{5kt} (T_p^5 - T_c^5) - \frac{2C_2}{kt} (T_p - T_c)} \quad (36)$$

and rearranging the variables,

$$\frac{dT_p}{dL} = -\sqrt{\frac{2C_1 T_c^5}{5kt}} \sqrt{\frac{T_p}{T_c} - 1} \sqrt{\left(\frac{T_p}{T_c}\right)^4 + \left(\frac{T_p}{T_c}\right)^3 + \left(\frac{T_p}{T_c}\right)^2 + \left(\frac{T_p}{T_c}\right) + 1 - \frac{5C_2}{C_1 T_c^4}} \quad (37)$$

Because Equation 37 is not easily integrated in this form,

a substitution can be made where

$$x = \sqrt{\frac{T_p}{T_c} - 1} \quad (38)$$

or

$$x^2 = \frac{T_p}{T_c} - 1 \quad (39)$$

Differentiating Equation 39,

$$dT_p = 2xT_c dx \quad (40)$$

Substituting values from Equations 38, 39, and 40 into Equation 37, and rearranging terms,

$$\frac{dx}{\sqrt{(1+x^2)^4 + (1+x^2)^3 + (1+x^2)^2 + (1+x^2) + 1 - \frac{5C_2}{C_1T_c^4}}} = -\sqrt{\frac{C_1T_c^3}{10kt}} dL \quad (41)$$

Equation 41 was graphically integrated by plotting, in Figure 7, the value of

$$\frac{1}{\sqrt{(1+x^2)^4 + (1+x^2)^3 + (1+x^2)^2 + (1+x^2) + 1 - \frac{5C_2}{C_1T_c^4}}}$$

as a function of the transformed variable x for several values of $5C_2/C_1T_c^4$. The area under any given curve in Figure 7 is equal to the right-hand member of Equation 41. The measured areas were plotted in Figure 8 as a function of the temperature ratio Z .

However, use of Figure 8 is inconvenient because of the manner in which the unknown temperature T_c occurs in the ordinate, abscissa, and parameter. Therefore, the curves were adjusted in Figures 9 through 11 to be more usable. The ordinate was modified as

$$L_1 \sqrt{\frac{C_1T_c^3}{10kt}} = L_1 \sqrt{\frac{C_1T_h^3}{2kt}} \sqrt{\frac{1}{5Z^3}} \quad (42)$$

and the ordinate points of the curve were divided by the corresponding quantity $\sqrt{1/5Z^3}$. The resulting values of $L_t \sqrt{C_1 T_h^3 / 2kt}$ were plotted on Figure 9 versus Z for different values of the parameter $5C_2 / C_1 T_c^4$. This parameter was similarly modified as

$$\frac{5C_2}{C_1 T_c^4} = 5Z^4 \left[\frac{C_2}{C_1 T_h^4} \right] \quad (43)$$

The new parameter shown in Equation 43 as the bracketed term was then computed from the former parameter $5C_2 / C_1 T_c^4$ at a number of chosen values of Z. The value of the ordinate $L_t \sqrt{C_1 T_h^3 / 2kt}$ was then plotted in Figure 10 versus the new parameter, $C_2 / C_1 T_h^4$, at the selected values of Z. Points from these curves were then plotted in Figure 11 for the same ordinate, but the position of $C_2 / C_1 T_h^4$ and Z was interchanged. The temperature ratio Z can now be obtained from Figure 11 for a wide range of values of parameters $L_t \sqrt{C_1 T_h^3 / 2kt}$ and $C_2 / C_1 T_h^4$.

The heat transferred from the plate can be computed using the parametric relationships shown in Figures 10 and 11. The heat transferred into the plate from the hot source and thence lost by radiation from the plate surface can be obtained from Equation 31. The temperature gradient dT_p/dL (Equation 31) in the plate at the hot end can be taken from Equation 37 when T_h is substituted for T_p , or

$$\frac{dT_p}{dL} = -\sqrt{\frac{8C_1T_h^3}{9kt}} \sqrt{Z-1} \sqrt{Z^4+Z^3+Z^2+Z+1} - \frac{8C_2}{C_1T_h^4} \quad (44)$$

Substituting Equation 14 into Equation 31 gives

$$\frac{Q_p}{ktL_w} = \sqrt{\frac{8C_1T_h^3}{9kt}} \sqrt{Z-1} \sqrt{Z^4+Z^3+Z^2+Z+1} - \frac{8C_2}{C_1T_h^4} \quad (45)$$

and rearranging terms,

$$\frac{Q_p L_t}{ktL_w T_h} = L_t \sqrt{\frac{C_1 T_h^3}{8kt}} \sqrt{\frac{4}{9Z^3}} \sqrt{Z-1} \sqrt{Z^4+Z^3+Z^2+Z+1} - 8Z^4 \left(\frac{C_2}{C_1 T_h^4}\right) \quad (46)$$

Using either Figure 10 or 11, the quantity $Q_p L_t / ktL_w T_h$ can be computed for chosen values of the parameter $L_t \sqrt{C_1 T_h^3 / 2kt}$.

(Figure 10 was used for this paper.)

Values of $C_2 / C_1 T_h^4$ were chosen, and the corresponding values of $L_t \sqrt{C_1 T_h^3 / 2kt}$ were read from the curves for the values shown for Z. These parameter values were substituted in Equation 46, and values of $Q_p L_t / ktL_w T_h$ were computed and plotted in Figure 12. The heat transferred can then be computed from Figure 12 for a plate of known width, length, thickness, and material.

An alternate method of presenting the heat transfer, in a form useful for heat exchanger design, is by an efficiency term. The ideal heat transfer is defined as the amount of heat transferred from the same plate at a uniform temperature T_h in an ambient

condition where no radiant heat is received from the environment,
or

$$Q_{T_h} = L_f L_w C_1 T_h^4 \quad (47)$$

Using Equation 47 as a basis, the plate efficiency can be written as

$$\Omega = \frac{Q_p}{L_f L_w C_1 T_h^4} \quad (48)$$

Equation 48 can be modified to

$$\Omega = \frac{\left[\frac{L_f Q_p}{k t L_w T_h} \right]}{\left[\frac{L_f^2 C_1 T_h^4}{k t} \right]} \quad (49)$$

The parameter in the numerator of the right-hand side of Equation 49 is the ordinate of the curves in Figure 12, and that of the denominator is twice the square of the abscissa. The efficiency was then easily computed, and the results are shown in Figure 13.

The actual heat transferred from a plate can also be calculated using the data of Figure 13. Values of C_1 and C_2 are obtained from Equations 27 and 28, respectively, and are then used to compute the plate parameters and the environment parameters. With the parameters computed, the plate efficiency can be

read from Figure 13. The ideal heat transfer can be obtained from Equation 47, and the actual heat transferred can be calculated by Equation 48.

CONCLUSION

Presented herein are a series of basic relationships which can be of great help to the designer of waste heat disposal systems. These relationships are valid when the density of matter around the radiant object is negligibly small and the only working mechanism for the transfer of heat to the outside is radiation. The design data presented can be used for a vehicle in free space or on the surface of a celestial body (the moon, for example) if the body has no appreciable atmosphere.

The parameters presented are flexible so that they can include not only the constants specifically mentioned but also any other influencing factors. They can account for reradiation from a number of bodies surrounding the radiating plate and for different plate surface finishes.

NOMENCLATURE

k	Thermal conductivity of plate material
p	Parameter in beta function
q	Parameter in beta function
r_m	Reflectivity of environmental surface
t	Plate thickness
x	Transformed variable for integration
A_p	Plate area
D	Integration constant
F_a	Radiation form factor for plate side facing sun
F_b	Radiation form factor for plate side away from sun
I_{w1}	Normalized beta function
L	Plate length, variable
L_t	Total plate length
L_w	Width of plate normal to heat flow
Q_g	External heat into plate
Q_l	Heat lost from plate by radiation
Q_p	Internal heat transferred into plate, equal to net heat lost by radiation, variable
Q_r	Heat lost by radiation

Q_{T_h}	Heat transferred from plate if temperature were uniform at T_h
Q_1	Heat transferred past Section 1 of plate
Q_2	Heat transferred past Section 2 of plate
S	Solar constant (heat received from sun per unit area in unit of time)
T_c	Temperature at cold end of plate
T_h	Temperature at hot end of plate
T_m	Surface temperature of environment
T_p	Plate temperature, variable
W	Transformed variable for integration
Z	Temperature ratio, T_h/T_c
a_a	Absorptivity of plate surface facing sun
a_b	Absorptivity of plate surface away from sun
β	Complete beta function
β_w	Incomplete beta function
ϵ	Surface emissivity
ϵ_a	Emissivity of plate surface facing sun
ϵ_b	Emissivity of plate surface away from sun
θ_m	Angle between sun's rays and a normal to environment surface

- θ_p Angle between sun's rays and a normal to plate surface
- σ Stefan-Boltzmann radiation constant
- Ω Plate efficiency

APPENDIX

SAMPLE PROBLEM

A missile electronic system dissipates 1 kw. of heat to its environment. This heat is transmitted to an aluminum fin which is painted white on both sides. The heat enters the fin at 1000°R , and the fin is 5 ft. long (length L_w).

Determine width L_t and thickness t for a minimum weight of fin for the following conditions. (The weight of the fin is proportional to the product $t L_t$, thickness times width.)

1. In free space.
2. On the surface of the moon when the plate is parallel to the moon's surface at the subsolar point. The distance from the fin to the moon's surface is large compared with the dimensions of the fin.
3. Same as condition 2, except the side of the fin facing the moon is coated with platinum black.

SOLUTION

The following data were assumed for the material of the fin:

k	133 Btu. / (hr.)(ft.)(°R)
$\epsilon_a = \epsilon_b$	0.95 for white paint
$\alpha_a = \alpha_b$	0.18

$$\begin{array}{l} \epsilon_b \\ a_b \end{array} \begin{array}{l} 0.93 \\ 0.97 \end{array} \left| \begin{array}{l} \text{for platinum black} \end{array} \right.$$

Condition 1

Using Equation 20,

$$Q_{T_h} = 2 L_f L_w \epsilon \sigma T_h^4$$

Substituting values,

$$Q_{T_h} = 2 L_f \times 5 \times 0.95 \times 0.173 \times 10^{-8}$$

or

$$Q_{T_h} = 16,435 L_f$$

From Equation 19,

$$\Omega = \frac{Q_p}{Q_{T_h}}$$

Substituting values,

$$\Omega = \frac{3413}{16,435 L_f}$$

or

$$L_f = \frac{0.208}{\Omega} \quad (\text{A-1})$$

The plate parameter per Figure 5 is

$$L_f \sqrt{\frac{5 \epsilon \sigma}{k t}} = \frac{L_f}{\sqrt{t}} \sqrt{\frac{5 \times 0.95 \times 0.173 \times 10^{-8}}{135}}$$

or

$$L_f \sqrt{\frac{5 \epsilon \sigma}{k t}} = 7.86 \times 10^{-6} \frac{L_f}{\sqrt{t}}$$

Solving for plate thickness,

$$t = \left[\frac{7.86 \times 10^{-8} L_t}{L_t \sqrt{\frac{5.6Q}{kt}}} \right]^2 \quad (\text{A-2})$$

The desired conditions are obtained by the following procedure:

1. A series of values for Ω are assumed.
2. The corresponding values for the plate parameter are read from Figure 5.
3. By substituting Ω in Equation 1, L_t is computed.
4. Using the plate parameter from step 2 and L_t computed in step 3, t is computed from Equation A-2.
5. The product $t L_t$ is computed.

The results of the above are plotted as curve a of Figure 14 to determine the conditions where the product $t L_t$ is a minimum. Using the minimum point, the value of the product $t L_t$ and the plate efficiency Ω are read. By using Equations A-1 and A-2, the required width L_t and the corresponding thickness t are as follows

$$\Omega = 0.55$$

$$t L_t = 1.45 \times 10^{-3} \text{ sq. ft.}$$

$$L_t = 0.378 \text{ ft or } 4.54 \text{ in.}$$

$$t = 3.83 \times 10^{-3} \text{ ft. or } 0.046 \text{ in.}$$

Condition 2

Using Equation 27, the value of C_1 is determined, or

$$C_1 = \sigma(\epsilon_a + \epsilon_b)$$

and, after substituting values,

$$C_1 = 0.173 \times 10^{-9} (0.95 + 0.95) = 3.285 \times 10^{-9}$$

From Equation 47, the ideal heat transfer Q_{T_h} is computed.

$$Q_{T_h} = L_f L_w C_1 T_h^4$$

or, upon substituting values,

$$Q_{T_h} = L_f \times 5 \times 3.285 \times 10^{-9} \times 10^{18} = 16,425 L_f$$

Using Equation 48,

$$\Omega = \frac{Q_p}{L_f L_w C_1 T_h^4}$$

and, by substituting values,

$$\Omega = \frac{3413}{16,425 L_f}$$

or

$$L_f = \frac{0.208}{\Omega} \quad (\text{A-3})$$

The values of the constant C_2 , which takes into account environmental conditions, can be computed from Equation 28.

$$C_2 = S(\alpha_a \cos \theta_p + F_a \alpha_a r_m \cos \theta_m + F_b \alpha_b r_m \cos \theta_m) + T_m^4 \sigma (F_a \epsilon_a + F_b \epsilon_b)$$

For the stated moon environment,

$$S = 430 \text{ Btu. / (hr.) (sq. ft.)}$$

$$\cos \theta_p = 1$$

$$\cos \theta_m = 1$$

$$F_a = 0$$

$$F_b = 1$$

$$r_m = 0.13$$

$$f_m = 674^\circ\text{R}$$

Substituting the known values into the previous equation

$$C_2 = 430 (0.18 \times 1.0 + 0 + 1 \times 0.18 \times 0.13 \times 1) + (674)^4 \times 0.173 \times 10^{-9} \times (0 + 1 \times 0.95)$$

or

$$C_2 = 424.5$$

The environment parameters Figure 3 can now be evaluated.

$$\frac{C_2}{C_1 T_h^4} = \frac{424.5}{3.285 \times 10^{-9} \times 10^{12}} = 0.1292$$

In a similar manner, the plate parameter of Figure 13 is equal to

$$L_1 \sqrt{\frac{C_1 T_h^3}{2kt}} = \frac{L_1}{\sqrt{t}} \sqrt{\frac{C_1 T_h^3}{2k}}$$

Solving the equation for t,

$$t = \left[\frac{L_1 \sqrt{\frac{C_1 T_h^3}{2k}}}{L_1 \sqrt{\frac{C_1 T_h^3}{2kt}}} \right]^2$$

and for known conditions

$$\sqrt{\frac{C_1 T_h^3}{2k}} = \sqrt{\frac{3.285 \times 10^{-9} \times 10^9}{2 \times 133}} = 0.1111$$

or

$$t = \left[\frac{0.1111 L_t}{L_t \sqrt{\frac{C_1 T_h^3}{2kt}}} \right]^2 \quad (\text{A-4})$$

To determine width and thickness, the following procedure (similar to that given for Condition 1) is used:

1. A series of values are assumed for Ω .
2. Using the environmental parameter already determined and Ω from step 1, the corresponding plate parameter $L_t \sqrt{C_1 T_h^3 / 2kt}$ is read from Figure 13.
3. Substituting the value of Ω assumed in step 1 into Equation A-3, the corresponding value of L_t is computed.
4. Using the plate parameters from step 2 and L_t computed in step 3, the plate thickness t is computed using Equation A-4.
5. Using t and L_t from step 4, the product $t L_t$ is obtained.

The results of these calculations are plotted as curve b of Figure 14. Using the minimum points from curve b in Equations A-2 and A-3, the following is obtained:

$$\Omega = 0.533$$

$$t L_t = 2.28 \times 10^{-3}$$

$$L_t = 0.39 \text{ ft. or } 4.68 \text{ in.}$$

$$t = 5.85 \times 10^{-3} \text{ ft. or } 0.0702 \text{ in.}$$

Condition 3

This problem is solved in much the same way as that for Condition 2 except different absorptivities and emissivities are used. With new values,

$$C_1 = 0.173 \times 10^{-6} (0.95 + 0.93) = 0.325 \times 10^{-6}$$

$$Q_{T_h} = L_1 \times 5 \times 0.325 \times 10^{-6} \times 10^{12} = 16,250 L_1$$

$$\Omega = \frac{3413}{16,250 L_1}$$

and

$$L_1 = \frac{0.21}{\Omega} \tag{A-5}$$

$$t = \left[\frac{0.1105 L_1}{L_1 \sqrt{\frac{C_1 T_h^3}{2kt}}} \right]^2 \tag{A-6}$$

Using the same procedure as for condition 2, and Equations A-5 and A-6 instead of Equation A-3 and A-4, curve c of Figure 14 is plotted. The following is obtained at the minimum point:

$$\Omega = 0.53$$

$$t L_t = 2.41 \times 10^{-3}$$

$$L_t = 0.393 \text{ ft. or } 4.72 \text{ in.}$$

$$t = 6.13 \times 10^{-3} \text{ ft. or } 0.0736 \text{ in.}$$

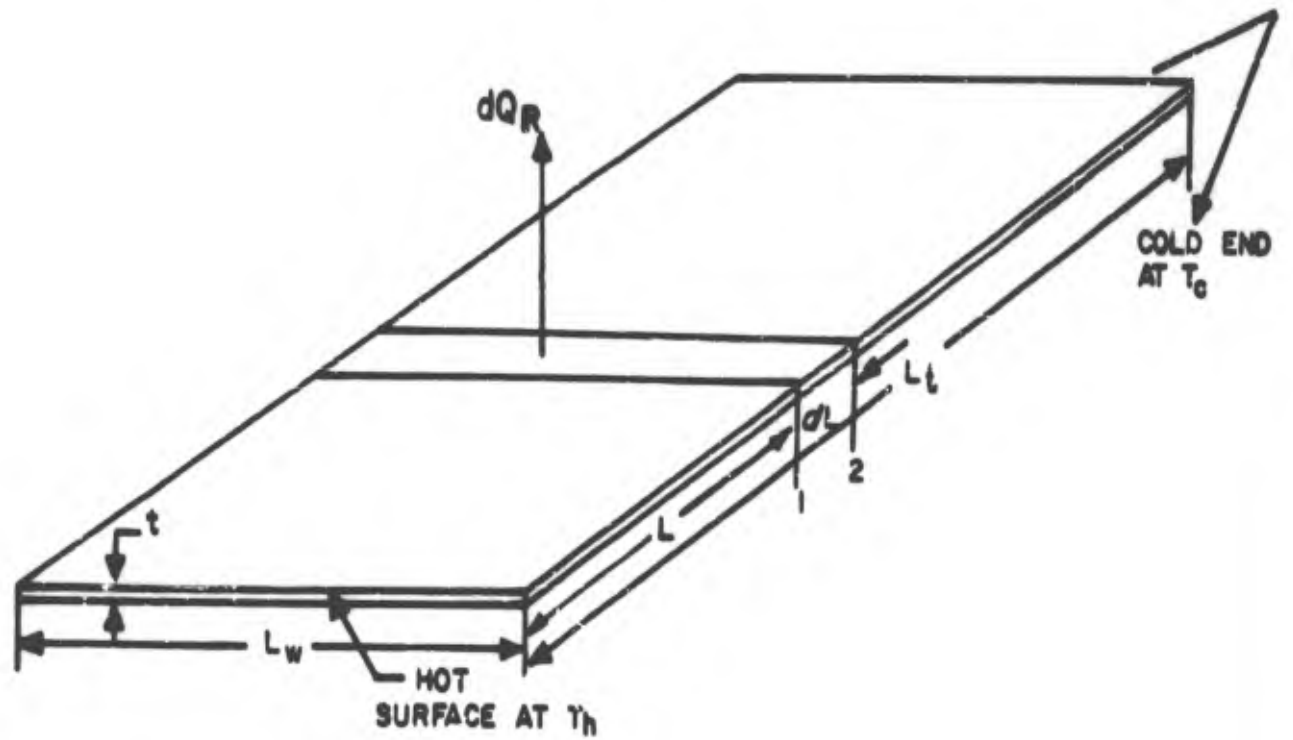


Figure 1. Typical Plate Schematic

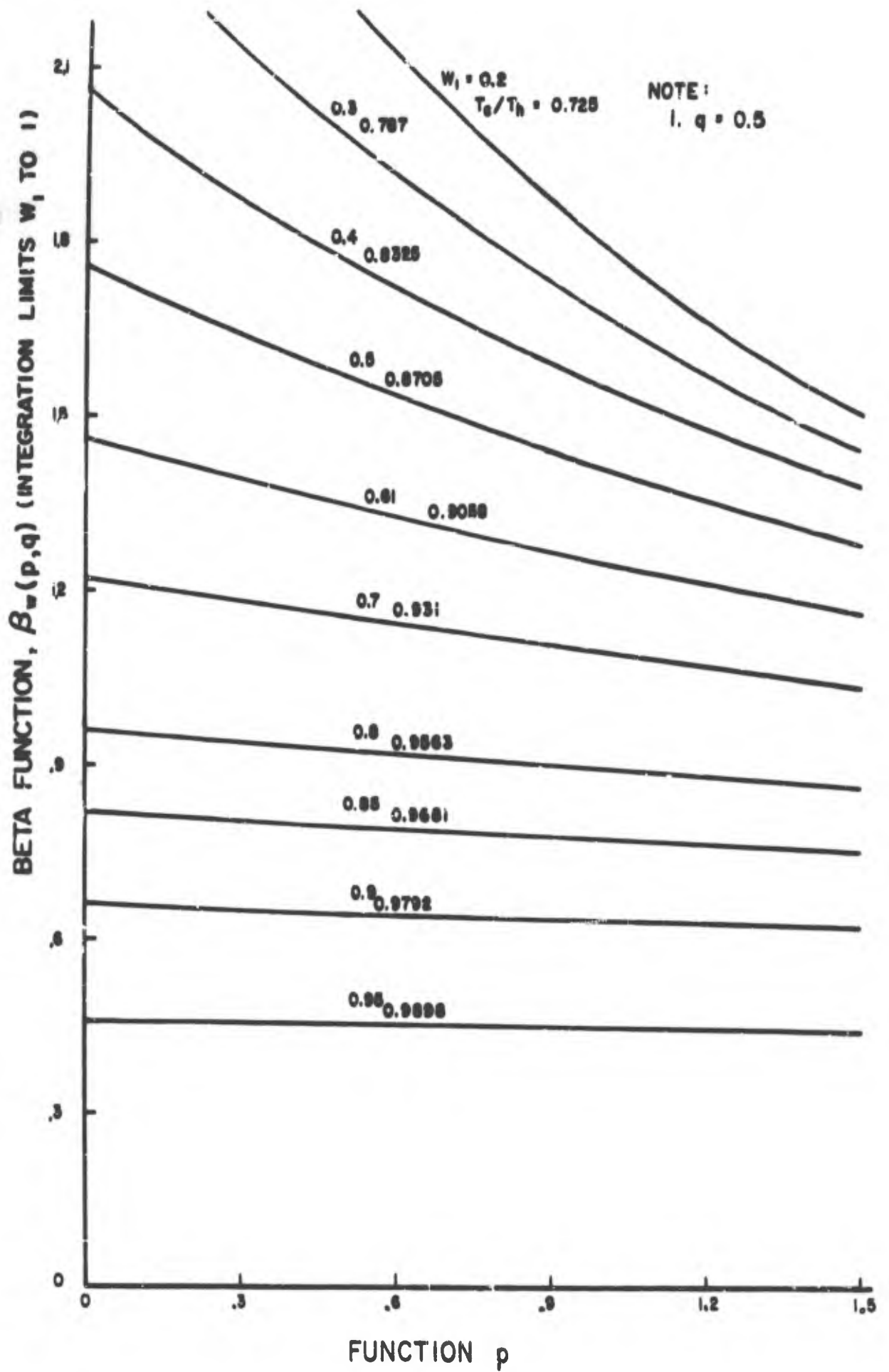


Figure 2. Evaluation of Beta Function

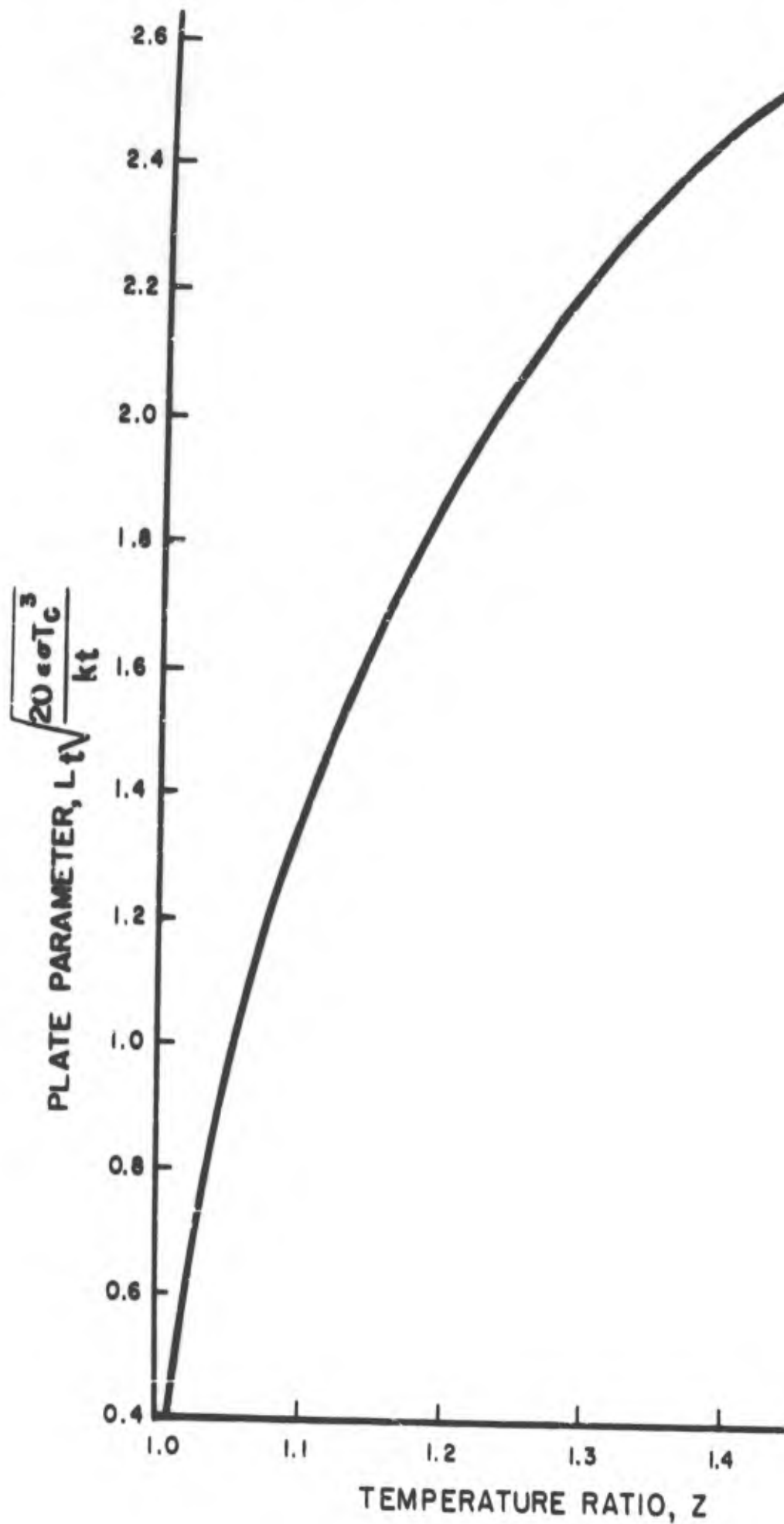


Figure 3. Relationship Between Plate Parameter and Temperature Ratio

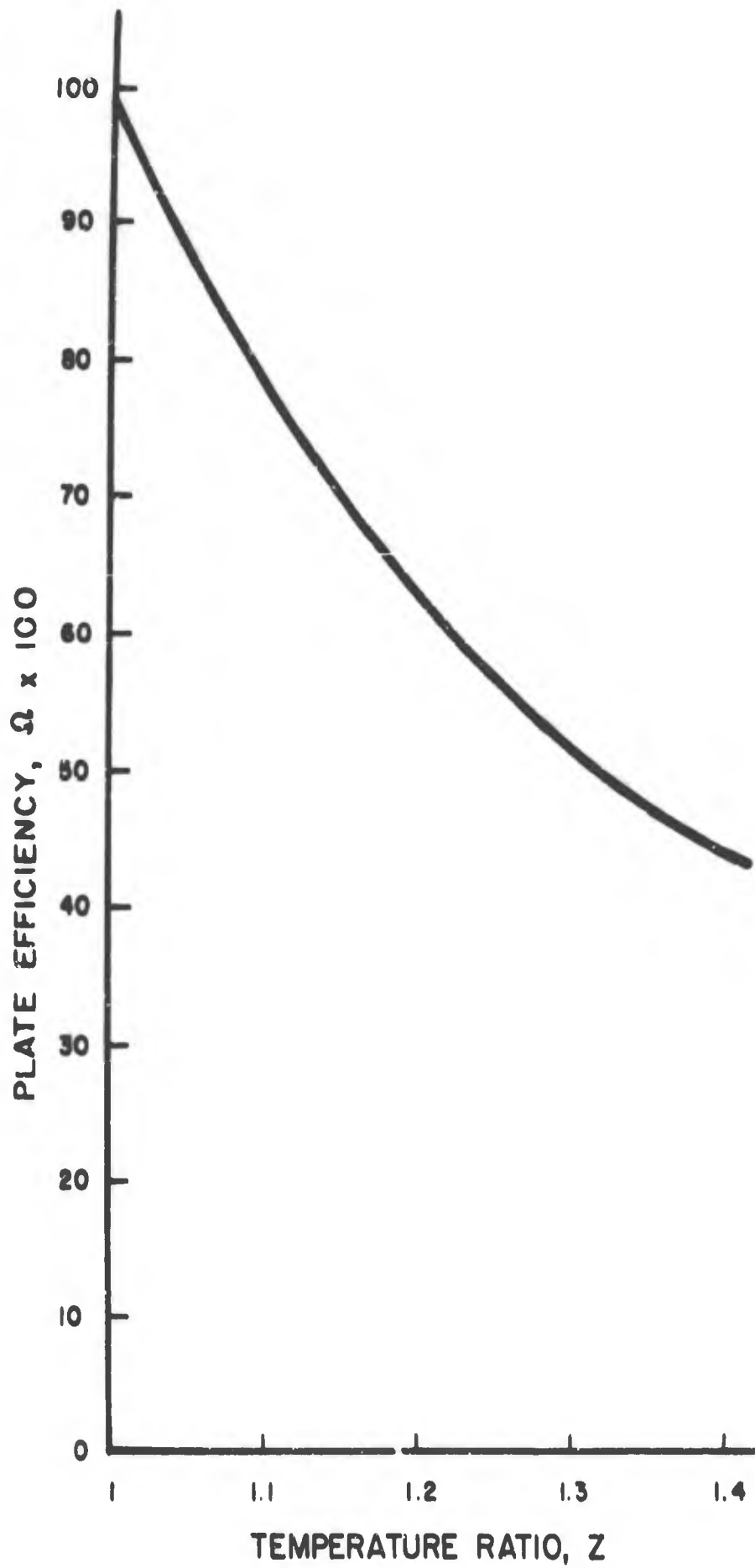


Figure 4. Plate Efficiency Versus Temperature Ratio

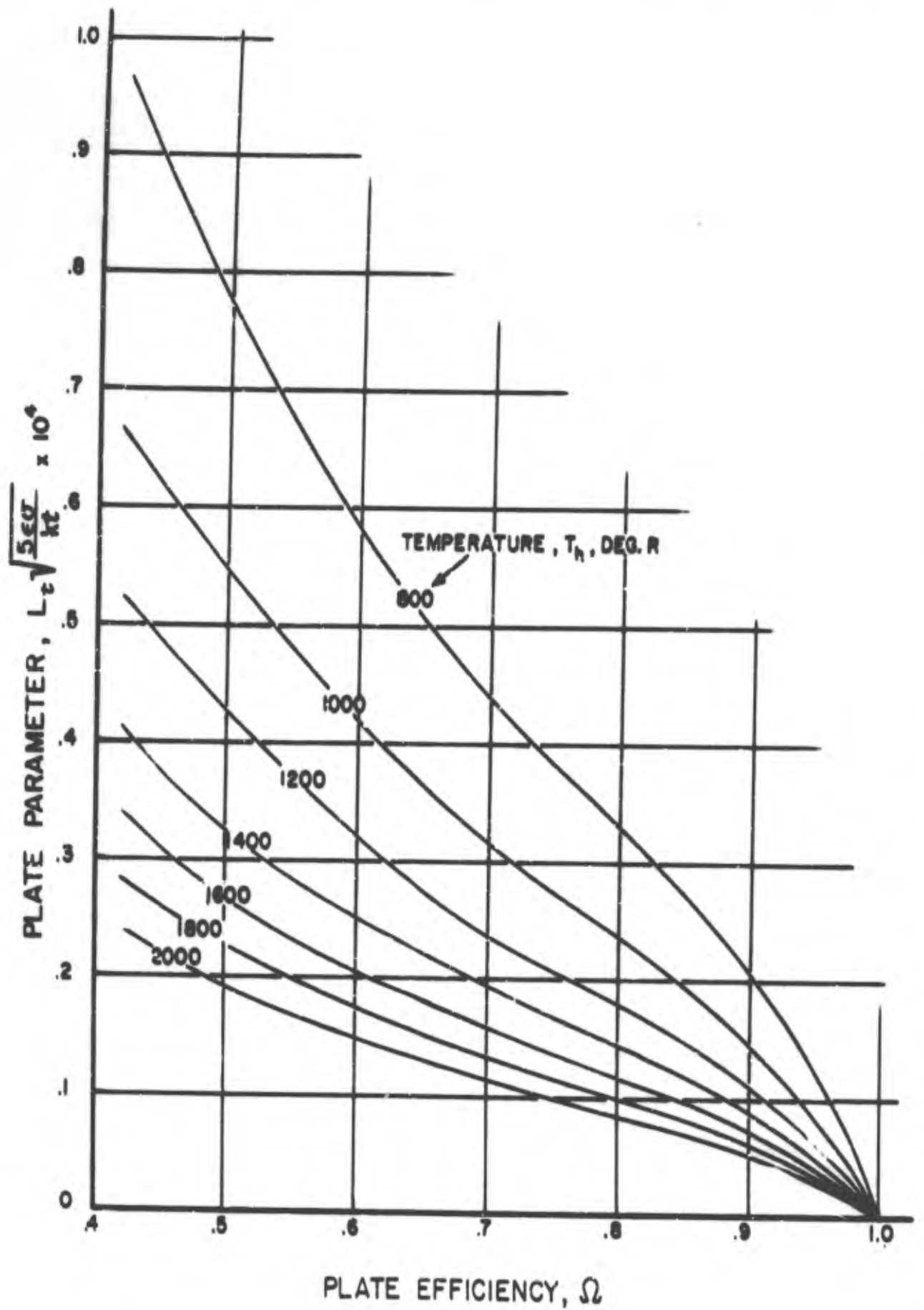


Figure 5. Plate Efficiency Versus Plate Parameter

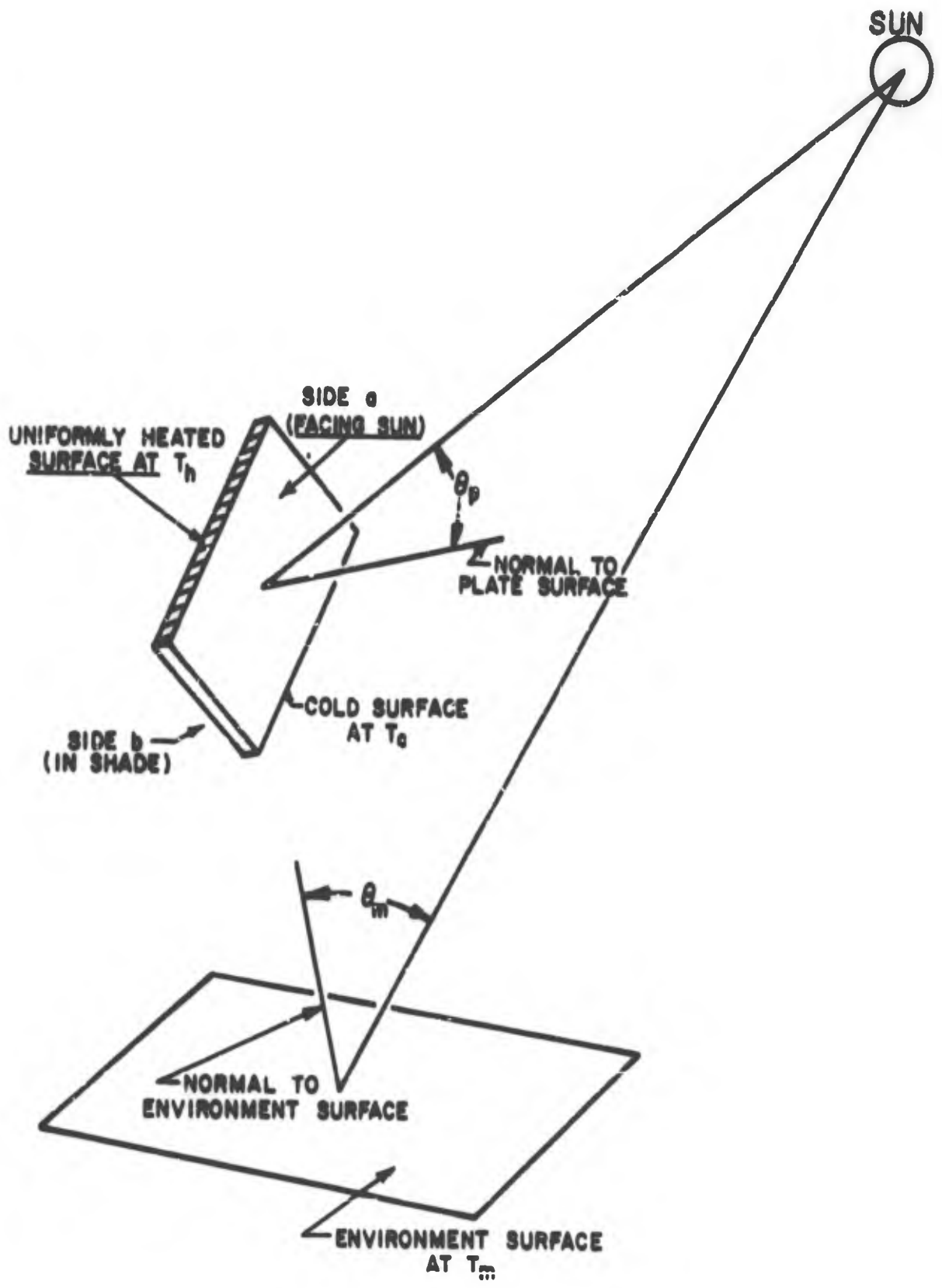


Figure 6. Radiating Plate Schematic

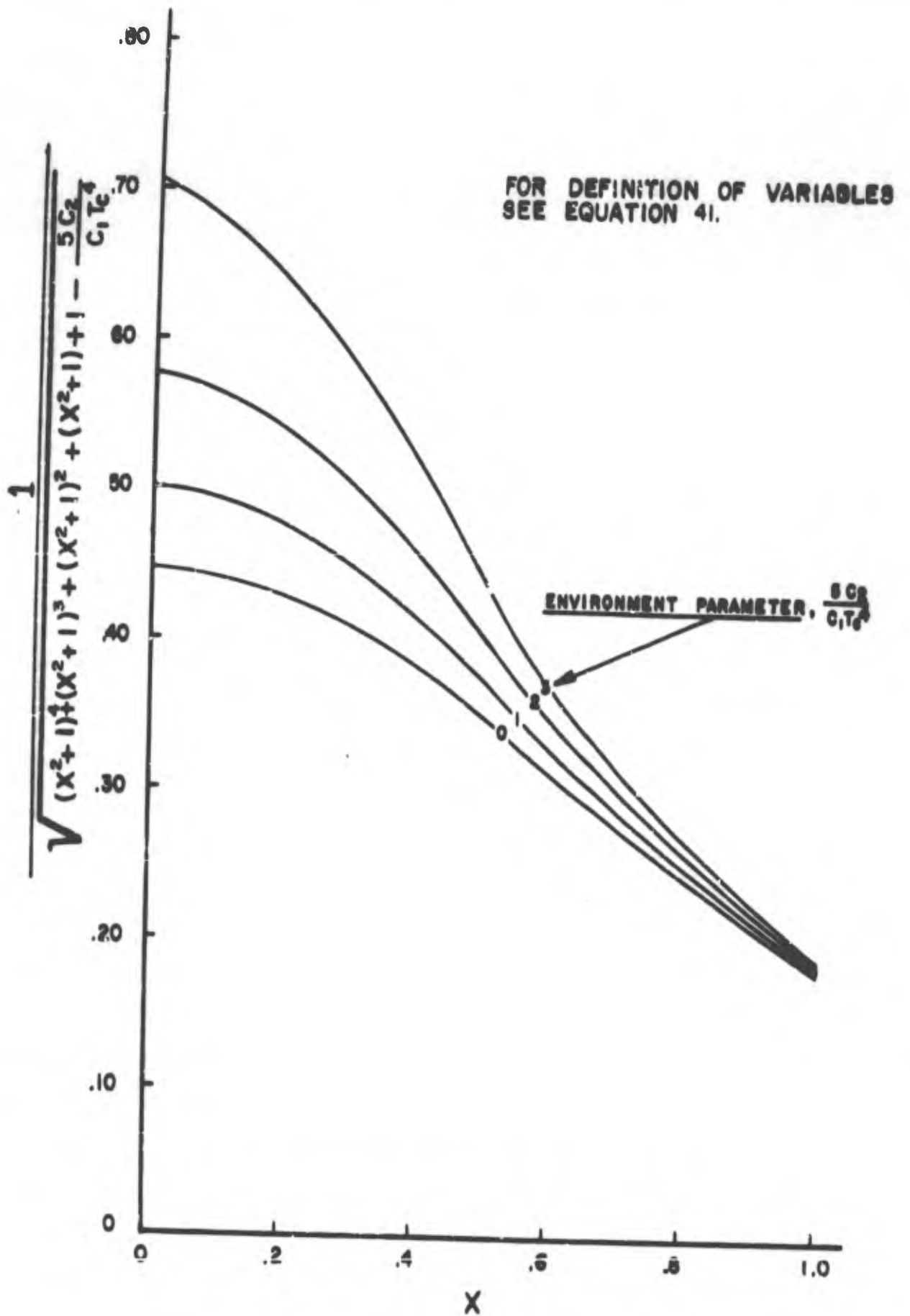


Figure 7. Curves for Graphical Integration

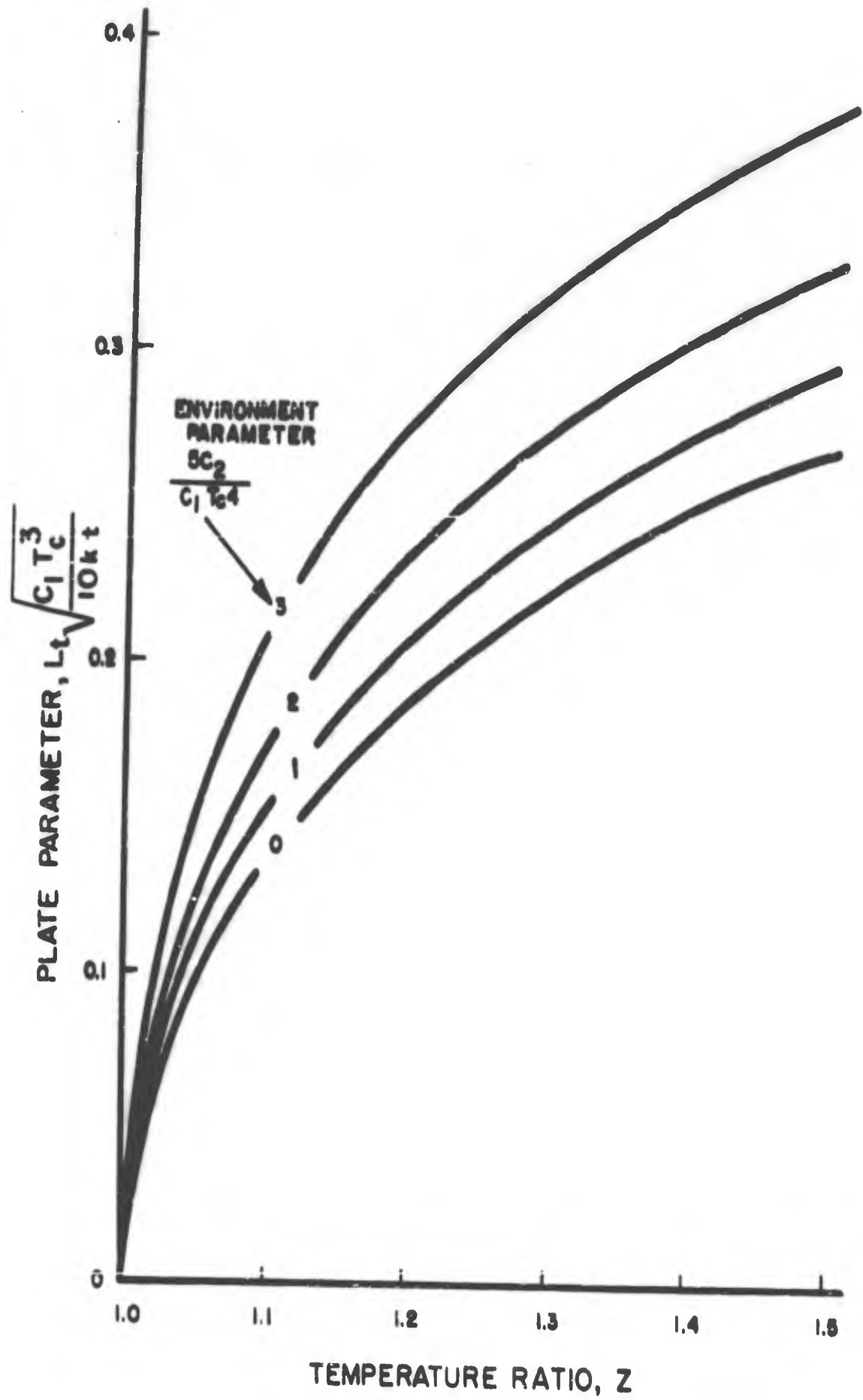


Figure 8. Parameter Relationship (Step 1)

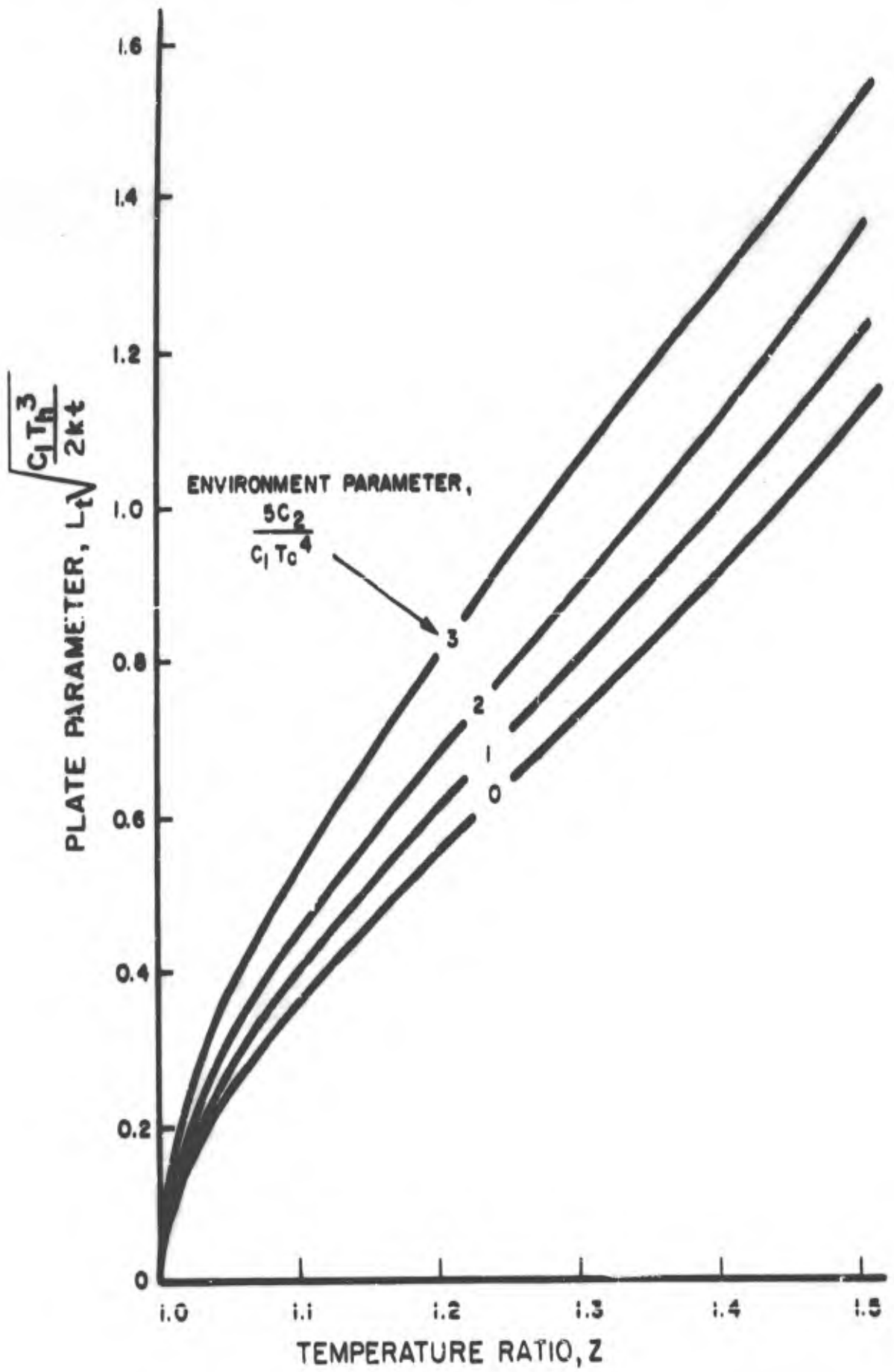


Figure 9. Parameter Relationship (Step 2)

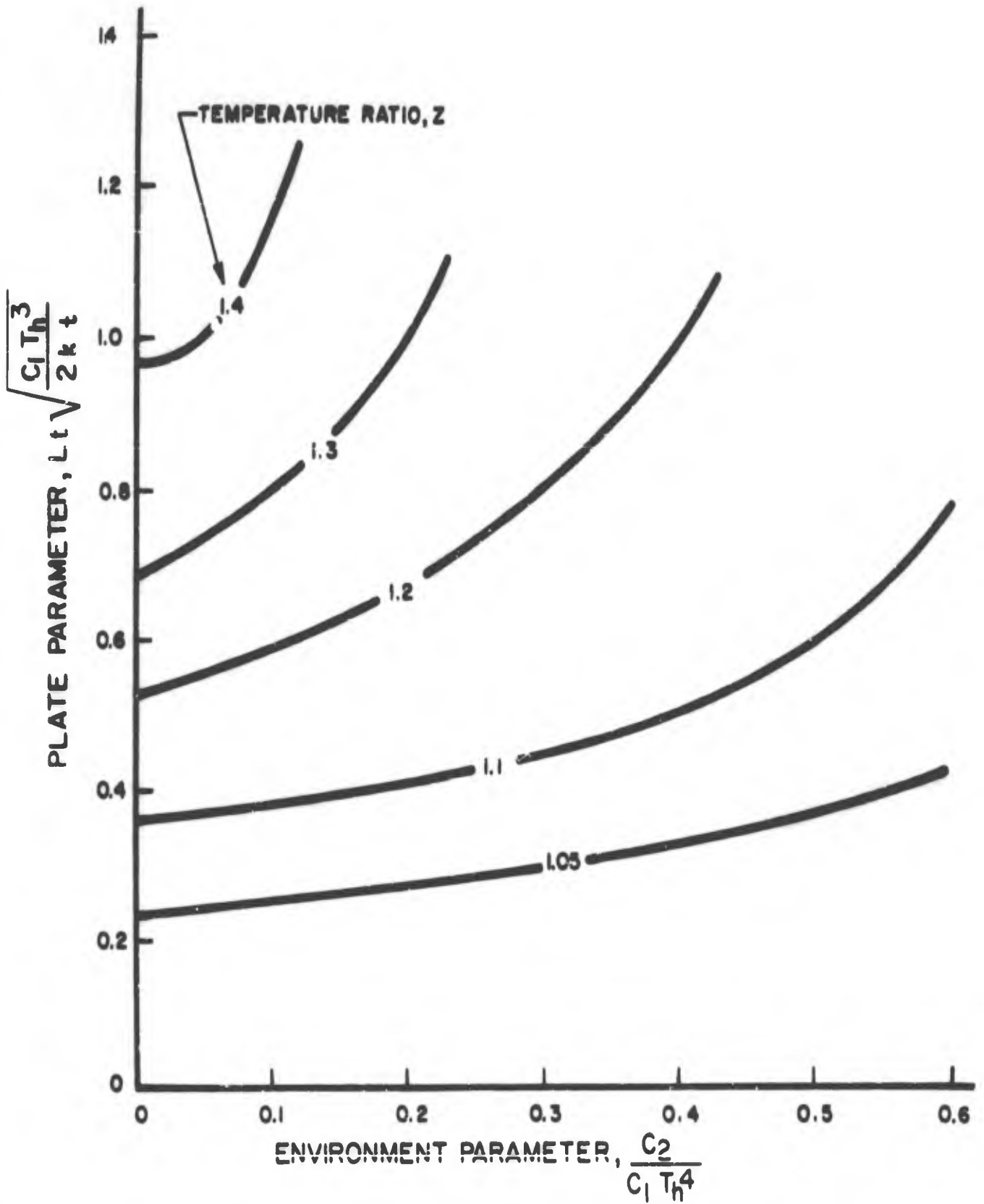


Figure 10. Parameter Relationship (Step 3)

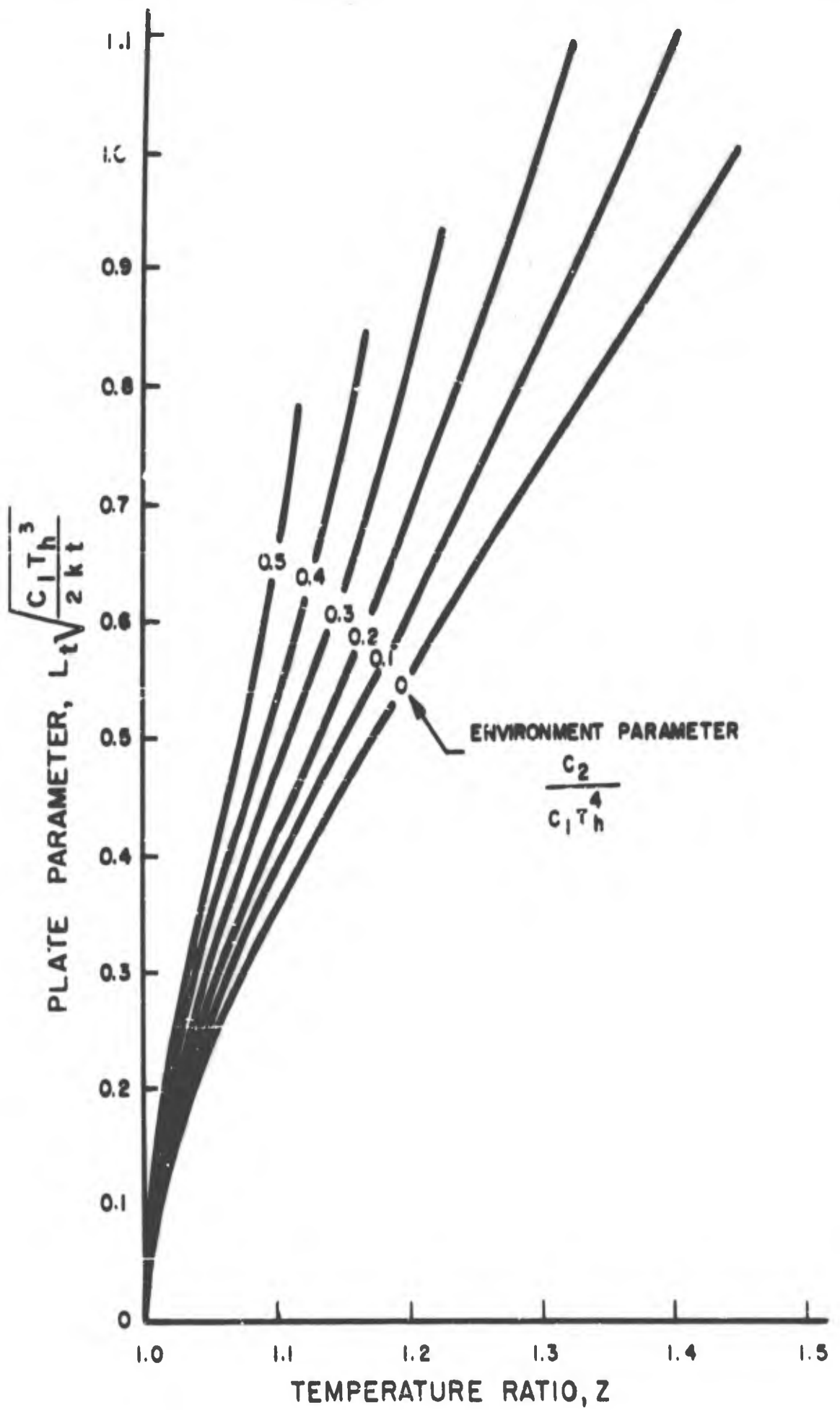


Figure 11. Parameter Relationship (Step 4)

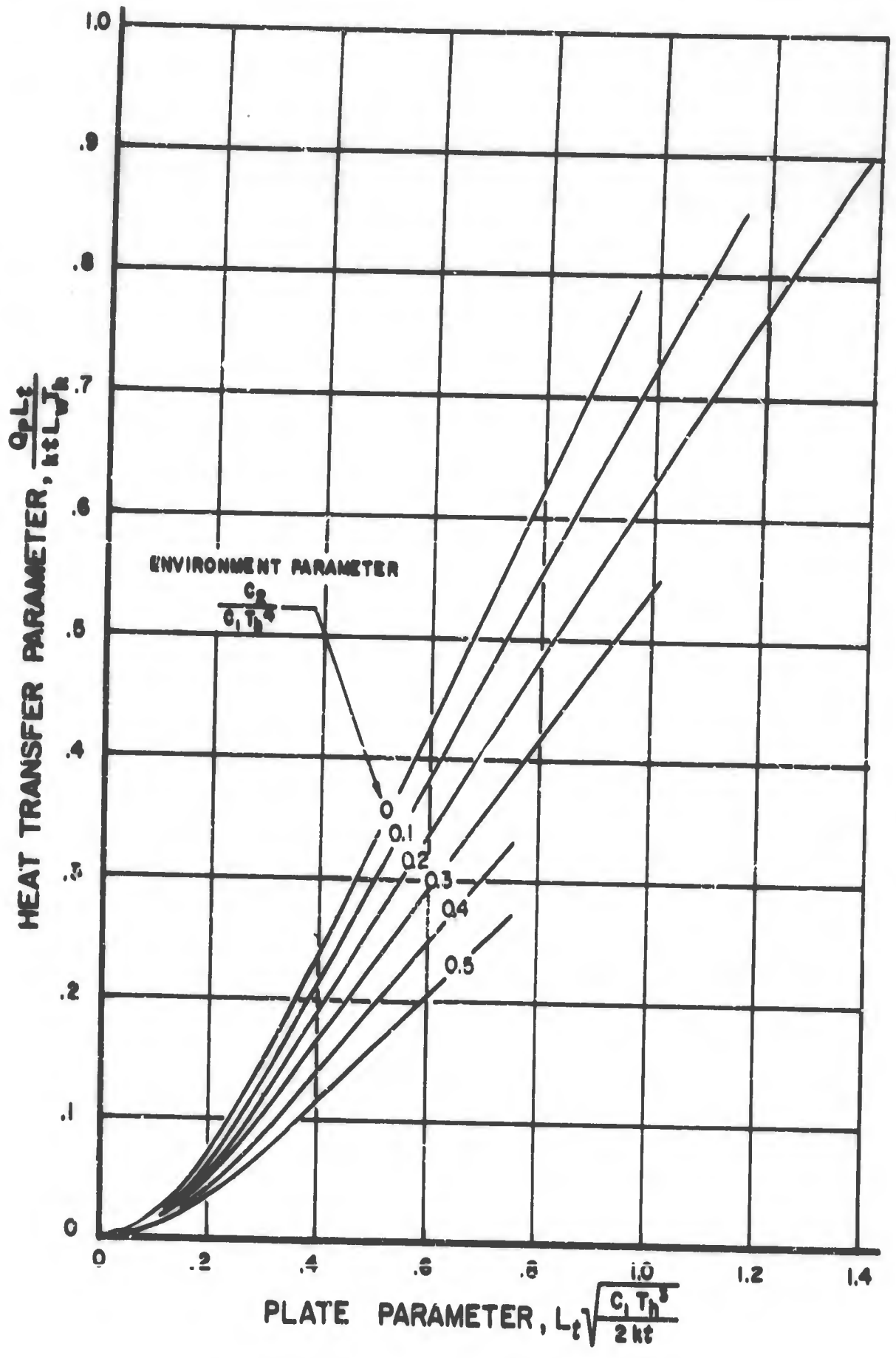


Figure 12. Plate Heat Transfer

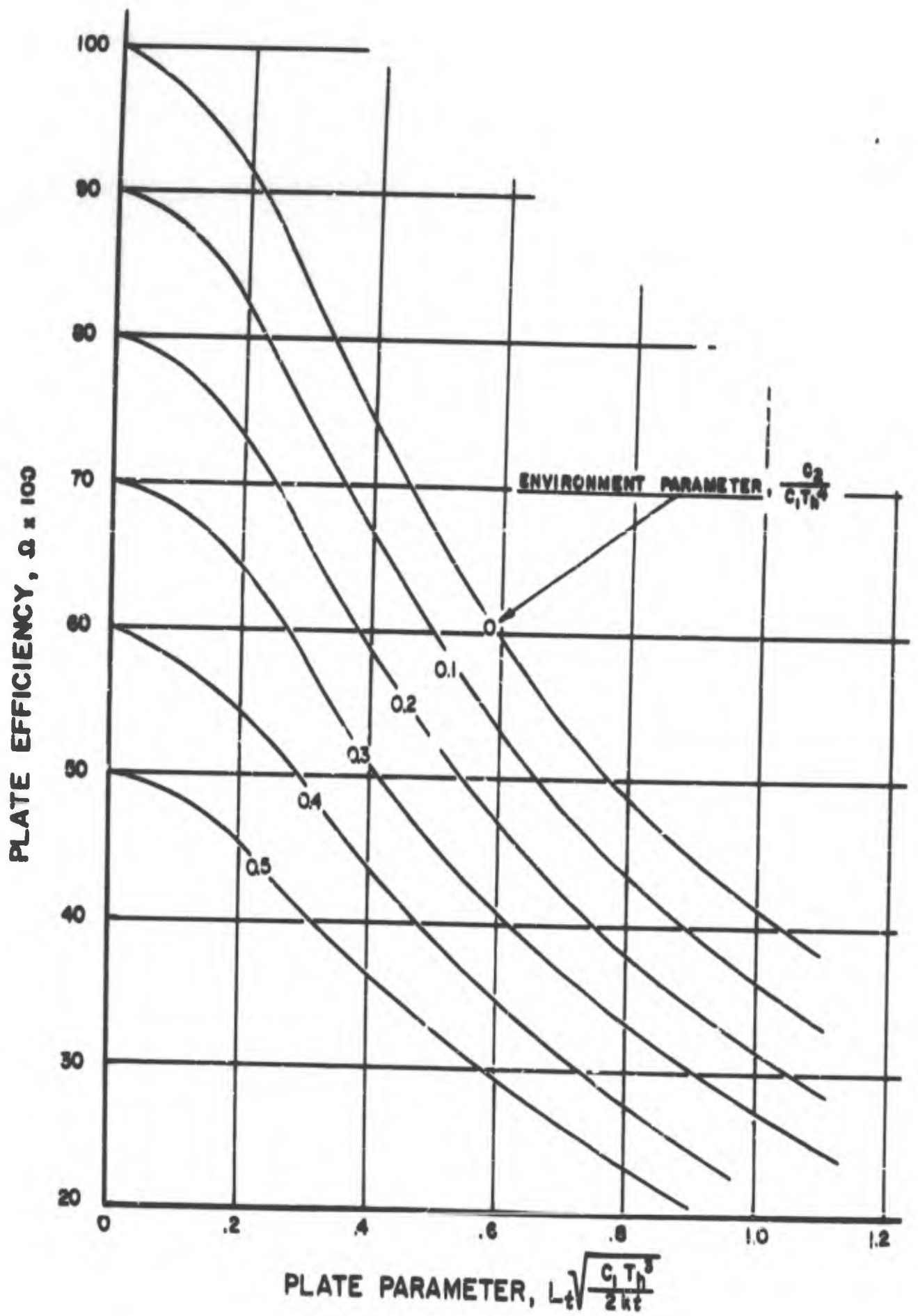


Figure 13. Plate Efficiency

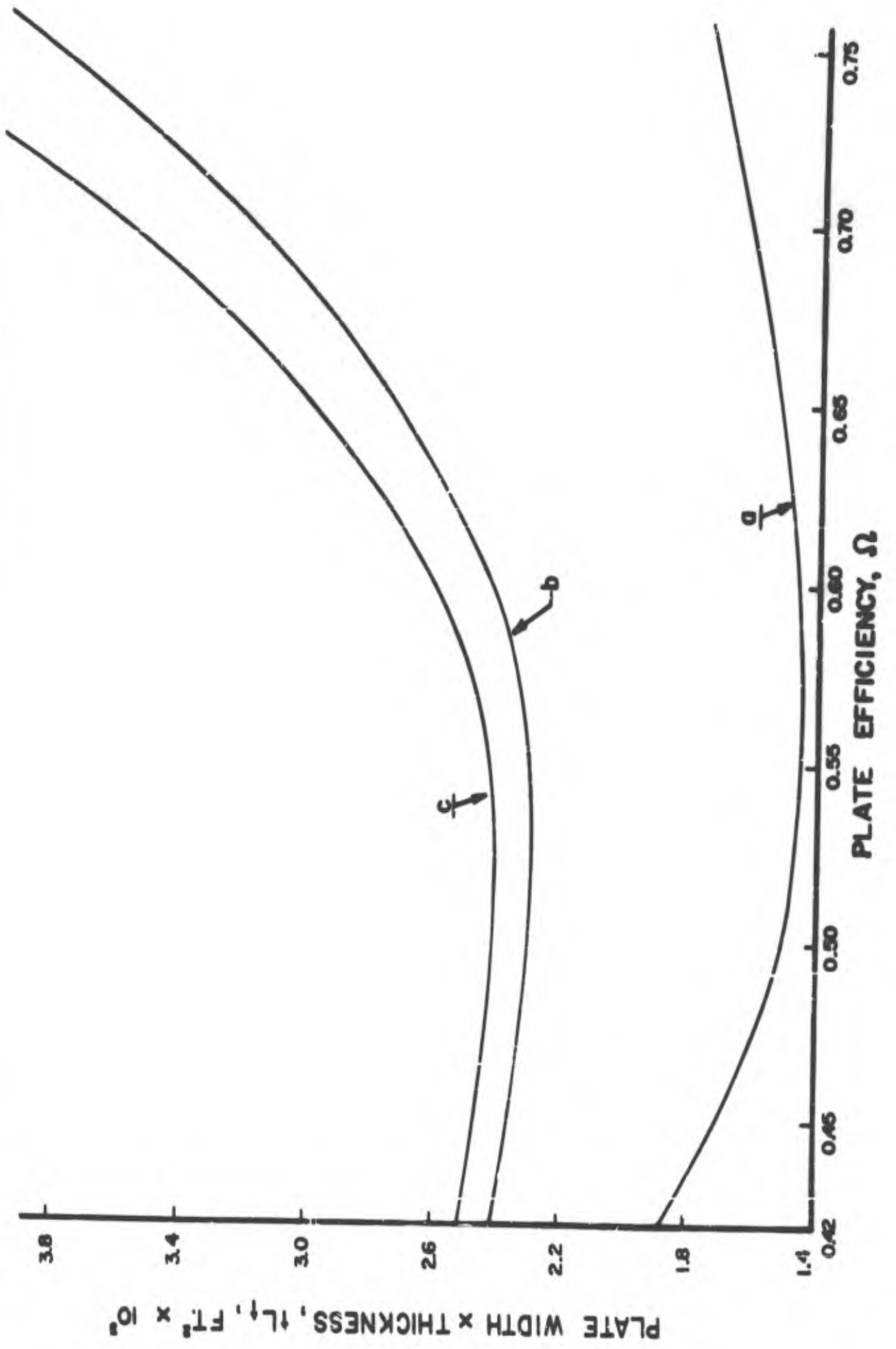


Figure 14. Illustrative Problem

APPENDIX B

RADIANT HEAT TRANSFER FROM TAPERED FIN WITH CONSTANT TEMPERATURE GRADIENT, UNIFORMLY HEATED AT ROOT SECTION

Donald B. Mackay

**Space and Information Systems Division
North American Aviation, Inc.**

This paper is included because it contains intermediate steps of derivation and development not included in the corresponding sections of the report. This should enable the user to follow the complete analyses which produce the physical and thermal relationships of the constant temperature-gradient fin.

This analysis is reproduced here in the form in which it was submitted for publication and presentation at the meeting of the American Institute of Chemical Engineers in August 1960 at Buffalo, New York. It is identified as Paper No. 24.

**RADIANT HEAT TRANSFER FROM TAPERED FIN
WITH CONSTANT TEMPERATURE GRADIENT,
UNIFORMLY HEATED AT ROOT SECTION**

by

Donald B. Mackay

**Missile Division
North American Aviation, Inc.
Downey, California**

ABSTRACT

A method is presented for determining the amount of heat that can be rejected from tapered fin surfaces by radiation heat interchange with the environment. A fin of minimum material with linear temperature gradient is emphasized. The removal of material from a fin to provide this gradient leaves the fin with a two-dimensional concave surface.

To this type of fin, mathematical analyses are directly applicable. For simplicity, the desired quantities of such factors as heat transfer and weight are expressed in terms of three parameters: (1) the fin root thickness, (2) the length, and (3) the ratio of the absolute temperatures of the hot and cold ends of the fin. The third parameter, in most instances, enters into

the equations as complicated functions which, for convenience, are grouped together. Because the evaluation of these groups was quite tedious, values were computed on an IBM machine and the results plotted for use in graphical form. Most problems encountered can be solved with the use of these graphs.

Methods are presented for computing heat transfer, fin weight, and fin contour as well as for design optimization. Sample problems illustrate the method and the magnitude of results to be expected. Approximate evaluation of triangular fins is also presented.

INTRODUCTION

The rejection of waste heat from either a powerplant or a temperature control system is a major problem in a space vehicle. Even for the somewhat futuristic powerplant described in Reference 1, the radiator was estimated to account for 35 percent of the total powerplant weight. For one refrigeration plant studied, which was to operate on the moon, the condenser area (assuming heat dissipation from both sides of the radiator) was found to be in excess of 20 sq. ft. /kw. of heat removed from the refrigerated space.

One way of reducing weight is by the use of extended surfaces. With this design, the probability of disabling meteoric damage is reduced almost in proportion to the percent of area used in the extended surfaces. The heat transfer from a radiator using constant-thickness flat plates for the extended area surfaces was considered in Reference 2, and the use of a uniform triangular taper was analyzed in Reference 3. The triangular taper is lighter in weight than a fin of constant thickness, but it is still not the lightest configuration. The Reference 3 analysis of the triangular tapered fin was limited to space applications where the presence of other surfaces would not influence the amount of heat transferred. A more rigorous and more general analysis is presented herein.

MATHEMATICAL ANALYSIS

To explain the nature of the problem and to establish useful relationships between the variables, the internal heat transfer in a tapered fin was considered first. From Fourier's law, the amount of heat passing a given section of a fin, such as shown in Figure 1, can be written as

$$Q_1 = k\delta L_w \frac{dT_f}{dL} \quad (1)$$

The amount of heat Q_1 can be computed providing the value of the temperature gradient dT_f/dL at the given section is known.

For convective heat transfer in a gaseous medium, as analyzed in Reference 4, the maximum amount of heat dissipation from a fin per unit weight of material occurs when a linear temperature gradient is established along the length L of the fin. At most, only a small error should result from assuming this as optimum from a weight standpoint for radiant heat transfer. Further, this assumption greatly simplifies the analysis and therefore warrants consideration.

Assuming a linear gradient, the temperature along the fin can be drawn as illustrated in Figure 2 and the temperature at any point along the fin can be written as

$$T_f = T_c + \frac{L}{L_h} (T_h - T_c) \quad (2)$$

and

$$\frac{T_f}{T_c} = 1 + \frac{L}{L_h} \left(\frac{T_h}{T_c} - 1 \right) \quad (3)$$

Differentiating Equation 2 with respect to L ,

$$dT_f = \left(\frac{T_h - T_c}{L_h} \right) dL \quad (4)$$

Combining Equations 1 and 4,

$$Q_i = \frac{k \delta L_w}{L_h} (T_h - T_c) \quad (5)$$

This heat must be equal to the heat lost by radiation through both sides of the fin or, by referring to Figure 1,

$$Q_i = Q_a + Q_b \quad (6)$$

However, the quantity of heat, $Q_a + Q_b$, radiated to space from a fin of nonuniform taper can be expressed in the same form as derived in Equation 30 of Reference 2 for a flat plate.

When end effects are neglected and the taper is small, the heat can be assumed to radiate from both sides of the projected area. The quantity of heat lost from the elemental area shown in Figure 3 can be written

$$dQ_f = (C_1 T_f^4 - C_2) L_w dL \quad (7)$$

where

$$C_1 = \sigma (\epsilon_a + \epsilon_b) \quad (8)$$

and C_2 is a constant which takes into account the heat transferred to the element from the environment.

Equation 8 can be integrated throughout the entire surface for special conditions providing the values of C_1 and C_2 are constant. Combining Equations 4 and 7 and indicating the limits for integration,

$$\int_0^{Q_f} dQ_f = \int_{T_c}^{T_f} \left(\frac{L_w L_h}{T_h - T_c} \right) (C_1 T_f^4 - C_2) dT_f$$

After integrating and simplifying,

$$Q_f = \frac{C_1 L_w L_h T_c^4}{5} \left[\frac{\left(\frac{T_f}{T_c} \right)^5 - 1}{Z - 1} \right] - \frac{C_2 L_w L_h}{(Z - 1)} \left(\frac{T_f}{T_c} - 1 \right) \quad (9)$$

where

$$\frac{T_h}{T_c} = Z \quad (10)$$

Because the quantity of heat lost from the end section of the fin (Equation 9) is equal to the amount entering the section (Equation 5), the two equations can be combined as

$$\frac{k\delta L_w}{L_h} (T_h - T_c) = \frac{C_1 L_w L_h T_c^4}{5} \left[\frac{\left(\frac{T_f}{T_c}\right)^5 - 1}{Z - 1} \right] - \frac{C_2 L_w L_h}{(Z - 1)} \left(\frac{T_f}{T_c} - 1\right) \quad (11)$$

After rearranging terms and solving for the fin thickness,

$$\delta = \frac{C_1 L_h^2 T_h^3}{5k Z^3 (Z - 1)^2} \left[\left(\frac{T_f}{T_c}\right)^5 - 1 \right] - \frac{C_2 L_h^2 Z \left(\frac{T_f}{T_c} - 1\right)}{k T_h (Z - 1)^2} \quad (12)$$

By combining Equations 12 and 3 and simplifying,

$$\delta = \frac{C_1 L_h^2 T_h^3}{5k Z^3 (Z - 1)^2} \left\{ \left[1 + \frac{L}{L_h} (Z - 1) \right]^5 - 1 - \frac{5C_2}{C_1 T_h^4} Z^4 (Z - 1) \frac{L}{L_h} \right\} \quad (13)$$

Equation 13 gives the thickness of the fin at any point L in terms of the other parameters. However, it should be pointed out that values of Z cannot be chosen indiscriminately. The value of δ can never be less than zero at any point in the fin and can be equal to zero only at the tip. Thus, by examining the terms of Equation 13, the limiting value of Z can be obtained.

Because the group of multiplying factors on the right-hand side of Equation 13 is positive, the positive terms within the bracket on the right-hand side must be larger than the negative terms. Therefore

$$\left[1 + \frac{L}{L_h} (Z-1) \right]^5 > 1 + \frac{5C_2}{C_1 T_h^4} Z^4 (Z-1) \frac{L}{L_h} \quad (14)$$

The left-hand term can be expanded by the binomial theorem to

$$\begin{aligned} \left[1 + \frac{L}{L_h} (Z-1) \right]^5 &= 1 + \frac{5L}{L_h} (Z-1) + 10 \left(\frac{L}{L_h} \right)^2 (Z-1)^2 + \quad (15) \\ &\quad \dots + \left(\frac{L}{L_h} \right)^5 (Z-1)^5 \end{aligned}$$

However, for small values of L/L_h , only the first two terms of the expansion need be considered, and

$$1 + 5 \frac{L}{L_h} (Z-1) > 1 + \frac{5C_2}{C_1 T_h^4} Z^4 (Z-1) \frac{L}{L_h}$$

After eliminating equal quantities,

$$1 > \frac{C_2}{C_1 T_h^4} Z^4 \quad (16)$$

From Equation 16, the maximum value of the temperature ratio

Z is

$$Z_{\max} = \sqrt[4]{\frac{C_1 T_h^4}{C_2}} \quad (17)$$

Combining Equations 17 and 10 for this condition,

$$(T_c)_{\min} = \sqrt[4]{\frac{C_2}{C_1}} \quad (18)$$

The condition of Equation 18 represents zero heat flow to the tip and zero heat transfer from the tip end to the environment.

When the generalized data are analyzed, the maximum value of the temperature ratio Z must be kept within the limits expressed by Equations 17 and 18.

At the hot end of the fin, L is equal to L_h and the maximum thickness can be obtained from Equation 13, or

$$\delta_h = \frac{C_1 L_h^2 T_h^3}{5K Z^3 (Z-1)^2} \left[Z^5 - 1 - \frac{5C_2}{C_1 T_h^4} Z^4 (Z-1) \right] \quad (19)$$

Equation 19 can also be solved for the total length L_h , as

$$L_h^2 = \frac{k \delta_h}{C_1 T_h^3} \Phi_1 \quad (20)$$

where

$$\Phi_1 = \frac{5Z^3 (Z-1)^2}{Z^5 - 1 - \frac{5C_2}{C_1 T_h^4} Z^4 (Z-1)} \quad (21)$$

It is often desirable to have the thickness expressed as a fraction of the maximum thickness. An equation giving this ratio can be obtained by combining Equations 13 and 19.

$$\frac{\delta}{\delta_h} = \frac{\left[1 + \frac{L}{L_h} (Z-1)\right]^5 - 1 - \frac{5C_2}{C_1 T_h^4} Z^4 (Z-1) \frac{L}{L_h}}{Z^5 - 1 - \frac{5C_2}{C_1 T_h^4} Z^4 (Z-1)} \quad (22)$$

Having thus established the relationship between the main variables, it is easy to derive a number of possible heat transfer equations applicable to the fin.

The heat transfer Q_f from the entire fin can be obtained from Equation 9 by substituting the temperature T_h for T_f at the root of the fin.

$$Q_f = \frac{C_1 L_w L_h T_c^4 (Z^5 - 1)}{5 (Z - 1)} - C_2 L_w L_h$$

or

$$Q_f = C_1 L_w L_h T_h^4 \Phi_2 - C_2 L_w L_h \quad (23)$$

where

$$\Phi_2 = \frac{Z^5 - 1}{5 Z^4 (Z - 1)} \quad (24)$$

It is of interest that the term $C_1 L_w L_h T_h^4$ of Equation 23 is the quantity of heat which would leave the plate if the plate were in free space and had a uniform temperature equal to the hot temperature T_h . The multiplying factor Φ_2 accounts for the decrease in heat transfer due to the temperature gradient along the fin.

The second term on the right-hand side of Equation 23 represents the heat coming into the fin from the environment.

The efficiency Ω of the fin as a heat-dissipating device can be expressed as a ratio of the heat actually leaving the fin divided by the amount which would leave the fin under the aforementioned ideal conditions of free space and uniform temperature.

$$\Omega = \frac{C_1 L_w L_h T_h^4 \Phi_2 - C_2 L_w L_h}{C_1 L_w L_h T_h^4} \quad (25)$$

After simplification,

$$\Omega = \Phi_2 - \frac{C_2}{C_1 T_h^4} \quad (26)$$

By combining Equations 23 and 25, a useful formula for computing the heat transfer is obtained.

$$Q_f = C_1 L_w L_h T_h^4 \Omega \quad (27)$$

An alternate equation for expressing the heat transfer from a fin is obtained by combining Equations 20 and 23 and simplifying.

$$Q_f = L_w \sqrt{C_1 T_h^5 k \delta_h} \times \Phi_3 \quad (28)$$

where

$$\Phi_3 = \left(\Phi_2 - \frac{C_2}{C_1 T_h^4} \right) \sqrt{\Phi_1} = \sqrt{\frac{Z^5 - 1 - \frac{5C_2}{C_1 T_h^4} Z^4 (Z-1)}{5Z^5}} \quad (29)$$

Equation 28 is preferred to Equation 27 for optimizing a radiator design, but for other purposes either equation can be used.

Using relationships already expressed for the variables, the weight of the fin can be computed. For the differential element of Figure 3,

$$dW_f = \rho \delta L_w dL$$

Substituting values from Equation 13,

$$W_f = \frac{\rho L_w C_1 L_h^2 T_h^3}{5 k Z^3 (Z-1)^2} \int_0^{L_h} \left\{ \left[1 + \frac{L}{L_h} (Z-1) \right]^5 - 1 - \frac{5 C_2}{C_1 T_h^4} Z^4 (Z-1) \frac{L}{L_h} \right\} dL \quad (30)$$

The first term within the bracket can be integrated by substituting

$$y = 1 + \frac{L}{L_h} (Z-1) \quad (31)$$

and

$$dy = \left(\frac{1}{L_h} \right) (Z-1) dL \quad (32)$$

Further, the new integration limits are

$$\text{when } L = 0, y = 1$$

$$\text{when } L = L_h, y = Z$$

and

$$\int_0^L \left[1 + \frac{L}{L_h} (Z-1) \right]^5 dL = \frac{L_h}{(Z-1)} \int_1^Z y^5 dy = \frac{L_h}{(Z-1)} \left[\frac{1}{6} Z^6 - \frac{1}{6} \right] \quad (33)$$

The remaining terms in Equation 30 can be integrated directly. After performing the integration and rearranging the terms, Equation 30 becomes

$$W_f = \frac{\rho C_1 L_w L_h^3 T_h^3}{5k Z^3 (Z-1)^3} \left[\frac{1}{6}(Z)^6 - Z + \frac{5}{6} - \frac{5}{2} \left(\frac{C_2}{C_1 T_h^4} \right) Z^4 (Z-1)^2 \right] \quad (34)$$

A more useful formula is obtained when L_h^3 in Equation 34 is eliminated by combining Equations 34 and 20, or

$$W_f = \rho L_w \left(\frac{k \theta h^3}{C_1 T_h^3} \right)^{1/2} \Phi_4 \quad (35)$$

where

$$\Phi_4 = \frac{\sqrt{5} Z^3 \left[\frac{1}{6}(Z)^6 - Z + \frac{5}{6} - \frac{5}{2} \left(\frac{C_2}{C_1 T_h^4} \right) Z^4 (Z-1)^2 \right]}{\left[Z^5 - 1 - \frac{5 C_2}{C_1 T_h^4} Z^4 (Z-1) \right]^{3/2}} \quad (36)$$

The fin weight per unit of heat dissipated to space is usually of paramount interest in preliminary design. This unit can be obtained by dividing the value of W given in Equation 34 by the heat rejected to the environment from the fin (expressed by Equation 28). Dividing Equation 34 by Equation 28 and simplifying,

$$\frac{W_f}{Q_f} = \frac{\rho L_h^2}{k T_h} \Phi_5 \quad (37)$$

where

$$\Phi_5 = \frac{Z \left[\frac{1}{6} Z^6 - Z + \frac{5}{6} - \frac{5}{2} \left(\frac{C_2}{C_1 T_h^4} \right) Z^4 (Z-1)^2 \right]}{\left[Z^5 - 1 \right] (Z-1)^2 - 5 \left(\frac{C_2}{C_1 T_h^4} \right) Z^4 (Z-1)^3} \quad (38)$$

For the special case of a fin designed to operate in free space where no heat is transferred in from other bodies, $C_2 = 0$ and

$$\Phi_5 = \frac{Z \left[\frac{1}{6} Z^6 - Z + \frac{5}{6} \right]}{(Z^5 - 1)(Z-1)^2} \quad (39)$$

The fin weight per unit of heat transfer can also be written in an alternate and more useful form by substituting into Equation 37 the value for L_h^2 given by Equation 20

$$\frac{W_f}{Q_f} = \frac{\rho \delta_h}{C_1 T_h^4} \Phi_5 \quad (40)$$

where

$$\Phi_5 = \Phi_1 \Phi_5 = \frac{5 Z^4 \left[\frac{1}{6} Z^6 - Z + \frac{5}{6} - \frac{5 C_2}{2 C_1 T_h^4} Z^4 (Z-1)^2 \right]}{\left[Z^5 - 1 - \left(\frac{5 C_2}{C_1 T_h^4} \right) Z^4 (Z-1) \right]^2} \quad (41)$$

The function ϕ_6 depends only upon the temperature ratio Z and the environmental parameter $C_2/C_1 T_h^4$. The remaining terms in Equation 40 are usually fixed by the design requirements and the available materials. The problem, therefore, is reduced to selecting the best temperature ratio for the conditions encountered.

In optimizing a system, it is necessary to know the ratio between the increase in weight and the increase in heat transfer resulting from increasing the temperature ratio in a fin. This ratio can be obtained by differentiating Equation 40, or by a more direct method in which

$$\frac{dW_f}{dQ_f} = \frac{\frac{dW_f}{dZ}}{\frac{dQ_f}{dZ}} \quad (42)$$

However, to simplify the analysis, Equation 35 can be written as

$$W_f = C_3 \sqrt[5]{\left[\frac{Z}{\phi_8} \right]^3} \cdot \phi_7 \quad (43)$$

where

$$C_3 = \rho L_w \left[\frac{k \delta h^3}{C_1 T_h^3} \right]^{1/2} \quad (44)$$

$$\Phi_7 = \frac{1}{6} Z^6 - Z + \frac{5}{6} - \frac{5}{2} \left(\frac{C_2}{C_1 T_h^4} \right) Z^4 (Z-1)^2 \quad (45)$$

$$\Phi_8 = Z^5 - 1 - 5 \left(\frac{C_2}{C_1 T_h^4} \right) Z^4 (Z-1) \quad (46)$$

Similarly, Equation 28 can be written as

$$Q_f = C_4 \sqrt{\frac{\Phi_8}{5 Z^5}} \quad (47)$$

where

$$C_4 = L_w \sqrt{C_1 T_h^5 k \delta h} \quad (48)$$

Differentiating Equations 43 and 47 with respect to Z and simplifying,

$$\frac{dW_f}{dZ} = C_3 \sqrt{\frac{5Z}{\Phi_8}} \left[\frac{Z}{\Phi_8} \frac{d\Phi_7}{dZ} + \frac{3}{2} \frac{\Phi_7}{\Phi_8} - \frac{3\Phi_7}{2\Phi_8^2} Z \frac{d\Phi_8}{dZ} \right] \quad (49)$$

and

$$\frac{dQ_f}{dZ} = \frac{C_4}{2 \sqrt{5 \Phi_8 Z^5}} \left(Z \frac{d\Phi_8}{dZ} - 5\Phi_8 \right) \quad (50)$$

Substituting values from Equations 49 and 50 into Equation 42,

$$\frac{dW_f}{dQ_f} = \frac{C_3 \sqrt{\frac{5Z}{\Phi_8}} \left[\frac{Z}{\Phi_8} \frac{d\Phi_7}{dZ} + \frac{3}{2} \frac{\Phi_7}{\Phi_8} - \frac{3}{2} Z \frac{\Phi_7}{\Phi_8^2} \frac{d\Phi_8}{dZ} \right]}{\frac{C_4}{2 \sqrt{5\Phi_8 Z}} \left(Z \frac{d\Phi_8}{dZ} - 5\Phi_8 \right)} \quad (51)$$

By further substituting the values from Equations 44 and 48 and simplifying,

$$\frac{dW_f}{dQ_f} = \frac{\rho \delta h}{C_1 T_h^4} \Phi_9 \quad (52)$$

where

$$\Phi_9 = \frac{Z^4}{\Phi_8^2} \left[\frac{2Z \frac{d\Phi_7}{dZ} + 3\Phi_7 \left(1 - \frac{Z}{\Phi_8} \frac{d\Phi_8}{dZ} \right)}{\frac{Z}{5\Phi_8} \frac{d\Phi_8}{dZ} - 1} \right] \quad (53)$$

Also, by differentiating Equations 45 and 46,

$$\frac{d\Phi_7}{dZ} = Z^5 - 1 - 5 \frac{C_2}{C_1 T_h^4} Z^3 (3Z - 2)(Z - 1) \quad (54)$$

and

$$\frac{d\Phi_8}{dZ} = 5 Z^3 \left[Z \left(1 - \frac{5C_2}{C_1 T_h^4} \right) + \frac{4C_2}{C_1 T_h^4} \right] \quad (55)$$

Although Equation 52 is complicated, it is important for optimization purposes. The computation of this equation requires the evaluation of Equations 45, 46, 54, and 55 for any value of Z and substituting the resultant values in Equation 52 in order to arrive at a final value for dW_f/dQ_f .

APPENDIX B

V. MODEL OF BUSINESS FOR
CONSUMER IN SPACE

DESIGN ANALYSIS

Equations in the previous discussion expressing dimensional relationships, heat transfer, and weight contain complicated temperature ratio functions ϕ which, in turn, can be evaluated for any given temperature ratio Z . Further, no practical method was found for eliminating the temperature functions. Therefore, it is necessary to consider three variables, δ_h , L_h , and Z , when determining the optimum fin configuration. Any two of these variables can, within limits, be chosen arbitrarily, and the third computed. (See Equation 20.) However, because the temperature ratio Z and the length L_h are in a sense specifying the same condition, the length parameter has been eliminated from most of the equations. This reduces the problem to one of choosing the temperature ratio and the root thickness best suited to the requirements. With these dimensions established, the fin length and shape can be computed.

The relationship existing between the basic factors (root thickness δ_h , overall length L_h , and temperature ratio Z) can be determined from Equations 19 and 20. Equation 20 is used for eliminating length from the other equations presented.

To aid in establishing the relationship which exists between the variables, the temperature function ϕ_1 has been plotted in Figure 4 for the expected range of temperature ratios. After the curves were plotted for a number of environment parameters, the locus of the point representing the theoretical limit as expressed by Equation 17 was drawn on the graph. The area below this locus line represents the useful region of the graph. However, actual fin designs will probably use temperature ratios in the region of one-half the difference between 1 and the value at the theoretical limit. This value is denoted as "midpoint locus" on Figure 4.

Curves of Figure 4 for environment parameters of high value are steep and give high values for ϕ_1 at comparatively low temperature ratios. According to Equation 20, a large value of ϕ_1 indicates a long fin length for a fixed root thickness or a thin root thickness for a fixed fin length. Therefore, in the applicable temperature ratio region, a fin designed for high environment parameters is either longer or has a thinner root section than a corresponding fin designed for a lower environment parameter.

To establish the best fin design for a particular application, a number of the more important equations must be analyzed. Fin efficiency is important because of its effect on the radiating area. (Efficiency is defined as a ratio of the actual heat dissipated divided by the heat which would be transmitted to free space from the same fin at a uniform temperature T_h .) Low efficiency means high total radiating area. The efficiency expressed by Equation 26 is a function of two dimensionless ratios, the environmental parameter $C_2/C_1 T_h^4$ and the temperature ratio Z . The relationship is shown graphically in Figure 5.

The best efficiency (100 percent) occurs in free space where $C_2 = 0$ and $Z = 1$. For this condition, however, the length of the fin is zero. Increasing the value of Z reduces the efficiency but permits heat to be dissipated from the fin. It is therefore evident that the use of fins in a heat exchanger will increase the total heat transfer area over the area required for prime surfaces.

An environment which restricts the loss of heat from a fin will cause an additional reduction in efficiency. This loss of efficiency is a function of the value of $C_2/C_1 T_h^4$. Minimum efficiency is encountered when the fin is designed so that the tip

of the fin reaches the equilibrium temperature of the environment. This limit was computed by Equation 17 and is shown on Figure 5. Thus, the possible fin efficiencies are confined by the environment to the region below the line of zero value for the environment parameter and above the line designated as locus of theoretical limit. Fin efficiencies at the theoretical limit may be higher than expected for the usual range of environment parameters, and temperature ratios approaching this limit could be considered but for weight and other practical considerations. Again, if the midpoint locus is regarded as a limit for the practical design, then the region of efficiencies at the high environment parameters is truly restricted to a narrow range of Z values.

It will be difficult, if not impossible, to manufacture a fin according to the established dimensions when the maximum temperature ratios are used. It is mathematically possible (by differentiating Equation 12 with respect to L) to show that the slope $d\theta/dL$ at the fin tip is zero. In other words, the fin would be more than razor sharp at the tip end.

To determine the quantitative increase in area resulting from a decrease in efficiency, it is only necessary to determine

the direct ratio of the efficiencies. For example, in an environment where the value of $C_2/C_1 T_h^4$ is 0.5, the prime surface radiation efficiency is 0.5. When the temperature ratio is equal to the theoretical limit, the efficiency is approximately 0.228. Dividing 0.5 by 0.228 gives a quotient of 2.19. Physically this means that the tapered fin designed for a temperature ratio of 1.185 would have 2.19 times as much area as a prime surface which has the same emissivity and is heated to a uniform temperature equal to the hot temperature, T_h .

Efficiencies are independent of both the thermal conductivity of the material and the maximum fin thickness. Thus, an aluminum fin designed for a given temperature ratio would have the same efficiency as one of plastic designed for the same temperature ratio, providing, of course, the surface emissivities are equal. By the same argument, a fin with a thick root has the same efficiency as one with a thin root. However, the aluminum fin would have to be longer than the plastic and a thick fin would have to be longer than the thin. Thus, while the efficiencies are equal, length and root thickness change drastically, when the material changes. The solution to a practical

problem involves more than efficiency; factors such as length and weight, must also be considered.

The heat actually lost from a fin can be computed in two ways, depending upon the conditions of the problem. Equation 27 shows that the heat transfer is a direct function of efficiency Ω , which can be obtained from Figure 5. The second method uses Equation 28 which expresses the heat transfer as a function of root thickness and temperature ratio. Because the latter equation gives a clearer representation of what to expect from a fin and is therefore more useful for optimization, the value of ϕ_3 has been plotted on Figure 6. It can be seen that the value of ϕ_3 increases rapidly as the temperature ratio increases above the value of one. The rate of increase is less as the value of Z becomes larger, however, and the curves reach a maximum at the locus of the theoretical limit. In the region near the theoretical limit, the magnitude of ϕ_3 changes very slowly, indicating that it is fruitless to use a temperature ratio approaching this limit.

A useful concept for establishing a practical limit is denoted by the midpoint locus. By comparing values along this line with those at the theoretical limit, some surprising figures

are obtained. When the environment parameter is 0.5, the value of ϕ_3 changes from 0.171 to 0.190, which represents only an 11.1 percent improvement in heat transfer in the last half of the ratio increase. At higher values of the environment parameter, the percentage gain is even less. When the environment parameter equals 0.2, only 8.1 percent improvement in heat transfer occurs in the last half of the ratio increase. The corresponding percentage increases in fin length L_h , computed from the data in Figure 4, are 132 and 122 percent for environment parameters of 0.5 and 0.2, respectively. In other words, it requires more than twice the fin length to obtain an approximate 10 percent increase in the heat transfer. From these comparisons, it would appear reasonable that the actual fin should be designed to temperature ratios below those shown by the midpoint locus.

It is also important to consider weight, which is expressed by Equations 34 and 35. When the temperature function ϕ_4 given by Equation 36 was plotted for a variety of temperature ratios, the curves were shaped somewhat like an inverted parabola. However, because the theoretical limit is exceeded for temperature ratios higher than the value obtained at the maximum, only the portions with positive slopes are applicable. These are

problem involves more than efficiency; factors such as length and weight, must also be considered.

The heat actually lost from a fin can be computed in two ways, depending upon the conditions of the problem. Equation 27 shows that the heat transfer is a direct function of efficiency Ω , which can be obtained from Figure 5. The second method uses Equation 28 which expresses the heat transfer as a function of root thickness and temperature ratio. Because the latter equation gives a clearer representation of what to expect from a fin and is therefore more useful for optimization, the value of ϕ_3 has been plotted on Figure 6. It can be seen that the value of ϕ_3 increases rapidly as the temperature ratio increases above the value of one. The rate of increase is less as the value of Z becomes larger, however, and the curves reach a maximum at the locus of the theoretical limit. In the region near the theoretical limit, the magnitude of ϕ_3 changes very slowly, indicating that it is fruitless to use a temperature ratio approaching this limit.

A useful concept for establishing a practical limit is denoted by the midpoint locus. By comparing values along this line with those at the theoretical limit, some surprising figures

shown in Figure 7. Although the locus line through the maximum points falls below portions of other curves, this neither invalidates any of the conclusions nor does it imply two theoretical limits. The question raised is why is it possible for a long fin designed for a temperature ratio equal to the theoretical maximum value to be lighter in weight than a somewhat shorter fin designed for the same temperature ratio but for a lower value of the environment parameter. The answer lies in the fin thickness which is less for the higher environment parameter. In fact, all fins designed for maximum temperature ratio are extremely thin for some distance back from the tip end. Because the values of ϕ_4 given in Figure 7 increase rapidly as a temperature ratio increases, low values must be used for Z if weight is important.

It is of paramount importance in radiator optimization to obtain the lightest fin per unit of heat dissipated. According to Equation 37, the density of the fin material should be low and the thermal conductivity high. Both of these qualities depend on the material. It would appear that the value of L_h should be small. However, for a fixed thickness δ_h at the root of the fin, a change of value in L_h would mean a change in the temperature ratio Z

and a change in the value of ϕ_5 . The value of ϕ_5 decreases rapidly as the temperature ratio increases. It is difficult to arrive at the optimum configuration because it is hard to visualize the product of two terms, one of which increases with the square of the length while the other decreases in an almost inverse manner. For this reason, Equation 40 which gives the weight per unit of heat transfer in terms of the root thickness is preferred over Equation 37 for design purposes.

Equation 40 shows that the weight per unit of heat transfer is directly proportional to the product of the density of the material and the root thickness and inversely proportional to the product of the constant C_1 and the fourth power of the temperature T_h . The temperature function ϕ_6 , the remaining item, takes into account all other factors. It is therefore important to study the temperature function. Its value is plotted for several environment parameters in Figure 8, which shows that the temperature function increases as the temperature ratio increases. The rate of increase is very modest for low values of the environment parameter, but with increasing values the rate of increase in ϕ_6 also becomes higher, and at an environment parameter of 0.5 the curve is extremely steep. In a practical design, when the

environment parameter is high, it is important to keep the temperature ratio as low as the conditions permit. Conversely, the temperature ratio can be comparatively high when the environment approaches the conditions in free space wherein the environment parameter is zero. A temperature ratio below the midpoint locus is suggested as a very rough approximation.

It is of interest that the weight per unit of heat transfer expressed by equation 40 is independent of the thermal conductivity of the material. While this is theoretically true, the thermal conductivity must be considered in a practical problem where the heat is generated near the root of the fin or in some way transported to the root. A fin of low-conductivity material designed for a given temperature ratio Z will, according to Equation 20, be shorter than a fin of high-conductivity material. The length is proportional to the square root of the thermal conductivity. The heat transferred from a fin, as expressed by Equation 27, is directly proportional to the length of the fin. Therefore, the heat radiated from a fin of given root thickness and fixed temperature ratio is proportional to the square root of the thermal conductivity. Thus, a material of high thermal conductivity

permits the use of longer, more effective fins, thereby reducing the length L_w .

By similar reasoning for a case where the fin length is fixed, a high-conductivity material will reduce the temperature ratio and thereby increase the amount of heat transfer. It is possible with a high-conductivity material to reduce the root dimension and thereby show a weight saving as well. Therefore, high thermal conductivity is important, but its influence appears in an indirect manner.

Using Figures 4 through 8 and the proper equations, it is possible to compute weight, heat transfer, and the ratio between them for fins.

HEAT EXCHANGER OPTIMIZATION

The data presented is not in itself adequate for optimizing a fin radiator system. For example, the equations predict reduced weight per unit of heat transfer when the temperature ratio (or the length) is reduced. Also, reduced weight per unit of heat transfer is indicated for a thin root section. Taking both of these literally and extending the reasoning to a logical conclusion, the optimum fin design would be obtained when using zero thickness and zero length. However, under these conditions, the ducting and tubing, or their equivalent, would have the total heat transfer task. A realistic optimization must include the system and all factors involved in fin design.

Finned surfaces will probably be used in a wide variety of applications, and it is impossible to obtain a general optimization procedure to fit all conditions. However, the largest amount of heat from a vehicle or lunar base will be lost from radiators associated with either the powerplant or the refrigeration equipment. In either case, the problem is one of condensing a working fluid, with the principal difference being in the temperature level maintained in the heat exchanger. An optimization study therefore has been directed to these particular applications.

To simplify the analysis, the working fluid was assumed to pass through rectangular passageways. The heat exchanger was assumed to be constructed with tapered fins in a manner illustrated by the two sections shown in Figure 9. It is of little consequence in a heat transfer study whether the fins are extruded, braised, welded, or attached in some other method, so long as they are fabricated as an integral part with the fluid passageway. With this configuration, it is possible to analyze the system and to determine the optimum thickness δ_h and length L_h for use with a given fluid passageway.

It is assumed here that the working fluid in the section is a condensing vapor which produces a uniform temperature throughout the length of the passageway. Further, the heat leaving a given section of the radiator of Figure 9 is very nearly equal to heat calculated to leave the projected centerplane area of the surface. This assumption is somewhat conservative since the passageways, which are the hottest part of the element, will transfer some heat from the end section to the colder fin surfaces. This will cause a slight increase in fin surface temperature and increase the amount of heat leaving the system. On the single section shown in Figure 10, three differential areas

are designated. One is obtained by adding the length dL_w to the fluid passageway and fins. The other two, which are equal, are obtained by adding the length dL_h to each of the fins. This involves adding material to the basic fin and extending its length. By analyzing the heat transfer and weight of the basic section and the differential areas, it is possible to establish the optimum configuration.

The heat output and weight of the section can be obtained by separately computing the heat outputs and weights of a rectangular passageway and of the fins. For the rectangular passageways, the values are computed in an ordinary manner; for the fins, the values are computed as outlined in this paper. The total heat transfer Q from the section can then be computed by adding the two parts.

If it is now assumed that the section must dissipate the additional quantity of heat dQ , one of the two methods mentioned can be used. Each method will result in a weight per unit of heat transfer which must be computed and compared. The weight per unit of heat transfer dW/dQ , resulting from an increase in length in the fluid passageway and fin dL_w , will be equal to the amount computed for the section. While the ratio dW_f/dQ_f resulting

from an increase in fin length dL_h can be computed using Equation 51, the method yielding the lower ratio should be used.

By continuing the same reasoning, it is possible to establish the optimum configuration. If the value of dW_f/dQ_f , corresponding to the additional fin length dL_h , is lower than the ratio W/Q computed for the original section, it is possible to shorten the length L_w and increase the fin length L_h . With this change, the same amount of heat could be dissipated from a configuration of lighter weight. At the optimum fin length L_h , the value of dW_f/dQ_f computed for the fin is equal to the value of W/Q for the section.

Having thus established the optimum length for a fin of given root section, it is now possible to analyze the effects of changing the root thickness. For each assumed thickness, the best overall weight-to-heat transfer ratio W/Q can be computed. The fin root thickness δ_h which yields the least total weight per unit of heat transfer is theoretically the optimum configuration.

To aid in this analysis, the value of ϕ_0 of Equation 53 has been computed and plotted in Figure 11. The temperature parameter can be used exclusively in the optimization work without regard to length because, for a fixed value of δ_h , the change in

the value of L_h is equivalent to a change in the temperature ratio Z . When the optimum fin thickness and temperature ratio have been determined, the associated length can be computed. As shown in Figure 11, the ratio dW_f/dQ_f increases rapidly with increasing temperature ratio. Therefore, the optimum design will probably use modest temperature ratios. Because the curves for higher environment parameters are much steeper than for lower parameters, lower temperature ratios for higher environment parameters are recommended. It can also be observed that the ratio dW_f/dQ_f is proportional to the root thickness δ_h and low values of δ_h should therefore be expected from an optimization.

To aid in understanding the optimization procedure, two illustrative problems are analyzed. For both of these, a vapor condenser of a refrigeration heat exchanger was assumed. The passageway for the vapor was assumed to be aluminum in a rectangular shape, as shown in Figure 12.

Problem 1 (Operation in Free Space)

In determining the best fin dimensions to be added to the vapor passageway of Figure 12, assume that the heat exchanger

is oriented so that the sun does not hit a face of the heat exchanger. Also assume the following:

$$T_h = 675 \text{ R.}$$

$$\epsilon_a = \epsilon_b = 0.95$$

$$\alpha_a = \alpha_b = 0.18$$

$$k = 133 \text{ Btu. / (hr.) (ft.) (}^\circ\text{R.)}$$

$$\rho = 172.8 \text{ lb. /cu. ft.}$$

The heat transfer from a 1-ft. length of the rectangular vapor passageway can be computed from the equation

$$Q_v = C_1 T_h^4 A_r$$

and

$$Q_v = (\epsilon_a + \epsilon_b) \sigma T_h^4 \frac{0.497}{12}$$

$$= 28.24 \text{ Btu. /hr. /ft.}$$

The weight W_v of 1 ft. of vapor passageway is 0.0216 lb.

Assuming a variety of temperature ratios Z in Equations 35 and 28, the weight and the heat transferred from a single fin

are computed. The respective values for the vapor passageway and the two fins are then totaled. The overall weight per unit of heat transfer W/Q is obtained and plotted for the useful region on Figure 13. Also, values of dW_f/dQ_f for the fins are computed by Equation 52 and superimposed on the other curves. The intersection of the W/Q and dW_f/dQ_f curves represents the best temperature ratio value for the given root thickness, and the locus line through the intersection points represents the best possibility for the system. For the case analyzed, the thinnest root section considered was 0.008 in. A thinner fin was considered impractical and only of academic interest.

The values obtained along the locus line demonstrate the possible reduction in weight per unit of heat transfer resulting from adding the fins. The passageway itself has a value of W_v/Q_v equal to 7.65×10^{-4} lb./Btu./hr. By comparison, the finned configuration with root section thickness δ_h of 0.030 in. has a value of 4.0×10^{-4} lb./Btu./hr. In other words, the weight of this configuration is only 51.7 percent of the weight of an unfinned passageway. Even greater savings are possible from using thinner fins. When the root section thickness is 0.008 in., the weight is only 27.5 percent of the weight of an unfinned

passageway. From the results of this problem, it would appear that very thin fins give the best performance.

The best fin is that which has the optimum combination of practical thickness and low weight per unit of heat transfer. A more detailed study of manufacturing processes and tolerances is needed to fully establish the best fin thickness.

Problem 2 (Operation on Moon)

Assume the same conditions as in Problem 1 except that the vapor condenser is designed for operation at mid-day on the lunar equator and is mounted vertically on a level terrain. The lunar conditions applicable to this exchanger were taken from Reference 2 and are as follows:

$$S = 430 \text{ Btu. / (hr.) (sq. ft.)}$$

$$\cos \theta_p = 0$$

$$\cos \theta_m = 1$$

$$F_a = F_b = 0.5$$

$$r_m = 0.13$$

$$T_m = 674 \text{ R.}$$

Using Equation 28 of reference 2,

$$\begin{aligned} C_2 &= S (\alpha_a \cos \theta_p + F_a \alpha_a r_m \cos \theta_m + F_b \alpha_b r_m \cos \theta_m) + \\ &\quad (F_a \epsilon_a + F_b \epsilon_b) \sigma T_m^4 \\ &= 341 \text{ Btu. / (hr.) (sq. ft.)} \end{aligned}$$

From the data of Problem 1,

$$\begin{aligned}C_1 T_h^4 &= (\epsilon_a + \epsilon_b) \sigma T_h^4 \\ &= 682 \text{ Btu. / (hr.) (sq. ft.)}\end{aligned}$$

By combining these two results,

$$\frac{C_2}{C_1 T_h^4} = 0.5$$

The heat transfer from 1 ft. of vapor passageway is

$$\begin{aligned}Q_v &= (C_1 T_h^4 - C_2) \frac{0.497}{12} \\ &= 14.12 \text{ Btu./hr.}\end{aligned}$$

As in Problem 1, the weight of 1 ft. of tube is 0.0216 lb.

The data of Figure 14 were obtained by computing and plotting the values of W/Q and dW_f/dQ_f as in Problem 1, with similar results. The weight per unit of heat transfer is very close to twice the amount for the condenser designed for free

space. This difference is largely due to the heat transfer for the lunar environment parameter being one-half the amount obtained for free space. Also, much lower values were found for the optimum temperature ratio than were obtained in Problem 1. For the thinnest fin analyzed, the optimum temperature ratio is shown to be approximately 1.12. The theoretical limit for an environment parameter of 0.5 is only 1.189 (Figure 4), and therefore a value of Z equal to 1.12 is 63.5 percent of the maximum temperature ratio increase.

It should be noted that the midpoint locus occurs in an area where there is little change in the weight per unit of heat transfer. Little reduction in weight is possible by using fins thinner than those shown at the midpoint locus. Although the thinner fins are more efficient from a weight standpoint, the best configuration will be a compromise between light weight and the practical considerations of fabrication and durability.

A further study of the fins of Problems 1 and 2 can be made to determine the actual fin lengths. Optimum temperature ratios for the various root thickness shown in Figures 13 and 14 are used with Figure 4 and Equation 20 to determine the lengths. The results are shown in Figure 15. All of the actual lengths fall

between approximately 1.75 and 2.2 in. , the larger root thickness requiring a shorter fin than the thinner root section. The fins for free space are longer than those for lunar operation, but with very small difference. The interaction of several parameters is responsible for the very slight variation of fin length with both root thickness and environment. Interacting factors are the length, shown by Equation 20 to be a function of both the root thickness and the temperature ratio value, and the marked change of the optimum value of the temperature ratio with the environment.

FIN SHAPE

The influence of temperature ratio on fin shape is shown in Figures 16 and 17. The data were obtained from Equation 22 and plotted for the thickness ratio δ/δ_h versus the length ratio L/L_h . The fin is almost triangular in shape at low temperature ratios but becomes more concave as the temperature ratio increases. Also, at a given temperature ratio, the fin becomes more concave as the value of the environment parameter increases.

For an environment parameter of zero, the fin shape does not change greatly as the temperature ratio changes from 1.05 to 1.5, as shown in Figure 16. Greater changes are shown in Figure 17, which was plotted for a more severe environment. For the environment parameter 0.2, the maximum temperature ratio at the theoretical limit is 1.49735, and at this value the fin is very concave. The mathematical theory of the Figure 17 curve for $Z = 1.5$ predicts a negative thickness near the tip end. However, the amount of negative thickness is so small that it cannot be detected on the plot. The 1.5 value was plotted to show the sharpness of the fin at the end section where conditions near the theoretical limit prevail.

TRIANGULAR FINS

The comparative ease of manufacture makes the triangular fin attractive for many uses. However, accurate computation of the heat transfer is difficult. Machine programs for calculating the radiation heat exchange are complicated and often require considerable machine time to perform the iterative processes. For these reasons, approximate answers are useful.

The shape of a fin having a constant temperature ratio of low value is not greatly different from that of a triangular fin, and the two types of fins have been compared. The weight of the triangular fin is equal to the volume times the density, or

$$W_f = \frac{\rho L_w \delta_h L_h}{2} \quad (56)$$

When equal length fins are compared, the value of L_h given by Equation 20 can be substituted into Equation 56.

$$W_f = \frac{\rho L_w \delta_h}{2} \sqrt{\frac{k \delta_h \Phi_1}{C_1 T_h^3}} \quad (57)$$

Dividing Equation 35 by Equation 57,

$$\frac{W_f}{W_t} = \frac{2 \Phi_4}{\sqrt{\Phi_1}} \quad (58)$$

Using Equation 58, a constant temperature gradient fin of a given temperature ratio Z can be compared with a triangular fin of the same length. The comparison is shown in Figure 18 where values for ϕ_4 and ϕ_1 were substituted into Equation 58. The weight ratio falls with increasing temperature ratio, and values from 0.75 to 0.85 can be expected. At the theoretical limit, values of 0.65 and less are encountered. In many cases, the fin is already of low weight and this 15 to 25 percent of additional weight is not excessive.

Figure 19 indicates the difference in the amount of material and temperature between the two fins. The distribution of this extra material in the triangular fin is less favorable to internal heat transfer than the distribution of material in the constant temperature gradient fin, and it is therefore much less effective to heat transfer. To illustrate the change resulting from the added material, the temperature along the triangular fin is also

compared in Figure 19 with the temperature in the constant gradient fin. Because the temperature at the tip is higher for the triangular fin, this type of fin will radiate more heat. However, the 15 to 25 percent more weight will increase the heat output by approximately 5 to 7 percent. The latter values were obtained by analyzing the probable effects of the added material.

CONCLUSIONS

The equations and methods presented permit computation of the heat transfer and weight of a tapered fin. Also, the optimization curves and procedures presented can aid the fin designer in performing preliminary design analysis and in selecting the best configuration.

In certain instances, particularly in the case of large vapor passageways connected to thin fins, considerable radiant heat transfer will take place between the end of the vapor passageway and the fin. This creates a condition where the radiation interchange factor along the fin is not constant as was assumed in this study. The overall effect is an increase in temperature along the fin, resulting in an increase in heat transfer from the system to the environment. Studies are needed to establish more accurately the amount of increase in heat transfer.

REFERENCES

1. English, R. E. , Slone, H. O. , Bernatowicz, D. T. , Davison, E. H. , and Lieblein, S. , "A 20,000-Kilowatt Nuclear Turboelectric Power Supply for Manned Space Vehicles, " Memo 2-20-59E, Lewis Research Center, National Aeronautics and Space Administration, Cleveland, Ohio, March 1959.
2. Mackay, D. B. , and Leventhal, E. L. , "Radiant Heat Transfer From Flat Plate Uniformly Heated on One Edge, " Paper presented to American Institute of Chemical Engineers, Buffalo, New York, August 1960.
3. Cornog, Robert, "Design Optimization of Thermal Radiators for Space Vehicles, " Preprint No. 59-10, American Astronautical Society, Los Angeles, California, 4-5 August 1959.
4. Eckert, E. R. G. , and Drake, R. M. , Jr. , "Heat and Mass Transfer, " McGraw-Hill Book Company, Inc. , New York, 1959.

NOMENCLATURE

A_f	Fin area
C_1	Radiation constant (Equation 8)
C_2	Radiation constant equal to heat received from environment by unit of fin area
C_3	Constant defined by Equation 44
C_4	Constant defined by Equation 48
F_a	Radiation form factor for fin side facing sun
F_b	Radiation form factor for fin side away from sun
k	Thermal conductivity of fin material
L	Fin length (variable) in direction of heat flow
L_h	Fin length (total) in direction of heat flow
L_w	Width of fin normal to heat flow
Q	Total heat lost from vapor passageway plus heat from connected fins
Q_a	Heat lost by radiation from fin surface facing sun
Q_b	Heat lost by radiation from fin surface not facing sun
Q_f	Heat lost by radiation from both sides of fin
Q_i	Internal heat passing through section of fin
Q_v	Heat lost from vapor passageway
r_m	Reflectivity of environmental surface

- S** Solar constant (heat received from sun per unit area in unit of time)
- T_c** Temperature at cold end of plate
- T_h** Temperature at hot end of plate
- T_m** Surface temperature of environment
- T_f** Fin temperature (variable)
- W** Weight of vapor passageway plus fins
- W_f** Weight of fin
- W_t** Weight of triangular fin
- W_v** Weight of vapor passageway
- y** Variable (Equation 31)
- Z** Ratio of absolute temperatures (root temperature divided by tip temperature)
- a_a** Absorptivity of fin surface facing sun
- a_b** Absorptivity of fin surface away from sun
- δ** Fin thickness (variable)
- δ_h** Fin thickness at root section
- e** Surface emissivity
- e_a** Emissivity of fin surface facing sun
- e_b** Emissivity of fin surface away from sun

θ_m	Angle between sun's rays and a normal to environment surface
θ_p	Angle between sun's rays and a normal to fin surface
ρ	Density of fin material
σ	Stefan-Boltzmann constant
ϕ_1	Temperature function defined by Equation 21
ϕ_2	Temperature function defined by Equation 24
ϕ_3	Temperature function defined by Equation 29
ϕ_4	Temperature function defined by Equation 36
ϕ_5	Temperature function defined by Equation 38
ϕ_6	Temperature function defined by Equation 41
ϕ_7	Temperature function defined by Equation 45
ϕ_8	Temperature function defined by Equation 46
ϕ_9	Temperature function defined by Equation 53
Ω	Fin efficiency

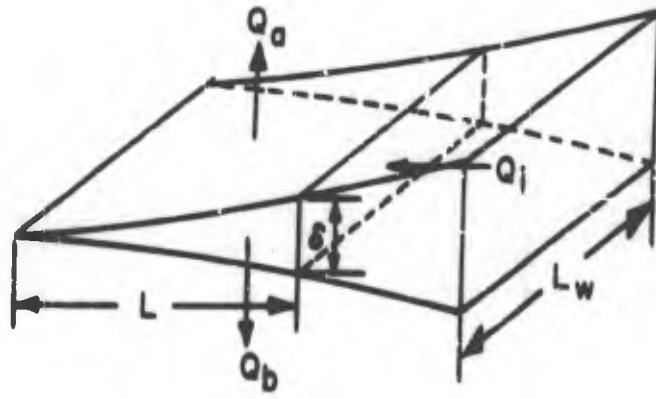


Figure 1. Fin Diagram

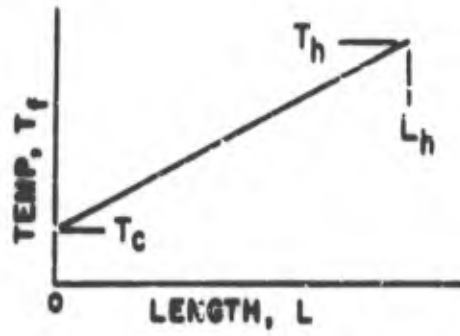


Figure 2. Temperature Profile

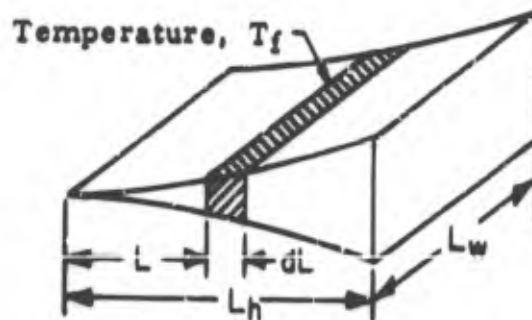


Figure 3. Element Analysis

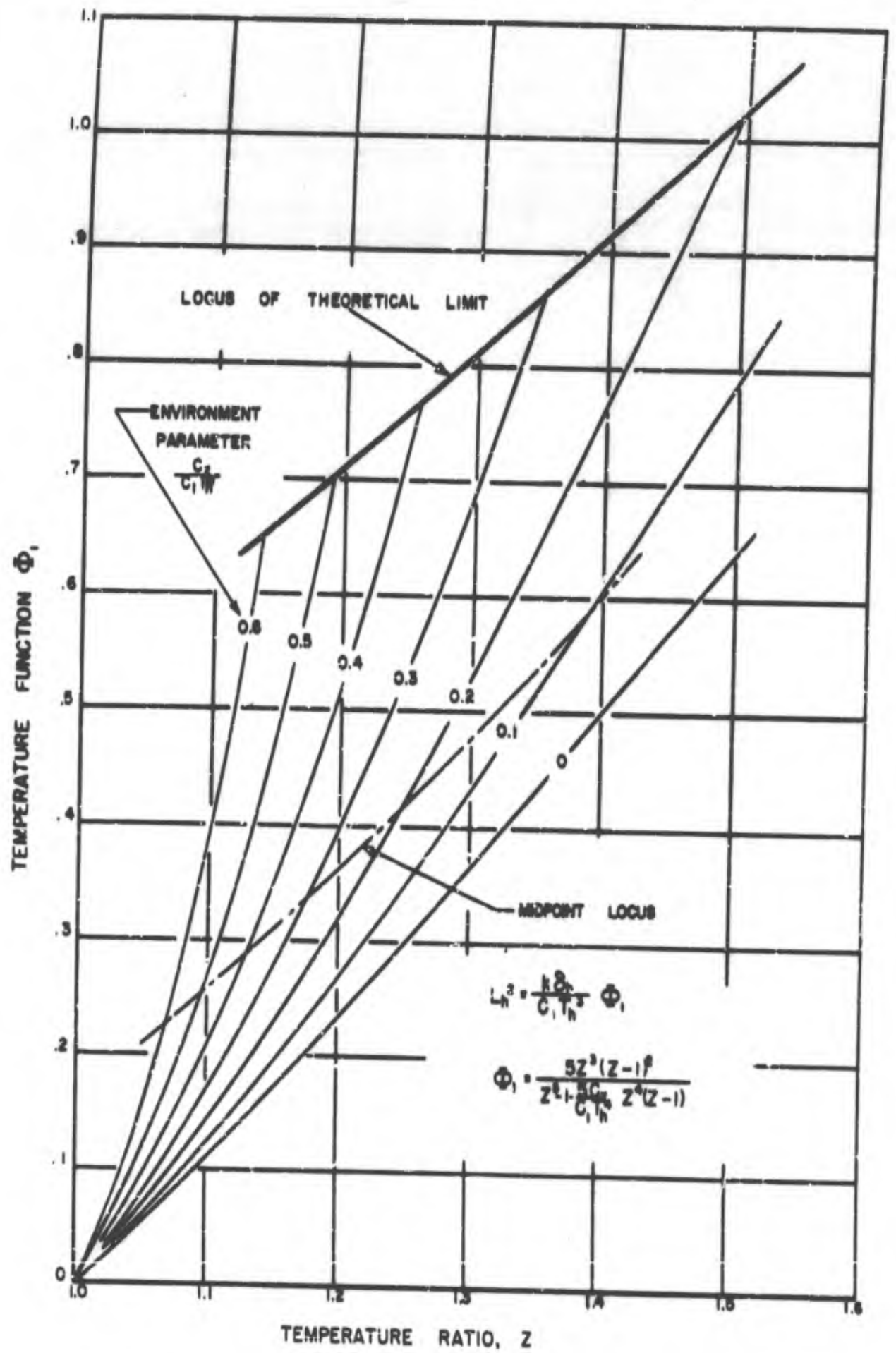


Figure 4. Length Function

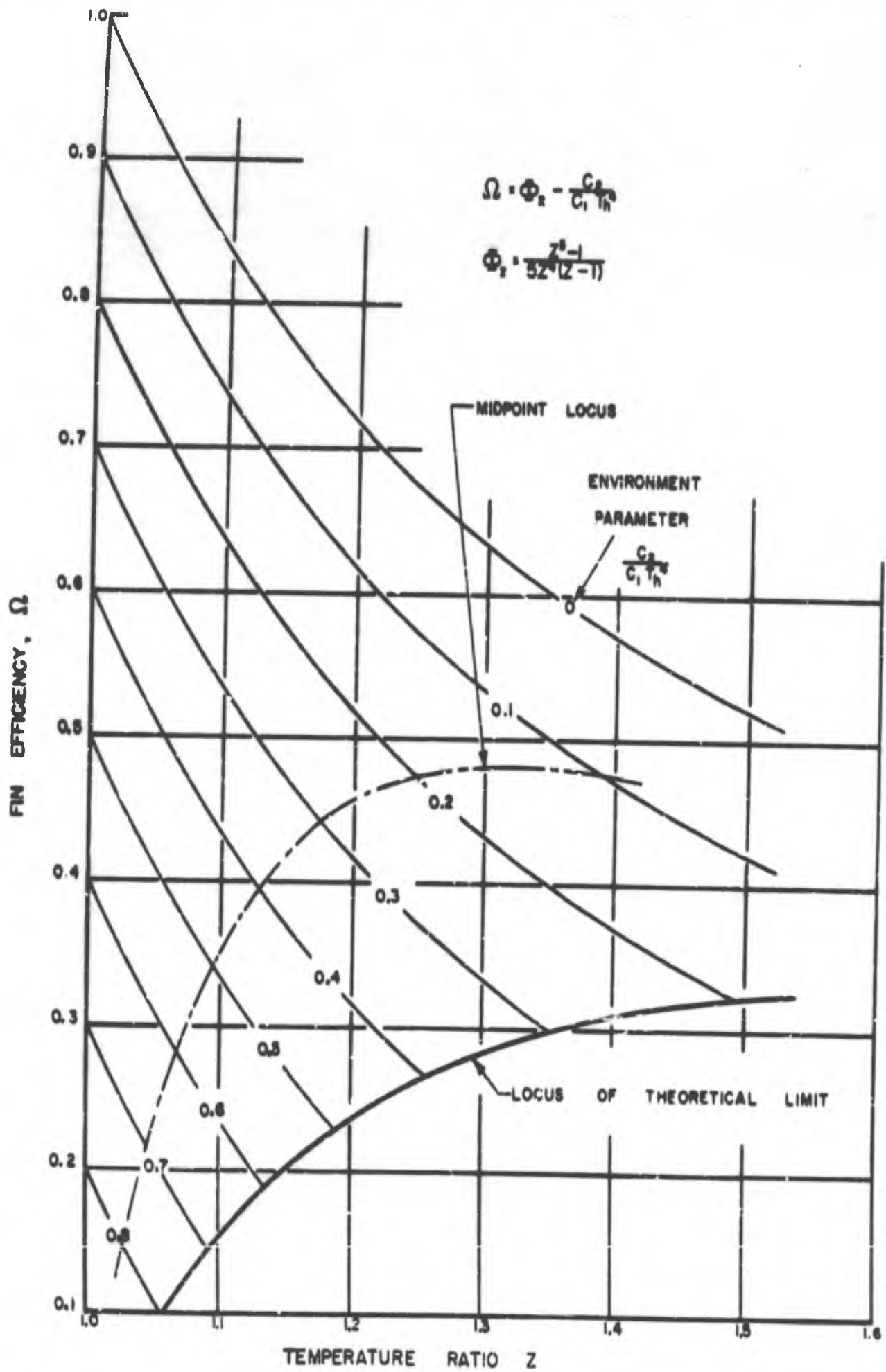


Figure 5. Fin Efficiency

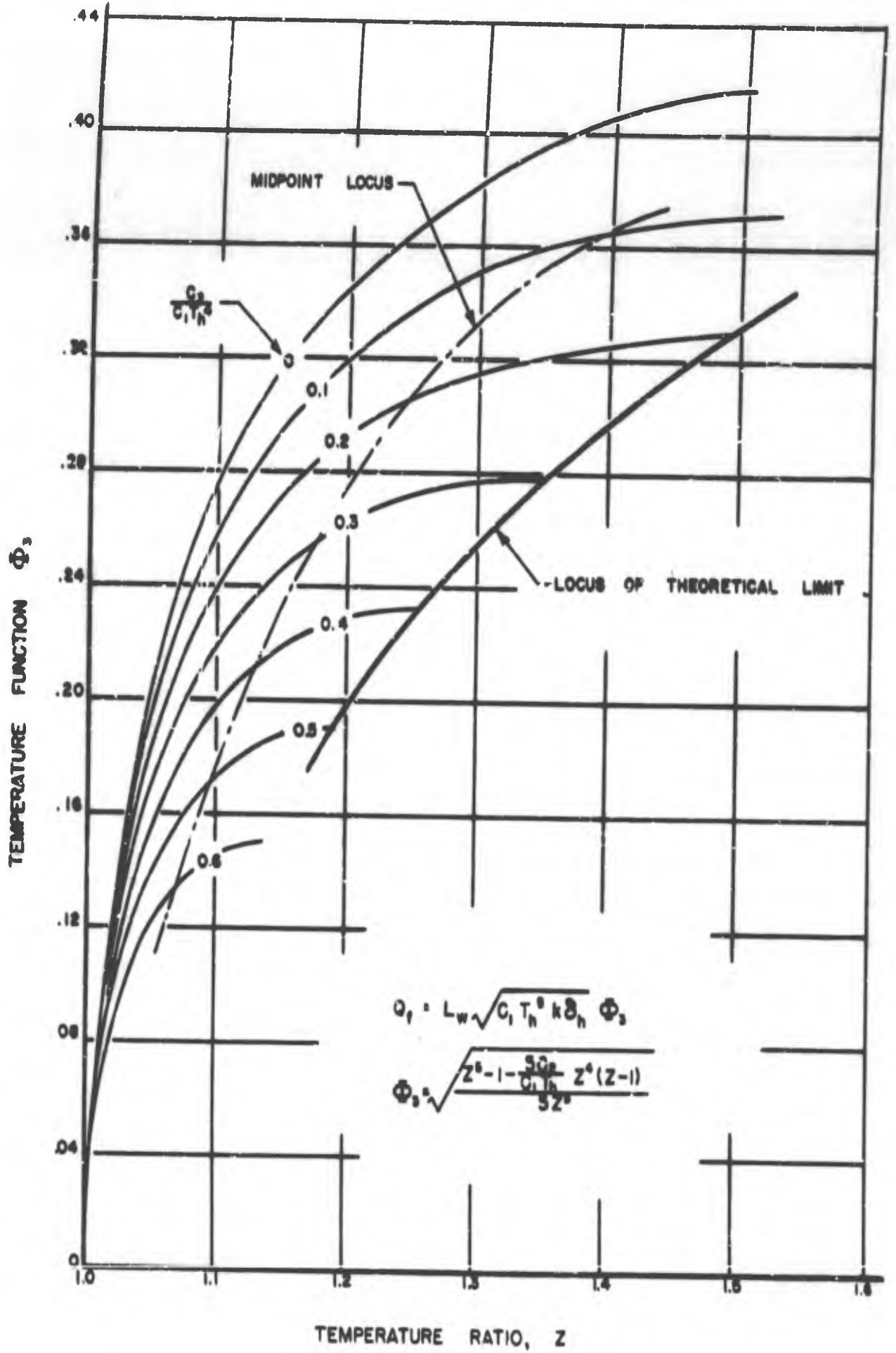


Figure 6. Heat Transfer Function

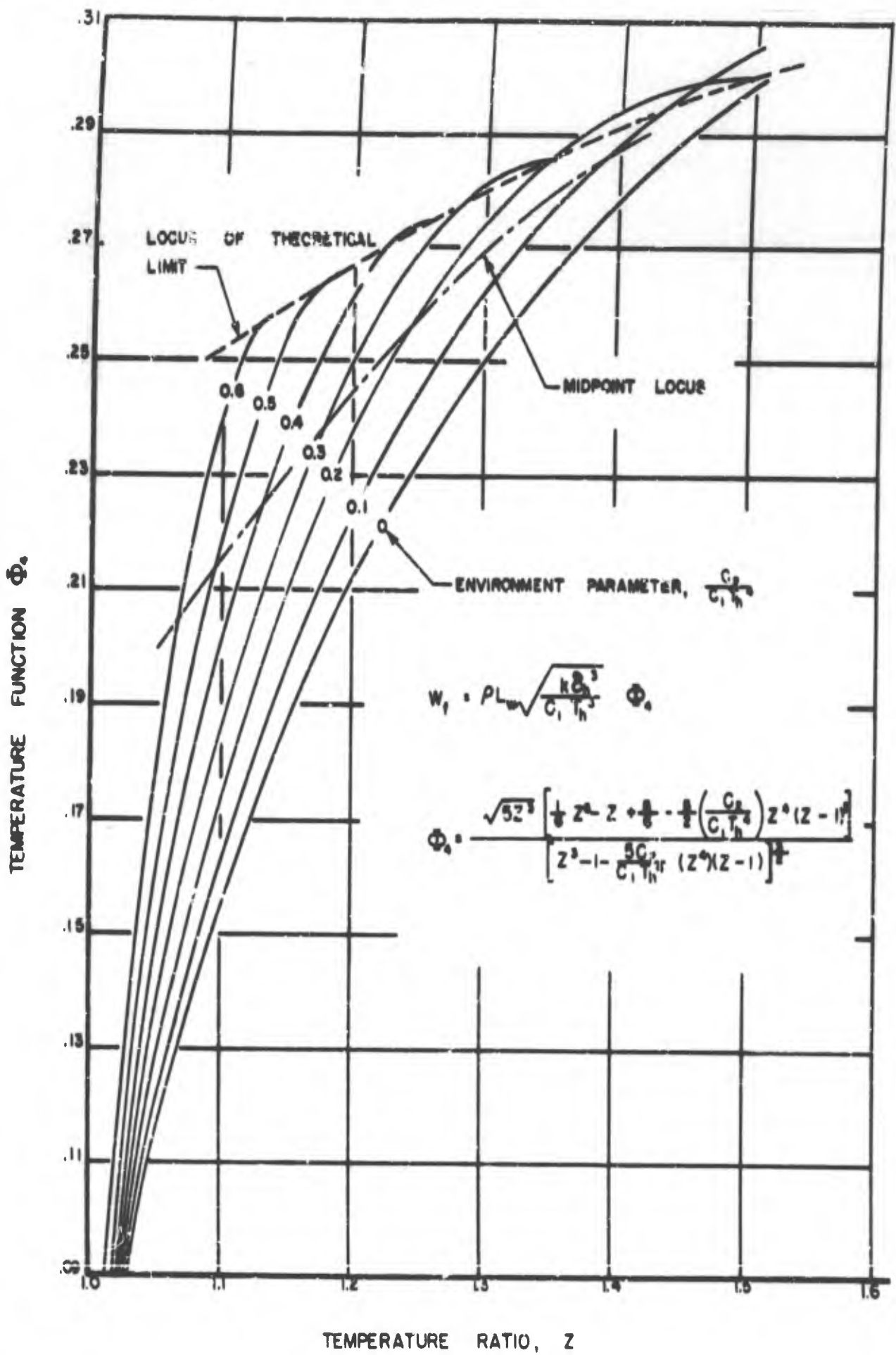


Figure 7. Weight Function

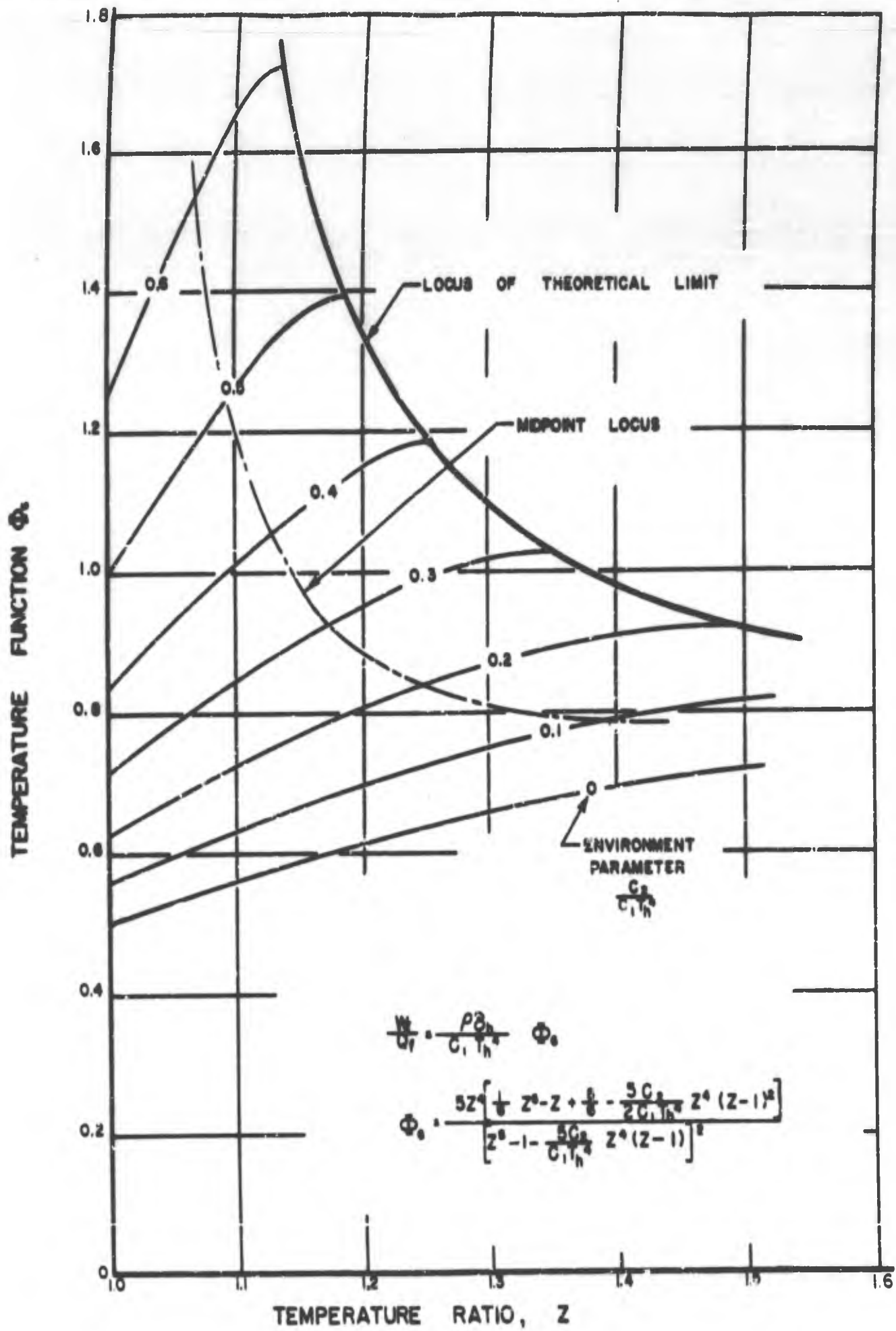


Figure 8. Function for W_f/Q_f

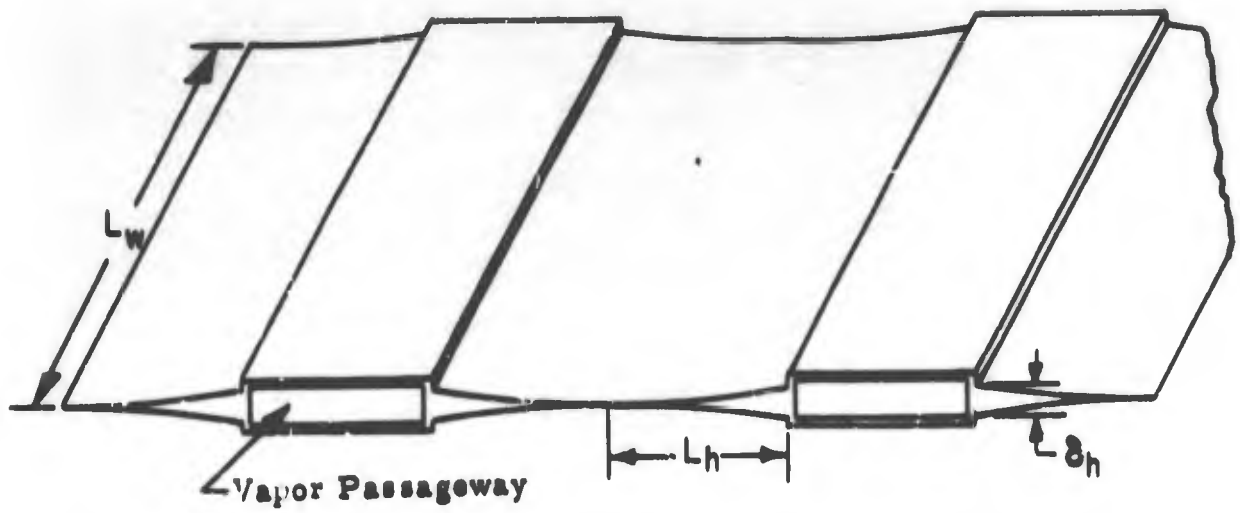


Figure 9. Heat Exchanger Configuration

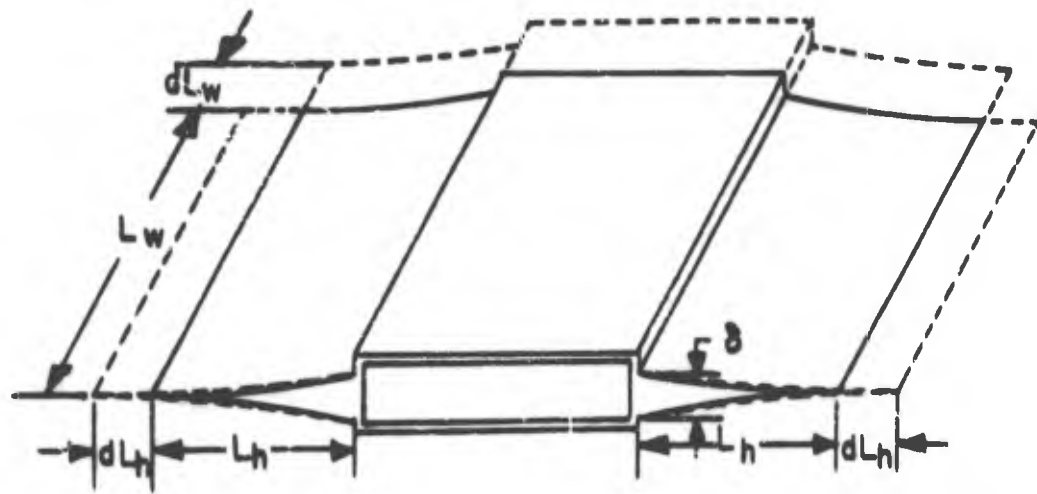


Figure 10. Heat Exchanger Section

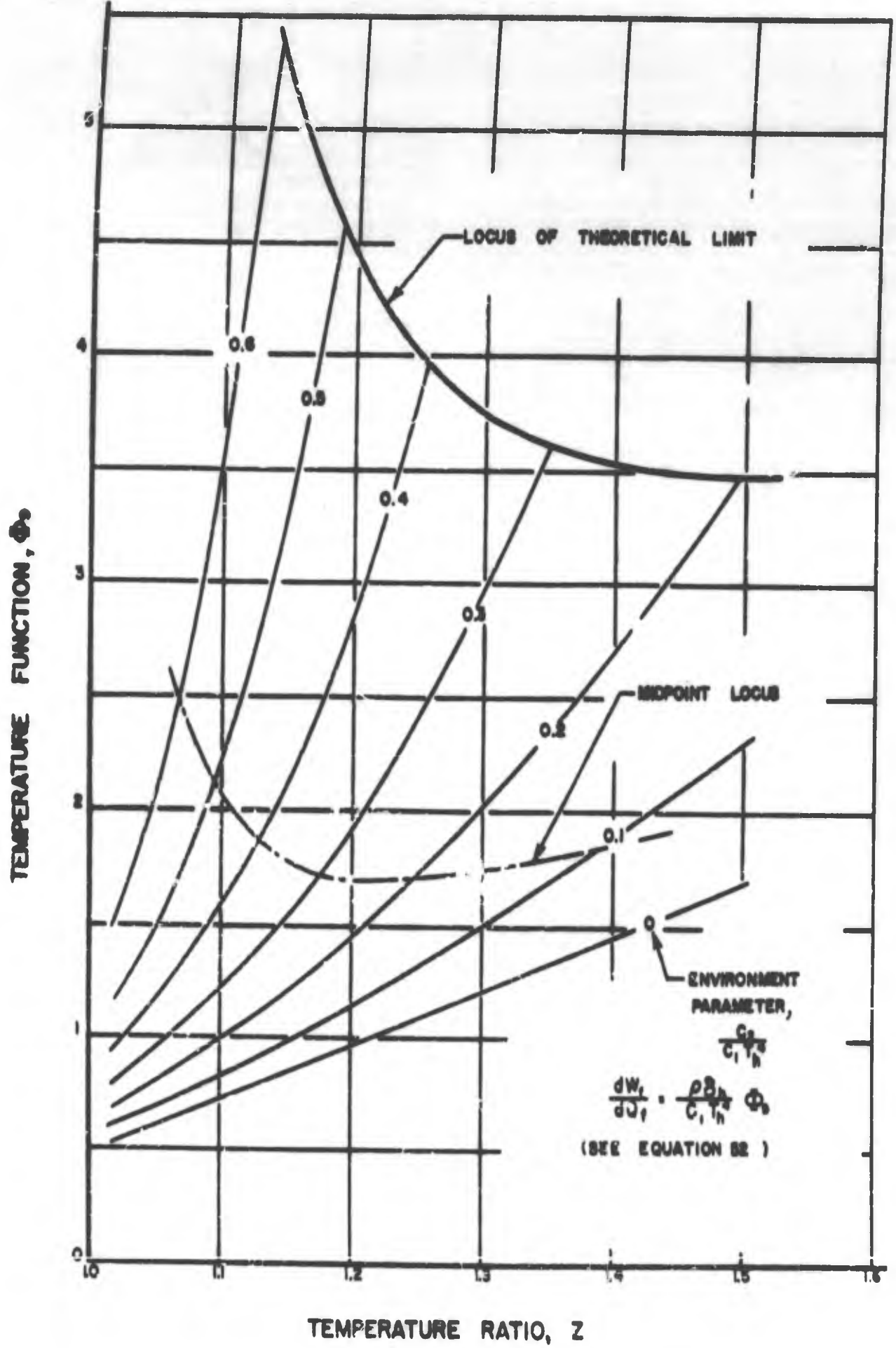


Figure 11. Function for dW_f/dQ_f

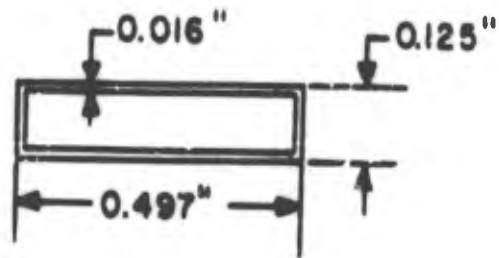


Figure 12. Passageway Dimensions

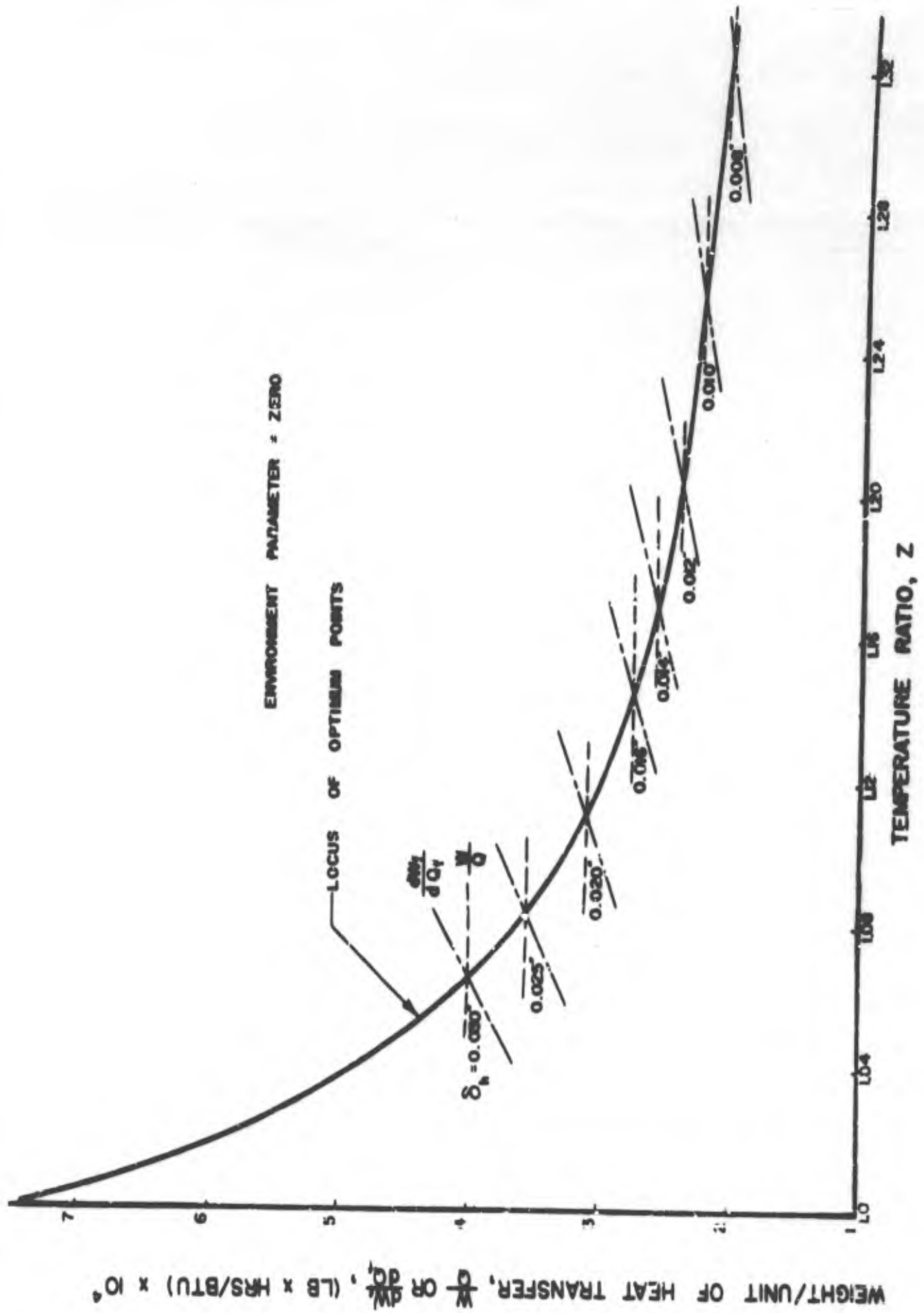


Figure 13. Problem 1 Solution

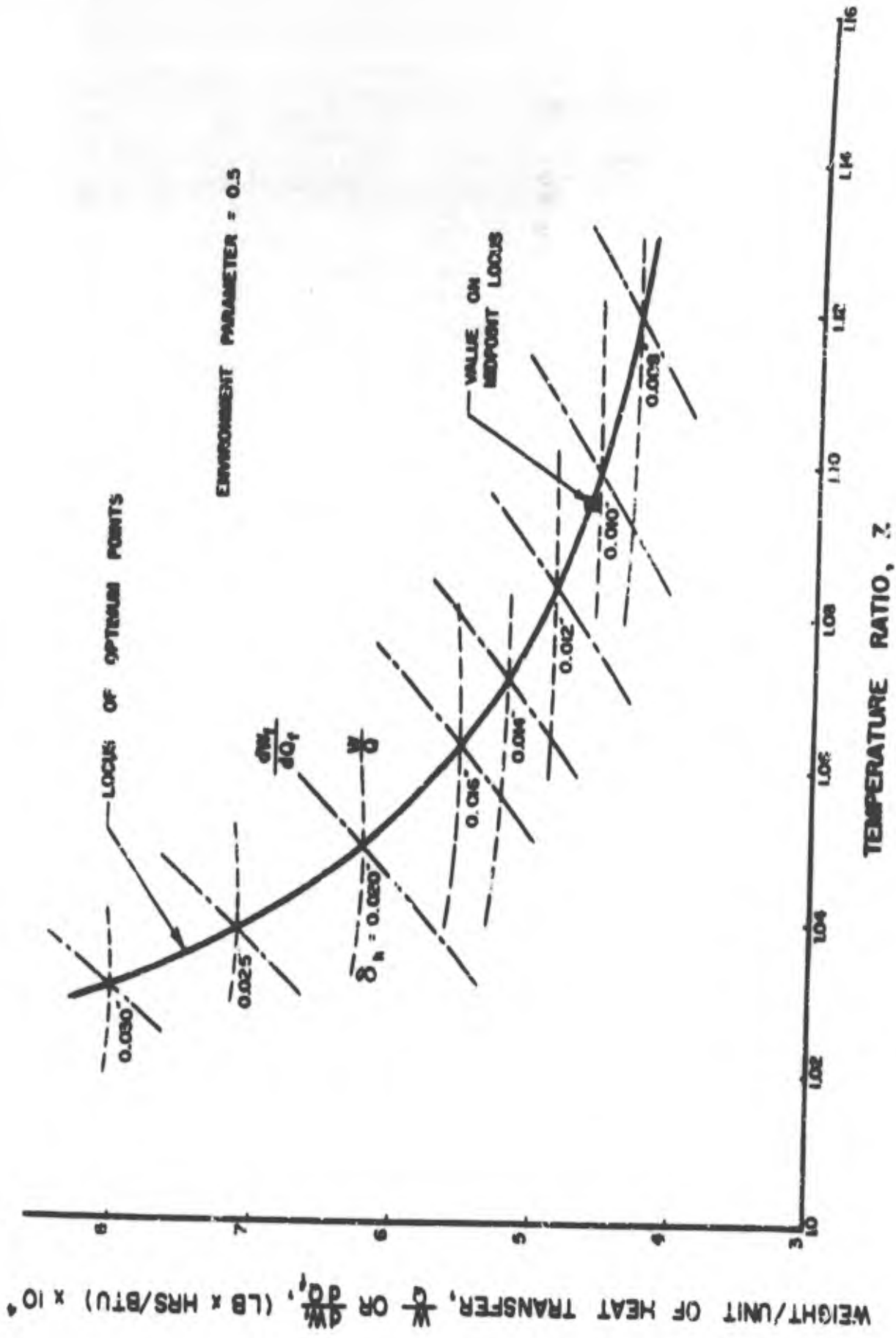


Figure 14. Problem 2 Solution

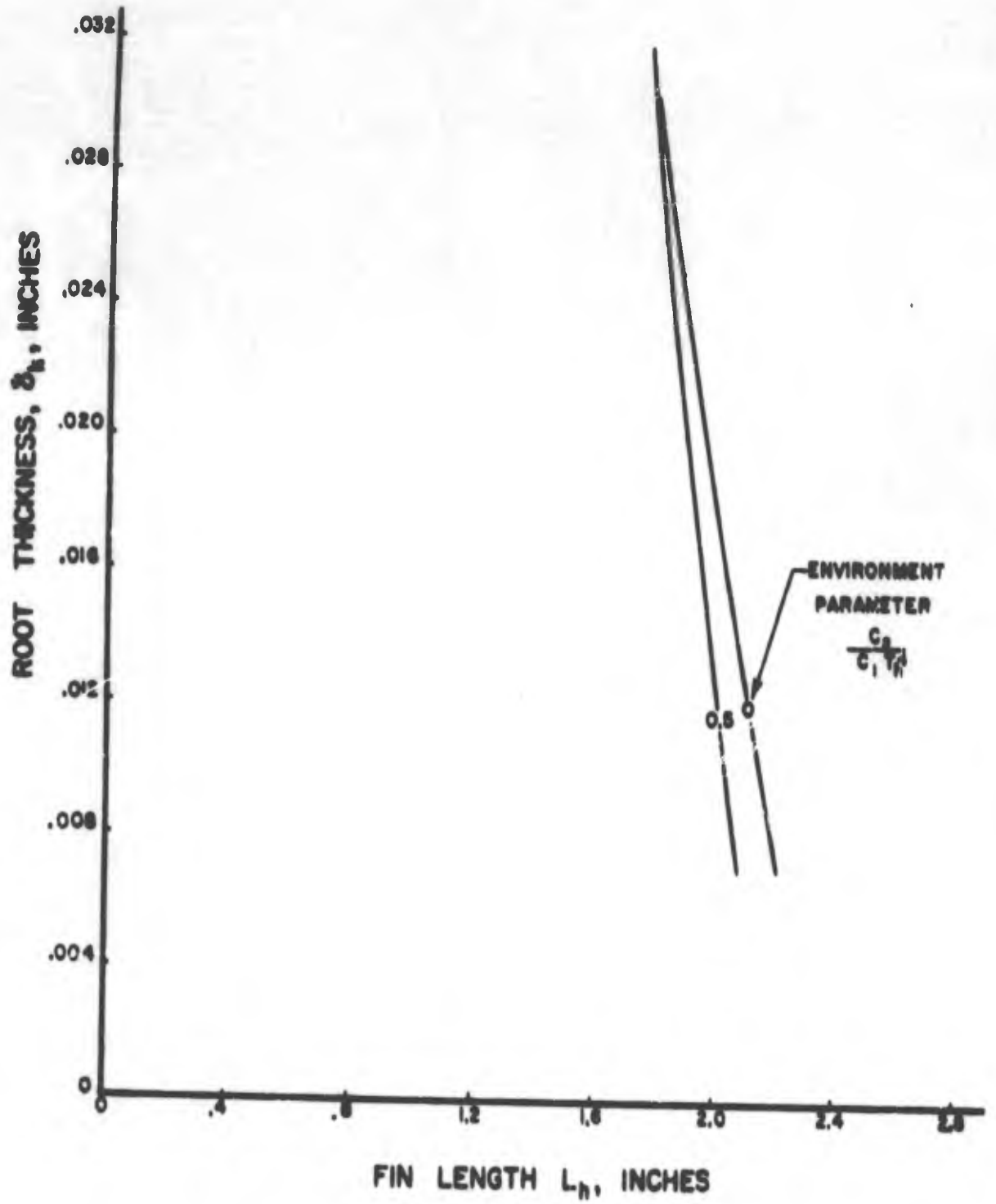


Figure 15. Fin Length (Problems 1 and 2)

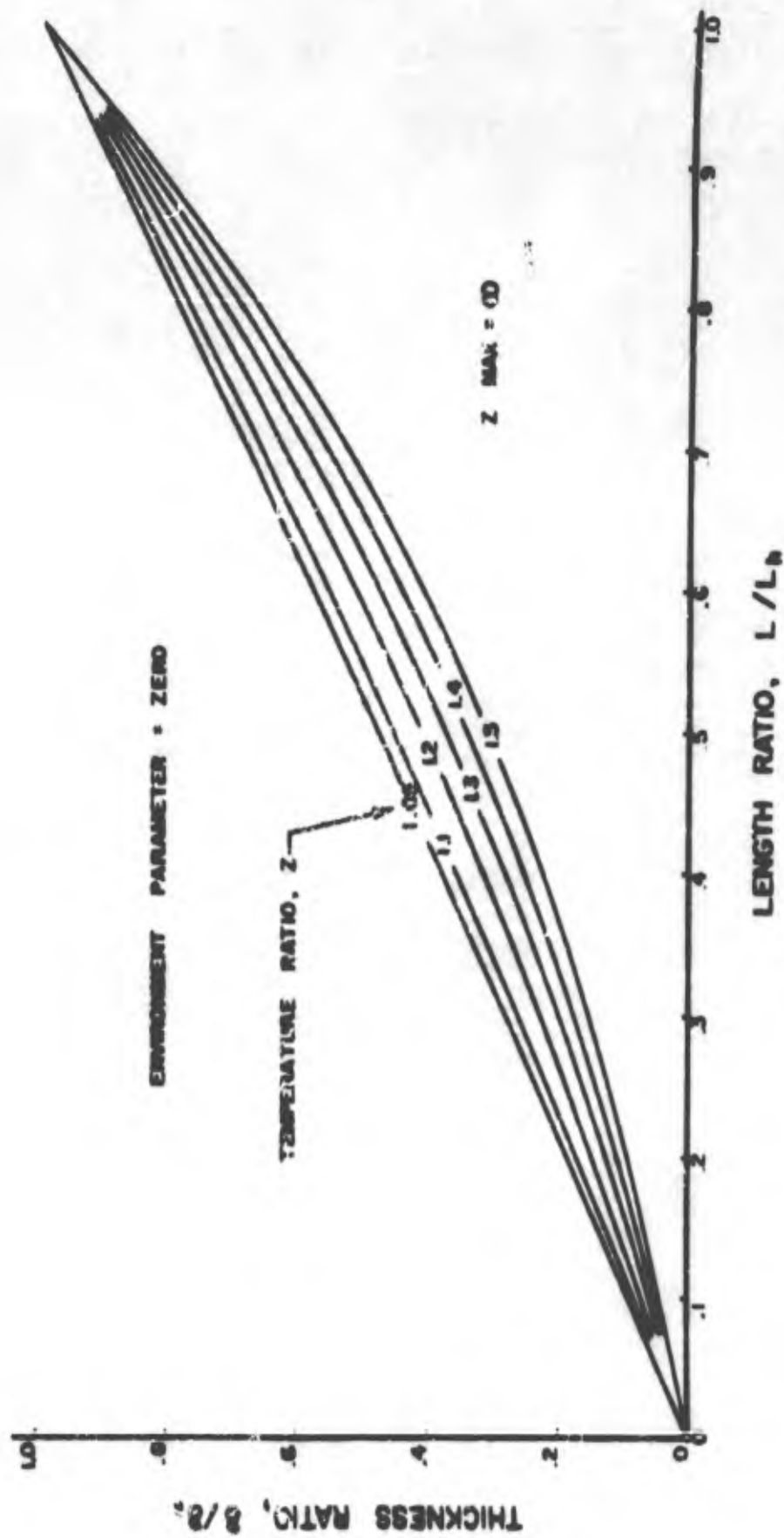


Figure 16. Fin Configuration for Free Space

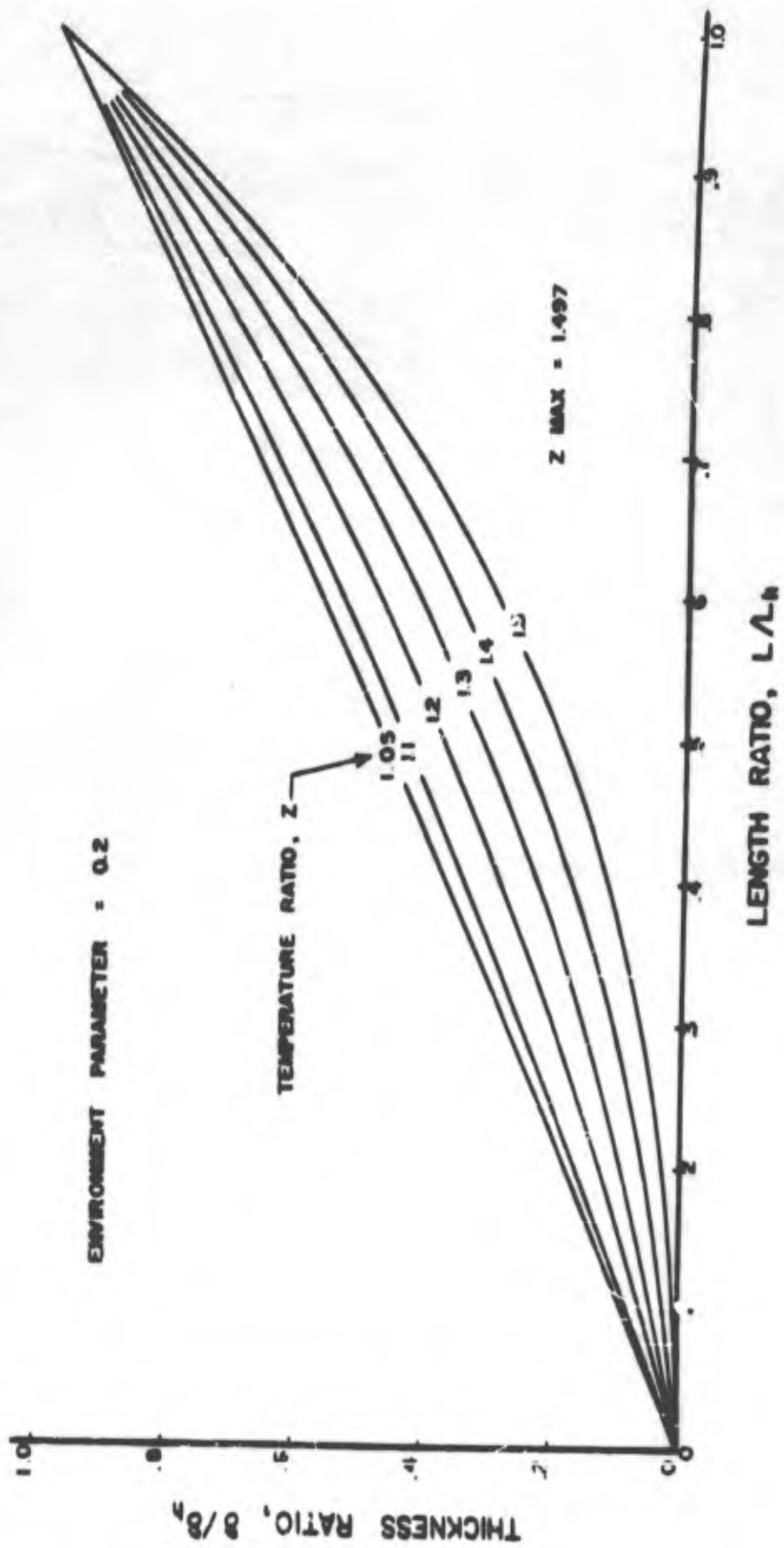


Figure 17. Fin Configuration for Environment Parameter 0.2

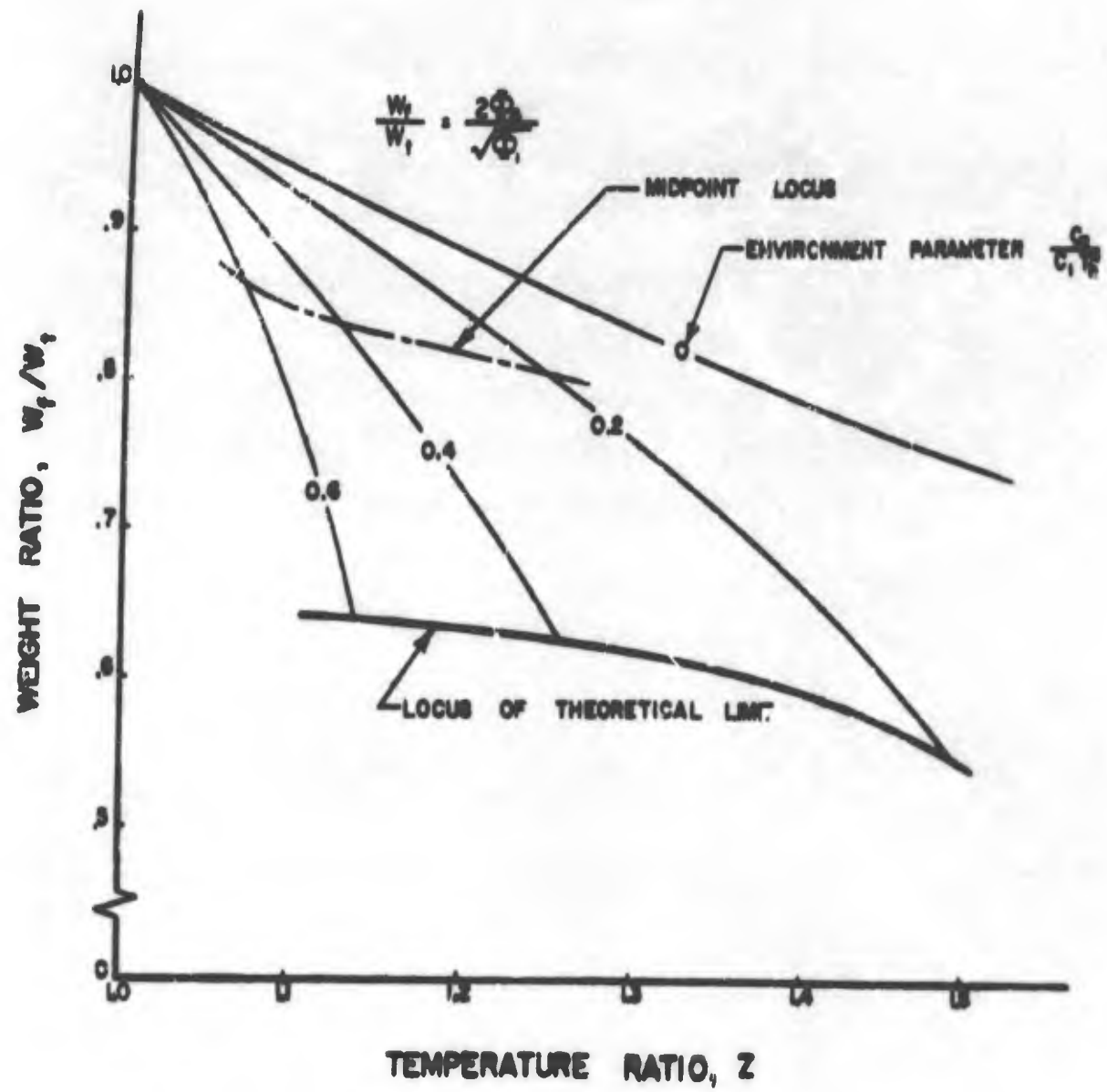


Figure 18. Weight Comparison

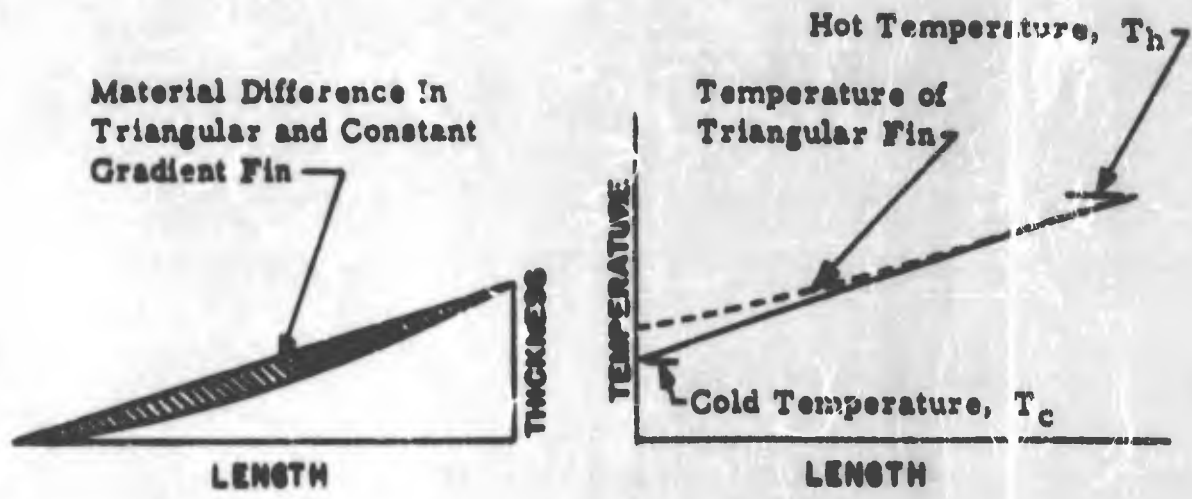


Figure 19. Fin Comparison

UNCLASSIFIED

UNCLASSIFIED